Protein prenylation reactions as tools for site-specific protein labeling and identification of prenylation substrates

Dissertation

zur Erlangung des akademischen Grades
eines Doktors der Naturwissenschaften (Dr. rer. nat.)
des Fachbereichs Chemie der Technischen Universität Dortmund

Angefertigt am Max-Planck-Institut für molekulare Physiologie
in Dortmund

Vorgelegt von
Dipl.-Chemikerin Thi Thanh Uyen Nguyen
aus Jülich

Dortmund, April 2009

Die vorliegende Arbeit wurde in der Zeit von Oktober 2005 bis April 2009 am Max-Planck-Institut für molekulare Physiologie in Dortmund unter der Anleitung von Prof. Dr. Roger S. Goody, Prof. Dr. Kirill Alexandrov und Prof. Dr. Herbert Waldmann durchgeführt.

1. Gutachter : Prof. Dr. R. S. Goody
2. Gutachter : Prof. Dr. H. Waldmann

The results of this work were published in the following journals:

"Exploiting the substrate tolerance of farnesyltransferase for site-selective protein derivatization"
U.T.T. Nguyen, J. Cramer, J. Gomis, R. Reents, M. Gutierrez-Rodriguez, R.S. Goody, K. Alexandrov, H. Waldmann, *Chembiochem* **2007,** *8* (4), 408-23.

"Development of selective RabGGTase inhibitors and crystal structure of a RabGGTase-inhibitor complex"
Z. Guo, Y.W. Wu, K.T. Tan, R.S. Bon, E. Guiu-Rozas, C. Delon, U.T.T. Nguyen, S. Wetzel,S. Arndt, R.S. Goody, W. Blankenfeldt, K. Alexandrov, H. Waldmann, *Angew Chem Int Ed Engl* **2008,** *47* (20), 3747-50.

"Analysis of the eukaryotic prenylome by isoprenoid affinity tagging"
U.T.T. Nguyen, Z. Guo, C. Delon, Y.W. Wu, C. Deraeve, B. Franzel, R.S. Bon, W. Blankenfeldt, R.S. Goody, H. Waldmann, D. Wolters, K. Alexandrov, *Nat Chem Biol* **2009**, *5* (4), 227-35.

Ba Má

Contents...i

Abbreviations...iii

ABBREVIATIONS

A	Ampère
Å	Angstrom (1 Å = 0.1 nm = 10^{-10} m)
AA	Amino acid
ACN	Acetonitrile
BG	Biotin-geranyl
BGPP	Biotin-geranyl pyrophosphate
CBR	C-terminal binding region
CHM	Choroideremia
CIM	CBR interacting motif
COMP	compactin
Da	Dalton
Dans / Dansyl	5-Dimethylaminonaphtalin-1-sulfonyl
DMSO	Dimethylsulfoxide
DTE	1,4-Dithioerythritol
DTT	1,4-Dithiothreitol
F	Farnesyl
FPP	Farnesylpyrophosphate
FTase	Farnesyltransferase
GAP	GTPase activating protein
GDF	GDI displacement factor
GDI	GDP dissociation inhibitor
GdmHCl	Guanidinium hydrochloride
GEF	Guaninenucleotide exchange factor
GF	Gel filtration
GG	Geranylgeranyl
GGPP	Geranylgeranylpyrophosphate
GGTase-I	Geranylgeranyltransferase-I
GGTI	GGTase-I inhibitor
GST	Glutathione *S*-transferase
GTPase	Guaninetriphosphate phosphatase
h	hour
HOPS	Homotypic fusion and vacuole protein sorting
HPLC	High performance liquid chromatography
Icmt	Isoprenylcysteine carboxymethyltransferase
IG	Immunoglobulin
IPTG	Isopropyl-β-D-thiogalactoside

LC-MS	Liquid chromatography-mass spectrometry
LRR	Leucine-rich repeat
MALDI-TOF-MS	Matrix assisted laser desorption/ionization-time of flight mass spectrometry
mant	N-methylanthraniloyl
min	minute
MudPIT	Multidimensional Protein Identification Technology
MWCO	Molecular weight cut off
NBD	7-Nitrobenz-2-oxa-1,3-diazol-4-yl
NSF	*N*-ethyl-maleimide sensitive factor
OD_{600}	Optical density at 600 nm
PP	Pyrophosphate
PTM	Posttranslational modification
Rab	Ras-like (protein) from Rat brain
RabGGTase	Rab Geranylgeranyltransferase
Ras	Rat adeno sarcoma
REP	Rab escort protein
Rho	Ras homologous protein
RP-HPLC	Reversed-phase high performance liquid chromatography
RT	Room temperature
SDS	Sodium dodecyl sulfate
Sec	Secretory protein
SNAP	Soluble NSF association protein
SNARE	Soluble NSF attachment protein receptor
TFA	Trifluoroacetic acid
wt	wild-type
Ypt	Yeast protein transport

1 INTRODUCTION

1.1 Posttranslational modifications

The deciphering of the human genome in 2001 constitutes a milestone in the history of biological research. Unexpectedly, it revealed that it contains just 30.000 genes; this is only twice as many as in lower eukaryotes such as worm or fly[1, 2]. Since the size of the human proteome, defined as the number of different protein molecules in humans, exceeds that of the genome, defined as the number of genes, by at least two orders of magnitude[3, 4], human complexity cannot be a direct consequence of the number of encoding genes. Instead, diversification of the coding capacity of the genome is achieved by two major mechanisms, first of all at the transcriptional level by mRNA splicing[5, 6], and secondly at the protein level by posttranslational modifications (PTMs)[3].
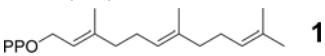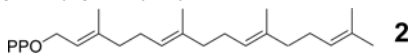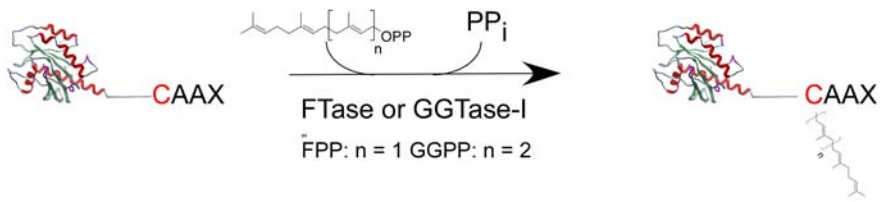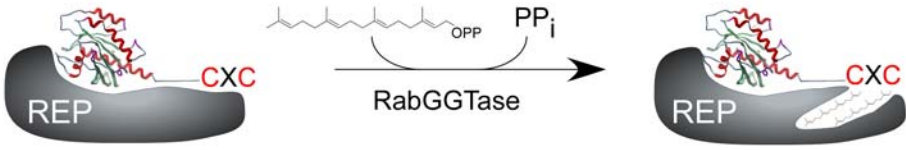
PTMs refer to covalent alterations that are usually added after a protein is expressed. They are mediated by specific enzymes which account for about 5 % of the genome of higher eukaryotes[3]. PTMs also occur in prokaryotes, but tend to be less common and less diverse compared to nucleated cells. They range from generic, widespread alterations (e.g. glycosylation) to highly specific and rare modifications (e.g. SUMOylation). Depending on the action of demodifying enzymes, PTMs can either occur transiently (e.g. phosphorylation, palmitoylation) or permanently (e.g. prenylation).

PTMs are important because they can add a vast array of different functionalities to their target proteins. By that, they are able to turn the 20 naturally occurring codon-encoded amino acids into a variety of amino acids with new characteristics, which cannot be achieved by mRNA splicing. Proteins can be modified by the same PTM at multiple sites or by different modifications within the same protein. This can create a dynamic library of properties, which is tightly controlled by protein modifying and demodifying enzymes in response to systemic stimuli[7].

A good example for the dynamic utilization of PTMs is the information retrieval system from chromatin[8, 9]. Histones are the chief protein component of chromatin. Their primary role is to condense DNA by acting as spools around which DNA winds. In addition, their tails can be modified at multiple sites by different PTMs e.g. methylations, acetylations, phosphorylations, ubiquitinations, SUMOylations, or ADP-ribosylations. This creates a large combinatorial library of histone PTMs which defines whether DNA is in a transcriptionally active or inactive state.

1.2 Protein prenylation

Posttranslational modification of proteins with isoprene lipids is a widespread PTM that affects up to 2% of the mammalian proteome[10]. The first reports on prenylated proteins and peptides were secreted pheromone peptides found in jelly fungi[11, 12]. Their structure resembles the α-factor mating pheromone from baker´s yeast and contains a farnesylated cysteine methylester at the C-terminus[13]. During the course of the discovery of the cholesterol biosynthesis pathway (see section 1.3.4), several groups reported that (i) one of the crucial steps in cholesterol biosynthesis was at the early step of mevalonic acid synthesis catalyzed by 3-hydroxy-3-methylglutaryl coenzyme A (HMG-CoA) reductase[14] and that (ii) a compound derived from mevalonic acid other than the final product cholesterol was specifically incorporated into proteins[15, 16]. Later, it became clear that protein prenylation is characterized by the attachment of a farnesyl or a geranylgeranyl moiety to one or two C-terminal cysteine residues of target proteins via a thioether linkage.

Table 1-1 Biochemistry of the protein prenyltransferases.

	FTase	GGTase-I	RabGGTase
Subunit composition (mammalian)	α 44 kDa β 48 kDa	α 44 kDa β 43 kDa	α 65 kDa β 37 kDa
Protein recognition motif	-CA$_1$A$_2$X X = Ala, Gln, Ser, Met, Phe A$_1$: flexible A$_2$: Ile, Val preferred	-CA$_1$A$_2$X X = Leu, Phe, rare: Met A$_1$: flexible A$_2$: Ile, Leu preferred	common: -CC, -CXC, -CCX, -CCXX, -CCXXX rare: -CXXX
Isoprenoid substrate	farnesyl pyrophosphate (FPP)	geranylgeranyl pyrophosphate (GGPP)	
Metal requirements:	Zn^{2+}, Mg^{2+}	Zn^{2+}	Zn^{2+}

Schematic representation of the reaction catalyzed by the two CAAX prenyltransferases FTase (n = 1) and GGTase-I (n = 2) **A** or RabGGTase in concert with REP (Rab Escort Protein) **B**. The enzymes catalyze the formation of a thioether linkage between the prenyl group and one or two C-terminal cysteines of the protein substrate.

The prenylation reactions are catalyzed by three different protein prenyltransferases: protein farnesyltransferase (FTase), protein geranylgeranyltransferase-I (GGTase-I), and Rab geranylgeranyltransferase (RabGGTase)[17, 18]. FTase and GGTase-I recognize their substrates via a short C-terminal recognition sequence, referred to as the CAAX box, where C is a cysteine, A is variable, and X is commonly Ala, Gln, Ser, Met, or Phe for FTase and Leu or Phe for GGTase-I. In contrast, protein substrate recognition by RabGGTase is more complex since it requires an additional protein, the Rab Escort Protein (REP), to recruit its substrates (Table 1-1).

1.2.1 Structural features of the protein prenyltransferases

All three protein prenyltransferases are α, β heterodimeric enzymes. FTase and GGTase-I share the same α subunit with a molecular mass of 48 kDa[19]. The α subunit consists of 14 α helices folded into 7 successive pairs to form a series of right-handed antiparallel coiled coils[20, 21], also known as "helical hairpins". These helices are arranged in a crescent-shaped superhelix that wraps around the β subunit (Figure 1-1 A)[22]. The first 50 amino acids on the N-terminus of the α subunit form a proline-rich disordered domain, which is not involved in catalysis and does not influence the structure of the rest of the enzymes[23, 24].
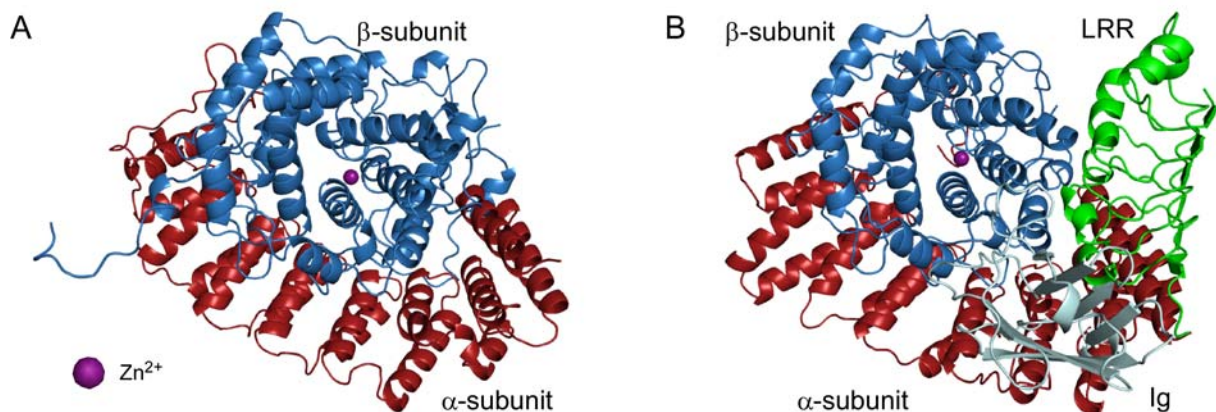
Figure 1-1 Overall structures of FTase **A** and RabGGTase **B**. Red: α-subunit, blue: β-subunit, gray: Ig-like domain, green: LRR-domain, purple: Zn^{2+} ion.

In contrast, the α subunit of RabGGTase contains an Ig-like and a leucine-rich repeat (LRR) domain in addition to the helical domain, which is highly similar to that of FTase/GGTase-I despite only 22 % sequence identity (Figure 1-1 B)[25]. Since these domains are absent in the structures found in lower eukaryotes, they are believed not to be involved in catalysis[26, 27], but their specific function is as yet unknown.

The β subunits of all three protein prenyltransferases share only 25 % sequence identity, but are also similar in their structure (Figure 1-1 A and B). They consist of 14, 13, or 12 α helices in FTase, GGTase-I, or RabGGTase, respectively. The helices fold into an α-α barrel forming

a funnel-shaped hydrophobic cavity with a diameter of 15 Å, which consists of several conserved aromatic residues. This cavity represents the active site of the enzymes and contains the lipid and protein substrate binding sites. The α and β subunits form an extensive interface burying about 20 % of accessible surface area of each subunit[20, 21].

Zn²⁺ binding site. All three protein prenyltransferases are zinc metalloenzymes with one Zn^{2+} located near the α, β subunit interface (Figure 1-1)[20, 21, 25, 28-33]. Zn^{2+} is coordinated by three strictly conserved residues: D297β, C299β, and H362β in FTase; D269β, C271β, and H321β in GGTase-I; and D238β, C240β, and H290β in RabGGTase. All three crystal structures reveal a stabilizing hydrogen bond between the Zn^{2+}-coordinated histidine residue and an aspartic acid residue (D359β, D318β, and D287β for FTase, GGTase-I, and RabGGTase, respectively; Figure 1-2).
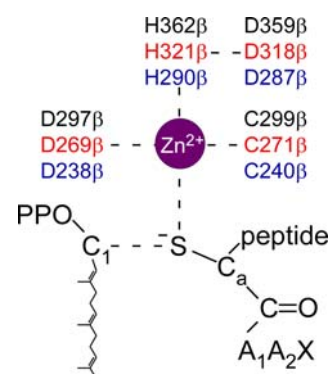
Figure 1-2 Zn^{2+} coordination. Black: FTase, red: GGTase-I, and blue: RabGGTase.

High-resolution substrate and product complexes indicate that the cysteine thiol of the CAAX motif interacts with Zn^{2+} at 2.3 Å distance in the substrate-bound and 2.6 Å distance in the product-bound state, resulting in a tetravalent coordination of the Zn^{2+} ion.

Lipid substrate binding. The lipid substrates of the CAAX prenyltransferases are buried next to the peptide binding site in the hydrophobic cavity of the β subunit[20, 34]. The pyrophosphate moieties of FTase and GGTase-I are sequestered within the diphosphate binding pocket. In FTase, this is mainly formed by R291β, K294β, both of which interact with the β-phosphate of FPP, and by Y300β, which forms a hydrogen bond with the α-phosphate of FPP[35] (corresponding residues in GGTase-I: R263β, K266β, and Y272β) (Figure 1-3). Both the pyrophosphate and the first three

Figure 1-3 Pyrophosphate coordination. Black: FTase, red: GGTase-I.

isoprene units of FPP and GGPP bind to FTase and GGTase-I in a similar conformation, which is mediated by analogous hydrophobic interactions with aromatic residues in their active sites. The additional fourth isoprene unit of GGPP is turned with an angle of 90° compared to the rest of the molecule (Figure 1-4). The active site of RabGGTase is structurally similar, but the exact conformation of the bound GGPP had not been determined until recently*.

---

* During the course of this work, our group published the RabGGTase structure in complex with its native substrate GGPP[36].

Isoprenoid substrate specificity. Both FPP and GGPP are tightly bound to all protein prenyltransferases in the nanomolar range, yet the enzymes display distinct lipid substrate specificities *in vivo*. This can be explained by the amino acids that occupy the bottom of their lipid binding site. In GGTase-I and RabGGTase, residues 49β and 48β, respectively, are always small amino acids like Thr or Ser, whereas the corresponding residue is a Trp in FTase (W102β). This bulky amino acid fills the space which is occupied by the additional fourth isoprene unit in the GGTase-I:GGPP complex (Figure 1-4).

Beese and co-workers showed that this amino acid determines whether the CAAX prenyltransferase accepts FPP or GGPP as a substrate. A single mutation W102Tβ was shown to interconvert the lipid substrate preference of both enzymes, surprisingly without changing the peptide substrate selectivity[20].

Figure 1-4 Bottom of the lipid binding pocket of the protein prenyltransferases. Blue: FTase:FPP; red: GGTase:GGPP; green: RabGGTase; light red or blue: pyrophosphate moieties of the respective isoprenoid. For further details, see text.

In RabGGTase, the bottom of the lipid binding site is further enlarged since Y154β (FTase) and Y126β (GGTase-I) are replaced by a much less bulky amino acid (L99β) at the corresponding position (Figure 1-4)[37].
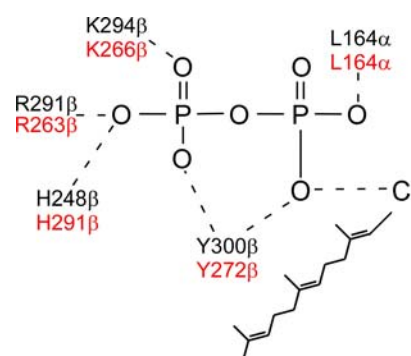
To explain the lipid substrate discrimination of FTase and GGTase-I, Beese and co-workers have postulated the "molecular ruler hypothesis", in which the depth of the lipid binding cavity of the two enzymes functions as a simple length-discriminating molecular ruler. In this hypothesis, larger non-cognate isoprenoids fill up the lipid binding pocket such that the diphosphate and C1 of the isoprenoid are mispositioned for efficient catalysis (Figure 1-5 C)[34].

Distefano and co-workers solved the structure of FTase in complex with GGPP and several other lipid analogs. From these data, they suggest a different explanation for the failure of FTase to transfer longer lipids than FPP, which they refer to as the "second site exclusion model"[38]. The pyrophosphate and the C1 atom of both GGPP and the benzophenone-functionalized GGPP **3** are correctly located at corresponding positions in the FTase:FPP complex (Figure 1-5 D and E). Interestingly, the isoprene conformation is perturbed in both cases, which stands in stark contrast to what the molecular ruler hypothesis had predicted. The crystal structure of FTase in complex with **3** revealed that the terminal benzophenone group bulges into the CAAX substrate binding pocket and prevents proper CAAX peptide binding. In contrast, the first two isoprene units of GGPP in the FTase:GGPP complex are perturbed and prevent the essential C1 move to produce a product complex due to steric

clashes with the peptide substrate (see section 1.2.2). The study indicated that the isoprenoid substrate specificity of FTase is not mediated by misalignment of the pyrophosphate group but by the inhibition of ternary complex formation (Figure 1-5 D) or by failure of the ternary complex to convert into product (Figure 1-5 B).
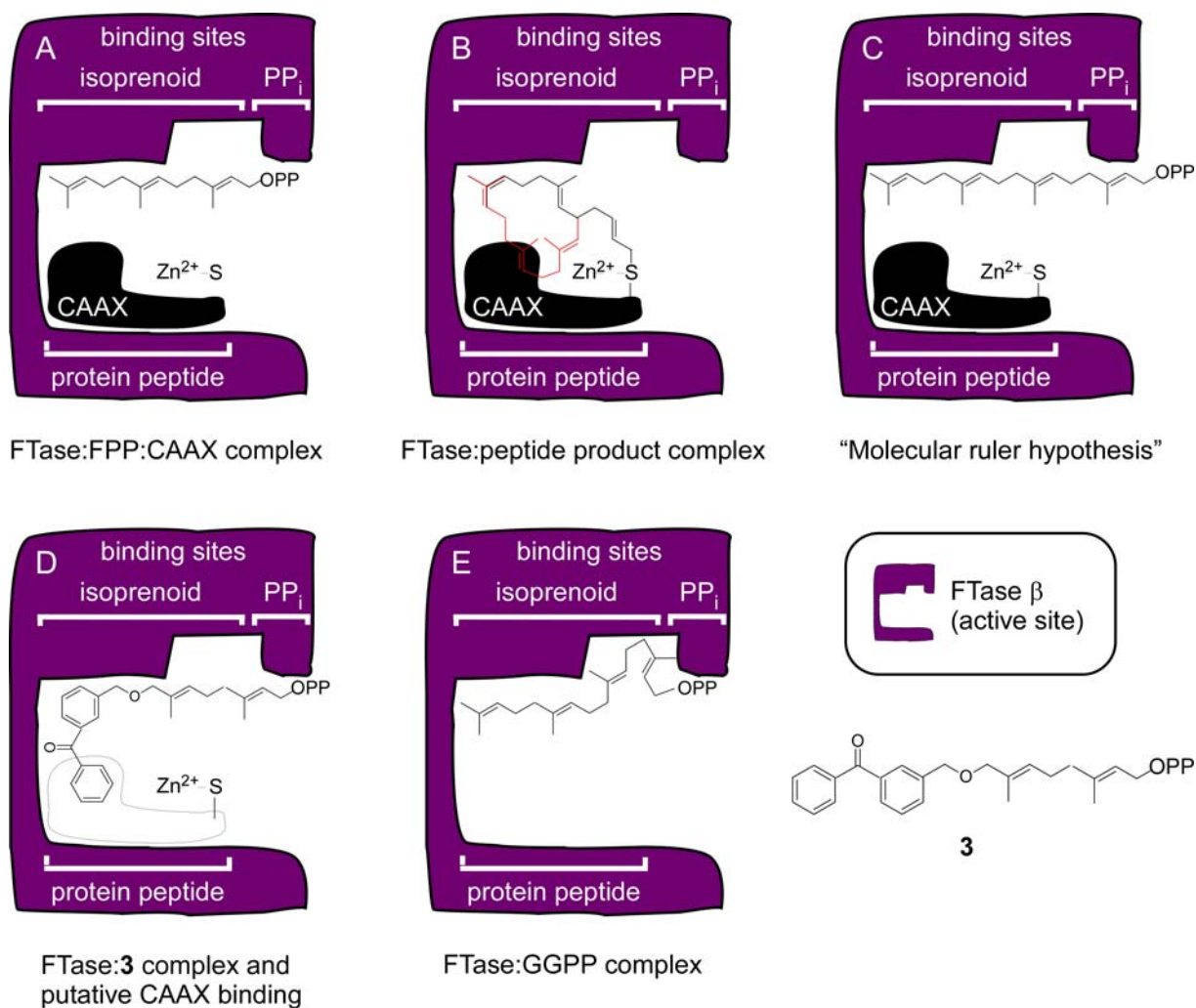
Figure 1-5 Schematic juxtaposition of the "molecular ruler hypothesis" and the "second site exclusion model" to explain the lipid substrate discrimination of FTase between FPP, GGPP, and other isoprenoid analogs. The β subunit of FTase (purple) contains the active site with the binding sites of the pyrophosphate, isoprene lipid, and the peptide substrate. The CAAX protein/peptide is shown in black and comprises the nucleophilic Zn^{2+}-coordinated thiol(ate). **A** Schematic representation of FTase lipid and peptide substrate binding based on the x-ray structure of FTase:FPP. **B** X-Ray structure of farnesylated peptide product (black) bound to FTase. Superimposed in red is the lipid conformation prior to product formation, which clashes with peptide binding. **C** "Molecular ruler model" proposed by Long et al.[34]. **D** X-ray structure of **3** bound to FTase. Superimposed is a putatively bound CAAX peptide, which leads to steric problems and prevents the formation of the ternary complex[38]. **E** X-ray structure of GGPP bound to FTase. Adapted from[38].

Peptide binding and substrate specificity. Bound next to the lipid substrate in the active site, the CA_1A_2X peptide forms direct van der Waals interactions with the second and third isoprene units of the lipid[39, 40]. Beese and co-workers have extensively investigated the CAAX requirements for FTase and GGTase-I. A_1 is solvent-exposed, therefore, any amino acid is tolerated at this position[20, 41, 42]. A_2 is buried in the "A_2 binding pocket" and forms a hydrophobic interaction with the pocket (Figure 1-6). The selection of amino acids at the A_2 position is constrained (A_2 can be Ile, Val, Leu, Phe, Tyr, Pro, Thr, or Met), yet it has little effect on CAAX specificity. X binds to the "specificity pocket" at the bottom of the peptide substrate binding site and represents the primary determinant of peptide substrate selectivity. The FTase specificity pocket is more polar and accepts Met (hydrophobic AA), Ser (small AA), and Glu (polar AA)- and to a lesser extent Ala, Thr, and Cys (small AA)- through a specific network of electrostatic interactions. Interestingly, Phe is too bulky for the specificity pocket, but is still tolerated by binding in an adjacent hydrophobic cavity[42].
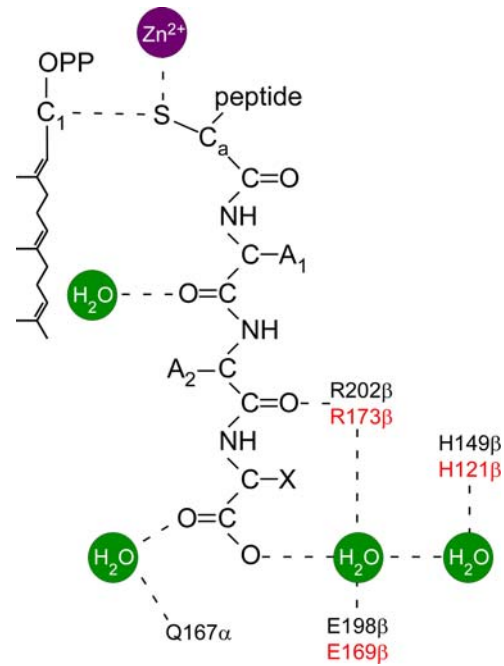
Figure 1-6 CAAX binding in active site. Black: FTase, red: GGTase-I.

In GGTase-I, the crystal structure revealed only one X-binding site that discriminates against polar, charged, and small amino acids. X is occupied by hydrophobic amino acids such as Leu or Phe and occasionally by Ile or Val.

The studies by Beese and co-workers suggest that the CAAX peptide is anchored to FTase/GGTase-I through the coordination of the cysteine thiol by Zn^{2+} and through water-mediated hydrogen bondings of the C-terminal carboxyl group. As a result, the enzymes are capable of discriminating against peptides that are too long or too short, or that lack a cysteine residue.

RabGGTase does not recognize its substrates via direct interaction, but needs REP to recruit its substrates[43, 44]. In line with this, Rab proteins (in most cases) do not carry a peptide recognition sequence such as the CAAX motif found in FTase and GGTase-I substrates. Usually, they are doubly prenylated at -CC, -CXC, -CCX, -CCXX, or -CCXXX upon formation of the quarternary complex that is composed of Rab, REP, RabGGTase, and GGPP. Some RabGTPases, however, have only one prenylatable C-terminal cysteine in a CXXX sequence. While most of them do not fulfill the classical CAAX motif requirements, Rab8 contains a CVLL motif, which was shown to serve as a substrate for GGTase-I *in vitro*. Nevertheless, the role of Rab8 geranylgeranylation by GGTase-I *in vivo* seems to play only a minor role[45].

1.2.2 Mechanism of the protein prenylation reaction

Due to the importance of prenylated proteins in many signaling pathways, the mechanisms of the prenylation reactions of the three protein prenyltransferases have been intensively investigated. FTase and GGTase-I display similar reaction mechanisms, whereas that of RabGGTase is fundamentally different.

Based on structural and metal substitution studies[29, 46], mutational analyses[35, 47], stereochemical[48, 49], kinetic isoptope effects[50, 51], and kinetic examinations[39, 52], as well as studies with non-natural substrates[53], an ordered substrate binding reaction pathway featuring a mainly associative mechanism with an "exploded" transition state has been proposed (Scheme 1-1)[54-56].
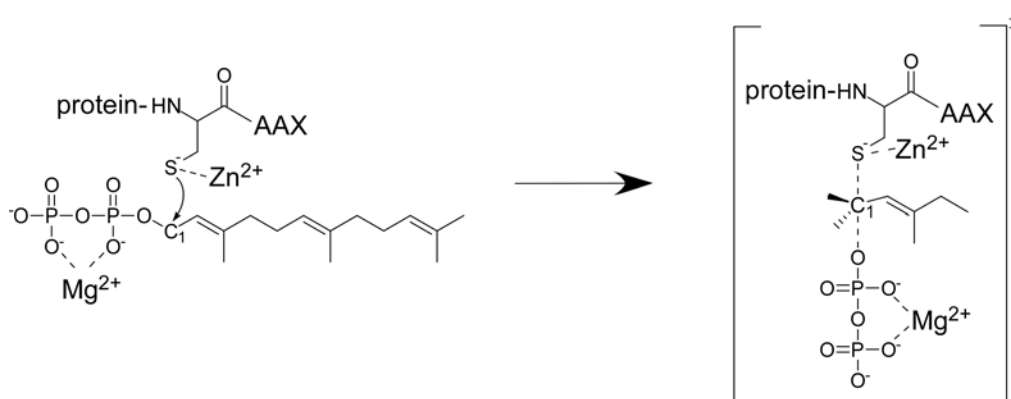
Scheme 1-1 Transition state model of the farnesylation reaction catalyzed by FTase. Adapted from[50].

According to this model, FPP first binds to the *apo* form of FTase in the hydrophobic funnel of the active site, followed by CAAX peptide association. The coordination of the reactive thiol by Zn^{2+} is essential for catalysis since it lowers the pKa of the thiol and thereby activates it for the nucleophilic attack[28-30, 57, 58].

Comparison of the structures of the CAAX protein prenyltransferases in complex with isoprenoids and CAAX peptides to the structures of the enzymes bound to the prenylated CAAX peptide products revealed that the conformation and the peptide backbone is practically identical prior to and after the chemical step. It is believed that the lipid substrate rotates at the third isoprene unit to move the C1 atom closer to the activated CAAX thiolate (Figure 1-5 B)[59]. In GGTase-I, the rotation takes place at the fourth isoprene unit in GGPP[20].

Under release of pyrophosphate, the reaction of the CAAX peptide with FPP and GGPP irreversibly forms a stable thioether bond. The negative charges of the diphosphate leaving group are stabilized by L164α (both in FTase and GGTase-I) and Y300β or Y272β in FTase or GGTase-I, respectively.

Interestingly, only FTase is dependent on Mg^{2+} for efficient catalysis[31, 60]. The Mg^{2+}-coordinating property of D352β in FTase is replaced by a Lys residue in GGTase-I (L311β),

which stabilizes the developing negative charge of the diphosphate group of GGPP and thereby renders GGTase-I independent of Mg^{2+}[47, 61].

Kinetic studies suggest that the rate-limiting step of the prenylation reaction is product release. This occurs upon competitive binding of lipid substrate to the enzyme by expelling the attached lipid chain of the prenylated product to an "exit groove" on the β subunit[20, 59]. Initially, it was believed that this is mainly stimulated through isoprenoid binding, but recently, Spielmann and colleagues postulate a more complex reaction mechanism which includes a CAAX peptide-stimulated product release[62].

The prenylation reaction catalyzed by RabGGTase is substantially different from the CAAX prenyltransferases since it (i) requires the additional protein REP to recruit its substrates and (ii) in most cases performs double geranylgeranylation. How the assembly of the ternary complex necessary for catalysis takes place is still debated[63-67]. In the "classical pathway", the unprenylated Rab interacts with REP first, which is then followed by RabGGTase binding. The observation that the affinity of REP for RabGGTase is increased upon binding of either Rab or GGPP led to the proposal of an alternative pathway: REP binds to GGPP-bound RabGGTase first, followed by the association of the RabGTPase[26, 68].

The mechanism of RabGGTase-mediated prenylation was studied using biochemical and structural methods[27, 36, 69, 70]. The crystal structure of the Rab:REP complex revealed two binding interfaces between (i) the Rab binding platform (RBP) of REP and the effector loops of Rab and (ii) the C-terminal binding region (CBR) of REP and the CBR interacting motif (CIM) of Rab[64, 69]. The binding between RabGGTase and REP is largely mediated through the interaction of two critical residues of REP-1 (F279 and R290) with the α-subunit of RabGGTase[27]. The CIM is a conserved motif among all RabGTPases and consists of two hydrophobic residues near the C-terminus of Rab proteins[36].

A structure of the ternary complex has not been solved to date, but modeling and biophysical studies indicate that the flexible C-terminus of Rab weakly associates with RabGGTase upon formation of the ternary complex. In doing so, it presents the cysteine residue to the reactive center with Zn^{2+}. The lipid binding site, which is formed by five helices, is located in domain II of REP-1. Upon prenyl transfer and the binding of a new isoprenoid, the conjugated isoprenes move from the hydrophobic funnel in the active site of the enzyme to the lipid binding site in domain II of REP-1. This results in the expansion of the cavity and in conformational changes of F279 and R290 of REP-1, leading to a decreased affinity of RabGGTase towards the prenylated Rab:REP complex and finally to product release from the enzyme.

1.3 Protein substrates of the protein prenyltransferases

Since the initial discovery of farnesylated fungal proteins, a broad variety of protein prenyltransferase substrates have been identified. The best studied ones belong to the Ras superfamily comprising the small GTPases Ras[71-73], Rho and Cdc42[74-79], Rac[80], Rap[81, 82], and Rab[83, 84], but also include the γ subunits of heterotrimeric G proteins[85-88], centromeric proteins[89], proteins involved in the regulation of cell cycle and apoptosis[90, 91], cellular framework[92-94], glycogen metabolism[95], as well as visual signal transduction[96-98].

1.3.1 The small GTPases of the Ras superfamily

The largest group of prenylated proteins belongs to the Ras superfamily of small GTPases. These display molecular weights ranging from 20 to 30 kDa[99, 100] and are also called G proteins due to their ability to bind guanine nucleotides. The Ras superfamily comprises more than 150 members and is divided into 5 subgroups based on homology studies of their amino acid sequence: Ras, Ran, Rho/Rac/Cdc42, Rab, and Arf/Sar1. All these proteins function as key regulators in a variety of important cellular processes: the Ras family regulates gene expression and proliferation, the Ran family nucleocytoplasmic transport and microtubule organization, the Rho/Rac/Cdc42 family the organization of the cytoskeleton as well as gene expression, and the Rab and the Arf/Sar family vesicular transport. Except for the Arfs, which are N-terminally myristoylated, and the Rans, which are not posttranslationally lipidated at all, all members of the Ras superfamily are posttranslationally prenylated at one or two cysteines within their C-terminal region.

Like all G proteins, the small GTPases from the Ras superfamily contain a conserved GTPase domain and specifically bind one molecule of guanine nucleotide. They function as molecular switches and cycle between a GDP-bound "off" and a GTP-bound "on" state (Figure 1-7)[101]. In the GDP-bound state, they are in an inactive conformation. Upon GTP binding, they are transformed into an active conformation, which allows them to interact with effector proteins and to initiate downstream signaling events.

The GTPase cycle of the Ras superfamily is highly regulated by accessory proteins. Most of the small GTPases exist in the cytosol in the inactive GDP-bound form due to their intrinsic GTPase activity. GDP release is the rate-determining step in the GTPase cycle with a half-life in the range of hours. Additional factors are needed to speed up this process in a regulated, i.e. signal-dependent manner. The release of GDP is catalyzed by guanine nucleotide exchange factors (GEFs)[102]. GTP readily binds to the nucleotide-free GTPase due to a 10-fold excess of GTP in comparison to GDP in the cell (1 mM compared to 100 µM). Remarkably, the additional phosphate group switches the GTPase from the inactive to the active state by causing conformational changes of the so-called switch I and switch II

10

regions[103]. These regions are part of the effector-binding domain that engage downstream signaling only upon GTP binding.

Without external regulation, the active GTP-bound state is defined by the intrinsic GTPase activity of the protein, which hydrolyzes GTP to GDP under release of an inorganic phosphate. Since the intrinsic GTPase hydrolysis rate is low (e.g. 0.028 min^{-1} for Ras[104]) additional proteins are needed to efficiently inactivate the GTPases and thus to prevent permanent activation of the proteins, which could lead to misregulation. The intrinsic GTPase activity is dramatically enhanced by up to 5 orders of magnitudes by GTPase activating proteins (GAPs)[105, 106].
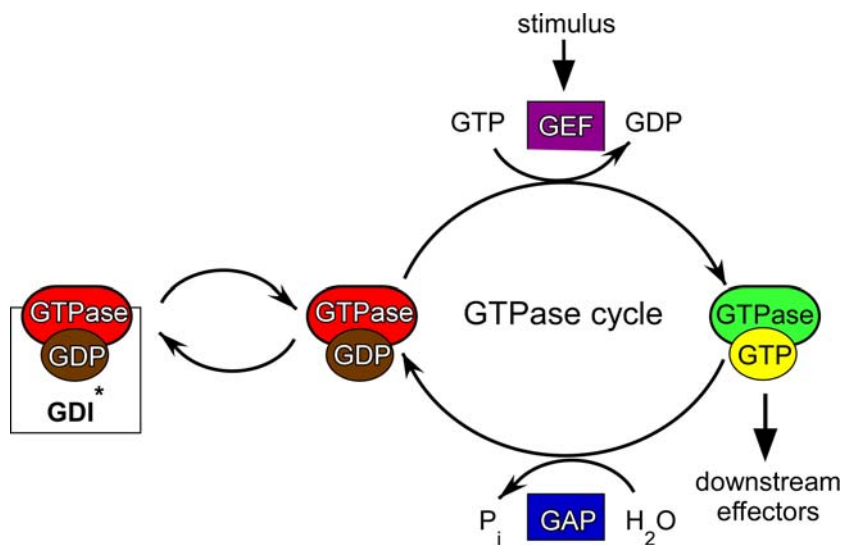
Figure 1-7 Schematic representation of the GTPase cycle. Upon an external stimuli, the GTPase switches from an inactive GDP-bound to an active GTP-bound state, which is tighly controlled by its GEFs. Once activated, it can recruit its effectors and enables downstream signaling processes. Inactivation is achieved through GTP hydrolysis, which is catalyzed by GAPs. *For Rab- and RhoGTPases, an additional level of regulation through GDIs is present, which keep the prenylated GDP-bound protein in the cytosol. GEF: guanine nucleotide exchange factor; GAP: GTPase activating protein; GDI: GDP dissociation inhibitor.

For Rabs and Rhos, GDP dissociation inhibitors (GDIs) bind to the GDP-bound GTPases and inhibit GDP release, preventing the GTPases from activation, and thus acting as an additional control mechanism to keep the proteins in the inactive state[79, 107]. More significantly, the GDP form of the proteins can be extracted from membranes by GDIs.

1.3.2 Ras and Rho/Rac/Cdc42 families: post-prenylation processing, localization, and signaling

The GTPases from the Ras superfamily share common structural, biochemical, and regulatory features, but still are involved in a variety of different signaling and trafficking pathways.

Ras family. The interest in small GTPases and in particular Ras stems from the discovery that Ras genes encoded by *ra*t *s*arcoma viruses (v-H-ras, v-N-Ras, and v-K-Ras) are heavily associated with cancer (see section 1.3.4)[108-112]. Since then, Ras has been intensively investigated and has become the prototype of a small monomeric GTPase with (both structural and functional) characteristics which can be generally applied to the rest of the members of the Ras superfamily. There are four types of Ras proteins, N-, H-, K-Ras4A, and K-Ras4B (the two latter are splice variants of the *kras* gene), which are ubiquitously expressed in eukaryotic cells. These Ras isoforms are structurally surprisingly very similar and differ virtually only in the hypervariable C-terminal region, also called the target domain. Upstream of the CAAX motif, N-, H-, and K-Ras4A possess additional cysteine(s) (C181; C181 and C184; and C180, respectively) that can undergo posttranslational palmitoylation[113]. In contrast, a polybasic domain with 11 lysines, forming a net charge of +9 and lacking a palmitoylation site, can be found at the C-terminus of K-Ras4B[114].
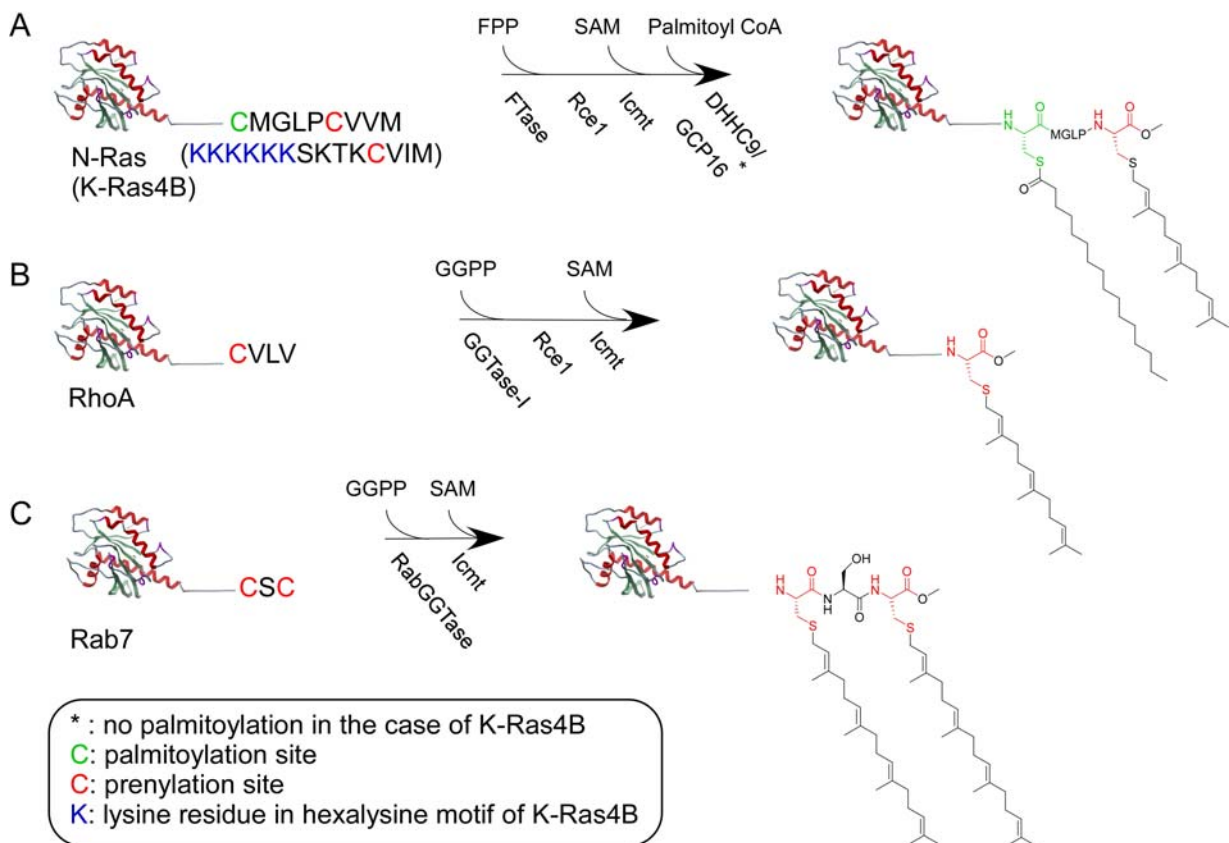
Scheme 1-2 Schematic representation of the posttranslational processing of N-Ras or K-Ras4B, RhoA, and Rab7. **A** N-Ras is farnesylated on one cysteine (red) by FTase, which is followed by -AAX removal by Rce1, carboxy-methylation by Icmt, and palmitoylation on one cysteine by DHHC9/GCP16 (green). K-Ras4B is similarly posttranslationally processed, but does not contain any palmitoylation site. Instead, it contains a hexalysine repeat in the target domain (blue). **B** RhoA is geranylgeranylated by GGTase-I on one cysteine (red), -AAX cleaved, and carboxymethylated. **C** Rab7 undergoes double geranylgeranylation on two cysteines (red), followed by carboxymethylation. Rab proteins with two cysteines as the terminal residues are not carboxymethylated.

Ras proteins are synthesized as soluble proteins on free polysomes in the cytosol and are subsequently targeted to cellular membranes by several PTMs (Scheme 1-2)[115]. After farnesylation on the C-terminal cysteine by FTase, the S-isoprenyl CAAX moiety becomes a substrate of Ras converting enzyme 1 (Rce1)[115-117], which is a protease located in the ER membrane that cleaves off the -AAX group adjacent to the prenylated cysteine. Subsequently, a second ER membrane protein, Isoprenylcysteine carboxymethyltransferase (Icmt), methylates the carboxyl group[118]. The transfer of Ras proteins from the endogenous membrane to the inner leaflet of the plasma membrane requires a second signal found in the above mentioned target domain. For N-, H-, and K-Ras4A, palmitoylation, which is catalyzed by DHHC9/ GCP16, occurs on the cysteine(s) found in this C-terminal hypervariable region at the Golgi. This significantly increases the affinity for membranes and precedes the translocation of N- and H-Ras via vesicular transport mechanisms to the plasma membrane[119, 120]. In contrast, K-Ras4B does not contain additional cysteine lipidation sites. Instead, the polybasic sequence is thought to ensure complete plasma membrane localization via electrostatic interactions (Scheme 1-2).

Initially, it was believed that the inner cytoplasmic side of the plasma membrane is the predominant location of Ras action in a variety of signal transduction pathways. The best characterized one is the MAPK pathway (Figure 1-8). An external stimulus activates this pathway by the binding of growth factors at the extracellular domain of protein tyrosine kinase receptors (PTKRs)[121]. This leads to receptor dimerization, which is followed by autophosphorylation by the intrinsic kinase activity *in trans* within the cytoplasmic regions of the receptor. These phosphorylated tyrosine residues represent docking sites for adaptor proteins such as Grb2 (Growth factor receptor-bound protein 2), which recruits Sos (Son of sevenless) through its SH3 (Src homology domain 3) domain. Sos is a Ras GEF which, once recruited to a location near the membrane-anchored Ras protein, switches Ras to the active GTP-bound conformation. Following activation, Ras recruits one of its effectors, the serine/threonine kinase Raf-1. Raf-1 becomes activated by the association with membranes and in turn activates MEK (MAPK/Erk kinase, a dual specificity tyrosine/threonine kinase) by phosphorylation. MEK then phosphorylates and activates the serine/threonine kinases Erk1 and Erk2. Phosphorylated Erks form dimers and are translocalized into the nucleus. There, they phosphorylate the Ets family of transcription factors such as Elk-1 to activate transcription. Although the MAPK pathway is the best characterized one, it is only one of many that are regulated by Ras.

The MAPK pathway has for a long time served as a model for the prototypical unidirectional pathway that relays a signal from the extracellular space to the nucleus. Later, it became obvious that the situation is not so simple. First, the MAPK pathway cannot be regarded as an isolated pathway, but is rather embedded in a complex network of cellular processes with

many crosstalks between the GTPases of the Ras superfamily[122, 123]. Second, Ras has emerged as an important model system of compartmentalized signaling, which can be found both between different and within one membrane compartment[124, 125]. For example, the PTMs of Ras proteins are not static, but have been shown to be highly dynamic: the activation of N- and H-Ras at the plasma membrane triggers depalmitoylation and back-trafficking to the Golgi, where a set of effectors is recruited. Repalmitoylation redirects the proteins to the plasma membrane (the so-called "Ras acylation cycle")[126, 127]. K-Ras4B is dynamically regulated by either the binding of calmodulin[128-130] or protein kinase C, which phosphorylates the GTPase on S181[131].
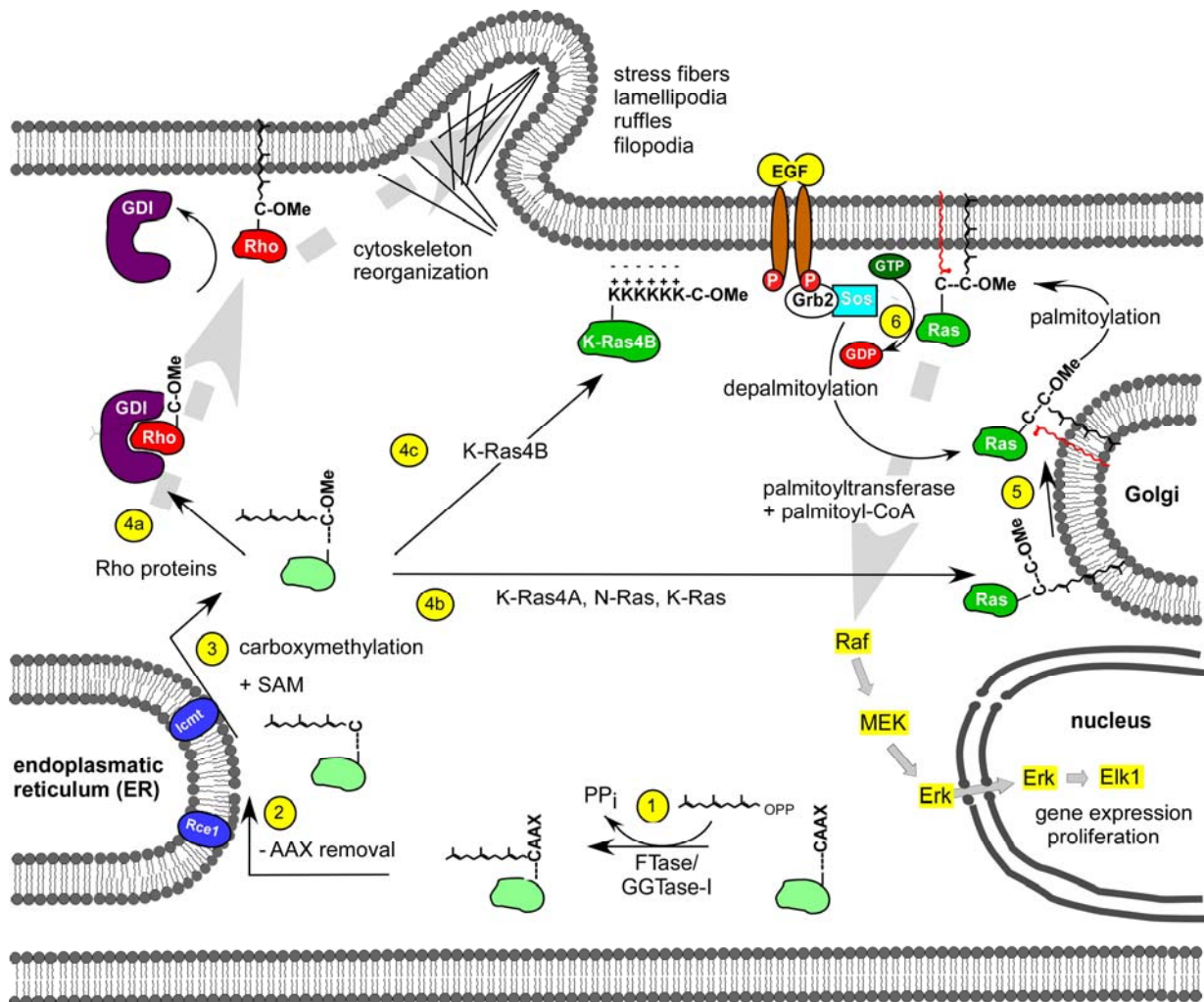
Figure 1-8 Overview of CAAX prenyltransferase-mediated protein prenylation, post-prenylation modifications, membrane targeting, and the function of the prenylated proteins. **A** Ras or Rho protein (light green) is prenylated by FTase or GGTase-I with FPP or GGPP, respectively **1**. -AAX removal by Rce1 **2** and carboxymethylation by lcmt **3** take place at the ER. In the case of Rho proteins (red), the protein is chaperoned by a Rho-specific GDI, which targets the Rho protein to the correct membrane **4a**. K-Ras4A, N-Ras, and K-Ras are targeted to the Golgi **4b**, where they are further palmitoylated on one or two cysteines **5**. Once palmitoylation, the mature protein trafficks to the plasma membrane. There, it recruits its GEF, which activates the protein **6** and engages downstream signaling, including the MAPK signaling pathway. Through depalmitoylation-repalmitoylation, it is subjected to a dynamic acylation cycle. K-Ras4B is targeted to the plasma membrane without additional palmitoylation through its hexalysine motif within its targeting domain **4c**. Membrane attachment is dynamically regulated by protein kinase C and/or calmodulin. For details, see text.

In addition to compartmentalization to different organelles, compartmentalization also takes place within an organelle. The best studied case is the plasma membrane, which can no longer be regarded as a homogenous platform of cell signaling. Instead, it consists of microdomains, which concentrate proteins and lipids to facilitate processes such as signal transduction events.

The most prominent, albeit still debated, concept of membrane microdomains are the lipid rafts[132]. These domains are rich in cholesterol and sphingolipids and are believed to contain liquid-ordered phases, partitioning into patches within the disordered glycerophospholipids of the membrane. The various mature Ras isoforms are thought to insert into lipid rafts with different distributions, depending on their PTM and the activation state of the GTPase.

Thus, both organelle-specific signaling and the heterogeinity of the plasma membrane play a role in the complexity of signaling outputs[124, 125].

Rho/Rac/Cdc42 family. Like Ras, *R*as *ho*mologous (Rho) proteins also play important roles within signaling networks that are extracellularly stimulated and lead to cell cycle progression, gene expression, and, most prominently, to actin reorganization (Figure 1-8)[133, 134].

The actin cytoskeleton is composed of actin filaments and many specialized actin binding proteins. It is essential in many cellular functions such as cell shape change, cell motility, cell adhesion, and cytokinesis[135, 136]. In most cases, filamentous actin is organized into a number of distinct structures, whose formation is regulated by the GTPases of the Rho family through the control of their GEFs and GAPs.

In particular, Rho proteins regulate the formation of actin stress fibers, which are bundles of actin filaments that span the cell and are linked to the extracellular matrix through focal adhesions. Rac proteins regulate the formation of (i) lamellipodia, which are thin protrusive actin sheets found on the edges of many migrating cells, and (ii) membrane ruffles, observed as lamellipodia at the leading edge of the cell that lift up and fold backwards. Cdc42 is a regulator of the formation of filopodia, which are finger-like protrusions with long actin filaments in the direction of the protrusion and are often found in motile cells.

Until now, 20 members of this Rho/Rac/Cdc42 subfamily have been identified, with RhoA, Rac1, and Cdc42 being the best characterized. RhoGTPases undergo post-prenylation processing as described for the RasGTPases. However, they do not contain polybasic patches or palmitoylation sites within their C-terminal hypervariable domain to target them to the plasma membrane. Instead, they are regulated by guanine nucleotide dissociation inhibitors (GDIs), which act as chaperones to mask the prenyl group, block spontaneous activation by maintaining them in the inactive GDP-bound form[137], and promote their membrane delivery.

1.3.3 The vesicular transport controlled by RabGTPases
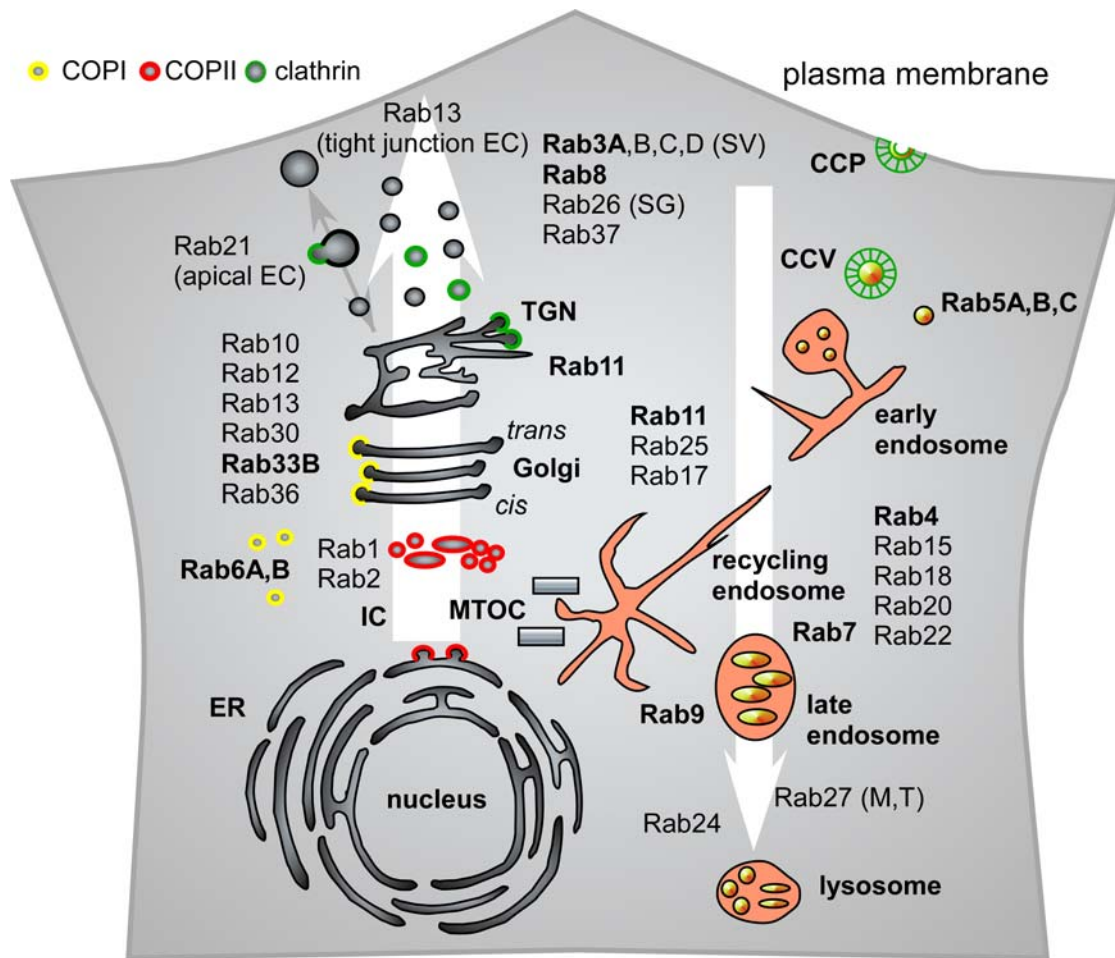
Figure 1-9 Overview of intracellular localization of specific Rab proteins in mammalian cells, which correlates to their compartment-related function in vesicular transport. The key Rab proteins regulating the main hubs of endocytosis, biosynthetic pathways, and secretion are shown in bold. Some proteins are cell-specific (e.g. Rab3A in neurons) or tissue-specific (e.g. Rab17 in epithelia) or show cell-type-specific localization (e.g. Rab13 in tight junctions). The large white arrows represent exocytosis and endocytosis. **Endocytosis** Cargo is packed in clathrin-coated vesicles (CCVs) and trafficked to the early endosome, mediated by Rab5, and subsequently to recycling endosomes or late endosomes. The back-transport to the plasma membrane (directly or via recycling endosomes) is regulated by Rab4. Cargo trafficking from the recycling endosomes to the plasma membrane is mediated by Rab11. Rab7 regulates the transport from early to late endosomes as well as to the lysosome, while receptor recycling from late endosomes to the TGN is mediated by Rab9. **Exocytosis** COPII-coated vesicles are transported from the ER to the Golgi apparatus, which is facilitated by Rab1 and in part by Rab33B. Rab6 controls the retrograde Golgi-ER as well as the intra-Golgi transport of COPI-coated vesicles. Subsequently, the vesicles are passaged through the Golgi to the TGN, which serves as the major distribution center along the biosynthetic pathway to different destinations. Rab3A mediates the secretion of transmitters from synaptic vesicles in neurons. Rab8 is involved in the TGN-plasma membrane transport. Abbreviations: CCV, clathrin-coated vesicle; CCP, clathrin-coated pit; EC, epithelial cells; IC, ER–Golgi intermediate compartment; M, melanosomes; MTOC, microtubule-organizing centre; SG, secretory granules; SV, synaptic vesicles; T, T-cell granules; TGN, *trans*-Golgi nextwork. Adapted from[138].

Intracellular vesicular transport. One of the characteristic features of eukaryotic cells are intracellular organelles, which are separated from the rest of the cell by membranes. They can be regarded as autonomous units that have to sustain their specific structural, functional, and biochemical properties such as pH, redox potential, viscosity, or membrane composition. Continuous flow of biomaterial takes place in a highly regulated fashion between these organelles.

The study of membrane traffic was hallmarked by discoveries of Palade[139], Schekman[140], and Rothman[141] and colleagues. Using electron microscopy audiography, genetic manipulation of yeast, and *in vitro* reconstitution, respectively, these pioneering studies established the hypothesis that the transfer of cargo molecules between organelles is mediated by shuttling transport vesicles, both in endocytotic (which serves for the uptake of nutrients and signaling molecules as well as for the internalization of receptors) and exocytotic pathways (secretory export of proteins and lipids).

Exocytosis is initiated by the translocation of newly synthesized proteins into the ER. After correct protein folding, the proteins exit the ER and are transported through the Golgi apparatus, which is accompanied by maturation and often by PTMs of the cargo. Subsequently, the mature proteins are trafficked to their final destination at the lysosome, the plasma membrane, or the extracellular space.

Conversely, in endocytosis, newly internalized material is transported to the early endosome, which functions as a central sorting station. Then, the cargo is "sorted", either to early and recycling endosomes for the recycling of the material to the plasma membrane (e.g. membrane receptors), or to late endosomes and the lysosome for degradation.

Vesicular trafficking processes can be divided into four essential steps: (i) vesicle formation and budding at the donor membrane, (ii) transport, (iii) tethering, and (iv) fusion with the acceptor membrane, all of which have to be tightly regulated to ensure the correct transport processes[142-144].

Rab proteins have been implicated in the control of each of these steps (Figure 1-9)[138, 145, 146]. Upon synthesis and posttranslational prenylation of the RabGTPase by RabGGTase in concert with REP, the enzyme dissociates from the ternary complex, and REP delivers the prenylated Rab to the membrane. The membrane represents the site where the RabGTPase is subjected to the GTPase cycle, switches from the inactive to the active state, and functions as a regulator of vesicular trafficking (Figure 1-10).
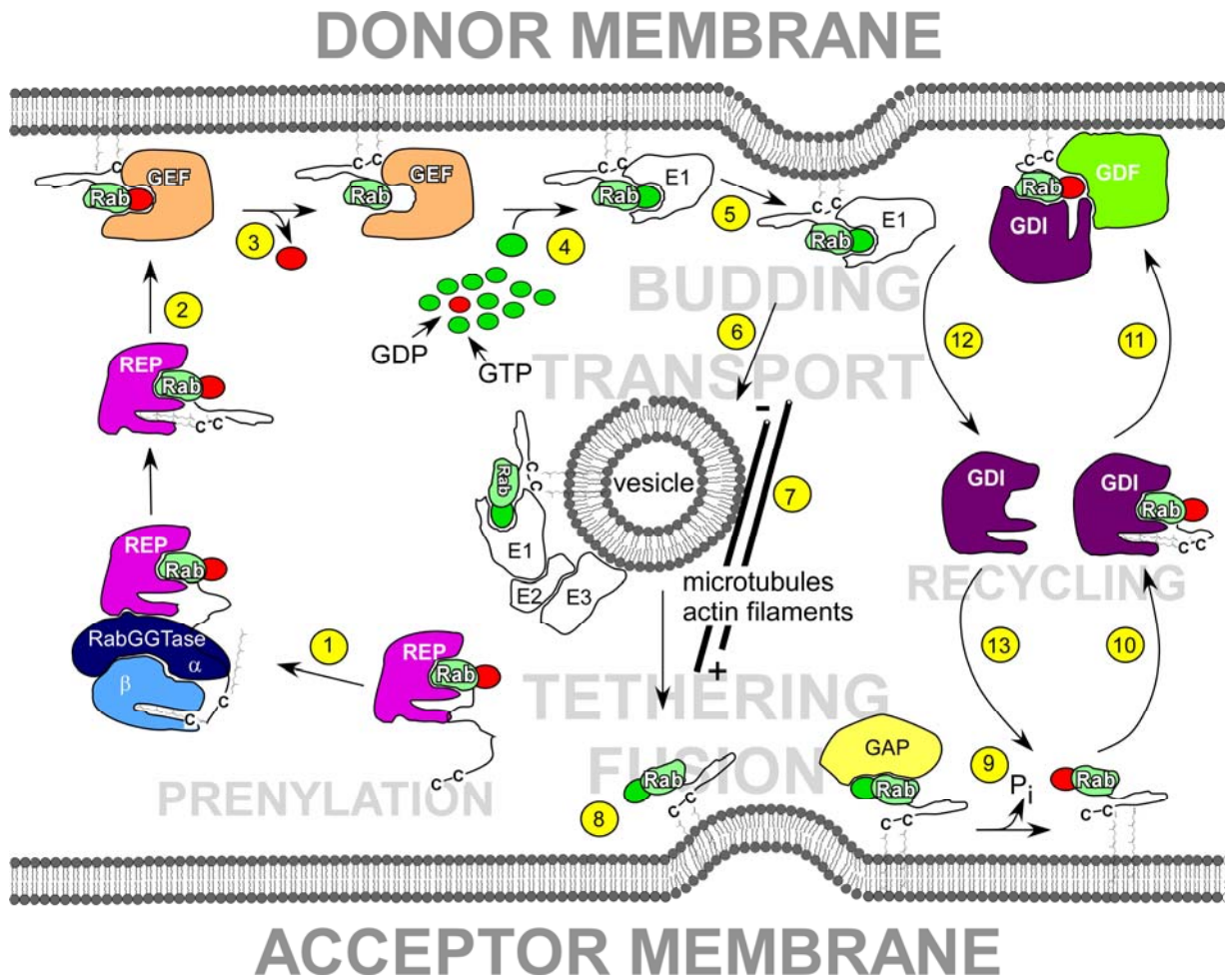
Figure 1-10 Schematic representation of the Rab-mediated vesicular transport. After (usually) double prenylation **1**, the GDP-bound proteins are delivered to the membrane by REP **2**. Following membrane insertion, GEF binding releases the bound nucleotide **3**. Due to a 10-fold excess of GTP over GDP, GTP binds to Rab **4**. The active GTPase initiates specific vesicle-mediated transport processes (budding **6**, transport **7**, tethering, and fusion **8**) through the recruitment and binding of specific effector proteins **5**. The active GTP-bound Rab is turned off by the action of GAPs **9**, and the GDP-bound Rab is recycled back to the acceptor membrane by Rab-specific GDIs and GDF(s) **10**, **11**. GDI is relased and can undergo another Rab extraction cycle **12**, **13**. For details, see text.

Budding. The first step of a typical vesicle trafficking event is budding, which can be considered as a process of simultaneous cargo selection and vesicle formation. Budding is mediated by protein coats, which are highly dynamic supramolecular assemblies that cycle on and off membranes (Figure 1-11)[147-149]. There are three main classes of coated vesicles: (i) clathrin-coated vesicles (CCV), (ii) vesicles covered with either the coat protein complex-I (COPI) or (iii) the coat protein complex-II (COPII).
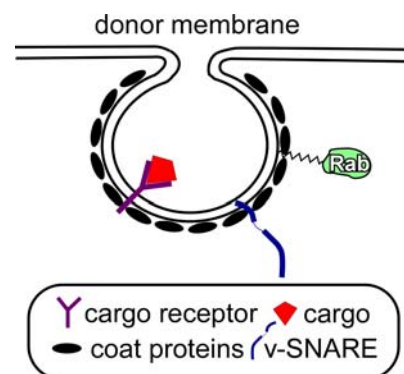
Figure 1-11 Vesicle budding.

CCVs are mainly derived from the plasma membrane or the trans-Golgi network (TGN) and are transported to endosomes[150], whereas COPI and COPII mediate the vesicular trafficking in the early secretory pathway. COPI predominantly regulates the vesicle transport from the

Golgi to the ER as well as within the Golgi cisternae, while COPII mediates the traffic from the ER to the Golgi (Figure 1-9)[151, 152].

Coat assembly and disassembly is believed to be regulated by Arf and Sar1 for COPI/CCVs and COPII, respectively[153]. The small GTPases are in turn tightly controlled by their specific GAPs and GEFs. The majority of cargo material is actively concentrated in the coated buds and vesicles prior to export to the acceptor membrane. Coat proteins recognize sorting signals found in the cytosolic domains of transmembrane cargo proteins.

In addition, the GTPases of the Rab family have been associated with cargo selection[154, 155] and vesicle formation[156, 157] as well. In particular, TIP47, an effector of Rab9, has been shown to be intimately involved in the formation of vesicles containing mannose 6-phosphate receptors (MPRs) that are recycled from late endosomes to the Golgi. Activated Rab9 increases both the association of TIP47 with late endosomes and its affinity for MPRs.

Once the cargo is concentrated at the site of vesicle budding, the flat membrane patches are deformed into round buds. After vesicle fission, which is mediated by Arf/Sar1 (COPI and COPII) or dynamin (CCV), the coated vesicles are released.

Transport. After budding, the vesicles are transported through the cytoplasm toward their final destination at the acceptor membrane. This is often mediated by active trafficking processes using either actin-dependent motors (slow, short-range/local transport using myosins) or microtubule-dependent motors (high-speed, long-range transport using kinesins or dyneins; Figure 1-12). During the
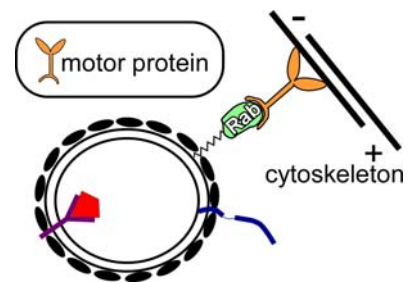
Figure 1-12 Vesicle transport.

last decade, the emerging role of Rab proteins in vesicle transport through the recruitment and the control of motor proteins has been demonstrated in multiple studies[158-163] (summarized in[164-167]). One interesting example for Rab-dependent recruitment of microtubule-based dynein/dynactin as well as myosin motors is the involvement of Rab7 and Rab27 in melanosome trafficking. Melanosomes are lysosome-related organelles which synthesize, store, and transport melanin and undergo rapid microtubule-dependent transport towards the melanocyte periphery. Subsequently, they are captured to actin filaments and slow actin-dependent retention at the cell periphery before they are transferred to neighbouring keratinocytes[168]. Rab7 has been shown to regulate microtubule-dependent melanosome transport through the recruitment of its effectors Rab-7 interacting lysosomal protein (RILP) and oxysterol-binding protein-related protein 1 L (ORP1L)[169, 170]. After transport to the cell periphery, the melanosomes are attached to the peripheral actin through the myosin motor Va[171]. The myosin Va, on the other hand, is recruited by active Rab27 through

its effector melanophilin/Slac2a[172]. Thus in this process, the melanosome is shifted from microtubule- to actin-based transport.

Tethering. Once the vesicle reaches the target membrane, a specific group of proteins, so-called tethering factors, functions in the initial recognition between the incoming vesicle and the target membrane and brings them in close proximity (Figure 1-13).

Figure 1-13 Vesicle tethering.

The membrane tethers identified so far can be grouped into two classes: long coiled-coil single protein-based tethers and large multi-subunit complexes[173, 174]. Characteristic for coiled-coil tethers are long stretches of heptad repeats with every seventh residue showing propensity to form an α-helix. These long, extended rod-like molecules (usually) form dimers and have been observed between vesicles and Golgi membranes and between Golgi cisternae[175]. Until now, 12 members of this class of tethers have been characterized, with p115, Uso1p, GM130, and Giantin being the best studied ones[174].

The second class of tethers are formed by the multi-subunit complexes, which include COG (8 subunits), Dsl1 (3 subunits), GARP (4 subunits), TRAPP I (7 subunits), TRAPP II (19 subunits), and the Exocyst (8 subunits).

The GTPases of the Rab family have been implicated in the regulation of tethering factors on the vesicle due to their compartment-specific localization along with their ability to specifically interact with their effectors. The tethers can function as both Rab effectors and Rab exchange factors. For example, active Rab1 promotes the binding of p115, a Rab effector, to membranes[176] (yeast homologs: Ypt1p binding to Uso1p[177]), whereas the HOPS complex acts as an effector of a RabGTPase (Ypt7p) and as its GEF at the same time[178, 179].

Fusion. The actual fusion event between an incoming vesicle and the acceptor membrane is mainly mediated by SNAREs (*soluble N*-ethylmaleimide-sensitive factor *attachment* protein *re*ceptors, Figure 1-14)[180, 181]. They have a simple domain structure with a characteristic SNARE motif, a region of 60-70 amino acids arranged in heptad repeats, which has been evolutionarily conserved and can undergo coiled-coil formation[182]. Most SNAREs are transmembrane proteins, with their functional N-terminal domains facing the cytosol and the C-terminus anchored in the membrane. Even though the mechanism of the SNARE-promoted fusion event is not fully understood, the prevailing "SNARE hypothesis" assumes that each vesicle carries a specific "v-SNARE" that pairs with a corresponding "t-SNARE" on the target membrane[183]. This *trans*-SNARE complex forms a very stable four-helix bundle, with one α-helix being contributed by the monomeric v-SNARE and the other three by the oligomeric t-SNARE[182, 184]. Careful analysis of *trans*-SNARE complex formation revealed that the
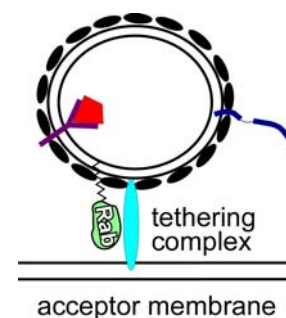
elongated coiled coils of four interwined parallel α-helices contain 16 stacked layers of interacting side chains, which are hydrophobic except for the central ´0´ layer that contains three highly conserved glutamine (Q) residues on the t-SNAREs and one arginine (R) residue on the v-SNARE[185]. As a consequence, an alternative nomenclature classifies them as Qa-, Qb-, Qc-, and R-SNAREs (Figure 1-14)[184].

According to the "zippering hypothesis", the SNARE motifs "zip" from the N-terminal ends towards their C-terminal membrane anchors, which clamps the membranes together. The *trans*-complexes transform from a loose state (in which the N-terminal parts of the SNARE motifs are "zipped up") into a tight state. Thereby, mechanical force is excerted on the membranes, which initiates the opening of a fusion pore and leads to vesicle fusion[186].

During the fusion event, the *trans*-complex relaxes into a *cis*-complex. The ATPase NSF (*N*-ethylmaleimide-*s*ensitive *f*actor), along with SNAPs (*s*oluble *N*SF *a*ssociation *p*rotein), functions as a cofactor to disassemble the *trans*-complex and thus recycles the SNAREs for other rounds of catalyses (Figure 1-14)[187, 188].

The GTPases of the Rab family have been implicated to participate in driving the fusion process. Acting in "Rab microdomains", they are believed to concentrate SNAREs, accessory proteins, and key lipids and to recruit their effectors at the fusion site[189], partly due to their specific intracellular compartmentalization[190], as shown earlier for the GTPases from the Ras and Rho family.
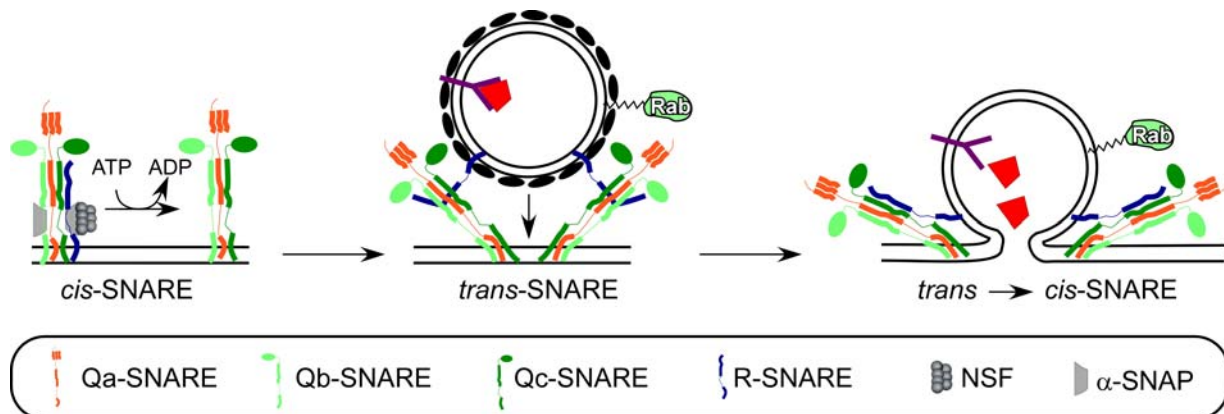
Figure 1-14 SNARE-mediated vesicle fusion. For details, see text.

Once the active GTP-bound Rab reaches the acceptor membrane, its function in the regulation of the four steps of vesicle trafficking is fulfilled. GAPs subsequently catalyze GTP hydrolysis and switch the GTPase to the inactive state. The Rab protein is then recycled back to the donor membrane for another round of catalysis. This process is mediated through GDP dissociation inhibitors (GDIs)[107, 191-193]. GDIs are structurally related to REP and extract the lipidated Rab from the acceptor membrane. The reinsertion of the prenylated protein into the donor membrane is thought to be mediated by GDI displacement factors (GDFs), which release the Rab protein from the Rab:GDI complex (Figure 1-10)[194].

1.3.4 Protein Prenyltransferases as therapeutic targets

As described in the previous sections the GTPases of the Ras superfamily are key players in many signaling and trafficking pathways. Consequently, it is not surprising that expression defects, mutations, or misregulation of the GTPases themselves, their effectors, their regulators, or their posttranslationally modifying enzymes affect this highly sophisticated network, which can lead to abnormalities in human beings.

Ras proteins have been heavily linked to tumor formation in cancer due to their regulatory function in the control of cell proliferation[195]. 20 % of all human cancers harbor mutant ras genes, but the isoforms involved and the incidence of mutations differ for various cancers. Point mutations in Ras can be most frequently found in KRAS (~ 85 %), followed by NRAS (~ 15 %) and HRAS (< 1%). One type of mutation in the Ras genes renders Ras oncogenic and makes it insensitive to the action of GAPs. Thereby, Ras is locked in the GTP-bound, active state and constantly activates downstream signaling, including the described MAPK pathway[109, 196]. Another class of mutation leads to proteins with abnormally high GDP dissociation rates, again leading to increased population of the GTP state even in the absence of an input signal.

Rho proteins have been implicated to be associated with vascular diseases due to their role in the reorganization of the actin cytoskeleton and other important cellular processes[197].

RabGTPases and their regulatory molecules and effectors have also been demonstrated to be altered in human diseases[198]. Loss of function mutations in the Rab genes, for example in the Rab27A gene, leads to Griscelli syndrome type 2. This autosomal recessive disorder is characterized by immune impairment, increased susceptibility to infections, and partial albinism as a result from defects in Rab27-mediated melanosome trafficking[199]. Genetic defects in Rab regulatory molecules are associated with retinal degeneration in choroideremia (point mutation(s) in REP, leading to an accumulation of unprenylated Rab27 incapable of regulating melanosome trafficking[200]), X-linked mental retardation (genetic defects in GDI[201]), and kidney disease in tuberous sclerosis (mutations in the tuberous sclerosis (TCS1) protein, which functions as a Rab GAP[202]).

Central to the action of the small GTPases of the Ras superfamily as regulators in the described signaling and vesicular trafficking pathways is their organelle-specific compartmentalization, which is in turn mediated by their PTM status. Interest in the therapeutic targeting of their PTM-mediating enzymes stems from the seminal observation that membrane detachment of Ras through inhibition of FTase can reverse the transformed phenotypes of cancer cells. Consequently, a variety of small-molecule inhibitors of FTase (FTIs), competing with the CAAX peptide, the lipid substrate, or both, have been developed (Figure 1-15)[203, 204]. Among these, three compounds, tipifarnib, lonafarnib, and BMS214662,

are currently being evaluated in anticancer clinical trials. Although FTIs have been shown to be effective in the treatment of hematologic malignancies[205, 206], their effects on solid tumors are limited[207, 208].
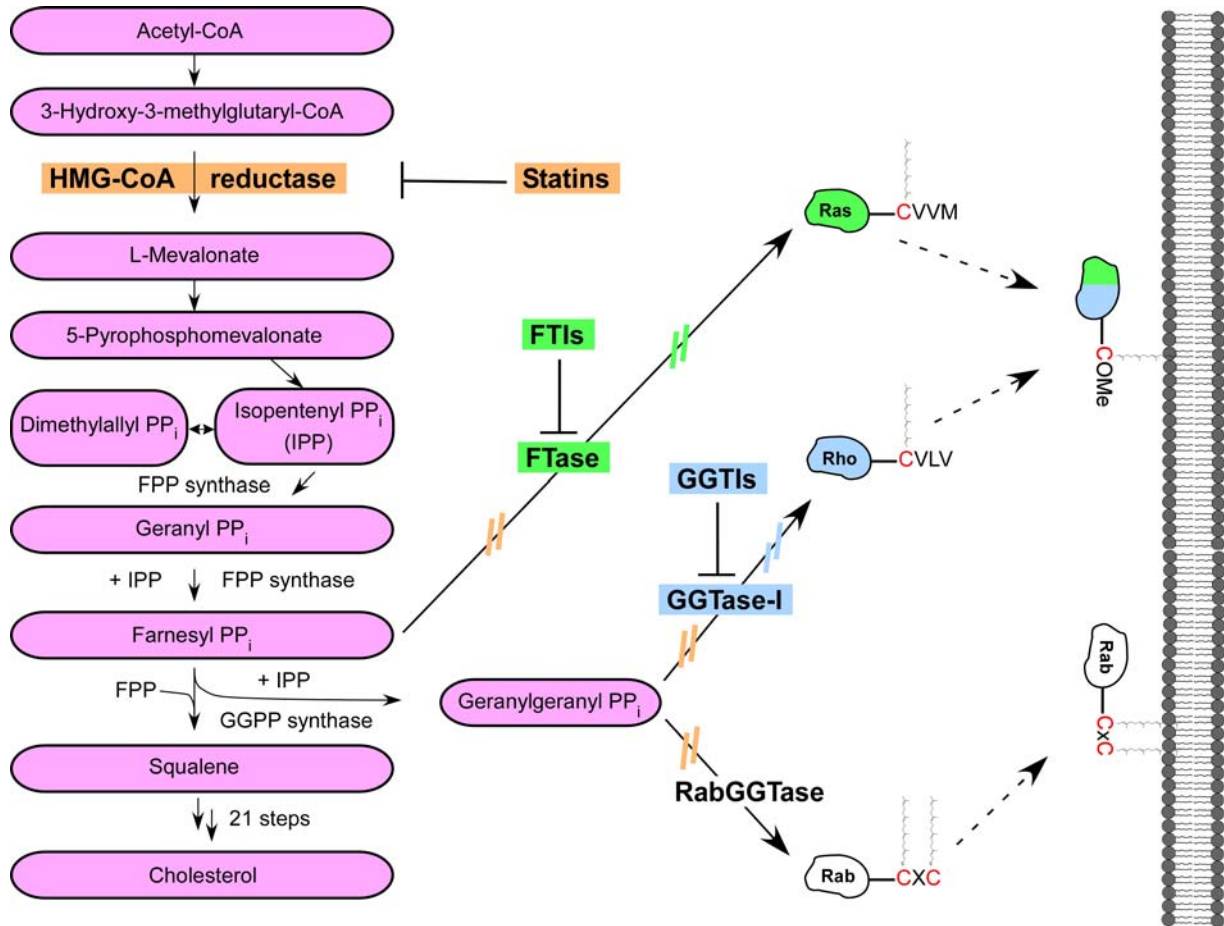
Figure 1-15 The cholesterol synthesis pathway and protein prenylation. Protein prenylation can be specifically inhibited by FTIs (green) and GGTIs (blue), which target the prenylation enzymes. Without isoprene modification, the protein substrates of FTase and GGTase are incapable of associating to membranes and thus cannot excert their role in signaling pathways. Alternatively, prenylation can be modulated by statins that inhibit the conversion of HMG-CoA to L-mevalonate through competitive inhibition of the rate-limiting enzyme HMG-CoA reductase. As prenyltransferase-unspecific drugs, their action leads to a decrease in the downstream biosynthesis of cholesterol and other intermediate metabolites including FPP and GGPP (orange). Consequently, the prenylation machinery of all three enzymes is shut down due to a lack of lipid substrates. Adapted from[209].

Surprisingly, the efficacy of FTIs in preclinical testing was not strictly associated with the presence or absence of activating mutations of Ras[210], probably because they do not inhibit the function of K-Ras4B (which is the Ras isoform most involved in human solid tumors), K-Ras4A, and N-Ras. The main reason for this is believed to be the alternative prenylation (cross-prenylation) of K- and N-Ras by GGTase-I in FTI-treated cells. This led to the recognition of GGTase-I as an additional therapeutic target in cancer and to the development of GGTase-I inhibitors (GGTIs). These attempts were supported by the observation that several geranylgeranylated CAAX proteins, including RalA and RhoC, are critical for oncogenesis downstream of Ras[211-216]. GGTIs have been shown to be able to impair tumor

growth *in vivo* and, in contrast to FTIs, cause inhibition of Rho signaling, cell cycle arrest at G0 and G1, and apoptosis[217].

Recently, the GTPases of the Rab family have been shown to be involved in cancer as well. RNA microarray analyses revealed that about half of the Rab genes are overexpressed in ovarian cancer. In prostate and transitional cell bladder cancer, upregulation of Rab25 was found[218]. Rab5A and Rab7 were demonstrated to be overexpressed in thyroid adenomas, wheras overexpression of Rab1B, Rab4B, Rab10, Rab22A, Rab24, and Rab25 has been well documented in hepatocellular carcinomas and cholangiohepatomas[219].

However, the effects of FTIs and GGTIs on the prenylation across the entire proteome have not been studied due to a lack of appropriate analytical methods. Despite the fact that some of these compounds are in clinical trials, the identity of the targets that mediate the therapeutic effects of those inhibitors is still debated; for example, compounds BMS1-4, initially developed by Bristol-Myers Squibb pharmaceuticals as specific FTase inhibitors, have reached clinics without a complete analysis of potential cross-inhibition of GGTase-I and/or RabGGTase. Ross-MacDonald and co-workers demonstrated that these compounds induced apoptosis by inhibiting RabGGTase and not FTase[220]. Yet the true *in vivo* potency towards both enzymes or other potential causes for the clinical outcome are not fully understood.

The second group of compounds that modulate prenylation are the cholesterol-lowering drugs known as statins (Figure 1-15). Statins are first-line therapeutics for the prevention of coronary heart disease and atherosclerosis[221]. They prevent the formation of FPP, which serves as a precursor for GGPP and cholesterol synthesis, by inhibiting the synthesis of mevalonate. Initially, the clinical use of statins was limited to the treatment of high cholesterol levels for cardiovascular indications. However, statins are currently being evaluated in the therapy of cancer as well as neurodegenerative and autoimmune diseases[209, 222, 223]. The therapeutic effects of statins in these disorders are believed to be due to their ability to suppress protein prenylation, but of which targets and to what extent is largely unknown, similar to the effects of FTIs and GGTIs described before.

1.4 Tools to investigate protein prenylation

Since the discovery that prenylated proteins act as key regulators in many signaling and trafficking processes protein prenylation has been thoroughly investigated. Yet many questions regarding the *in vivo* function of the three protein prenyltransferases remain unanswered, including the size and composition of the eukaryotic prenylome (the prenylated proteome), potential cell type-specific variations in the abundance and type of prenylation, cross-specificities among the enzymes, rates and order of prenylation, or the true therapeutic effects and toxicities of protein prenyltransferase inhibitors and statins. To address these questions, efforts have been made to develop methods to investigate protein prenylation.

There are several strategies to approach this task (Figure 1-16). First, one can utilize the changes in the physical or biochemical properties of the protein substrate upon the addition of the lipid group (Figure 1-16 B). Second, one can tag the peptide or protein substrate with reporter groups (C) or third, derivatize the isoprenoid with fluorophores or affinity tags (D).
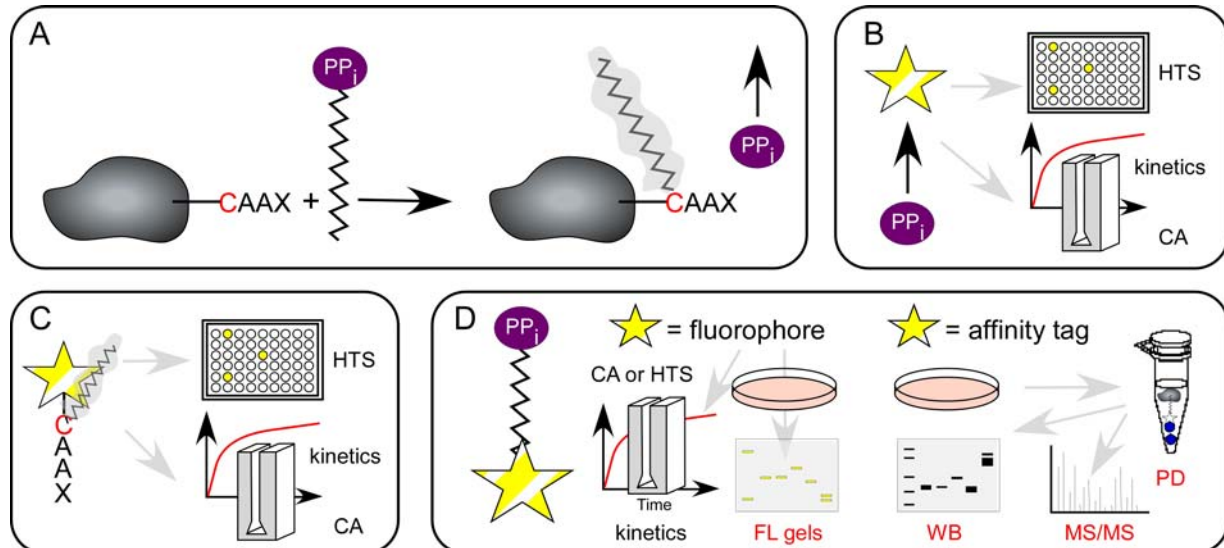
Figure 1-16 Schematic representation of the prenylation reaction and possibilities of its investigation. **A** Upon transfer of a prenyl group, the hydrophobicity of the protein/peptide is increased, and one molecule of pyrophosphate is released. **B** Pyrophosphate release can be measured to investigate the kinetics of the reaction (CA or HTS) *in vitro*[224]. **C** The increase in hydrophobicity can be sensed by a dansyl fluorophore coupled to a peptide substrate (CA or HTS) *in vitro*[225]. **D** For *in vitro*, in lysate, or *in vivo* applications, the isoprenoid moiety can be functionalized with either a fluorophore[226, 227] or, ideally, an affinity tag for subsequent Western blot or MS/MS analysis. Potential applications in lysate and/or *in vivo* are marked in red. HTS: high throughput screen; CA: cuvette assay; FL: fluorescence; WB: Western blot; MS: mass spectrometry; PD: pulldown.

Fierke and colleagues developed a coupled assay that reports on the prenylation reaction by monitoring the dissociation of the diphosphate upon attachment of a farnesyl group[224]. In an alternative approach, Pompliano and later Poulter and co-workers developed a prenylation assay which exploits the change in fluorescence of a dansylated peptide substrate due to a presumed increased hydrophobicity of the environment of the dansyl fluorophore upon prenylation[225, 228]. Despite wide successes of these approaches, particularly of the latter method, these technologies are prone to artefacts and, importantly, are limited to *in vitro* investigations.

Synthetic analogs of isoprenoid pyrophosphates have proven to be well suited as probes to investigate the features of protein prenyltransferase-mediated lipidation reactions. These include mechanistic probes to study the stereochemistry, the transition state, or kinetic isoptope effects; photoaffinity-labeled or other biophysical probes to investigate binding modes of the lipid and protein substrates; or stereospecific isomers to probe the lipid substrate tolerance of the enzymes[229].

One of the primary advantages of incorporating the reporter group within the lipid substrate is the direct read-out of the prenylated protein, even in complex mixtures such as cellular lysates or living cells.

Soon after the discovery of protein prenylation, radioactive labeling of the lipid substrates either via metabolic conversion of tritiated mevalonate into isoprenoids or by direct addition of radioactive isoprenoids as pyrophosphates or alcohols to cells or cell lysates was developed[230-232]. Using an excess of synthetic isoprenoids these analogs successfully competed with endogenous pools of isoprenoids. Alternatively, they were added *in vivo* using available pharmacological and biochemical tools that allow efficient manipulation of the pool of intracellular phosphoisoprenoids and prenylation protein substrates[233]. The prenylated products were detected by radio-audiography of samples separated by SDS-PAGE or affinity precipitates. In spite of high detection sensitivity, these procedures, however, are very laborious and poorly scalable.

To overcome these problems, efforts in incorporating chemical reporters into the isoprene chain have been undertaken. As in all cases of altering enzyme substrates, it is common experience that not every modification in the lipid substrate is tolerated. In the last two decades, many studies examined the effect of modifications within the farnesyl chain of FPP on FTase binding and/or catalysis.
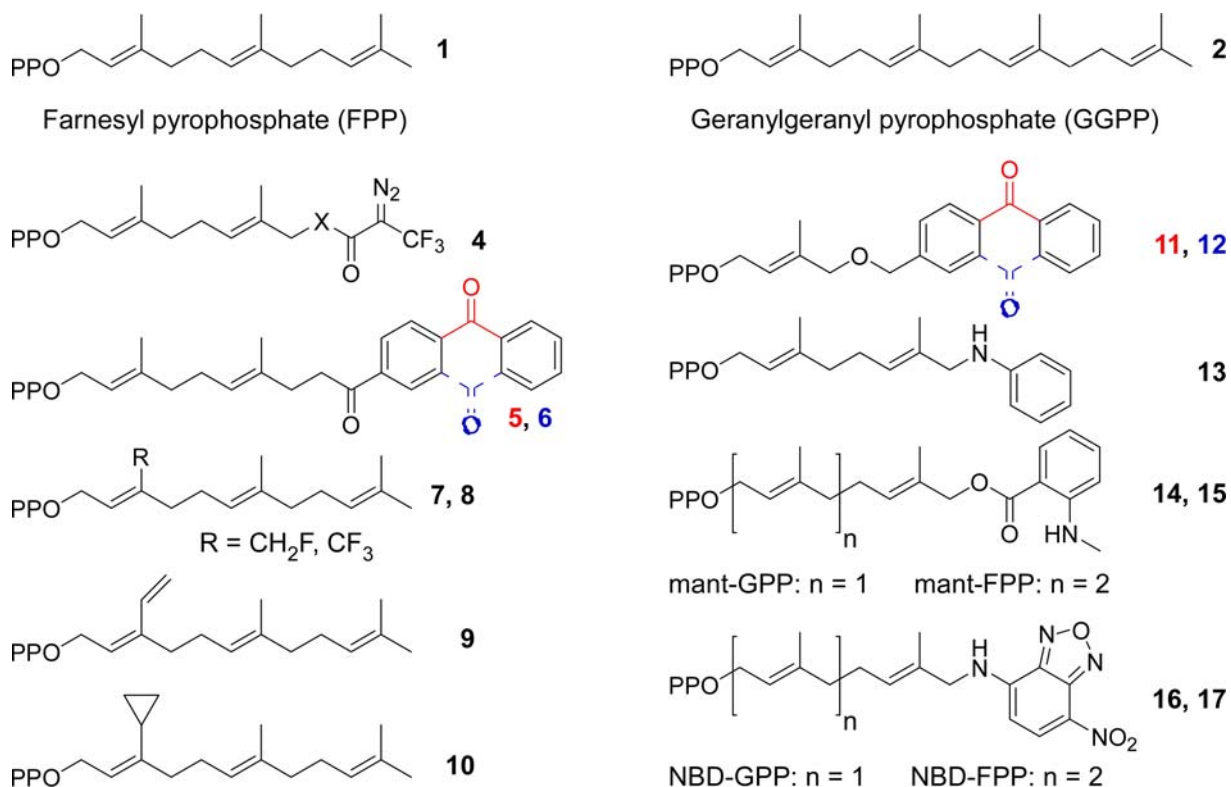

Figure 1-17 Synthetic analogs of FPP and GGPP. Red and blue indicate different constitutional isomers. For further details, see text.

The work of Das and Allen has paved the way for the design of functionalized farnesyl analogs[234]. The photo-affinity group diazotrifluoropropionyl (DATFP) was incorporated into the terminal isoprene moiety for cross-linking applications. They showed that the photoactive reagent was a good mimic of FPP for FTase binding, which gave insight into the tolerance for substitutions in the FPP analogs (**4**, Figure 1-17). The study revealed that the terminal isoprene unit was amenable to alterations, indicating the importance of size rather than hydrophobicity of the lipid substrate for successful competition with FPP. This analog, however, was shown not to be transferred by FTase onto peptide substrates.

Distefano and co-workers pursued a similar approach and designed a photo-affinity-tagged analog based on benzophenone as a photoactive core. This analog exhibited better chemical, thermal, and photochemical stability as well as a better tolerated wavelength for activation (**5, 6**, Figure 1-17)[235]. In contrast to the DATFP-based probe, the resulting analog was similar in polarity to FPP, but somewhat larger and also not a FTase substrate either.

The first studies on structural alterations in the lipid chain that were still tolerated by FTase for successful transfer were reported by Poulter, Gibbs and co-workers[53, 236]. These studies revealed that the incorporation of fluorines, a vinylic, or a cyclopropyl moiety (**7/8**, **9**, and **10**, respectively) at the C3 position resulted in alternate substrates for FTase, albeit often with lower transfer efficiency.

While these studies demonstrated that FTase displays flexibility in recognizing its lipid substrates, modification at the C3 position is not optimal when designing probes that contain reporter groups. The terminal position, in contrast, is much more suitable for derivatization. However, not every modification made here is tolerated by FTase, as shown for the cross-linking probes **5** and **6**. One of the reasons was anticipated to be the overall length of the isoprenoid analog. Therefore, Distefano and co-workers sought to design benzophenone-based probes with shorter spacers (**11**, **12**)[237-240]. These were accepted as lipid substrates in FTase-mediated catalysis and allowed two interesting conclusions to be drawn: firstly, the overall length should mimic the native substrate as closely as possible and secondly, the terminal isoprene substitution should not be too bulky.

Spielmann and co-workers developed isoprenoid analogs with alterations at the terminal isoprene unit, but kept the geranyl core structure (**13**)[241]. The C8 position was substituted with an aniline group, resulting in an analog that was an excellent substrate for FTase.

The first isoprenoid analog that contained a reporter group, enabling a direct readout of the prenylated product, was reported by Waldmann and co-workers[226]. A geranyl or a farnesyl chain was augmented with a *N*-methylanthraniloyl (mant) moiety at the C8 position (**14**, **15**). These analogs were used for the preparation of fluorescently prenylated Rab7 using RabGGTase. In further work, they developed 3,7,11-trimethyl-12-(7-*nitro*-benzo[1,2,5]oxa-diazo-4-ylamino (NBD)-tagged FPP and GGPP mimics (**16**, **17**), which have turned out to be

functional substrates of FTase, GGTase-I, and RabGGTase[227, 242]. Their application in cell lysate or *in vivo*, however, has been limited due to a generally low abundance of protein prenyltransferase substrates in mammalian lysate in combination with a moderate sensitivity of the developed methodology.

1.5 Strategies for site-specific protein labeling

The elucidation of the distribution, dynamics, and functions of proteins *in vivo* is essential for the understanding of their cellular functions. The site-specific labeling of proteins addresses these questions by introducing reporter groups that can be employed to monitor their physical or biochemical properties. One of the major challenges in this field is to develop a method that, ideally, is site- and chemoselective and can be applied to virtually any protein. One approach is to incorporate reporter groups into the substrates of PTM enzymes, which are posttranslationally transferred to their targets[243], as shown for prenylatable proteins in section 1.4. Since not all proteins are subjected to PTMs or substrate alterations may not be tolerated by the PTM-mediating enzyme, a more generic approach for site-specific protein derivatization is needed.

For *in vitro* applications, the reactive groups of proteins have been exploited by targeting small molecules that carry the desired functionality to the thiol(s) of solvent-exposed cysteine residues, amines of lysines or the N-terminus, as well as carboxylates of aspartate, glutamate, and the C-terminus. While these techniques are simple and display fast reaction kinetics, they do not provide any specificity, given that these groups are often found at multiple sites on the protein surface. Thus, efforts have been undertaken to develop protein labeling strategies with higher site-specificity[244, 245].

The easiest approach for targeting a small molecule to a protein sequence in a specific manner is to use a high-affinity binding interaction, where the protein tag capable of associating to the compound is fused to the protein of interest. This has been demonstrated with many examples including antibody tags fused to localization signal sequences to target various haptene-fluophores to specific cellular compartments[246]. In an alternative approach, the dihydrofolate reductase (DHFR) and the F36V mutant of FK506-binding protein 12 (FKBP12(F36V)) bind to the small molecules methotrexate and SLF´, a synthetic ligand for FKBP12[247].

One of the major concerns of the strategies mentioned is the large tag size (108-157 AAs, Table 1-2), which can significantly influence the native structure or function of the protein. In contrast to the fusion of a large protein tag, the introduction of a short peptide sequence presents a much less invasive approach. Similar to proteins, there are high-affinity interactions found between small molecules and peptides. Nolan and colleages evolved a

peptide tag of 38 amino acids, which binds to a Texas fluorophore[248]. In a different approach, Vogel and co-workers have used a hexa- or decahistidine tag that can be labeled with nickel-nitrilotriacetic acid (Ni-NTA) derivatives[249].

The most promising approach in non-covalent peptide-small molecule labeling was developed by Tsien and co-workers[250, 251]. In this system, fluorogenic biarsenical compounds (FlAsH) display intense fluorescence with varying colors upon binding to a tetracysteine peptide *in vitro* and *in vivo*[252]. Except for the FlAsH technology, whose drawbacks, however, are background labeling, residual arsenic toxicity, and long labeling times, protein-ligand dissociation followed by signal deterioration remains a concern in all non-covalent labeling strategies mentioned.
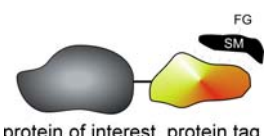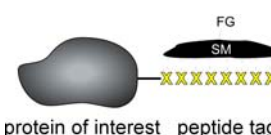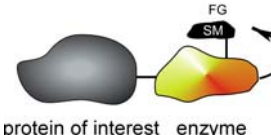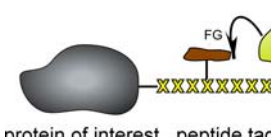
To circumvent signal loss through ligand dissociation, covalent labeling has emerged as the preferred approach for protein derivatization. The most prominent method in which the reporter group, in this case the fluorophore, is covalently attached to the target protein is to express it in fusion with the genetically encoded green fluorescent protein (GFP) or one of its variants[253, 254]. Despite enormous successes in the *in vivo* studies of protein function and localization, the utility of this strategy is limited because it is restricted to a defined (fluorescence) read-out. In line with the described non-covalent strategies, the need for chemically diverse protein labels has led to the development of covalent labeling strategies of fusion proteins with small molecules.

To guarantee specificity, researchers have exploited the specificity of enzymes for these purposes. Johnsson and co-workers fused the protein of interest with mutant forms of human O6-alkylguanine transferase (hAGT), which can be alkylated on C145 with different O6-benzylguanine suicide substrates[255-257]. In a different approach, the self-splicing proteins known as inteins were adapted to meet the needs for a selective labeling of proteins *in vitro* as well as in living cells[258-260]. The advantage of this approach is its "traceless" labeling since the intein splices itself out of the protein in an autocatalytic manner.

Again, despite many reported successful applications of hAGT- and intein-mediated labeling strategies, the protein tags are large (207 and 150 AA, respectively) and- even if temporary (intein)- prone to influence the structural or biochemical properties of the target proteins.

Instead of fusing the enzyme itself to the protein to ensure specificity, a different approach emerged that included the fusion of peptidic substrates of suitable enzymes. One class of enzyme that perfectly fulfills these needs are PTM-mediating enzymes. These enzymes show high fidelity in protein substrate recognition, bringing excellent specificity into the labeling approach. Depending on the type of PTM, these enzymes display moderately or significantly shortened recognition sequences, but are often tolerant to modifications made to the small molecule to be attached (Table 1-2).

Table 1-2 Different methods for the site-specific labeling of proteins.

	Method	Tag size[1]	Specificity	restrictions
Non-covalent tagging				
protein of interest protein tag	DHFR	157 (ProTS)	labels endogenous DHFR	protein-ligand dissociation
	FKBP12 (F36V)	108 (ProTS)	excellent	protein-ligand dissociation
protein of interest peptide tag	Tetracysteine biarsenicals	6-10 (PepTS)	background due to affinity to monothiols	reducing environment; fluorogenic; possible residual arsenic toxicity; long labeling times
	His$_6$/Ni-NTA	6 (PepTS)	unclear	fast off-rate, Ni quenches fluorescence
	Texas-red-binding peptide	23-38 (PepTS)	excellent	Texas-red only, ligand dissociation
Covalent tagging				
protein of interest GFP *et al.*	GFP et al.	238	excellent	restricted to fluorescence large tag size
protein of interest enzyme	hAGT	207 (ProTS)	labels endogenous AGT	large tag size limited scope of modification
	intein/NCL	150→1[2] (ProTS)	competition with endogenous cys	reducing environment slow rate
protein of interest peptide tag	ACP(PCP)/ PPTase	77 (ProTS)	excellent	cell surface proteins
	biotin ligase/ hydrazide	15 (PepTS)	excellent	one natural substrate in *E.coli*, cell surface proteins, 2-step labeling

[1]Tag size is given in number of amino acids; [2]Tag is temporary and cleaved-off inside the cell; PepTS: peptide target sequence; ProTS: protein target sequence; FG: functional group; X: amino acid; SM: small molecule; adapted from[245].

In one approach, the PTM-mediating enzyme phosphopantetheine transferase (PPTase) was exploited to label a 77 AA protein sequence derived from either peptide carrier protein (PCP)[261] or acyl carrier protein (ACP)[262] with 2´-phosphopantetheine-linked probes from coenzyme A (CoA). In spite of reduction of the length of the recognition sequence by a factor of two, the tag size is still large. Recently, Ting and co-workers developed a strategy in which the PTM-mediating enzyme *E.coli* biotin ligase (BirA) is capable of labeling a peptide sequence of 15 amino acids with either its natural substrate biotin or a synthetic ketone analog. In a second step, the ketone moiety was derivatized with hydrazide- or hydroxylamine-functionalized probes[263, 264] (summarized in Table 1-2).

Some considerations concerning the chemical entity to be incorporated into the small molecule have to be taken into account as well. In one approach, one can directly incorporate the reporter group (such as affinity tags, fluorophores, or any other biophysical probes). This has the advantage that the labeling is performed in one step and prevents loss in read-out signal. However, it bears the disadvantage that not all modifications may be tolerated by the enzyme, if the synthetic substrate significantly differs in size, polarity and/or chemical reactivity from the native substrate. Additionally, the synthetic efforts of preparing the functionalized probes for each application are high.

Alternatively, one can incorporate a chemical group into the small molecule that can be chemoselectively modified after being attached to the protein[243]. A potentially suitable chemical group and the reaction involved have to fulfill several criteria: (i) the functional group should be small to mimic the native substrate as closely as possible; (ii) the chemical reaction should be biocompatible, that means should be tolerated for protein or cellular functions (depending on the *in vitro* or *in vivo* application); (iii) the reaction should be orthogonal, that means the incorporated functionality should be absent in biological systems; and (iv) the reaction should tolerate water as a solvent and display sufficiently rapid kinetics.

So far, only a few chemical moieties have been reported that possess the required qualities of biocompatibility and selective reactivity (Table 1-3). Ketones and aldehydes are mild electrophiles and attractive scaffolds to be incorporated into biomolecules such as proteins[263], lipids, or glycans[265], since they can be derivatized with amine-bearing compounds. They are, however, limited to cultured cells due to a constraining pH optimum of the reaction as well as lack of "true" bioorthogonality in more complex physiological settings, since metabolites such as sugars often carry ketones and/or aldehydes.

The Diels-Alder cycloaddition is a reaction between a diene and dienophile that is known to proceed very well in water and has been used for protein labeling purposes. However, this reaction displays restricted chemoselectivity due to one of its reactants, the dienophile, which can undergo undesired side reactions with side chains of amino acids[266].

In contrast, azides have been shown to be excellent bioorthogonal chemical groups for labeling all classes of biomolecules. Azides are small, absent in animals, do not readily react either with water or with amine-bearing functionalities, and are not prone to decomposition or to reduction under physiological conditions. In recent years, azides have been incorporated in a vast array of biomolecules[243] upon the development of three distinct bioorthogonal reactions: the [3+2] cycloaddition of azides with activated alkynes (termed as the "Click reaction")[267, 268], the Staudinger ligation of azides with functionalized triarylphosphines[269, 270], and the strain-promoted cycloaddition (Table 1-3)[271]. The three types of reactions display excellent chemoselectivities, but the suitability of their application might vary on a case by case basis[272].

Table 1-3 Commonly used chemical reactions for *in vitro* and *in vivo* labeling of biomolecules.

Chemical reporter	Reactive partner	Ligation product	Target (R)
ketone/aldehyde	imine ligation oxime ligation		protein glycan
azide	Staudinger ligation "Click" chemistry Strain-promoted cycloaddition		protein glycan lipid
terminal alkyne	"Click" chemistry ´R−N₃		protein

Adapted from[243].

Similar to the azide, the phosphine employed in the Staudinger ligation is bioorthogonal as well, but can undergo oxidation by air or metabolic enzymes during the course of the ligation. However, the Staudinger ligation is a very mild reaction that is well tolerated by biological systems without showing toxicities. As a result, it has been applied to study many biological processes including tagging of recombinant proteins[273], glycan labeling on cell surfaces[274], or immobilization of small molecules and proteins on glass slides[275, 276].

The primary advantage of the copper-catalyzed click reaction over the Staudinger ligation is its faster rate (around 25 faster than the Staudinger ligation in lysates). Consequently, click chemistry is preferred when very small quantities of azide-labeled biomolecules need to be detected[277]. The big drawback, however, is the cellular toxicity of the metal catalyst, which often limits its application *in vivo*[278].

In an attempt to combine the advantages of the two approaches, an alternative azide-employing bioorthogonal reaction was developed. The strain-promoted cycloaddition exploits the ring strain of an alkyne embedded in a cyclooctyne compound for its activation without the need of accessory catalysts. This reaction has been used to label biomolecules both *in vitro* and on cell surfaces without observable toxic effects[271]. Despite slow reaction kinetics, this

reaction is considered to represent the next generation of azide-mediated protein labeling which compromises between the advantages of click chemistry and the Staudinger ligation*.

---

*In 2007, Bertozzi and co-workers reported on a strain-promoted click reaction with enhanced reaction kinetics[279].

2   AIMS OF THE PROJECT

Protein prenylation is a widespread PTM in eukaryotes which is mediated by three distinct protein prenyltransferases: FTase, GGTase-I, and RabGGTase. Among their protein substrates, the small GTPases from the Ras superfamily represent the largest group and are involved in a variety of signaling and trafficking pathways. Interest in the analysis of prenylation and its associated enzymes stems from the observation that changes in the prenylation status of the target proteins can lead to abnormalities in human beings. While the prenylation mechanisms have been thoroughly investigated, most studies were carried out *in vitro*. Therefore, many questions regarding the *in vivo* function and regulation of the three protein prenyltransferases have not been elucidated to date.

Recent advances in the field of chemical biology paved the way for the application of organic synthesis to introduce specific modifications into proteins. Such approaches are highly useful since they enable the investigation of various aspects of protein biochemistry *in vitro* and *in vivo*; this would not be possible using molecular biological techniques alone.

In particular, the combination of chemical and biochemical tools may also be valuable for the investigation of the posttranslational prenylation reactions catalyzed by FTase, GGTase-I, and RabGGTase. Generating isoprenoid analogs that contain reporter groups by classical organic synthesis could be suitable for tracking protein prenyltransferase substrates upon prenylation. These reporter groups can either be (i) fluorescence or affinity tags for a direct read-out or (ii) a chemical entity capable of further derivatization by an adequate site- and chemoselective reaction. Ideally, these functionalized analogs should be accepted as substrates by all three protein prenyltransferases.

As part of this study, different protocols were to be developed that would permit the tagging of all prenylatable protein substrates in mammalian cells with suitable reporter groups. This would allow researchers to track, isolate, and identify protein prenyltransferase substrates upon lipid attachment. In the first instance, this should be achieved by means of organic synthesis of lipid substrates modified with a suitable reporter group. If lipid analogs turned out to constitute poor substrates for wild-type protein prenyltransferases, the plan was to enhance their activity by protein engineering. If successful, the approach could address many unanswered questions: For instance, what is the size and composition of the cellular prenylome? What is the abundance of the different prenylation types and what is their tissue-specific distribution? At what rate and in which order do prenylation reactions occur *in vivo*? What are the therapeutic effects and toxicities of protein prenyltransferase inhibitors and statins?
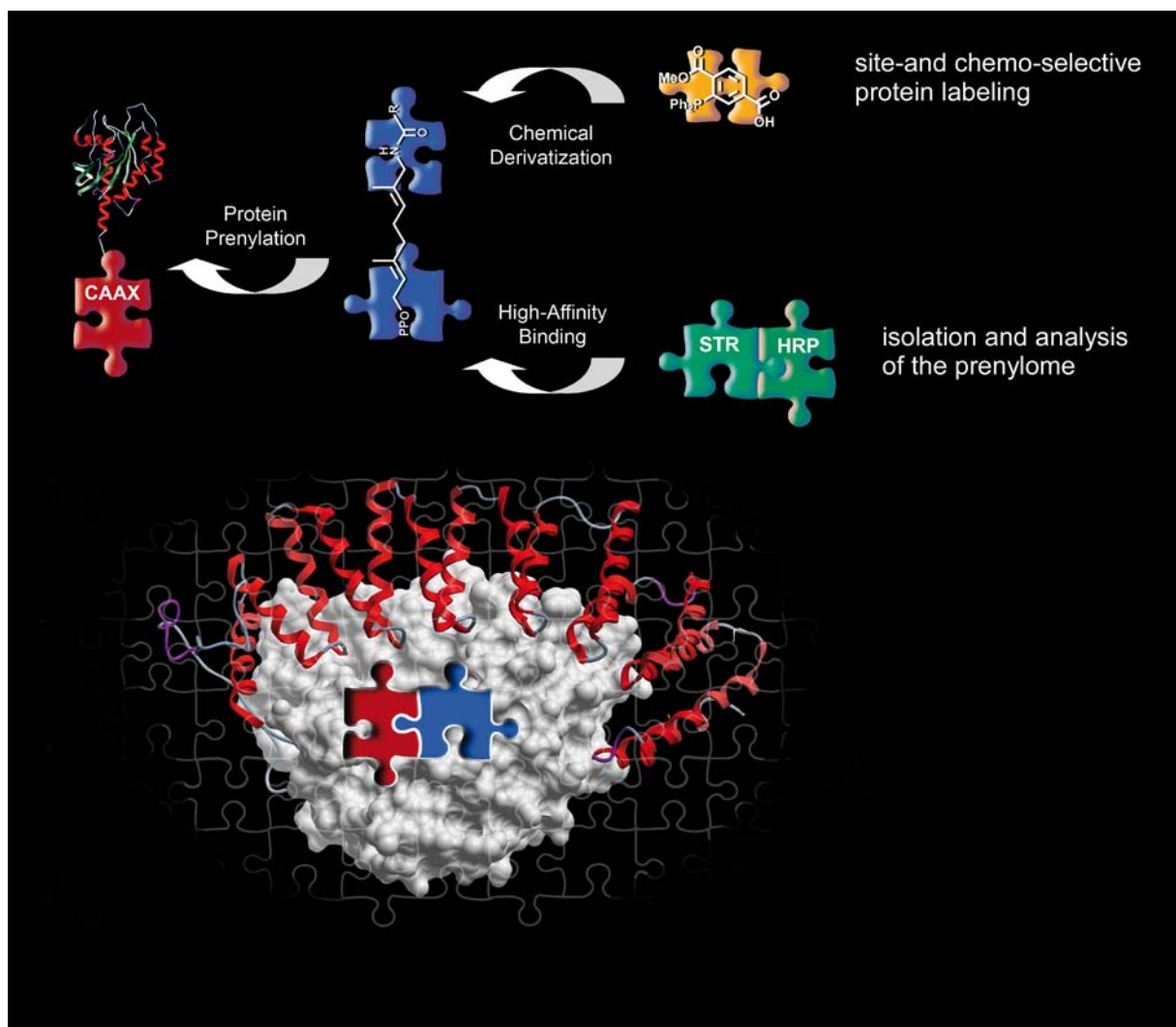
Figure 2-1 Schematic representation of the strategy for the incorporation of functional groups into the isoprene chain for (i) the investigation of the cellular prenylome or (ii) for a generic site- and chemoselective protein labeling technique. STR: streptavidin, HRP: horse-radish peroxidase.

In addition to being a useful tool to investigate protein prenylation, the strategy could also meet a long-standing demand in the field of site-specific protein labeling. A generic labeling strategy should be highly site- and chemoselective, but at the same time influence the target protein as little as possible. Enzymes that mediate PTM reactions have turned out to be suitable for these purposes because (i) they often recognize short protein or peptide sequences that can be genetically fused to the target protein and (ii) their small-molecule substrates are often amenable to modifications. PTM enzymes such as biotin ligase or phosphopantetheine transferase partly fulfill these requirements. However, they are either limited by insufficient enzyme specificity or, if higher specificity is required, a large protein tag. In contrast, the CAAX prenyltransferases FTase and GGTase-I recognize a peptide motif that is four amino acids short; this consitutes the smallest enzyme recognition sequence reported to date and can in theory be fused to the C-terminus of any protein. Additionally, it has been

established that the CAAX prenyltransferases tolerate modifications within the isoprenyl chain.

Hence, part of this work was aimed at the development of a generic protein labeling strategy that exploits the posttranslational prenylation reaction by (i) equipping the target protein with a genetically encoded CAAX sequence that is recognized by the prenyltransferase(s) and by (ii) synthesizing functionalized isoprenoid analogs that contain reporter groups.

3 RESULTS AND DISCUSSION

3.1 Exploiting the substrate tolerance of FTase for site-specific protein labeling

Central to the outlined objectives was the development of a generally applicable procedure for the site- and chemoselective derivatization of proteins carrying a short genetically encoded microtag. The posttranslational modification reactions catalyzed by FTase and GGTase-I fulfill these requirements. Their recognition sequences are four amino acids short and can be fused to the C-terminus of virtually any protein[242]. Previous studies have indicated that despite a rigid specificity for their protein substrate, variations in the lipid chain are tolerated by these enzymes (section 1.4).

This chapter describes the use of FTase for the site-specific derivatization of proteins with functionalized isoprenoids. The properties of the semi-synthetic proteins will be biochemically characterized. Finally, the advantages and disadvantages of the incorporated azide and diene groups used for subsequent chemical labeling by Staudinger ligation and Diels-Alder cycloaddition, respectively, will be discussed.

3.1.1 Strategy for the design of the genetically encodable microtag and the chemically functionalized isoprenoid analogs

FTase and GGTase-I are structurally and mechanistically similar enzymes that could both be suitable for the purposes pursued (Table 1-1). However, several lines of evidence suggest that FTase meets the different experimental needs and the general applicability of the method better than GGTase-I.

First of all, the catalytic prenylation efficiency among both CAAX prenyltransferases has been shown to be best in the case when FTase is used in combination with the CAAX box derived from the C-terminus of K-Ras4B, CVIM[242]. Secondly, since proteins produced by enzymatic lipidation reactions display a decrease in solubility, attachment of the shortest lipid chain, farnesyl, is desirable. Third, since Ras represents the best studied GTPase among the members of the Ras superfamily, its PTM-mediating enzymes, particularly FTase, have been studied extensively. A large amount of information on the mechanism of the farnesylation process and, most importantly for our studies, on the influence of modifications on both the lipid chain and the protein substrate are available.

In order to meet the experimental requirements, some criteria regarding the equipment of the isoprenoid analogs with functional groups have to be evaluated. As described in section 1.5, there are generally two different strategies for protein labeling.

A direct incorporation of the reporter group into the isoprene chain represents the ideal situation, since it enables a one-step labeling process. The most widely used labeling-detection system in medical research and diagnostics is the biotin-streptavidin system. Streptavidin is a bacterial protein from *Streptomyces avidinii* that consists of four subunits, each of which can bind one biotin molecule with K_D values in femtomolar range ($K_D \sim 10^{14}$–10^{15} M^{-1})[280]. Often referred to as the strongest non-covalent bond in biology, this system has been extensively used since (i) the biotin group can be attached to any small molecule (for example to a substrate of a PTM reaction) and (ii) streptavidin can be fused to reporter enzymes. Most prominently, horse-radish peroxidase (HRP) is very often utilized in immunhistochemistry and produces chemiluminescence upon cleavage of its substrate. Here, the read-out is coupled to an enzymatic reaction, which leads to a significant signal amplification. Thus, we envisaged an isoprenoid analog which is equipped with a biotin functionality at the terminal isoprene units.

Since we were concerned that a bulky and hydrophilic biotin-tagged analog might not be tolerated as a substrate by FTase, we sought to design an alternatively functionalized isoprenoid that contains a smaller chemical functionality in the terminal isoprene unit suitable for further chemoselective transformation (see section 1.5). Since it was not clear at this point to which extent the overall length, the bulkiness, and/or the hydrophobicity of the resulting isoprenoid would influence the FTase substrate recognition, two paths were followed in parallel. In the first, we made use of the observation that alterations in the hydrophobicity of the analogs by adding or removing unsaturated bonds were well tolerated (see section 1.4). Additionally, designing probes that mimic the lipid chain in structure, but not in polarity, might help to develop probes with reduced aggregation and/or precipitation potential of the target protein after prenylation. For reasons discussed in section 1.5, we designed FPP analogs that contain an azide group for further Staudinger ligation, click chemistry, or strain-promoted cycloaddition.

In the second approach, the development of a FPP analog that better mimicked the native structure in hydrophobicity was attempted. The Diels-Alder cycloaddition has been intensively studied, shown to proceed in water without any additives, and to be biocompatible in protein biochemistry[266]. We expected that one of the reactants in this reaction, the diene, would mimic the lipid chain in polarity better than the hydrophilic azide group*.

---

* During the course of this PhD thesis, several other groups reported on similar strategies to incorporate azides into the isoprenyl chain. These synthetic analogs were efficiently transferred to CAAX peptides and proteins and used for peptide and protein labeling[281-285], protein immobilization[286, 287], proteomics applications[288], and the preparation of protein-DNA conjugates[289] by means of click chemistry and Staudinger ligation.

Dr. Joaquín Gomis (Prof. Waldmann, Department of Chemical Biology, Max-Planck-Institut für molekulare Physiologie, Dortmund) synthesized two azide-, one diene-, and one biotin-functionalized isoprenoid analog. The developed probes are shown in Figure 3-1 in comparison with the native substrates FPP and GGPP[290].
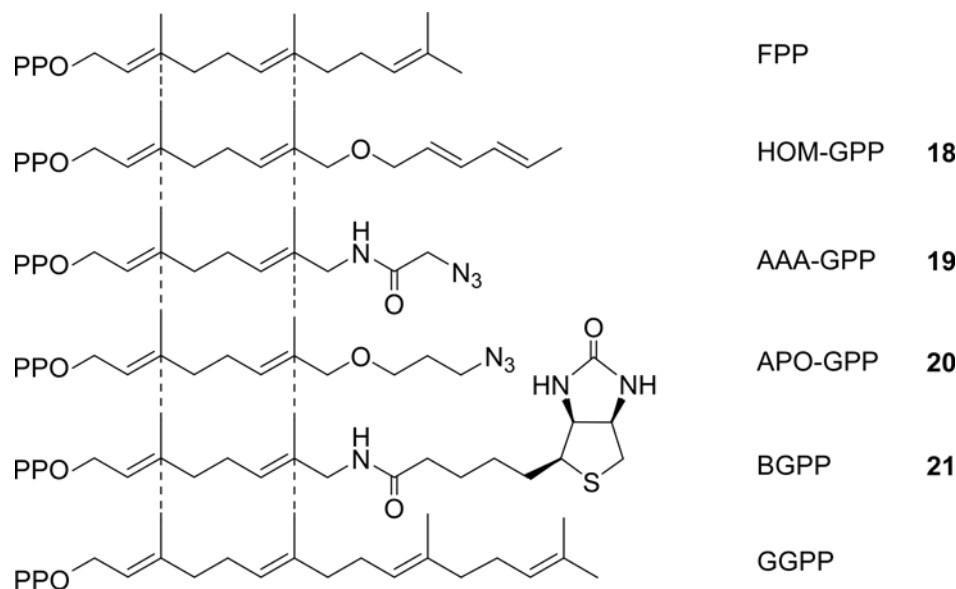
Figure 3-1 Chemical structure of the functionalized isoprenoid analogs in comparison with the native substrates FPP and GGPP[290]. The analogs were synthesized by Dr. Joaquín Gomis.

3.1.2 Prior work

Previous studies have shown that FTase is flexible in its substrate recognition; it can transfer isoprenoids with lengths of up to 15 atoms that also contain additional ether groups[291]. The developed analogs can be regarded as hybrid molecules compared to the typical protein prenyltransferase substrate. Containing GPP as a core structure, the isoprenyl chain was then augmented with the respective functional groups. In order to fulfill certain synthetic needs, such as the prevention of thermal interconversion or ester hydrolysis[290], the resulting analogs differ in the overall lengths of the linear chain. The length of the diene-functionalized isoprenoid HOM-GPP (15 atoms) is closer to that of GGPP than that of FPP since the lipid contains only one carbon fewer than GGPP. Additionally, it bears an ether group at position C9, while instead of an additional geranyl unit at position C10 it has a conjugated diene functionality at carbons C11 to C14. The chain length of the azide-functionalized analog AAA-GPP is comparable to that of FPP, but the terminal methyl group is substituted by an azide moiety. APO-GPP has one additional terminal azide group relative to FPP and comprises an ether functionality at the same position as in HOM-GPP. The hydrophobicity of the three analogs is expected to be significantly lowered due to the presence of less unsaturated carbon-carbon bonds as well as the incorporation of azide, amide, and/or ether moieties.

To analyze the interactions of the designed FPP analogs with FTase, Dr. Janina Cramer (Prof. Roger S. Goody, Department of Physical Biochemistry, Max-Planck-Institut für molekulare Physiologie, Dortmund) made use of a previously established fluorescent prenylation assay[227]. In this assay, the affinity of the non-fluorescent phosphoisoprenoid is estimated by its influence on the interaction between the enzyme and the fluorescent isoprenoids NBD-GPP or NBD-FPP. In competitive titration experiments the preformed complex of NBD-FPP and FTase was titrated with the respective isoprenoid. The resulting dequenching of the NBD-FPP fluorescence indicated that the analogs were displaced from FTase. The titration data were fitted numerically by a previously described approach and resulted in the K_D values summarized in Table 3-1.

Table 3-1 K_D values of the analogs towards FTase binding and mode of competition.

Isoprenoid analog	K_d / nM	competition
NBD-FPP	5[290]	
FPP	2.8[292]	
HOM-GPP	16.4 ± 0.9	full displacement
AAA-GPP	26.5 ± 1.8	partial displacement
APO-GPP	2.3 ± 0.3	partial displacement
BGPP	32.3 ± 2.7	full displacement

The affinities were determined by Dr. Janina Cramer.

In spite of significant changes in the structure of the lipid chain, the azide-functionalized analog APO-GPP bound FTase with an affinity comparable to that of the native isoprenoid FPP (2.8 nM). The other azide-functionalized AAA-GPP, which is shortened by one carbon atom and lacks one double bond, bound FTase about 9 times less tighly than did FPP. Compared to the native substrates FPP and GGPP, it is striking that the isoprenoid HOM-GPP is much closer to GGPP in its length than to FPP. Yet this analog still displayed an affinity of 16.4 nM for FTase, which is about three times stronger than GGPP. The reason for this might be found in the diene group, which may cause an increased hydrophobicity of the isoprenoid and compensate for the longer chain. The biotin-functionalized analog contains the same core structure as AAA-GPP from postions 1-11 in the linear chain, but is then augmented by three additional carbon atoms and the terminal biotin group. While the length of BGPP is much closer to that of GGPP than to FPP it binds to FTase with an affinity comparable to that of AAA-GPP (32 nM).

HOM-GPP and BGPP showed full displacement of NBD-FPP out of the complex; this suggests that these analogs share the binding site with FTase. In contrast, the azide-functionalized analogs displayed only partial displacement, which hints at a different binding mode.

3.1.3 The isoprenoid analogs as efficient lipid donors for the prenylation reaction catalyzed by FTase

Transferrability of the analogs onto CAAX-tagged peptides. Since tight binding of the lipid substrate to FTase does not necessarily correlate with efficient catalysis, the next step was to evaluate whether the functionalized isoprenoids could serve as native lipid donors in the prenylation reaction catalyzed by FTase.

Using the fluorescence assay developed by Pompliano and colleagues (Figure 3-2 A), the prenylation reaction was monitored by the increase in fluorescence of dansyl-GCVLS upon prenylation. The reaction was initiated by mixing the fluorescently labeled peptide with catalytic amount of FTase and excess of either FPP (Figure 3-2 B, black line) or the isoprenoid analog APO-GPP (red), HOM-GPP (blue), and AAA-GPP (green). All four isoprenoids showed a significant fluorescence increase upon addition of the prenylation machinery, which strongly suggests that these analogs serve as lipid substrates for FTase.

Two major differences between the functionalized isoprenoids were observed. First, the relative fluorescence increase varied from 4.6-fold (FPP) and 4.2-fold (APO-GPP and HOM-GPP) to 3.3-fold (AAA-GPP). Since this assay is sensitive to hydrophobicity changes in the environment of the dansyl fluorophore, these observations most probably resulted from different hydrophobicities of the analogs. As expected, the more hydrophobic HOM-GPP and APO-GPP, which comprise a diene group and an aliphatic azide, respectively, showed a higher fluorescence increase than AAA-GPP which contains the azide moiety next to an amide functionality.

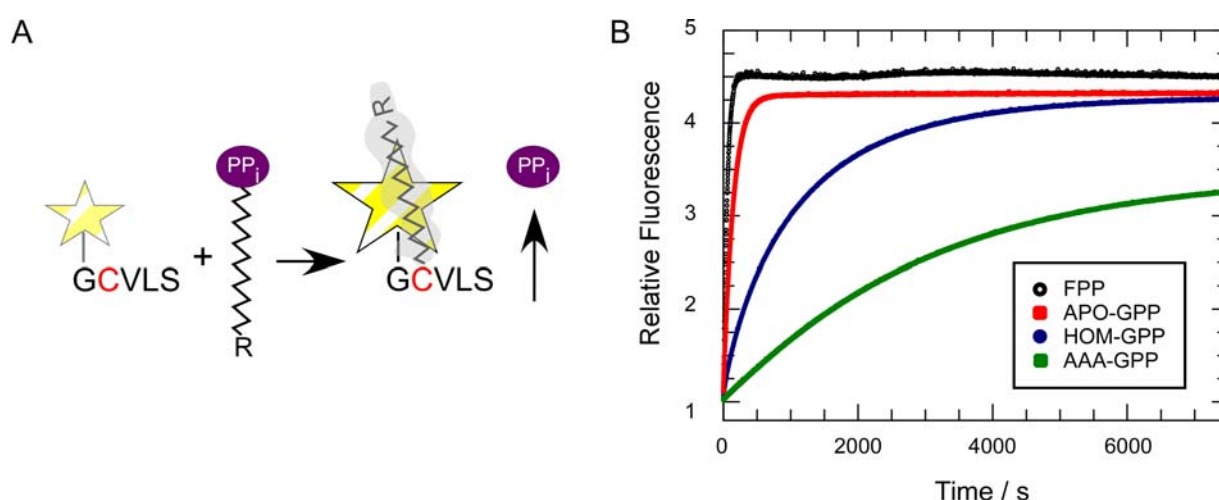**Figure 3-2** Fluorescence increase of dansyl-GCVLS upon prenylation. **A** Schematic representation of the fluorescence assay. **B** Relative fluorescence increase upon addition of FPP (black), APO-GPP (red), HOM-GPP (blue), and AAA-GPP (green).

Addition of BGPP to the reaction mixture had no impact on the fluorescence, indicating that this analog was either no lipid donor for FTase or that its incorporation into dansyl-GCVLS did not cause a hydrophobicity change affecting the fluorescent group. To examine these two possibilities, all prenylation reaction mixtures were analyzed by ESI-MS. In accordance with the fluorescence assay, the prenylation reactions using APO-GPP, HOM-GPP, and AAA-GPP as lipid donors showed full conversion of dansyl-GCVLS into the prenylated species, whereas no product was detected for BGPP. Hence, despite nanomolar affinity, the biotin-functionalized analog does not serve as an efficient FTase substrate; this can be explained by its overall length, hydrophilicity, and/or its bulky biotin group.

While the importance of the hydrophobicity of the farnesyl group for Ras function and processing in biological systems is well established[293, 294], Spielmann and co-workers demonstrated that hydrophobicity is not the primary determinant for lipid transferability by FTase[295, 296]. By utilizing a number of isoprenoid analogs that differ in size, shape, and hydrophobicity, these studies revealed that the shape and the size of the functionalized lipids are more important for FTase-catalyzed transfer.

As mentioned in section 1.2.1, there are two prevailing hypotheses that explain the lipid substrate specificity of FTase. In the molecular ruler hypothesis, the depth of the lipid binding pocket of the enzyme is a simple length-discriminating molecular ruler[34]. Isoprenoids larger and/or bulkier than FPP such as BGPP fail to be transferred because the pyrophosphate and the C1 of the isoprene chain are misaligned for efficient catalysis. Considering the tight binding between BGPP and FTase, it is unlikely that the C1 carbon and the pyrophosphate in BGPP are mispositioned, given that numerous mutagenesis and computational modeling studies have suggested that pyrophosphate binding is the primary energy source of lipid binding[297, 298]. Several studies on lipid analogs that are longer than FPP suggest that the conformation of the bound lipid rather than simply the length of the lipid determines whether it is transferred by FTase or not. For example, Gibbs and co-workers found that 2Z-GGPP was in fact a substrate for FTase, in contrast to the native *all-trans* GGPP. Distefano and co-workers solved the structure of the benzophenone-derivatized analog **3** and GGPP in complex with FTase, which revealed that the pyrophosphate group and the C1 atom of the isoprenoids were correctly located (Figure 1-5)[38]. Instead, the conformation was perturbed in both cases which interfered with the CAAX peptide binding site or prevented the conversion into product, respectively.

Thus, the most plausible explanation for BGPP´s failure not to serve as a FTase substrate is its conformation due to the overall length and/or bulkiness of the biotin group, as postulated by the second site-exclusion model. However, the crystal structure of FTase in complex with BGPP should clarify this matter (section 3.2.4).

Kinetics of FTase-mediated transfer of the analogs onto CAAX-tagged peptides. Key to a universal chemical derivatization tool is the efficiency of labeling, since long labeling times and excess enzyme or substrate concentrations are undesirable. Substitutions in the lipid chain have been shown to potentially affect the rates of FTase catalysis[229]. Therefore, the fluorescence assay described above was employed to study the kinetics of the FTase-catalyzed reaction with the isoprenoid analogs as lipid donors. The initial velocities of the prenylation reactions were measured at various isoprenoid concentrations to calculate the kinetic constants. To directly correlate fluorescence units to actual product concentrations, the completion of the reaction was verified by adding excess FTase to the prenylation mixture when the fluorescence had reached its maximum. Since this did not lead to any further fluorescence change, the total fluorescence increase was subsequently correlated to the peptide concentration to give the Michaelis-Menten curves shown in Figure 3-3.
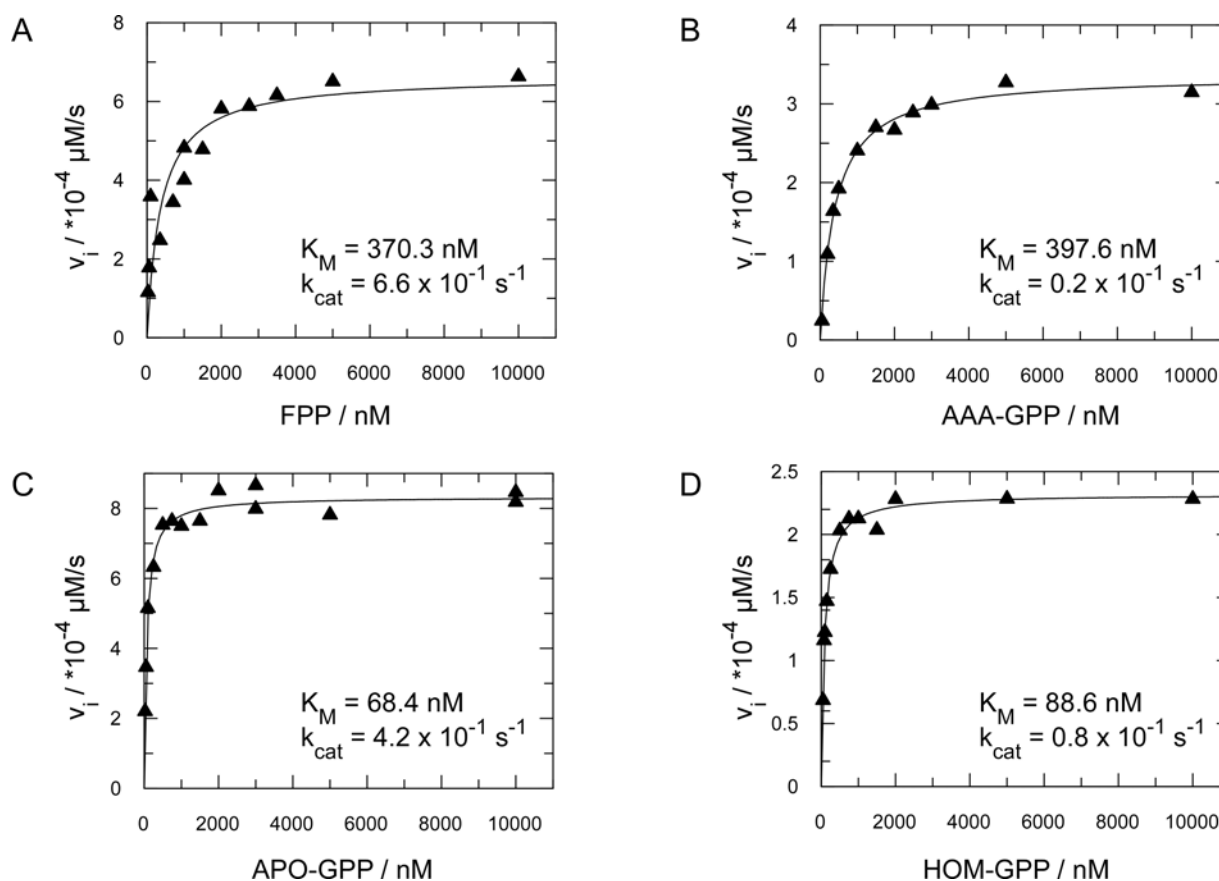
Figure 3-3 Michaelis-Menten kinetics of dansyl-GVLS prenylation. Kinetics of prenylation of dansyl-GVLS using FPP (A), AAA-GPP (B), APO-GPP (C), and HOM-GPP (D). The kinetic parameters are indicated in the corresponding panels.

The K_M values obtained for the three analogs were in the low (APO-GPP and HOM-GPP) and in the high nanomolar range (HOM-GPP, Figure 3-3). Notably, substrate binding and product release are rate-limiting for steady-state catalysis under conditions of subsaturating and saturating substrate concentrations for mammalian FTase, respectively[39, 52]. Therefore, the K_M

for lipid substrates does not simply reflect the K_D when peptide concentration is saturating, assuming that FTase follows an ordered binding mechanism. The K_M may reflect the binding of the lipid to the E*product complex to accelerate product dissociation[52, 291]. Spielmann and co-workers postulate that K_M is reciprocally dependent on the hydrophobicity ($\propto 1/K_M$) and on the lipid binding geometry[291]. In accord with their findings, the rather hydrophobic APO-GPP and HOM-GPP display lower K_M values than the hydrophilic AAA-GPP.

Since the ratio between k_{cat} and K_M provides a measure of catalytic efficiency of enzymatic reactions, the transfer efficiencies of the prenylation reactions with the respective analogs were judged by k_{cat}/K_M. APO-GPP was an excellent alternative substrate for the enzyme, with a 3.5-fold enhancement in catalytic efficiency over the natural substrate FPP. It appears that the linear carbon chain in APO-GPP with a terminal azide moiety is a good mimic for the ω-prenyl unit in FPP, which is in accord with the observation by Spielmann and co-workers for compound **23** (Table 3-2)[285]. The catalytic efficiency of HOM-GPP, in contrast, was 2-fold lower than FPP. This could be due to the overall length of the analog, which is elongated by three atoms compared to the native substrate and may result in a suboptimal accommodation of lipid and peptide substrate in the FTase active site. AAA-GPP represented the poorest analog and was transferred 36 times less efficiently than FPP. This result is rather surprising since its overall length is very similar to FPP.

The study of Spielmann and co-workers mentioned before also investigated the influence of hydrophobicity, size, shape, overall length, and conformational flexibility of the substituted isoprenoid analogs on the catalytic efficiency of the FTase-mediated prenylation reaction. Their findings suggest that there is no correlation between transfer efficiency and hydrophobicity [295, 296]. Instead, there is a compromise between the conformation of the ternary complex best suited for catalysis and the optimal interaction of the lipid with the FTase-product complex to accelerate product dissociation [291, 297]. In particular, using benzyloxyisoprenyl pyrophosphates of various lengths, Spielmann and co-workers demonstrated that conformational flexibility plays an important role in the kinetics of the prenylation reaction[291, 297]. They suggest that by incorporating a linker chain with flexible methylene units a large number of available conformations is created. Therefore, the analogs may be less organized and, once bound to the lipid binding site, have to find the optimal geometric fit, leading to a decreased overall transfer rate. In contrast, the isoprene units of FPP may preorganize the molecule to fit into the isoprenoid binding site and thereby reduce the number of conformations needed to place the lipid pyrophosphate into the active site. In thermodynamic terms, this would mean that a more flexible chain creates an entropic disadvantage. Therefore, Spielmann and colleagues postulate that an ideal accommodation of the lipid donor in the FTase lipid binding pocket involves an optimal interplay between flexibility and conformational rigidity of the lipid. While the overall length of AAA-GPP may be

optimal for a good fit in the FTase lipid binding pocket, it is possible that the rotational flexibility of the amide group of AAA-GPP may create various conformations that could lead to such a dramatic decrease in the overall catalytic efficiency.

Taken together, compared to other reported azide- or alkyne-functionalized FPP analogs used for selective chemical reactions involving azides, APO-GPP represents the azide-tagged analog with the highest catalytic efficiency reported to date (Table 3-2). HOM-GPP is as efficient as other commonly used azide- or alkyne-containing analogs, while AAA-GPP represents a rather poor substrate.

Table 3-2 Comparison of the kinetic parameters of the functionalized isoprenoids in comparison to other reported azide- or alkyne-tagged FPP analogs.

Structure	K_M / nM	k_{cat} / s^{-1}	k_{cat}/K_M / s^{-1}
(PPO-isoprenoid)	here: 370.3 40-1710[53, 241, 285]	0.66 0.07-2.3	1.78 0.77-2.25
22 (PPO-isoprenoid-N$_3$)	2120[285]	0.45	0.21
23 (PPO-isoprenoid-N$_3$)	670[285]	1.1	1.64
24 (PPO-isoprenoid-NH-benzyl-N$_3$)	1050[285]	0.35	0.33
25 (PPO-isoprenoid-NH-benzyl-N$_3$)	4230[285]	0.48	0.11
26 (PPO-isoprenoid-O-propargyl)	1900[285]	1.06	0.55
APO-GPP	68.4	0.42	6.14
AAA-GPP	397.6	0.02	0.05
HOM-GPP	88.6	0.08	0.90

Transferrability of the analogs onto CAAX-tagged proteins. Next, the ability of FTase to transfer the developed isoprenoid analogs onto proteins that contain a genetically encoded CAAX box was tested. As hydrophilic, easily detectable model protein substrates, Cyan Fluorescent Protein (CFP) and its red variant (Cherry) were chosen. The yeast Rab protein Ypt7 was included into the test group to represent an average protein that is not as robust as a fluorescent protein under non-native conditions. For reasons discussed earlier, the proteins were expressed in *E.coli* with the C-terminal motif TKCVIM, derived from a mammalian K-Ras4B protein[242]. Incubation of CFP-CAAX and Ypt7-CAAX with equimolar enzyme and excess of the respective isoprenoid analog led to full conversion of the proteins, which was confirmed by ESI-MS.

The reaction conditions of the prenylation reaction were optimized to compromise between (i) the amount of reagents used, since the preparation of FTase and particularly the isoprenoids is laborious, and (ii) labeling time, which should be as short as possible to prevent protein denaturation. AAA-GPP was chosen as a model isoprenoid since it displayed the slowest kinetics (Figure 3-3).

In this experiment, 60 µM of CFP-CAAX was premixed with 1-20 eq of AAA-GPP. The reaction was initiated by addition of 4.6 µM FTase, stopped with 6 M GdmHCl at the indicated time intervals, and analyzed by ESI-MS. Conversion of CFP-CAAX into the prenylated product was estimated by the height of the mass peaks. Except for a 1:1 equimolar composition of protein and AAA-GPP, the reaction was found to be completed with only two equivalents of lipid substrate following an incubation for 12 h at room temperature (Figure 3-4 A, B). A similar situation pertained for the other two analogs led to the same result, which was confirmed by ESI-MS (Figure 3-4 C, D).
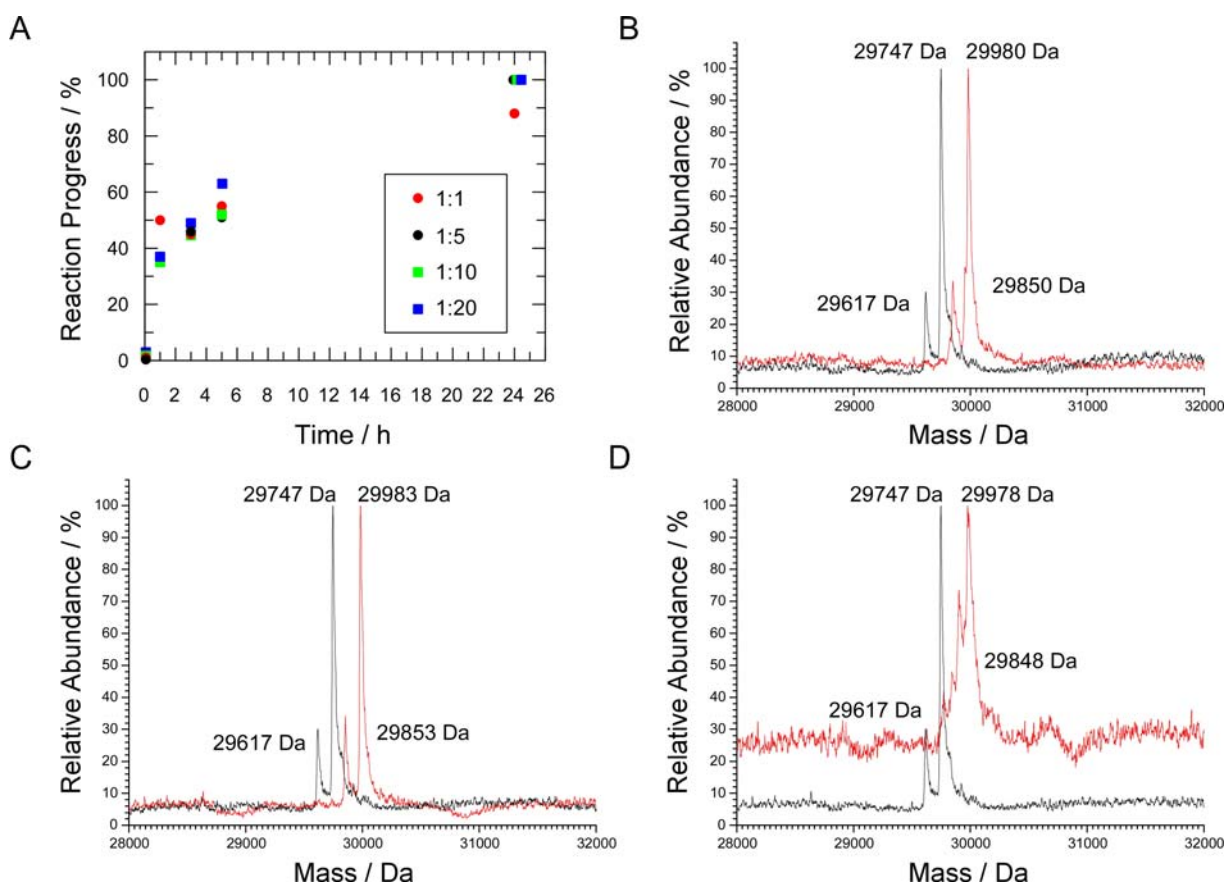
Figure 3-4 Incoproration of AAA-G, APO-G, and HOM-G into CFP-CAAX as evidenced by ESI-MS. **A** Monitoring of prenylation of CFP-CAAX by ESI-MS using different amounts of AAA-GPP. **B**-**D** ESI-MS of prenylated CFP-CAAX for AAA-GPP (**B**, expected: 29982 Da; found: 29983 Da), APO-GPP (**C**, expected: 29983 Da; found: 29980 Da), and HOM-GPP (**D**, expected main peak: 29980 Da; found: 29978 Da). The mass spectrum of unprenylated CFP-CAAX (experimentally determined mass: 29747 Da) was included in black in all spectra. All spectra showed a minor peak of [M-131]$^+$ that reflected the removal of the N-terminal translation initiator Met by methionine aminopeptidase. Additionally, **D** showed a fragmentation peak of [M-80]$^+$ typically corresponding to the loss of the hexadienyl group during ionization[266, 299].

To verify that the performed ESI-MS analysis gave a quantitative assessment of the sample and that the flight efficiencies of unprenylated and prenylated sample were comparable, equimolar amounts of CFP-CAAX and CFP-CAAX-F were premixed and analyzed by ESI-MS, which revealed that their flight efficiencies were similar. These results suggest that efficient protein labeling with FTase can be achieved using catalytic amounts of enzyme and two equivalents of lipid donor.

3.1.4 Biochemical features of proteins derivatized with the isoprenoid analogs

As mentioned earlier, it is desirable that the envisaged protein derivatization strategy should not change the physical, biochemical, or functional properties of the target protein. To fulfill these requirements, three aspects have to be examined.

(1) First, the native folding of the target protein should not be influenced under the reaction conditions used. In spite of the extended reaction time no protein degradation was observed (Figure 3-5 A).
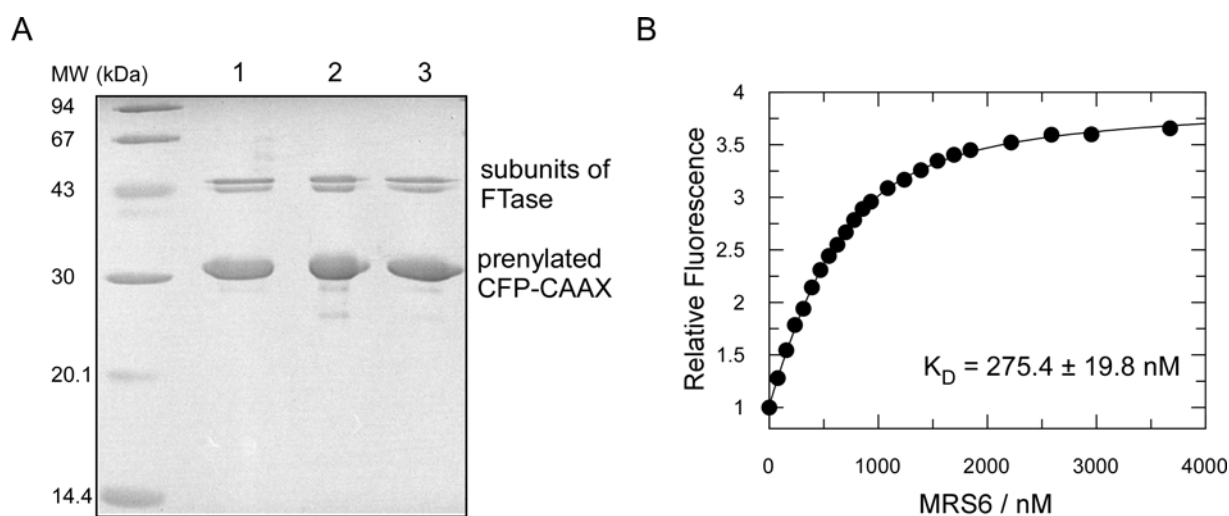
Figure 3-5 Biochemical characterization of the prenylated proteins. **A** Investigation of potential protein degradation after prenylation under the established prenylation conditions by SDS-PAGE. **B** Determination of the affinity of NBD-geranylated Ypt7-CAAX for MRS6 by fluorescence spectroscopy.

To examine the compatibility of the established labeling time of 12 h at room temperature with protein folding, a binding interaction of Ypt7-CAAX with one of its known binding partners was utilized. Ypt7 is a yeast GTPase of the Rab family, which is known to bind many of its regulators, including MRS6, the yeast equivalent of mammalian REP. Since the functionalized analogs do not contain any reporter group that can be used to quantify the binding interaction, Ypt7-CAAX was prenylated with NBD-GPP under the developed prenylation conditions instead. Excess lipid substrate was removed by a NAP-5 column, and the binding interaction between Ypt7-CAAX and MRS6 was monitored by fluorescence spectroscopy using 100 nM

Ypt7-CAAX-NBD-G and increasing amounts of MRS6. This resulted in a large and saturable increase in NBD fluorescence, which reflected hydrophobicity changes in the fluorophore environment. The obtained data could be fitted to a K_D value of 275.4 ± 19.8 nM (Figure 3-5 B); this is very close to that determined earlier[242]. The data strongly suggests that the established prenylation conditions are mild enough to preserve the native protein fold.

(2) A further stringent criterion for a generic protein labeling method is the hydrophobicity of the protein derivative produced. When increased, hydrophobicity tends to reduce protein solubility and is often associated with protein aggregation and/or precipitation. Isoprene lipids normally render proteins more hydrophobic, given their native function to mediate association of the prenylated substrates with membranes. However, reduction of chain length or substitution of parts of the structure with non-isoprenyl moieties can reduce the hydrophobicity of the isoprenoid[242].

In search of a technique that provides information about the hydrophobicity of biomolecules, reversed-phase High Performance Liquid Chromatography (rp-HPLC) was chosen. To investigate the influence of the functionalities incorporated into prenylated CFP-CAAX, the retention times of the various conjugated analogs and farnesyl were determined under identical conditions on a C4 reversed-phase column. The retention times of the derivatives including the three analogs were shorter compared to that of CFP-CAAX, which eluted at 11.85 min prior to and at 12.35 min upon addition of the farnesyl group (Table 3-3).

Table 3-3 Retention times of CFP-CAAX on a C4 HPLC column upon prenylation	
prenylated CFP-CAAX	**Retention Time / min**
no prenylation	11.85
FPP	12.35
HOM-GPP	12.20
AAA-GPP	11.90
APO-GPP	12.08
The prenylated proteins were eluted with a linear gradient of 20-70 % buffer B (0.1 % formic acid in ACN) in buffer A (0.1 % formic acid in water) over 10 min.	

CFP-CAAX-AAA-G showed no significant change in retention time relative to unprenylated CFP-CAAX (11.90 min), while CFP-CAAX-APO-G and CFP-CAAX-HOM-G eluted at 12.08 min and 12.20 min, respectively. These results are consistent with the increase in fluorescence obtained in the fluorescent prenylation assay, suggesting that prenylation with the isoprenoid analogs influences the hydrophobicity of the target proteins to a lesser extent than FPP. In particular, AAA-GPP appears not to influence the hydrophobicity of the tested proteins at all.

(3) Third, key to a successful derivatization of the incorporated diene and azide functionalities by a chemical reaction is the accessibility of the reactive groups to the solvent. The oligomeric state of the protein and its association to FTase upon prenylation have to be investigated since studies on FTase prenylation have indicated that (i) farnesylated proteins remain in complex with FTase without excess isoprenoid and/or protein substrate[52] and that (ii) farnesylated proteins oligomerize in the absence of detergents. Gel filtration analysis was chosen for this purpose as a technique that provides information on the oligomerization state of biomolecules.

CFP-CAAX and Ypt7-CAAX were prenylated under the optimized reaction conditions using 60 µM protein, 0.08 eq FTase, and 2 eq FPP, AAA-GPP, APO-GPP, or HOM-GPP. After completion, the reaction mixtures were separated on a 10/30 Sephadex-200 column in prenylation buffer without detergent and analyzed by SDS-PAGE. As shown in Figure 3-6, the elution profiles for the prenylated CFP-CAAX and Ypt7-CAAX proteins were highly similar for the respective isoprenoid, which suggests that the nature of the lipid defines the oligomeric state of the proteins to a large extent.

As anticipated, farnesylated Ypt7-CAAX (Figure 3-6 A) and CFP-CAAX (Figure 3-6 E) eluted as oligomers and partly in complex with FTase owing to increased protein hydrophobicity and lack of excess lipid and/or protein substrate for product release, respectively. In accordance with the HPLC-based experiments, Ypt7-CAAX-AAA-G (B) and CFP-CAAX-AAA-G (F) were completely soluble and eluted exclusively in monomeric form. Ypt7-CAAX-APO-G (C) and CFP-CAAX-APO-G (G) were almost completely monomeric, while the most hydrophobic Ypt7-CAAX-HOM-G (D) and CFP-CAAX-HOM-G (H) existed partly in monomeric and partly in dimeric, trimeric, and oligomeric form.

The proteins that had eluted as monomers were confirmed to be fully prenylated by ESI-MS, as shown for CFP-CAAX (red: CFP-CAAX-AAA-G, blue: CFP-CAAX-APO-G, green: CFP-CAAX-HOM-G, Figure 3-6 I).

From these data, it appears that the proteins modified with the more hydrophilic isoprenoids AAA-GPP and APO-GPP are readily released by FTase and stay in the monomeric form even in the absence of detergent and excess substrates.
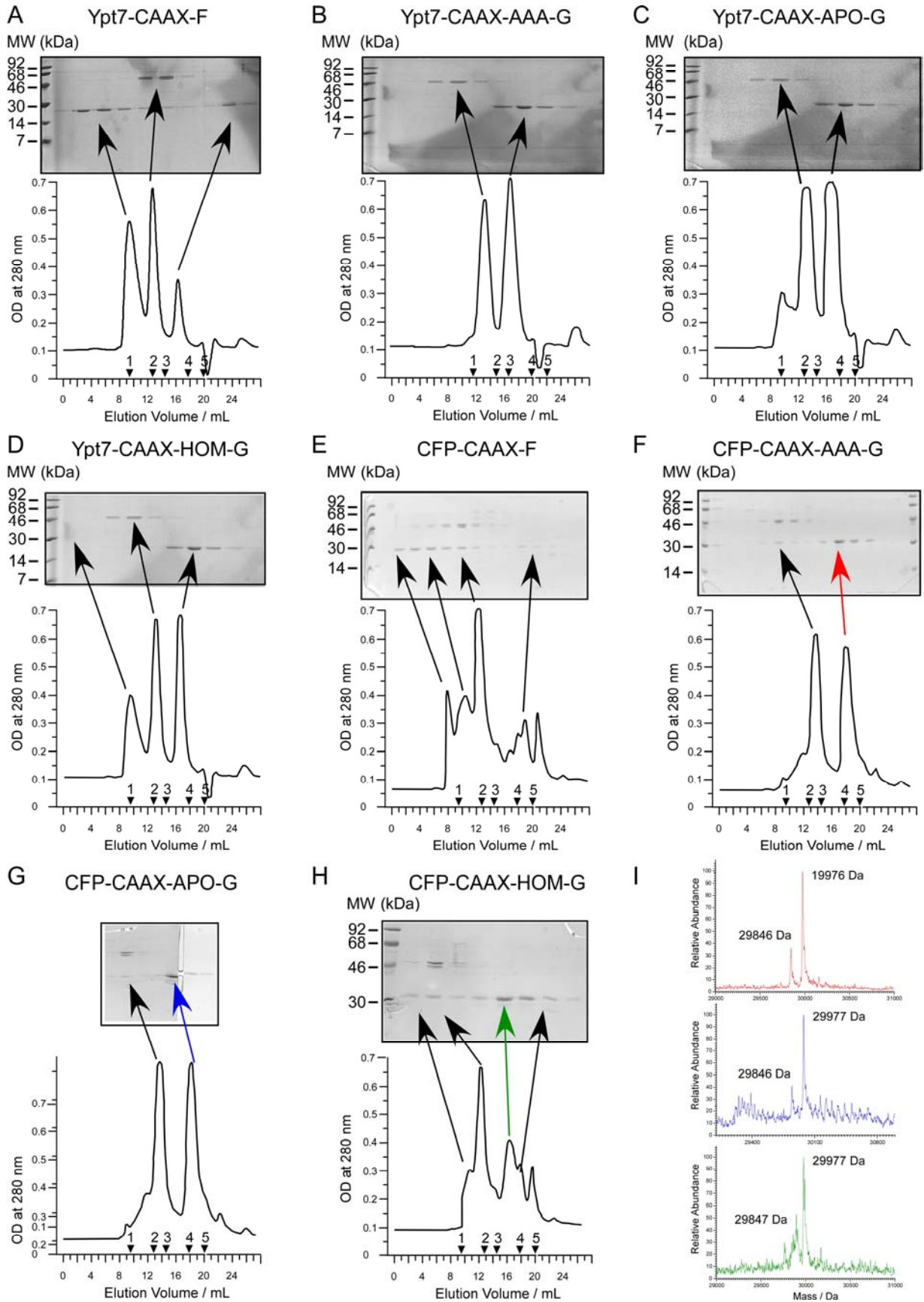
Figure 3-6 Gel filtration analysis of prenylation mixtures of CFP-CAAX and Ypt7-CAAX upon prenylation with FPP, AAA-GPP, APO-GPP, and HOM-GPP followed by analysis of the fractions by SDS-PAGE. The molecular weight of each peak was determined by comparison with protein standards of known molecular weight (1–670 kDa, 2–158 kDa, 3–44 kDa, 4–17 kDa, 5–1.3 kDa, shown as arrow heads). For further details, see text.

3.1.5 Further chemoselective derivatization of the prenylated proteins by Staudinger ligation and Diels-Alder cycloaddition

The incorporated azide and diene groups on the prenylated proteins were tested for their ability to be modified by a chemoselective reaction (Scheme 3-1).
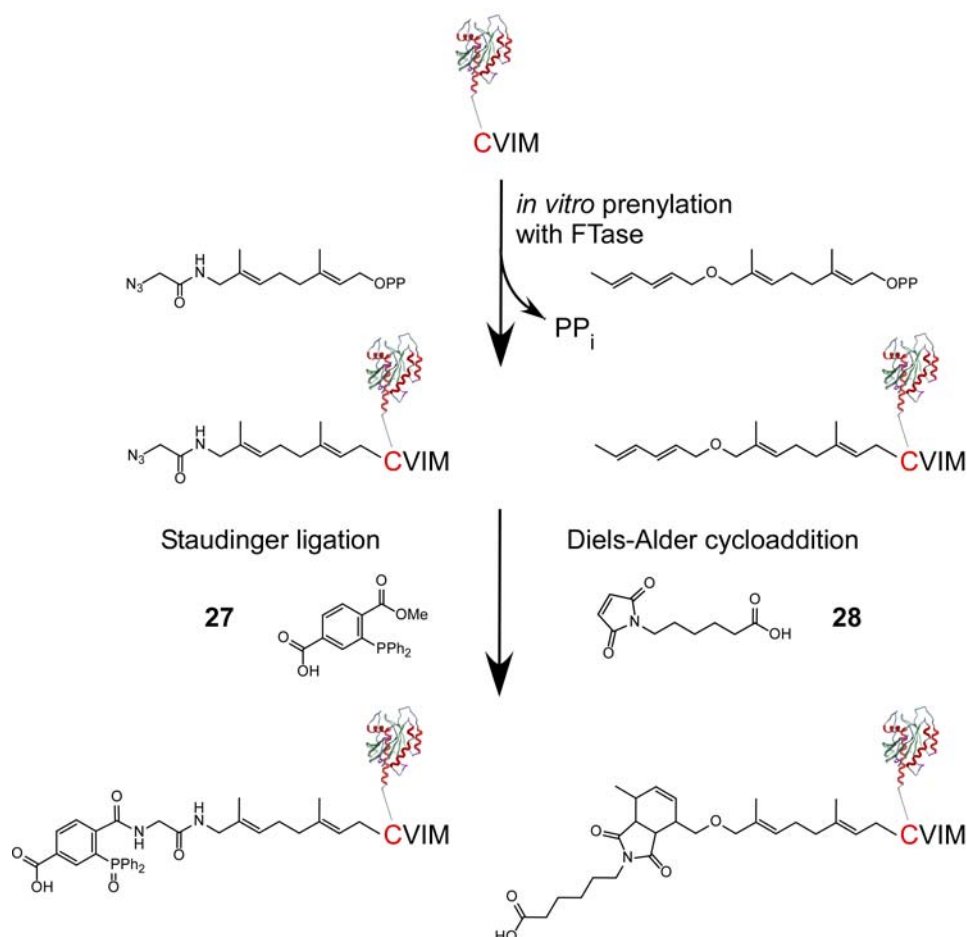
Scheme 3-1 Schematic representation of the two-step labeling approach involving prenylation with the azide- and diene-tagged analogs and subsequent Staudinger ligation with phosphine **27** or Diels-Alder cycloaddition with maleimide **28**.

Staudinger ligation. Farnesylated proteins and peptides containing azide tags can be derivatized either by the "Click reaction", Staudinger ligation, or strain-promoted cycloaddition, as described in section 1.5. Staudinger ligation was selected as the reaction of choice since (i) it does not require catalysts such as Cu^{2+} or the use of a triazolyl ligand necessary for click chemistry, which in many cases results in protein denaturation during the course of the reaction[300]; (ii) the synthetic effort to prepare the cyclooctyne compound is quite high; and (iii) much knowledge about protein derivatization by Staudinger ligation has accumulated in the research group of Prof. Waldmann[301, 302]. We chose the variation of the Staudinger ligation developed by Bertozzi and co-workers, since the reaction proceeds in a very specific

manner between an azide and a phosphine group. The latter can be provided in the form of an aryl phosphine that is relatively stable in aqueous solution[274, 303].
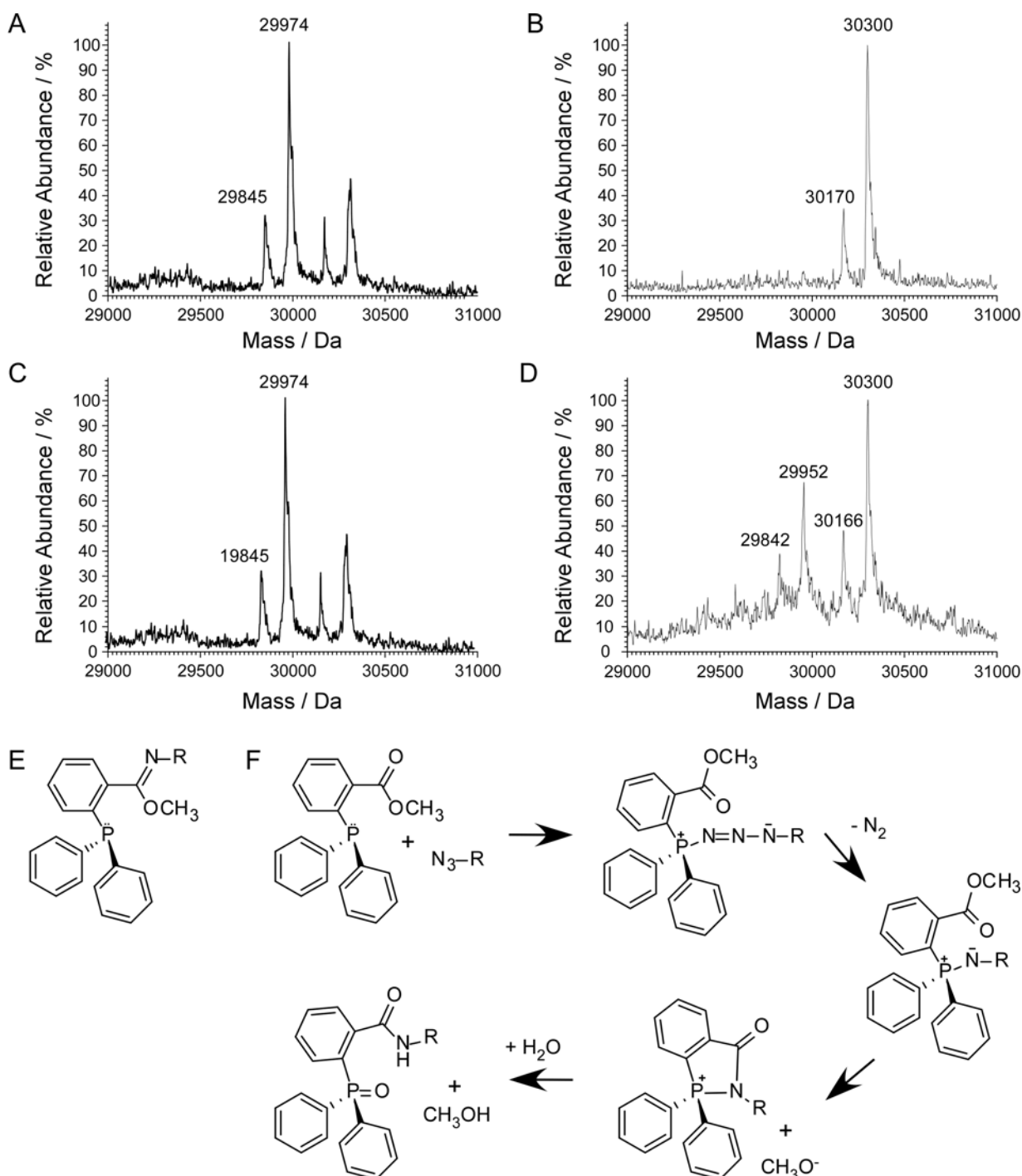
Figure 3-7 Chemoselective derivatization of the incorporated azides by Staudinger ligation. **A-D** ESI-MS spectra of CFP-CAAX-AAA-G (unligated protein: 29975 Da, expected ligated protein: 30298 Da) and CFP-CAAX-APO-G (unligated protein: 29976 Da, expected ligated protein: 30299 Da) upon incubation with DMSO **A**, **C** or phosphine **27 B**, **D**. The minor additional peaks in the control reactions represent contaminations from the positive samples. Each spectrum showed a minor peak of $[M-131]^+$ that reflected the removal of the N-terminal translation initiator Met by methionine aminopeptidase. **E** Chemical structure of the alkoxyimidate side product as reported by Distefano and co-workers[282]. **F** Mechanism of the Staudinger ligation as proposed by Bertozzi and colleagues[304].

In initial ligations, 50 μM CFP-CAAX prenylated either with AAA-GPP or with APO-GPP was reacted with 250 μM phosphine **27** in 25 mM HEPES, pH 7.2, 40 mM NaCl, 2 m, MgCl$_2$ in the presence or absence of 0.05 (v/v) % Tween-20 and/or 2 mM DTE for 8 h at 25 °C. Conventional separation methods such as HPLC or SDS-PAGE could not be used since the ligated and unligated proteins had similar hydrophobicities and masses (<< 1 kDa). Therefore, the reaction yields were estimated by mass spectrometry. While the control reaction with CFP-CAAX-F showed no protein modification, the reaction mixtures containing CFP-CAAX-AAA-G or CFP-CAAX-APO-G resulted in complete ligation in the absence or presence of DTE or Tween-20 (Figure 3-7 B, D), suggesting that both reagents were compatible with the Staudinger ligation.

Importantly, the control reactions with CFP-CAAX-AAA-G and CFP-CAAX-APO-G without the addition of phosphine **27** showed that the stability of the azides was not affected inspite of the presence of DTE as a reducing reagent, which stands in contrast to previous reports on azide reduction to amines by thiols (Figure 3-7 A, C)[305].

In addition to the major (desired) amide-linked product of the Staudinger reaction between phosphine **27** and an azide (Figure 3-7 F)[304], several groups have reported on an alternative alkyoxyimidate product (Figure 3-7 E)[282]. Mass spectrometric analysis of a reaction mixture containing CFP-CAAX-AAA-G and CFP-CAAX-APO-G and phosphine **27** showed a peak with the expected mass of the amide-linked reaction product (Figure 3-7 B, D) but no evidence for either the alkoxyimidate compound or the starting material.

In the case of CFP-CAAX-APO-G, an additional peak at 29952 Da was observed. This corresponded to the mass of unreacted CFP-CAAX-APO-G with an amine instead of an azide. Since this could not be due to a reduction of the azide as evidenced by the control sample, additional phosphine conjugations to Cherry-CAAX-APO-G and Ypt7-CAAX-APO-G were performed to establish that this phenomenon was not CFP-CAAX-specific. Both cases also yielded two reaction products. The origin of the side-product is still unknown, and further experiments are required to clarify this matter.

It is widely established that the Staudinger ligation displays significantly slower reaction kinetics than the click reaction[243]. To monitor the Staudinger ligation in a time-resolved manner the reaction was allowed to proceed under the conditions described and stopped at the indicated time intervals by passing it over a spin gel filtration column to remove the phosphine from the reaction mixture. Estimated by ESI-MS analysis, the reaction yields of either CFP-CAAX-AAA-G or CFP-CAAX-APO-G were plotted against reaction times (Figure 3-8), which revealed that the reaction kinetics were quite different for the two analogs. Ligation of CFP-CAAX-AAA-G was complete after 1.5 h while that of CFP-CAAX-APO-G afforded more than 4 h. This can be explained from the perspective that the analogs vary in the electrophilicities of their azide groups. The azide moiety in AAA-GPP is more electrophilic

than that in APO-GPP owing to the presence of the amide functionality. The azide in APO-GPP has aliphatic carbon atoms as neighbors, which make it less electrophilic. While the attack of the lone pair of the phosphorus of the triaryl phosphine on the azide might be enhanced in AAA-G in the initial formation of the phosphazide, the real cause is still unknown, given that mechanistic investigations of the Staudinger ligation indicate that intramolecular amide bond formation rather than phosphazide formation is the rate-determining step of the reaction (Figure 3-7 F)[304, 306].

The results demonstrate that the Staudinger ligation is fully chemoselective, is tolerant to detergents and reducing agents, and proceeds rapidly in aqueous media in the presence of a relatively small excess of phosphine (5 eq).
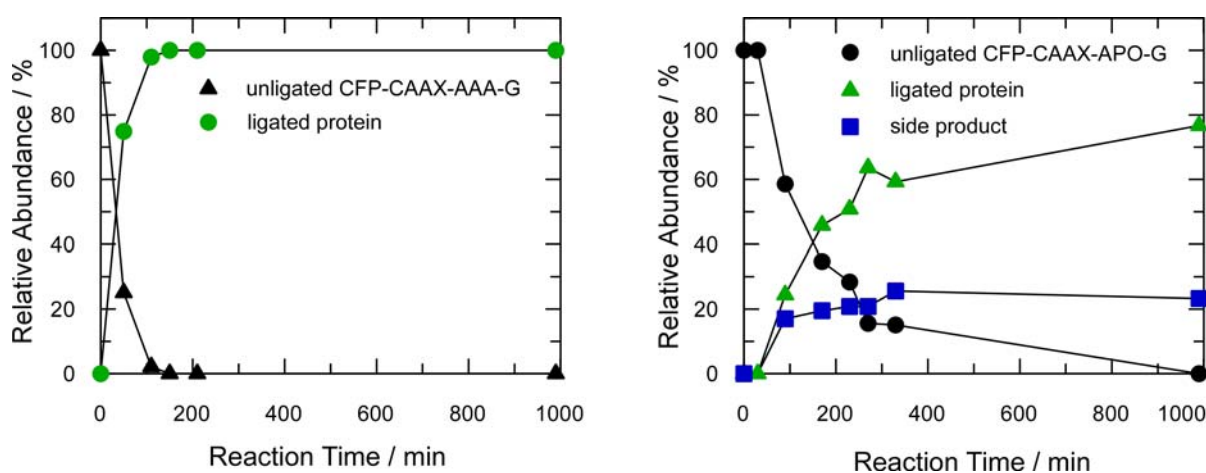
Figure 3-8. Time course of the Staudinger ligation monitored by ESI-MS for CFP-CAAX-AAA-G (left) and CFP-CAAX-APO-G (right). 50 µM CFP-CAAX-AAA-G or CFP-CAAX-APO-G was reacted with 250 µM phosphine **27** for the indicated time periods at room temperature.

Diels-Alder cycloaddition. The Diels-Alder reaction is known to be a selective cycloaddition between a diene and a dienophile that can proceed in aqueous media with a higher velocity and selectivity than in organic solvents[307-309]. Its compatibility with biomolecules has been explored in the bioconjugation and immobilization of oligonucleotides[310, 311] and other biomolecules[312] as well as in microarray applications[313-315]. Recently, the applicability of the Diels-Alder cycloaddition on the functionalization and immobilization of proteins has been demonstrated in the group of Prof. Waldmann[266, 299].

As shown in Scheme 3-1, dienophile **28** was chosen as a model substrate. Since it is a substrate of a Michael addition reaction with thiols as well, all cysteines in the reaction mixture had to be protected. This was necessary to prevent (i) either unspecific protein labeling, if solvent-accessible cysteines were present on the protein surface (in the case of CFP-CAAX there were no solvent-exposed cysteines other than that in the CAAX motif) or (ii) the decrease of free substrate concentration due to multiple cysteines present in FTase that would be labeled with the maleimide (Figure 3-9). A reaction mixture containing CFP-CAAX-

HOM-G was first treated with Ellman´s reagent (5,5´-dithiobis(2-nitrobenzoic acid), DTNB) to block all accessible cysteines of FTase and then subjected to Diels-Alder cycloaddition using 50 µM protein and 40-fold excess of dienophile at 25 °C. In contrast to the reaction conditions previously used to couple a bodipy-functionalized maleimide to a diene-tagged Rab7 protein [266, 299], conditions were chosen that did not affect protein folding and induce protein precipitation. Therefore, the reaction was allowed to proceed for 15 h at 25 °C.
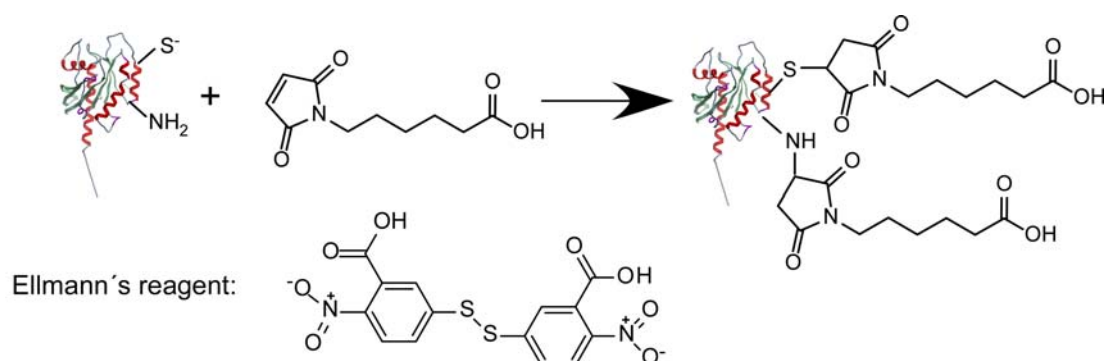
Figure 3-9 Michael addition of intrinsic solvent-exposed cysteine or lysine residues to maleimide **28** and chemical structure of Ellman´s reagent

To evaluate the chemoselectivity of the reaction, control reactions were carried out in which CFP-CAAX-HOM-G was substituted by CFP-CAAX-F. As in the case of the Staudinger ligation, the reaction could not be monitored by SDS-PAGE or HPLC. Therefore, it was judged by ESI-MS. CFP-CAAX-HOM-G reacted with one molecule of dienophile both at pH 6.0 and pH 7.2 (Figure 3-10 A, B). At pH 7.2, however, the control sample prenylated with FPP, which cannot undergo Diels-Alder cycloaddition, clearly showed a mass peak (30156 Da, Figure 3-10 D). Corresponding to the addition of one molecule of dienophile **28** to CFP-CAAX-F, the obtained result suggests that the Diels-Alder cycloaddition is not chemoselective at neutral pH, most likely owing to a Michael addition reaction of the lysines present in the protein structure to the maleimide. By lowering the pH, all lysines appear to be protonated, which inhibits the undesired side reaction, in agreement with earlier studies (Figure 3-10 C)[266, 299].

With 40-fold excess of dienophile **28** and a reaction time of 15 h at 25 °C, the yield of the cycloaddition was only 30 %, significantly lower than in the previous report. That study utilized a Rab7 concentration of 40 µM in combination with a 40-100-fold excess of reagent and a reaction time of 24 h, which led to protein precipitation and yielded 50-90 % product. The significantly lower yield of 30 % in our case can be approached by (i) a shorter reaction time and (ii) the observation that CFP-CAAX-HOM-G partially exists in oligomeric forms (Figure 3-6). Thus, the diene moiety may be buried within the protein core or between protein interfaces and not fully accessible to the reactive dienophile.
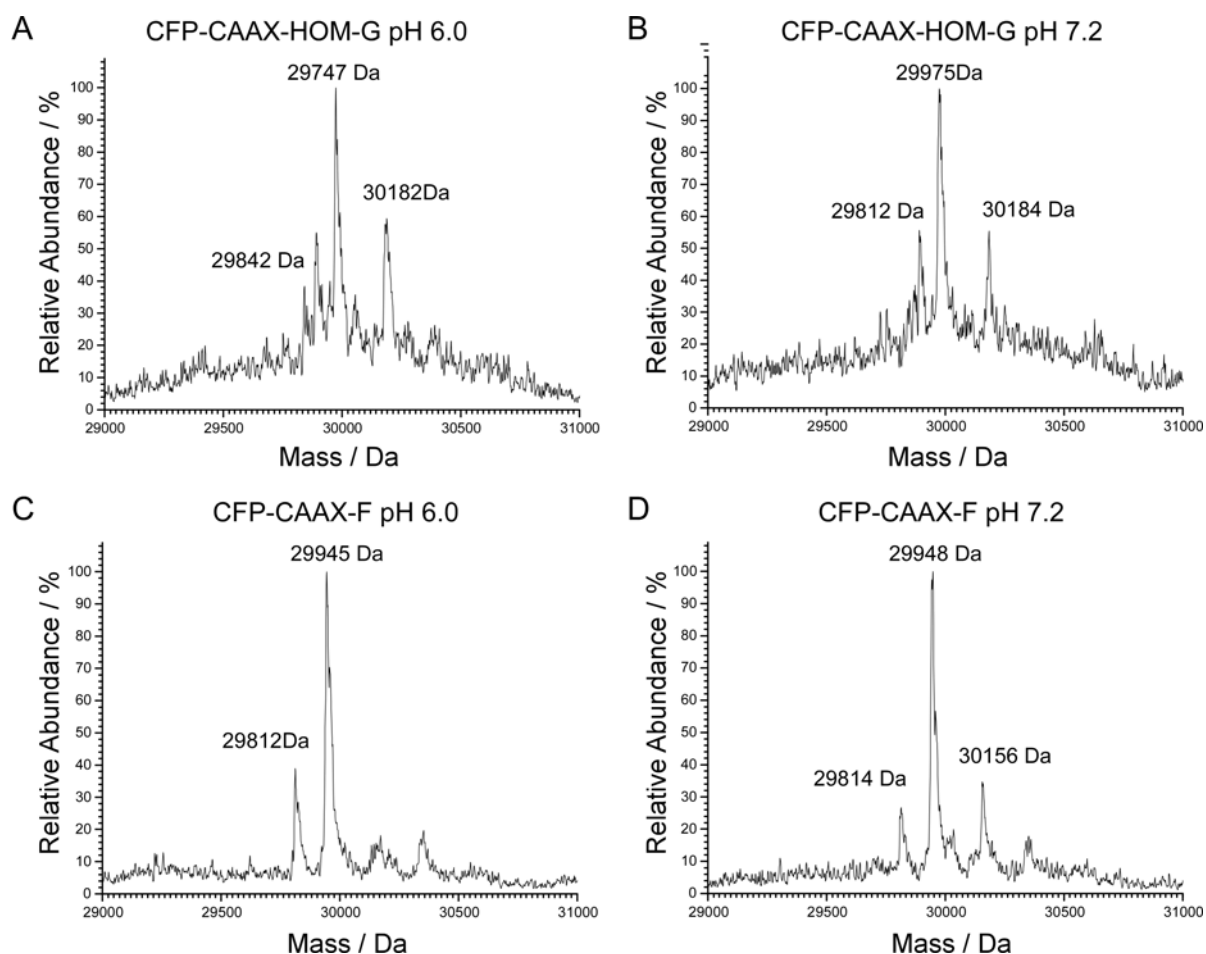
Figure 3-10 Ligation of CFP-CAAX-HOM-G with 6-maleimidohexanoic acid **28**. **A**, **B** ESI-MS spectra of CFP-CAAX-HOM-G reacted with **28** at pH 6.0 and 7.2, respectively (unligated protein: 29974 Da, expected ligated protein: 30185 Da). **C**, **D** ESI-MS spectra of control reactions of CFP-CAAX-F incubated with reagent **28** at pH 6.0 and 7.2, respectively (unligated protein: 29945 Da, expected ligated protein: 30156 Da). All spectra showed a minor peak of [M-131]$^+$ that reflected the removal of the N-terminal translation initiator Met by methionine aminopeptidase. In addition, the spectrum of **A** and **B** showed a typical fragmentation peak of [M-80]$^+$ corresponding to the loss of the hexadienyl group during ionization.

3.2 Towards the isolation and analysis of the cellular mammalian prenylome

The aim of the second part of this work was to develop a technique that allows for (i) sensitive detection of prenylatable proteins, even in complex mixtures such as cell lysates or living cells, and (ii) simultaneous analysis of the activity of the three protein prenyltransferases *in vivo*.

Initially, we anticipated that the strategy described in section 3.1 would be suitable for this purpose. During the course of the project, Zhao and co-workers published a study that followed an almost identical approach, designated as the "Tagging-via-substrate technology", to label and identify FTase substrates *in vivo*[288]. After metabolically incorporating a related azide-tagged farnesyl pyrophosphate analog (compound **22**, Table 3-2) into FTase substrates in cultivated cells, the azide moiety was further functionalized with a biotin-phosphine conjugate in the resulting lysate. This allowed for a moderately sensitive detection and identification of the prenylated proteins by means of streptavidin pulldown and mass spectrometry.

This approach represented an important further development towards the direct read-out of biotin-tagged and enriched prenylated proteins. However, the methodology suffered from a limited detection sensitivity, which prevented the authors from identifying all known FTase substrates. This could be a result of the two-step labeling procedure that was dependent on the chemical step, the Staudinger ligation. This reaction, as mentioned earlier, displays rather slow reaction kinetics. Additionally, the approach was restricted to the labeling of FTase substrates and did not allow for the investigation of either the GGTase-I or the RabGGTase action.

We conjectured that incorporating the biotin moiety directly into the isoprene chain, as in BGPP, may minimize signal loss and therefore increase the detection sensitivity. Ideally, the biotin-functionalized isoprenoid should be an efficient lipid donor for all three protein prenyltransferases to enable a proteome-wide analysis of prenylation.

This chapter describes the use of biotin-geranyl pyrophosphate BGPP as an efficient substrate in the RabGGTase-mediated prenylation reaction, enabling the isolation and analysis of RabGTPases *in vitro* and in lysate. The strategies for engineering FTase and GGTase-I mutants capable of faithfully delivering BGPP to their cognate substrates by site-directed mutagenesis will be described. Finally, the scope of applications of the developed strategy will be discussed.

3.2.1 BGPP as an efficient lipid donor for the RabGGTase-mediated prenylation reaction *in vitro*

BGPP represents an extended, bulky, hydrophilic isoprenoid hybrid molecule that is not accepted as a lipid donor by FTase (section 3.1.3). Compared to the native substrates FPP and GGPP (Figure 3-11 A), the BGPP structure is much closer to GGPP in size than to FPP and thus may be tolerated as a substrate by GGTase-I and/or RabGGTase.
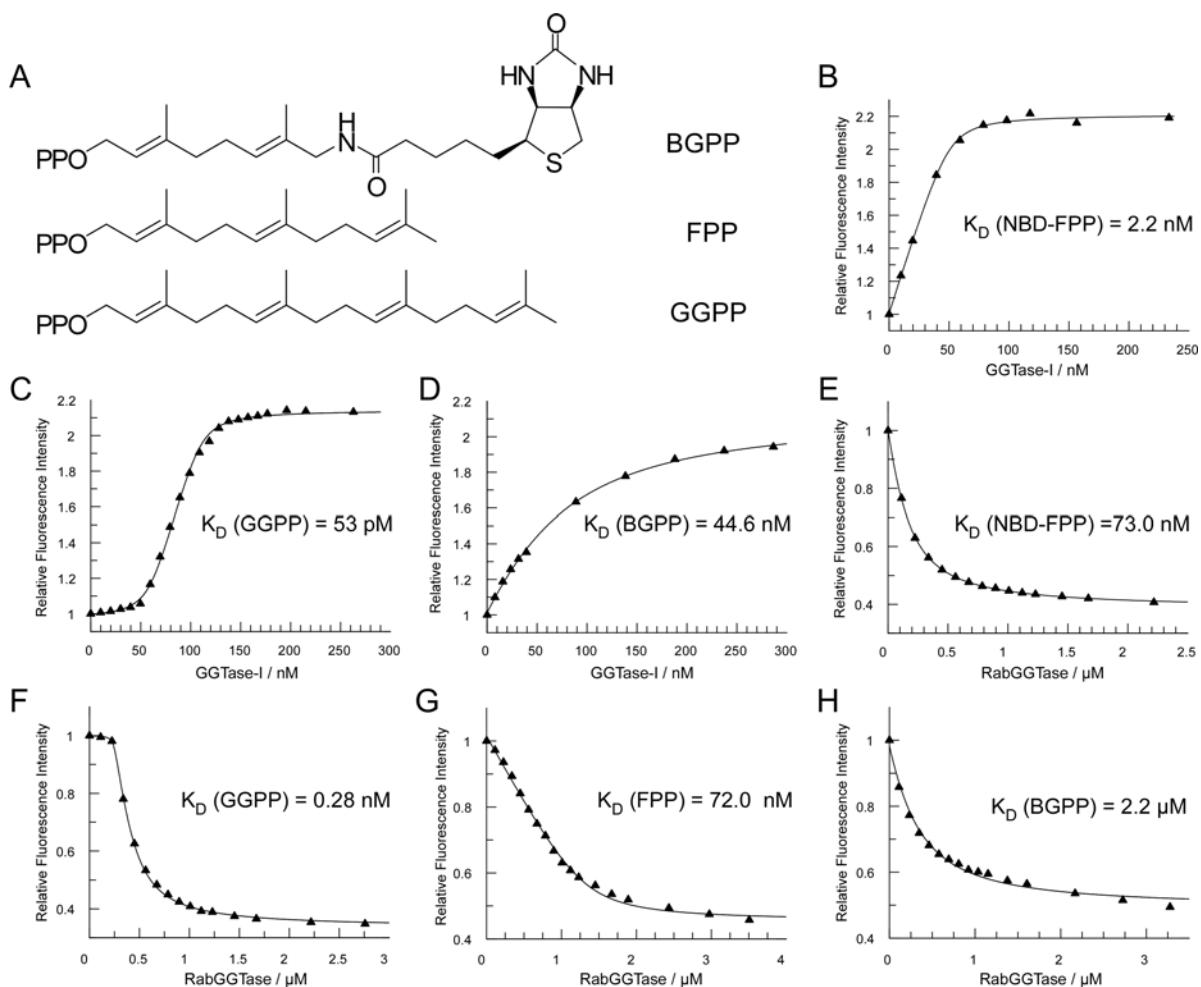
Figure 3-11 BGPP and its interaction with protein prenyltransferases. **A** Chemical structure of BGPP in comparison with the natural substrates FPP and GGPP. **B** Titration of 50 nM of NBD-FPP GGTase-I. The changes of NBD-FPP fluorescence were followed at 25°C in 50 mM Hepes pH 7.2, 50 mM NaCl, and 5 mM DTT in a volume of 1 mL. The NBD fluorescence was excited at 487 nm and data were collected at 530 nm. The data was fitted to a quadratic equation. **C**, **D** Competitive titration in which 50 nM NBD-FPP was mixed with 50 nM GGPP **C** or 1 µM BGPP **D** and then titrated with GGTase-I. The data was fitted numerically using the program Scientist. **E** Titration of 200 nM of NBD-FPP with RabGGTase. The experiments were performed as in **B**, but the fluorescence data was collected at 550 nm. The data were fitted as in **B**. **F-H** Competitive titration in which 200 nM NBD-FPP was mixed with 200 nM GGPP **F**, 200 nM FPP **G**, or 4 µM BGPP **H** and then titrated with RabGGTase. The data was fitted as in **C** ,**D**. The K_D values of the respective isoprenoids for GGTase-I or RabGGTase are shown in the corresponding panels.

To analyze the interaction between BGPP and the enzymes, the affinity of BGPP for GGTase-I and RabGGTase was determined using competitive titration experiments as described in 3.1.2. While BGPP bound to GGTase-I as tightly as to FTase (45 nM, Figure 3-

11 D), its affinity for RabGGTase was 49-fold lower (Figure 3-11 H). This result was quite surprising, since we had anticipated that the longer and bulkier BGPP would be better accommodated in the larger active site of RabGGTase. One of the reasons may be the rotational flexibility of the amide moiety within the lipid chain.
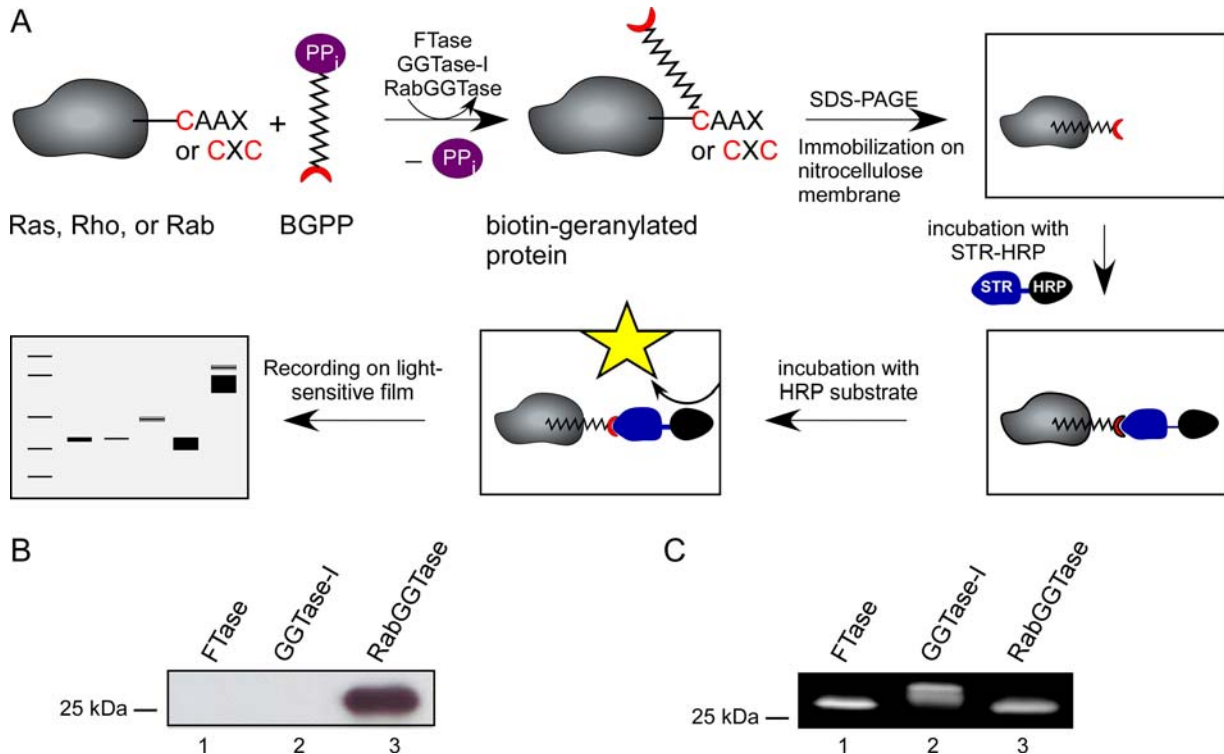
Figure 3-12 Evaluation of the incorporation of synthetic isoprenoids by wild-type protein prenyltransferases into recombinant GTPases. **A** Schematic representation of the prenylation procedure for recombinant GTPases followed by subsequent Western blot analysis using a STR-HRP conjugate. **B** Prenylation of K_i-Ras (lane 1), RhoA (lane 2), and Rab7 (lane 3) by FTase, GGTase-I, or RabGGTase/REP-1, respectively, using BGPP as a lipid donor. The reaction products were detected by Western blot with STR-HRP. **C** as in **B** but using NBD-GPP (lane 1) or NBD-FPP (lanes 2 and 3) as lipid donors. The reaction products in **C** were visualized by fluorescence scanning of the SDS-PAGE gel.

The ability of BGPP to serve as a protein prenyltransferase substrate was examined using recombinant K_i-Ras, RhoA, and Rab7 in combination with FTase, GGTase-I, and RabGGTase, respectively. 2 µM of the respective recombinant protein was mixed with an equimolar amount of enzyme (and REP-1 for RabGGTase), and the reaction was initiated by the addition of excess BGPP. The efficiency of transfer was evaluated by loading 0.5 pmol of protein on an SDS-PAGE gel followed by Western blot developed with a streptavidin-horseradish peroxidase (STR-HRP) conjugate (Figure 3-12 A). Western blot analysis showed that BGPP was efficiently transferred by RabGGTase (Figure 3-12 B, lane 3), whereas no or minimal transfer activity was detected for FTase and GGTase-I, respectively (lane 1 and 2). When this experiment was repeated with the fluorescent analogs NBD-GPP and NBD-FPP, all three protein substrates were lipidated to a similar extent (Figure 3-12 C, lanes 1-3). The results indicate that BGPP is only recognized as an efficient substrate by RabGGTase.

To confirm that the incorporation of biotin-geranyl was not specific to Rab7, the experiment was repeated using Rab27 as an alternative RabGTPase. In both cases, strong signals were detected, which were enzyme-dependent since omission of either RabGGTase (Figure 3-13 A, lane 3 and 6) or REP-1 (lane 2 and 5) resulted in lack of a chemiluminescent signal. To assess the efficiency of the prenylation reaction and whether BG was transferred to one or two C-terminal cysteines of the Rab proteins, the reaction mixture was further analyzed by ESI-MS. Under the conditions employed, Rab7 and Rab27 were fully converted into the doubly prenylated species, as shown for Rab7 in Figure 3-13 B (black: before, red: after prenylation).
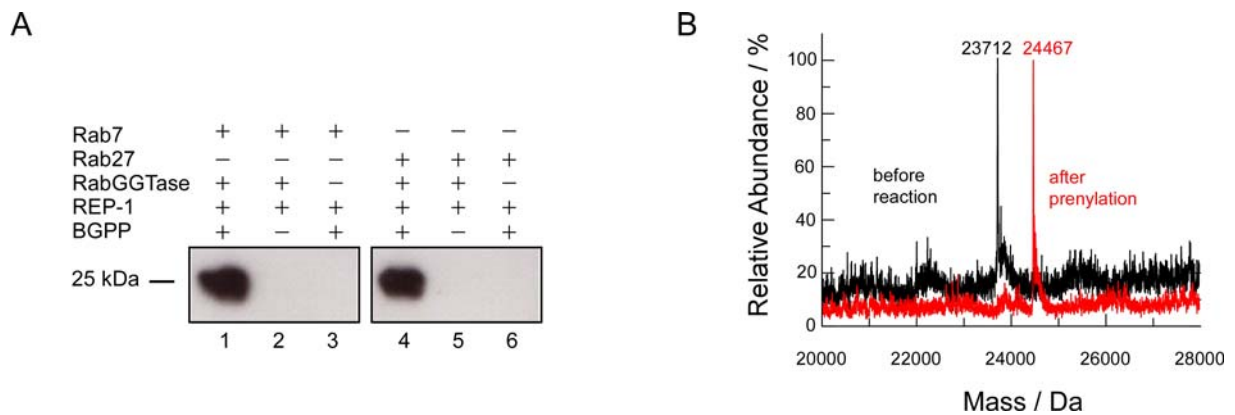
Figure 3-13 Analysis of RabGGTase-catalyzed biotin-geranyl transfer onto recombinant RabGTPases. **A** Western blot analysis of Rab7 and Rab27 *in vitro* prenylated with BGPP. Proteins were incubated with equimolar amounts of RabGGTase and REP-1 as well as 5 eq of BGPP. The samples were resolved on SDS-PAGE and subjected to Western blotting with STR-HRP to detect the incorporation of biotin-geranyl into the proteins (lane 1 and 4 for Rab7 and Rab27, respectively). Omission of either BGPP or RabGGTase resulted in a lack of chemiluminescent signal (lane 2, 3 and 5, 6 for Rab7 and Rab27, respectively). **B** ESI-MS of unprenylated Rab7 (23713 Da, in black) and doubly-biotin-geranylated Rab7 (expected: 24468 Da, found: 24467 Da, in red). The mass spectra revealed the doubly prenylated species only, suggesting that the prenylation reaction had proceeded to completion.

3.2.2 BGPP as an efficient lipid donor for the RabGGTase-mediated prenylation of endogenous RabGTPases in COS-7 lysate

Subsequently, the sensitivity of the strategy was explored by labeling endogenous RabGTPases in mammalian lysates with BGPP. As a model cell strain for this study, COS-7 cells, kidney cells derived from the green monkey, were utilized. The cells were grown in Dulbecco's Modified Eagle's medium supplemented with 10% fetal bovine serum, 1% penicillin, and 1% streptomycin. To increase the pool of unprenylated proteins *in vivo*, 20 µM compactin, an inhibitor of isoprenoid synthesis, was included in the medium, and the cells were grown overnight at 37 °C (Figure 3-14). After cell lysis, the resulting lysates were subjected to prenylation with 2 µM recombinant RabGGTase, REP-1, and 10 µM BGPP for typically 2-4 h at room temperature.

Analysis of the reaction mixture by Western blot revealed three prominent bands in the range of 25 kDa. These bands presumably represented the endogenous RabGTPases in COS-7 cells retained in the unprenylated form owing to the lack of GGPP substrate due to compactin treatment (Figure 3-14).
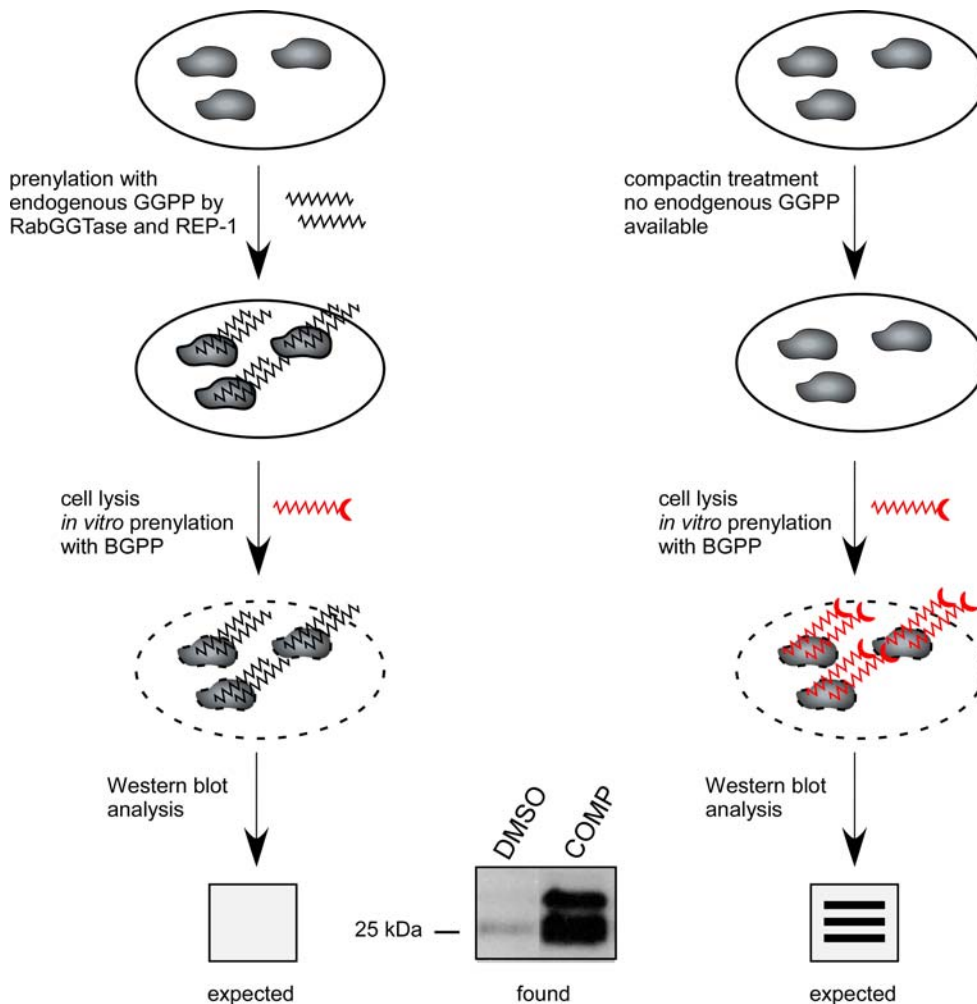
Figure 3-14 Incorporation of biotin-geranyl into endogeneous RabGTPases in COS-7 lysates. Schematically shown is the treatment of COS-7 cells with either DMSO (left) or compactin (right) followed by lysate preparation and *in vitro* prenylation with BGPP as a lipid substrate. At the bottom, the outcome of the experiment after Western blot analysis reveals that specific incorporation of biotin-geranyl was achieved when the RabGTPases had been rendered unprenylated upon compactin treatment, whereas only faint bands appeared without statin incubation. COMP: compactin.

In contrast, when cells pretreated with only DMSO were *in vitro* prenylated with BGPP, only very faint bands in the same molecular range were detected. These bands were enzyme-specific and disappeared when RabGGTase and/or REP-1 were omitted in the prenylation mixture. This suggested the existence of a minor pool of unprenylated RabGTPases, which may originate from either newly synthesized Rab proteins on their way to prenylation, a pool of RabGTPases that are not prenylated under physiological conditions, or a mixture of both.

.

3.2.3 Enrichment of biotin-geranylated RabGTPases by means of streptavidin chromatography

To investigate the origin of the detected bands, the biotin group on the transferred prenyl moiety was utilized to enrich the minor pool of unprenylated proteins by means of streptavidin pulldown (Figure 3-16 A).

Establishing prenylation conditions for subsequent streptavidin pulldown. Before testing whether the endogenous RabGTPases in compactin-treated cells could be enriched on streptavidin beads, optimal prenylation conditions were elaborated to achieve a compromise between (i) sufficient BGPP concentration to drive the biotin-geranylation reaction to completion with sufficiently high reaction kinetics and (ii) a minimal required volume of beads ensuring a quantitative elution with SDS sample buffer. *In vitro* prenylation using 0.5 µM Rab7, RabGGTase, and REP-1 for 2 h at room temperature reached maximal prenylation efficiency using only a two-fold excess of BGPP.
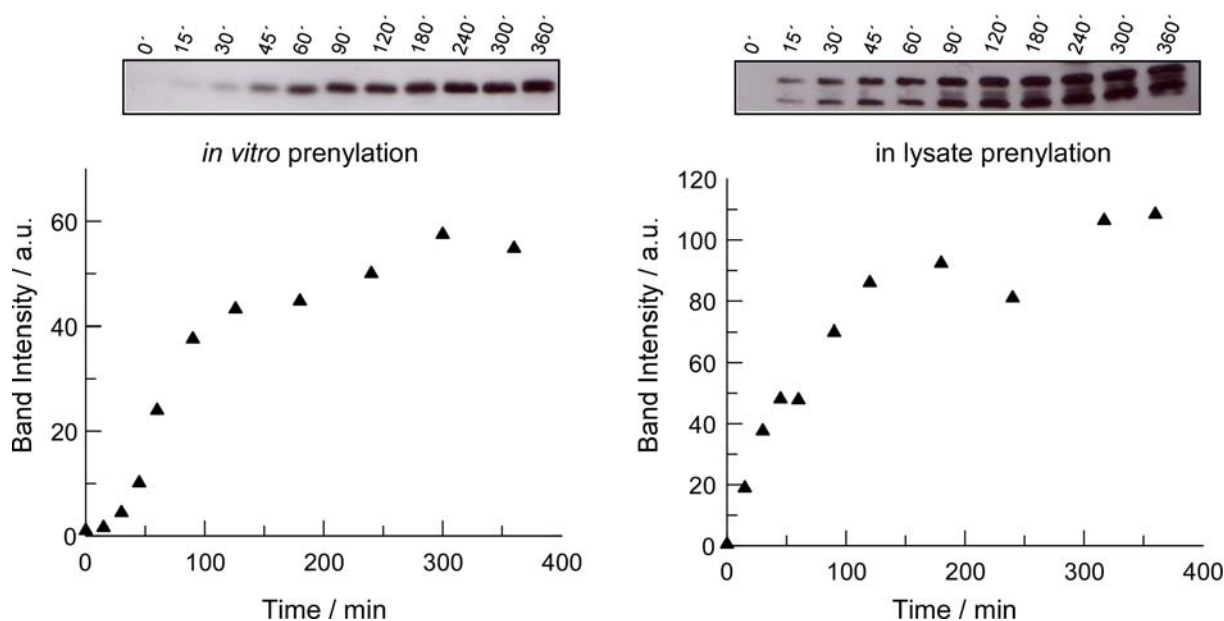
Figure 3-15 Juxtaposition of prenylation of recombinant (left) or endogenous RabGTPases in compactin-treated COS-7 cells (right). In a volume of 10 µL, 0.5 µM Rab7, RabGGTase, REP-1 was mixed with 1 µM BGPP. The reaction was allowed to proceed for 2 h at room temperature. Alternatively, 10 µL of compactin lysate was supplemented with the Rab prenylation machinery and 1 µM BGPP for 2 h at room temperature.

Judging from the band intensities on the Western blot in comparison to biotinylated protein standards of known amount, the concentration of total endogenous RabGTPases in COS-7 lysate was estimated to be 0.5 µM. Thus, the same experiment was repeated in compactin-treated COS-7 lysate using 1 µM BGPP to test whether the prenylation kinetics were comparable or whether a higher amount of the lipid substrate was required. The latter is

theoretically possible if a partial dephosphorylation of BGPP in the lysate by endogenous phosphatases takes place.

As shown in Figure 3-15, the transfer efficiencies were very similar, suggesting that a small excess of BGPP is enough to drive the prenylation of the RabGTPases to completion in a reasonable time both *in vitro* and in lysate.

Having established the optimal prenylation conditions for subsequent streptavidin pulldown, we next wanted to test whether the biotin group(s) on the RabGTPases were accessible for streptavidin under non-denaturing conditions. The shielding of the biotin group may occur since the biotin-geranylated RabGTPases may stay in complex with REP-1 after prenylation. Indeed, gel filtration and subsequent SDS-PAGE/Western blot analysis of the reaction mixture revealed that Rab7 was only partially released from REP-1/RabGGTase upon prenylation with BGPP (Figure 3-16 B).
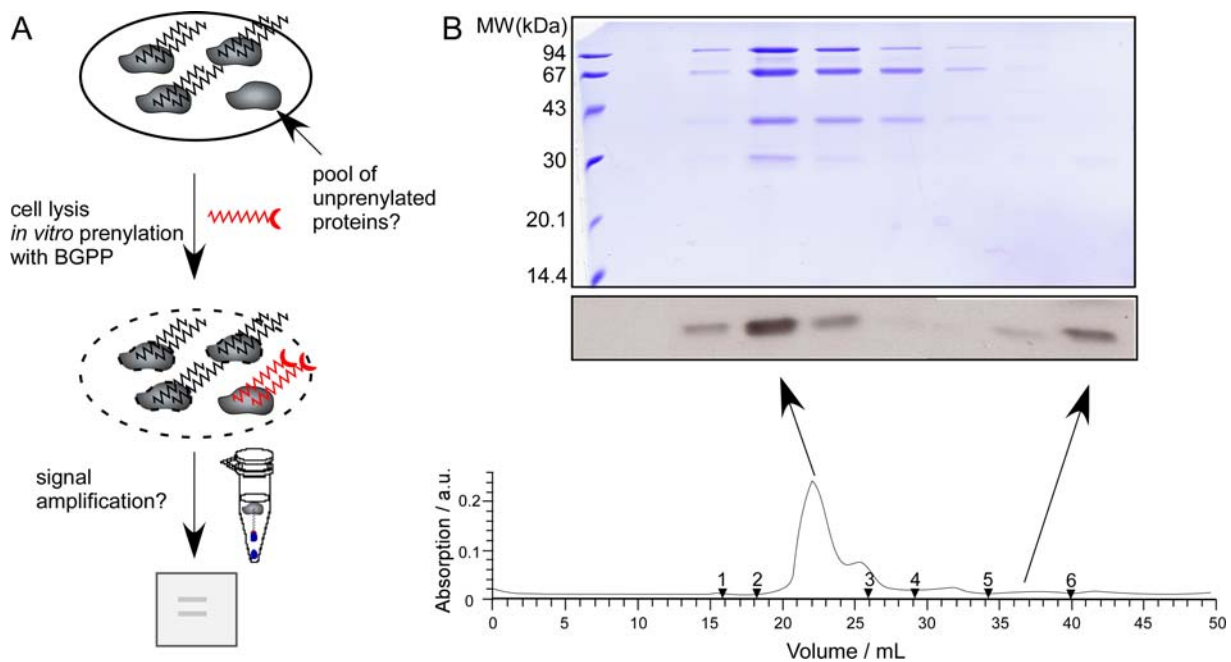
Figure 3-16 Enrichment of biotin-geranylated RabGTPases by means of streptavidin pulldown. **A** Schematic representation of the strategy to enrich the minor pool of unprenylated RabGTPases in COS-7 lysate. **B** Gel Filtration analysis of recombinant Rab7 prenylated with RabGGTase, REP-1, and BGPP *in vitro*. Fractions were subjected to SDS-PAGE and the proteins were visualized by either Coomassie Blue staining or subjected to Western blot analysis. The molecular weight of each peak was determined by comparison with protein standards of known molecular weight (1–670 kDa, 2–158 kDa, 3–4 kDa, 4, 4–17 kDa, 5–1.3 kDa, shown as arrow heads).

Nonetheless, even as part of the ternary complex, it is conveivable that only one of the two transferred biotin group might be buried in the lipid binding site. To test this possibility, compactin-treated lysate was prenylated under the optimized reaction conditions and subsequently incubated with magnetic streptavidin beads for 1 h at room temperature, washed three times with PBS, and eluted with 2x SDS sample buffer. Western blot analysis revealed that all biotin-geranylated proteins bound to the streptavidin beads. This suggests

that at least one biotin group on the RabGTPase was accessible to streptavidin, possibly located at the "exit groove" (section 1.2.2). Judging from the Western blot signals, the overall recovery was nearly quantitative (Figure 3-17 A, lanes 1 and 5).
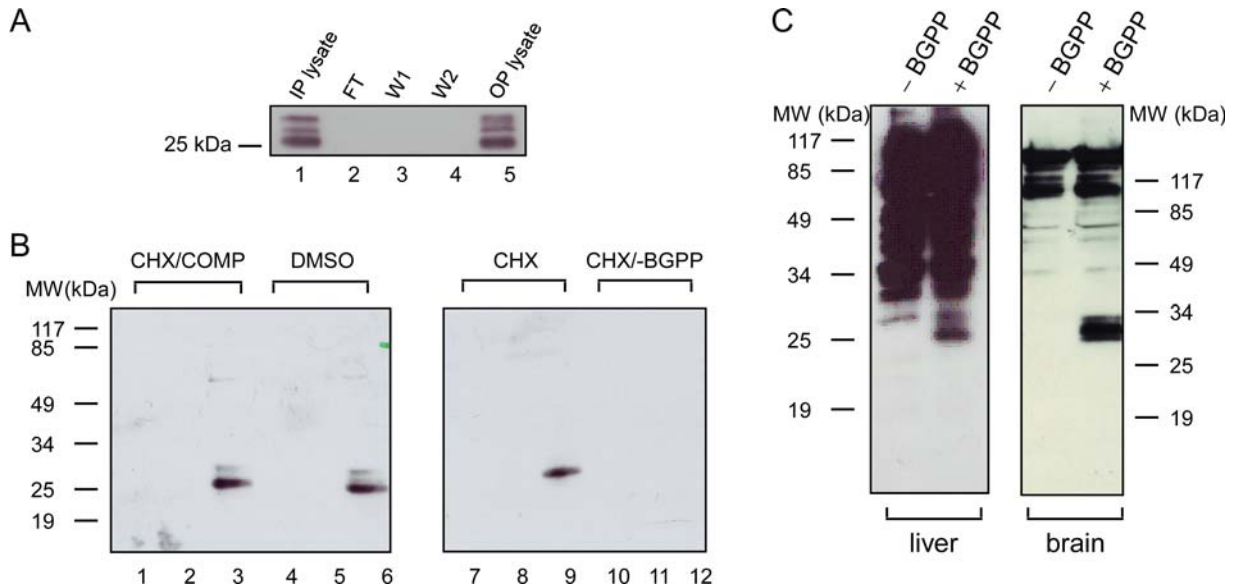
Figure 3-17 Enrichment of endogenous RabGTPases prenylated with biotin-geranyl using streptavidin affinity chromatography. **A** Recovery of biotin-prenylated Rabs in compactin-treated lysate after pulldown on streptavidin beads. The recovery of the prenylated Rabs was nearly quantitative as judged by visual inspection of Western blots. **B** Inhibition of isoprenoid and protein synthesis to elucidate the origin of the pool of unprenylated RabGTPases. COS-7 cells were treated with DMSO (lanes 4-6), cycloheximide (lanes 7-12; negative control without BGPP addition: lanes 10-12), or a combination of cycloheximide and compactin (lanes 1-3) overnight. The resulting lysates were prenylated with RabGGTase/REP-1 and BGPP as a lipid donor *in vitro*, incubated with magnetic streptavidin beads, washed with PBS, and eluted with 1x SDS sample buffer. Input lysate: lanes 1, 4, 7, and 10; flowthrough: lanes 2, 5, 8, 11; output lysate: lanes 3, 6, 9, and 12. **C** Enrichment of the pool of unprenylated proteins from the lysates of untreated mouse liver (left) or mouse brain (right). Strong signals in the high-molecular weight range represent endogenous biotinylated proteins. IP: input; FT: flow-through; W: wash; OP: output; CHX: cycloheximide; COMP: compactin; PD: pulldown.

Detection of the minor pool of unprenylated RabGTPase in COS-7 cells and mouse tissue. After demonstrating that the biotin-geranylated proteins can be enriched *in vitro* and in compactin-treated lysate, the biotin-geranylated lysates from untreated COS-7 cells were subjected to a streptavidin pulldown. As can be seen in Figure 3-17 B, enrichment resulted in signal amplification of a dominant lower and faint upper bands around 25 kDa (lane 6), while a negative control, where BGPP had been omitted, showed no signal at all (lane 12).

To test whether these bands resulted from newly synthesized Rab proteins on their way to be prenylated, protein synthesis in COS-7 cells was blocked with cycloheximide. The resulting lysate was biotin-geranylated with RabGGTase and enriched on streptavidin beads prior to Western blot analysis. If the observed bands originated from newly synthesized RabGTPases they should disappear upon inhibition of protein synthesis. Conversely, if they were a result of a pool of unprenylated proteins, they should remain unaffected. The pool of unprenylated proteins in COS-7 cells was reduced but not abolished by cycloheximide treatment (Figure 3-17 B, lane 9). Several minor bands disappeared following the treatment, which suggests that

they may represent newly synthesized proteins on their way to be prenylated. The intensity of the most dominant lower band remained essentially unchanged, indicating that the RabGGTase substrate(s) is/are present in the cell in the unprenylated form for several hours. To verify this assumption, COS-7 cells were incubated with cycloheximide and compactin to simultaneously block isoprenoid and protein synthesis. This resulted in a mixture of endogeneously unprenylated proteins and of unprenylated newly synthesized RabGTPases, similar to the untreated case (Figure 3-17 B, lane 3).

In order to test whether the unprenylated RabGTPase pool could also be detected directly in the tissues of living organisms, as shown for COS-7 cells, mouse brains and livers, provided by Oliver Leske (Prof. Heumann, Ruhr-Universität Bochum), were lysed, *in vitro* prenylated with recombinant RabGGTase/REP-1/BGPP, and enriched by streptavidin pulldown. Enzyme-independent high molecular weight bands were detected that most probably represented endogenous biotinylated proteins in mouse tissue (Figure 3-17 C).

For the lysate derived from mouse liver, these endougenously biotinylated proteins dominated the Western blot. Only a minor band in the 25 kDa range was detected, which was absent in the control experiment where BGPP had been omitted.

The abundance of RabGTPases in lysate derived from mouse brain was much higher and clearly visible (Figure 3-17 C). This finding is not surprising since Rab proteins were first identified as ras-related genes expressed in rat brains[316]. Thus, using BGPP as a protein prenyltransferase substrate even the minor pool of unprenylated RabGTPases in lysates derived directly from mouse tissue could be isolated.

3.2.4 Engineering FTase and GGTase-I mutants capable of BGPP transfer

The developed methodology allows for an efficient detection and isolation of RabGGTase substrates in mammalian cells and tissues. Compared to other methods (e.g. radioactive labeling; prenylation with derivatized isoprenoids such as the NBD-tagged isoprenoids **16**, **17** or the aniline-functionalized AGPP **13**, which can be detected by specific antibodies[317]; or the use of anti-farnesyl/geranylgeranyl antibodies[318, 319]) the developed technology is less laborious, displays higher sensitivity, enabling a detection of as little as 10 fmol of prenylated protein, and is highly efficient in enriching the prenylation products.

Using this approach, questions regarding RabGTPase biogenesis, e.g. expression profiles in different cell types, the rates of Rab expression and prenylation, and the effect of prenylation modulators (section 1.4), can be clarified. Given the importance of the prenylation substrates of the other two protein prenyltransferases for cellular biogenesis and disease, it would be of great value to expand this methodology to the other two enzymes. However, BGPP is an efficient lipid donor for RabGGTase only. The finding that the isoprenoid analog retains the

ability to bind to FTase with high affinity but fails to be transferred can be explained either by the molecular ruler hypothesis or the second site exclusion model, which was discussed in the introduction. The second model was favored since the diphosphate group of the lipid makes the largest contribution to the overall binding energy by interaction with the positively charged part of the active site (section 3.1.3).

Structural analysis of the FTase:BGPP complex. In order to provide the experimental proof for this assumption, Dr. Zhong Guo (Prof. Roger S. Goody, Department of Physical Biochemistry, Max-Planck-Institut für molekulare Physiologie, Dortmund) crystallized wild-type FTase in complex with BGPP and determined its structure by X-ray crystallography to 2.8 Å resolution. Structural analysis revealed that BGPP binds to the active site of FTase in a bent conformation. As anticipated, the diphosphate and geranyl group of BGPP bind to the same site as FPP in the FTase:FPP:protein substrate complex (Figure 3-18 A, B).

In contrast, the terminal part of the molecule is bent by 90°, pointing towards the opening of the active site due to the overall length and the bulkiness of the terminal biotin moiety. Superimposition of the FTase:BGPP and the FTase:FPP:protein substrate complexes provides an explanation for the failure of FTase to transfer BGPP. The distal part of the lipid cannot be optimally accommodated by the lipid binding pocket present in the FTase active site. Therefore, it protrudes into the peptide binding site of the enzyme and prevents the proper positioning of the protein substrate (Figure 3-18 C). Consistent with the arguments from the biochemical view point mentioned earlier (section 3.1.3), this strengthens the assumption that the failure of FTase to accept BGPP as a substrate can be explained by the second site exclusion model, as postulated by Distefano and co-workers[38].

Comparison of the recently solved high resolution structure of RabGGTase in complex with GGPP[36] with the structures of CAAX prenyltransferases in complex with their respective lipid substrates provides insight into the possible structural differences between RabGGTase and the other protein prenyltransferases, which turns out to be coupled to their ability to transfer BGPP[22, 36]. At first glance, it seems likely that the size of BGPP in combination with the depth of the lipid binding pocket of the CAAX prenyltransferases is the origin of the inability of BGPP to serve as an efficient substrate. The length of BGPP, however, is unlikely to be the only explanation since GGTase-I, which possesses a sufficiently deep isoprenoid binding site to accommodate GGPP, is also inefficient in transferring BGPP. As shown in the next section (Figure 3-19 A-C), this is in accord with the finding that the mutants FTase_{W102T_Y365F} and FTase_{W102T}, which constitute mutations that have been shown to interconvert the FTase and GGTase-I lipid specificity[20, 320], transferred biotin-geranyl onto CFP-CAAX very inefficiently and not at all, respectively.
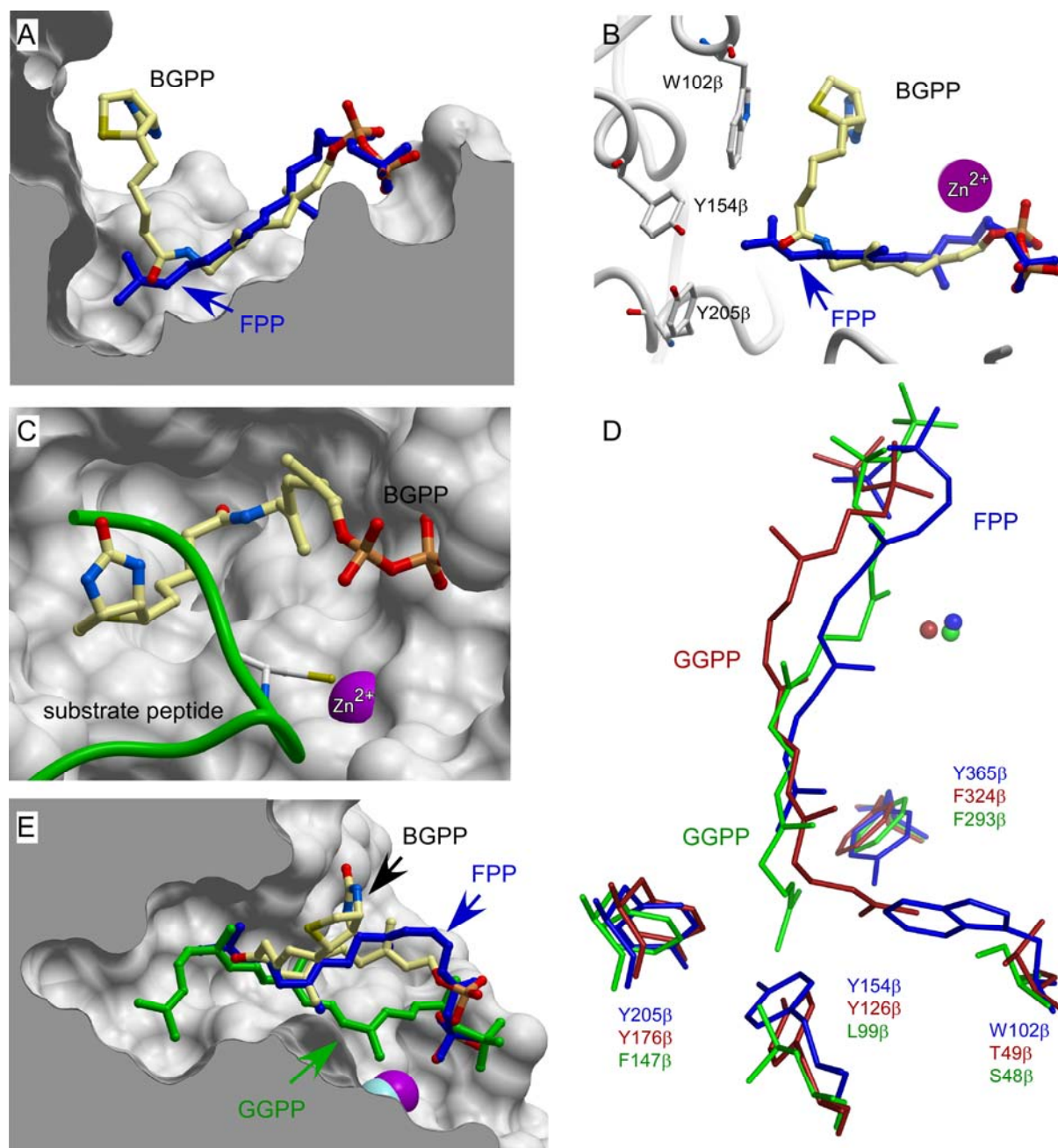
Figure 3-18 Structural analysis of the BGPP:FTase complex. **A** Side view of the optically sliced active site of FTase in surface representation with bound BGPP. BGPP is shown in ball-and-stick representation, colored according to atom type. The FPP molecule colored in blue is placed for comparison into the active site based on the FPP analog:FTase:peptide complex structure (PDB:1D8D). **B** Worm representation of the active site of FTase complexed to BGPP. The aromatic residues of the beta subunit, W102β, Y154β, and Y205β, that form the bottom of the lipid binding site, are displayed in ball-and-stick representation. The isoprenoid molecules are labeled as in **A**. **C** Top view of the FTase active site in surface representation with bound BGPP displayed as in **A**. The peptide substrate displayed as a green worm is placed into the active site based on the FPP analog:FTase:peptide complex. The reactive cysteine is shown in ball-and-stick representation, while the catalytic Zn^{2+} ion is displayed as a magenta van der Waals sphere. **D** Superimposition of the critical amino acids at the bottom of the lipid binding pocket in complex with the respective lipid in the FTase:FPP (PDB:1D8D), GGTase-I:GGPP (PDB:1N4P), and the RabGGTase:GGPP (PDB:3DST) complex. **E** Optical slice through the active site of the RabGGTase: GGPP complex structure superimposed with structures of FPP:FTase:peptide and BGPP:FTase complexes.

Analysis of GGPP in complex with RabGGTase and GGTase-I showed that the coordination of the fourth isoprene unit of GGPP is substantially different in the two enzymes (Figure 3-18 D, E). In GGTase-I, the terminal isoprenoid unit is directed towards T49β and F324β in the GGTase-I:GGPP complex. In RabGGTase, in contrast, the fourth isoprene unit points towards S48β and L99β (analogous to T49β and Y126β in GGTase-I), as revealed in the recently solved RabGGTase:GGPP complex[36]. Compared to the corresponding amino acids in FTase and GGTase-I, the leucine is replaced by a bulky tyrosine side chain in both FTase and GGTase-I (Y154β and Y126β, respectively). This may provide a mechanistic explanation for the ability of the bulky BGPP to penetrate more deeply into the lipid binding cavity of RabGGTase, which may not be possible in FTase and GGTase-I (Figure 3-18 D, E). This reasoning is in accordance with studies with *cis* and *trans*-isoprenylpyrophosphate synthases, which carry conserved amino acids in the active site. These bulky amino acid residues have been demonstrated to play essential roles in determining the product chain length by blocking further product elongation[321, 322].
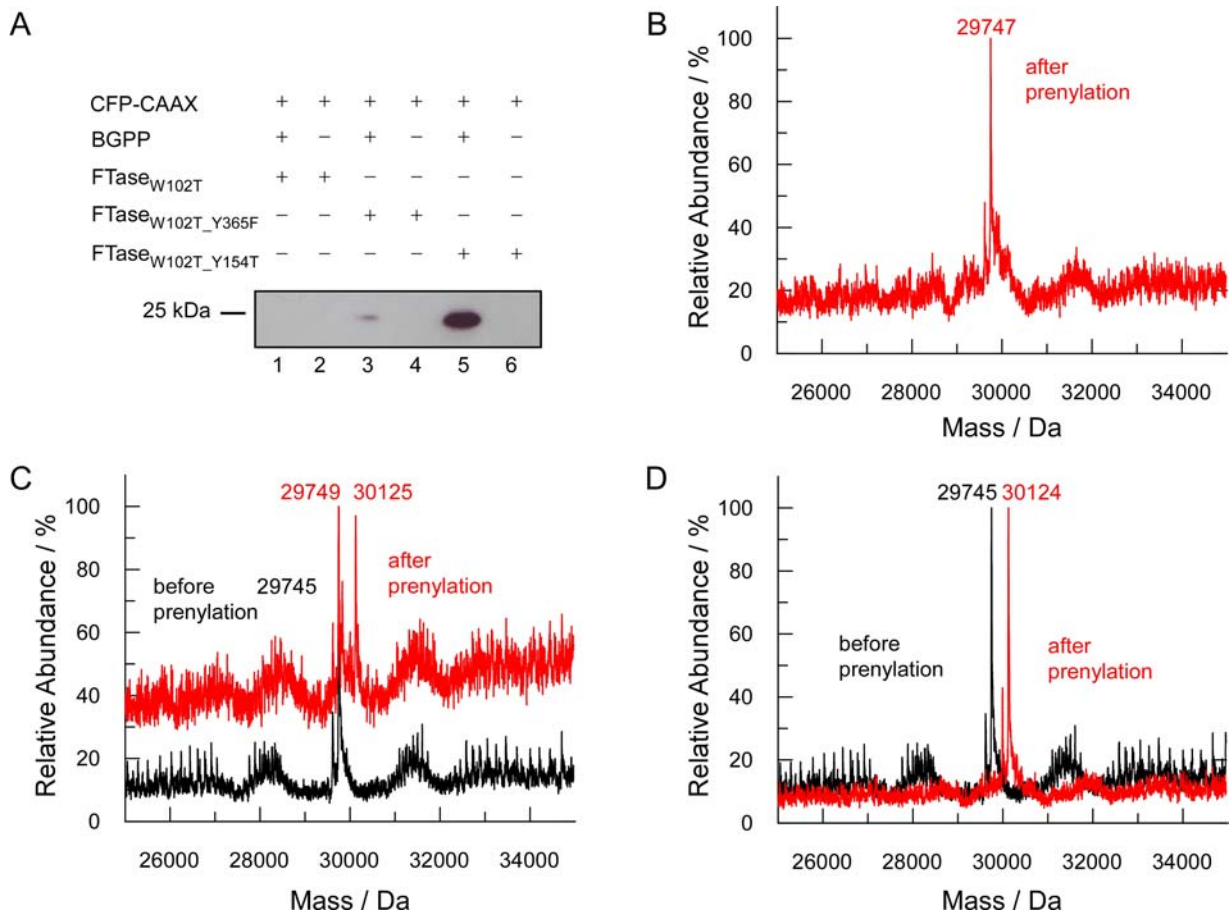
Figure 3-19 First round of engineering of an FTase mutant capable of utilizing BGPP as a lipid donor. **A** Western blot analysis of CFP-CAAX (CFP-TKCVIM) *in vitro* biotin-geranylated with FTase$_{W102T}$ (lane 1 and 2), FTase$_{W102T\_Y365F}$ (lane 3 and 4), and FTase$_{W102T\_Y154T}$ (lane 5 and 6). **B-D** ESI-MS analysis of CFP-CAAX *in vitro* biotin-geranylated by FTase$_{Y154T}$ **B**, FTase$_{W102T\_Y365F}$ **C**, or FTase$_{W102T\_Y154T}$ **D** (black: spectra of unprenylated CFP-CAAX, red: mono-prenylated CFP-CAAX). For better illustration, the unprenylated spectrum was omitted for **B**.

Design of a BGPP-transferring FTase mutant. The structural differences in the depth and width of the active sites between FTase, GGTase-I, and RabGGTase provided guidance for the design of FTase and GGTase-I mutants that would be capable of utilizing BGPP as a substrate. Interestingly, a similar strategy has been employed to engineer *trans*-isoprenylpyrophosphate synthases that can produce longer lipid polymers[323, 324].

To mimic the lipid binding site of RabGGTase, a double mutant FTase$_{W102T\_Y154T}$ was engineered by site-directed mutagenesis, which has threonines instead of the more bulky native groups at the bottom of the isoprenoid binding pocket. The mutant efficiently transferred biotin-geranyl onto recombinant K$_i$-Ras or other CAAX-tagged proteins such as CFP-CAAX *in vitro*, as confirmed by Western blot (Figure 3-19 A). ESI-MS analysis revealed that CFP-CAAX was entirely converted to the biotin-geranylated product (Figure 3-19 D).

Compared to wild-type RabGGTase, however, the catalytic efficiency of the mutant enzyme was low. In order to elucidate the structural changes that occurred in the FTase$_{W102T\_Y154T}$:BGPP complex compared to the wild-type enzyme and to find a solution to further improve the activity of the mutants, Dr. Zhong Guo solved the complex structure to 2.75 Å resolution.

Superimposition of the complexes of BGPP bound to wild-type FTase and FTase$_{W102T\_Y154T}$ revealed that the mutation to the less bulky amino acids resulted in an expansion of the active site, similar to that of RabGGTase. As a result, the terminal part of BGPP is inserted into the newly formed cavity in an almost completely extended conformation (Figure 3-20 A). The first 15 carbon atoms of BGPP are located at positions nearly identical to the lipid chain of FPP and BGPP in the wild-type FTase:FPP and wild-type FTase:BGPP structures, respectively.

As can be seen in Figure 3-20 B, however, the location of the oxygen group of the biotin moiety is still very close to the side chains of the CAAX peptide; this may result in sterical clashes between the two substrates and hence a lower catalytic efficiency (Figure 3-20 C, D). We anticipated that an additional mutation of the bulky tyrosine Y205β to a smaller amino acid would further expand the active site and improve the activity of the mutant enzyme. *In vitro* prenylation of recombinant K$_i$-Ras using wild-type FTase, FTase$_{W102T\_Y154T}$, FTase$_{W102T\_Y205T}$, or FTase$_{W102T\_Y154T\_Y205T}$ (Figure 3-20 E, lanes 1-4, respectively) showed that the extent of prenylation at excess BGPP and equimolar concentrations of enzyme and protein substrate was similar after 4 h reaction time *in vitro*.

However, when the same experiment was repeated in lysate of compactin-treated COS-7 cells, the efficiencies of the mutants were different. Several prenylatable proteins were labeled by the FTase mutants (Figure 3-20 F, lanes 1-4). In all cases, the Western blots were dominated by high molecular weight species (~50-80 kDa), which are likely to represent nuclear lamins. The observation that the high molecular weight substrates were the most abundant ones among FTase substrates is in accord with earlier findings by Zhao and

Spielmann and co-workers[288, 317]. Additional intermediate (~ 40 kDa) and low molecular mass products (~ 25 kDa) could be detected even without an enrichment step. The 25 kDa signals probably represent small GTPases of the Ras family.

Notably, the detection of the RasGTPases underscores the sensitivity of the developed methodology in comparison to other developed functionalized isoprenoid analogs.

While being a good mimic of FPP, the incorporation of NBD-GPP into endogenous FTase substrates derived from compactin-treated COS-7 lysates does not result in detectable signals on SDS-PAGE gels (Dr. Christine Delon, unpublished results).

Spielmann and co-workers metabolically incorporated the aniline-derivatized isoprenoid analog **13** into compactin-treated HEK-293 cells. After lysate preparation, visualization of protein substrates that had been labeled was achieved by using antibodies directed against the aniline moiety, which enabled them to detect substrates in the 45-66 kDa range[317]. However, endogenous RasGTPases could only be detected when overexpressed, probably because of the limited detection sensitivity of their system (Figure 3-20 G).

Zhao and co-workers followed the same procedure to incorporate the azide-tagged lipid donor **22** into endogenous FTase substrates of COS-1 cells[288]. The prenylation pattern obtained in their experiments displayed numerous bands, in addition to the two prominent high molecular weight bands detected by Spielmann and co-workers. While some very faint bands were observed in a range corresponding to small RasGTPases and γ-subunits of trimeric G proteins, these bands were overlaid by background signals of the biotin-functionalized phosphine reactant (Figure 3-20 H). Nevertheless, the overall pattern looks very similar to that obtained in our studies, suggesting that our engineering procedures retained the substrate specificity of the resulting FTase mutants. Thus, comparison of our strategy to existing methodologies underlines the further improvement in sensitivity and a minimized background labeling in our system.

The prenylation pattern of the double and triple FTase mutants was similar, but the intensity of the bands, especially in the low and high molecular weight range, as mentioned earlier, was significantly different. While the double mutant displayed more intense bands in the low molecular weight range, the triple mutant showed a higher extent of prenylation of high molecular weight substrates. Since maximal biotin-geranylation of the unprenylated proteins is desirable, an equimolar mixture of $FTase_{W102T\_Y154T}$ and $FTase_{W102T\_Y154T\_Y205T}$ was chosen for further work.
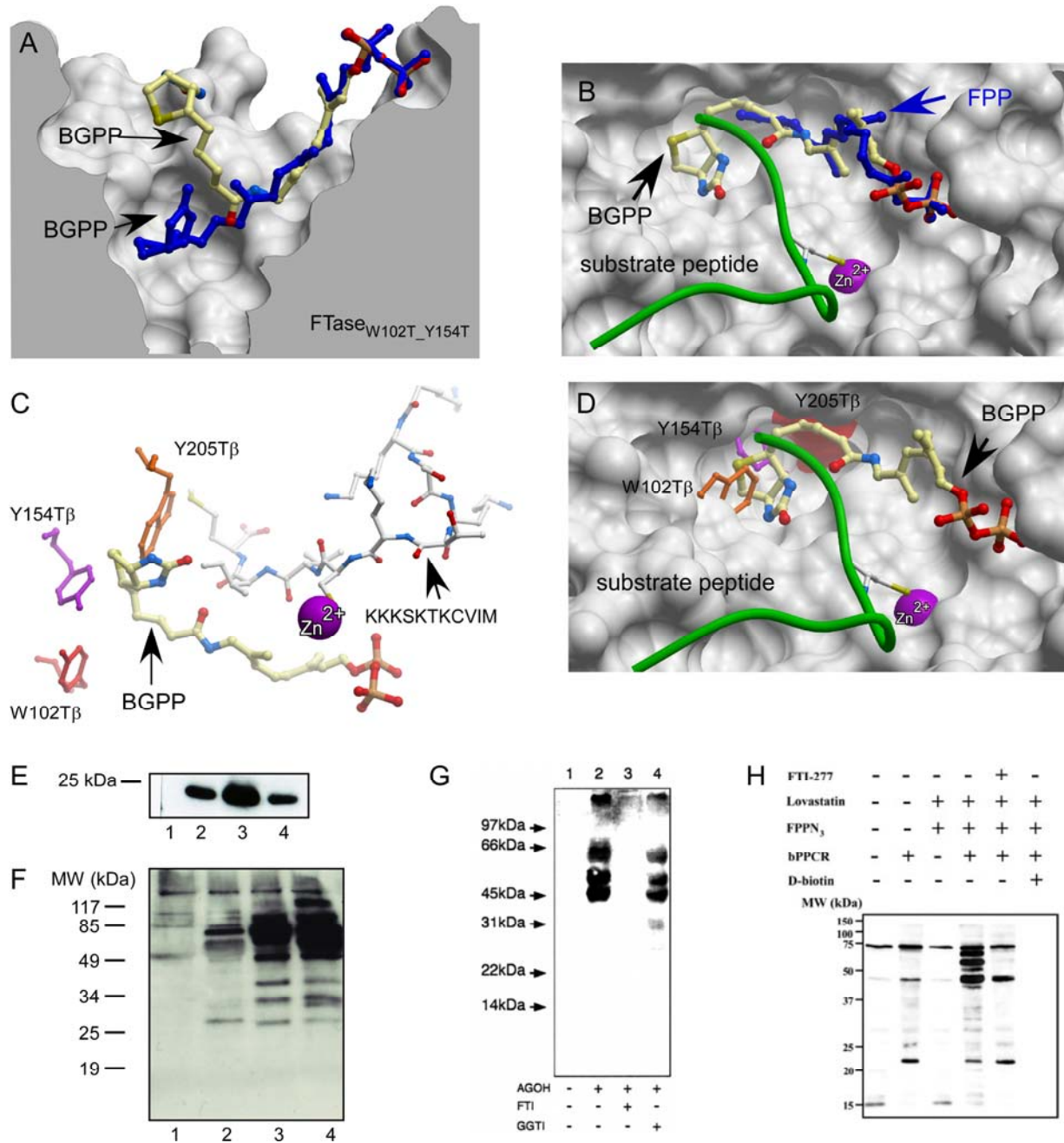
Figure 3-20 Second round of engineering of FTase mutants capable of utilizing BGPP as a lipid donor. **A** Optical slice through the active site of the FTase$_{W102T\_Y154T}$:BGPP complex superimposed with the structure of the wt FTase:BPP complex. The picture is drawn as in Figure 3-18 **A**, and the isoprenoid from the BGPP:FTase complex is shown in atomic colors while the BGPP in complex with the mutant is colored in blue. **B** Ball and stick representation of the active site of the wt FTase in complex with the FPP analog and peptide substrate superimposed with the BGPP from the BGPP:FTase$_{W102T\_Y154T}$ complex. **C** Worm representation of the active site of FTase complexed to BGPP. The aromatic residues of the β-subunit, W102β, Y154β, and Y205β, which form the bottom of the lipid binding site, are displayed in ball-and-stick representation. The isoprenoid molecules are labeled as in **A**. **D** as in **B**, and the residues W102β and Y154β of the wt FTase are displayed in ball and stick representation and colored in orange and pink, respectively. The residue Y205β which is mutated in the triple mutant is colored in red. **E**, **F** Comparison of the FTase mutants in their ability to prenylate the recombinant substrate K$_i$-Ras **E** or endogenous substrates in compactin-treated COS-7 lysate **F**. Lane 1- FTase wild-type, lane 2- FTase$_{W102T\_Y154T}$, lane 3- FTase$_{Y154T\_Y205T}$, lane 4- FTase$_{W102T\_Y154T\_Y205T}$. **G**, **H** Prenylation pattern of FTase prenylation in mammalian lysate reported by Spielmann and co-workers **G**[317] and Zhao and co-workers **H**[288].

Design of a BGPP-transferring GGTase-I mutant. We followed the same strategy for expanding the lipid binding pocket to engineer a variant of GGTase-I capable of accepting BGPP as an efficient substrate. Since the bulky amino acid W102β in FTase is already occupied by a Thr residue in the GGTase-I active site, a single mutation (Y126Tβ) was introduced to mimic the RabGGTase lipid binding pocket. An *in vitro* prenylation assay showed that the Y126Tβ mutant could catalyze the biotin-geranylation of recombinant GST-RhoA (Figure 3-21 A). The efficiency of transfer was slightly enhanced compared to wild-type GGTase-I (Figure 3-21 B), but was still much lower than that of RabGGTase or the engineered double and triple FTase mutants. In addition, prenylation with BGPP never reached completion and could not be detected when using less than 20 pmol of recombinant protein on the Western blot. This result was surprising, since the active site of the GGTase-I mutant was expanded to a comparable extent to that of RabGGTase or FTase$_{W102T\_Y154T}$. This suggests that there might be a second structural requirement for BGPP to function as an efficient protein prenyltransferase substrate, other than just an enlarged lipid binding cavity.
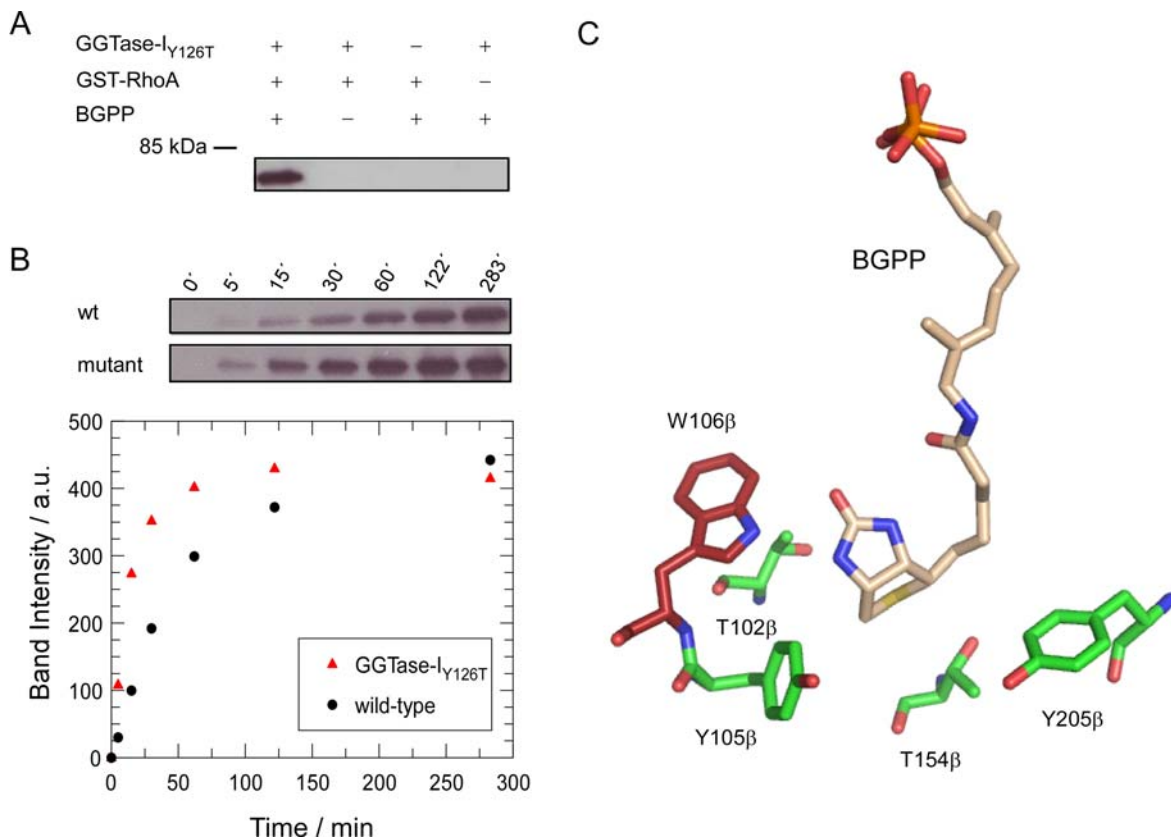
Figure 3-21 First round of engineering of a GGTase-I mutant capable of utilizing BGPP. **A** Mutation of Y126Tβ in GGTase-I leads to a specific incorporation of biotin-geranyl into GST-RhoA. **B** Comparison of the prenylation efficiencies of GGTase-I$_{Y126T}$ and the wild-type enzyme, which was analyzed by Western blot analysis. The band intensities were determined using the AIDA software. **C** Representation of the mutated amino acids as well as Y105β and W106β at the bottom of the lipid binding pocket of FTase$_{W102T\_Y154T}$ in complex with BGPP

Therefore, the structures of the three wild-type enzymes in complex with their respective isoprenoid substrates were re-analyzed, revealing the presence of two conserved residues, Y105β/W106β and Y51β/W52β, in wild-type FTase and RabGGTase, respectively, which are replaced by phenylalanine in wild-type GGTase-I (F52β and F53β). Interestingly, the benzyl ring of F53β and of the analogous amino acids in FTase and RabGGTase point into the isoprenoid binding pocket. This could hint at an important hydrogen bonding to the oxygen of the terminal carbonyl group of BGPP that might be important for catalysis, as shown in Figure 3-21 C. Therefore, one could conjecture that a replacement of F53β by a tyrosine would enhance the catalytic efficiency of GGTase-I by positioning the biotin group in the active site for efficient catalysis. In contrast, the control mutation F52Yβ should not have such an effect, since the side chain of this amino acid does not point towards the bound BGPP in the active site (Figure 3-21 C).

Comparison of the transfer efficiency of GGTase-I$_{Y126T}$, GGTase-I$_{F52Y\_Y126T}$, GGTase-I$_{F53Y\_Y126T}$, and GGTase-I$_{F52Y\_F53Y\_Y126T}$ demonstrated that, as expected, mutation to tyrosine at position 53β led to a dramatic increase in the extent of prenylation of recombinant RhoA along with an enhanced catalytic activity, while a mutation at position 52β did not improve, but instead lowered the efficiency of BGPP transfer (Figure 3-22 A).

Similar results were obtained when the same experiment was repeated in lysate derived from compactin-treated COS-7 cells (Figure 3-22 B). The extent of prenylation was highest for GGTase-I$_{F53Y\_Y126T}$ and GGTase-I$_{F52Y\_F53Y\_Y126T}$. We chose to further work with GGTase-I$_{F53Y\_Y126T}$, since the potency of this mutant was essentially the same as the triple mutant.
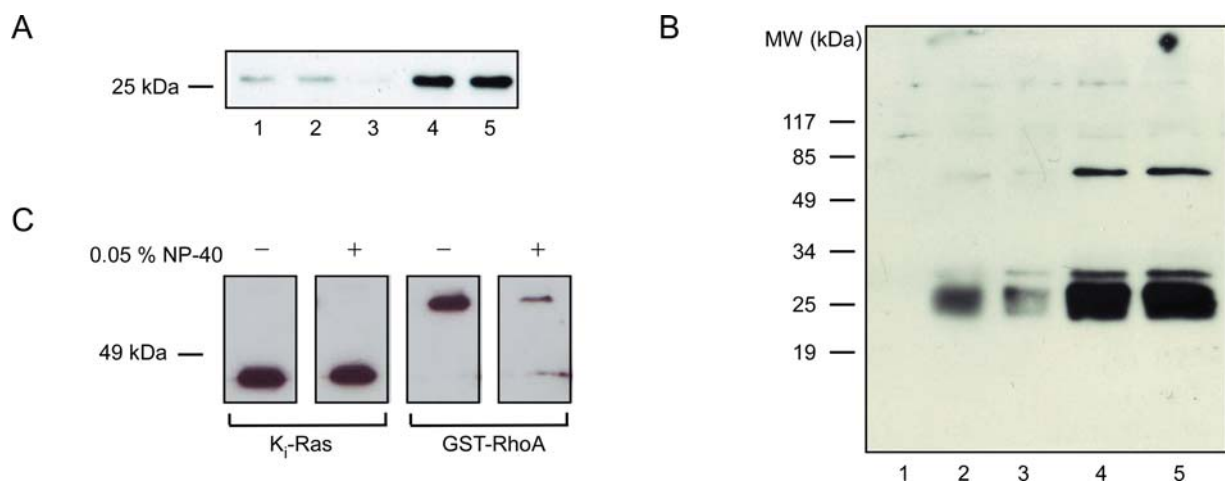
Figure 3-22 Second round of engineering of a GGTase-I mutant capable of transferring BGPP. **A**, **B** Comparison of the prenylation efficiencies of the designed GGTase-I mutants using Western blot analysis of equal amounts of recombinant RhoA **A** or of the lysate of compactin-treated COS-7 cells **B**. Lane 1- wild-type GGTase-I, lane 2- GGTase-I$_{Y126T}$, lane 3- GGTase-I$_{F52Y\_Y126T}$, lane 4- GGTase-I$_{F53Y\_Y126T}$, and lane 5- GGTase-I$_{F52Y\_F53Y\_Y126T}$. **C** To investigate the effect of NP-40 detergent on the biotin-geranylation of K$_i$-Ras and RhoA by mutants of FTase and GGTase-I, respectively, *in vitro* prenylation experiments were carried out as in **A** in the presence or absence of 0.5 % NP-40, and the samples were analyzed by Western blot. The presence of detergent did not significantly affect the FTase-mediated prenylation but significantly inhibited the activity of GGTase-I.

The prenylation pattern of GGTase-I$_{F53Y\_Y126T}$ in compactin-treated COS-7 lysate was substantially different from that of the FTase mutants. It was dominated by numerous signals that were exclusively in the 20-25 kDa range, most probably representing Rho/RacGTPases (Figure 3-22 B). The prenylation pattern was practically identical to that obtained with NBD-FPP as a lipid donor in combination with wild-type GGTase-I; NBD-FPP constitutes the only GGPP analog equipped with a reporter group available so far that allows for the labeling of endogenous GGTase-I substrates in mammalian lysate (Dr. Christine Delon, unpublished). A major difference, however, is the sensitivity of BGPP, which is significantly higher compared to NBD-FPP.

The protocol for lysate preparation had to be adapted to the conditions of prenylation using GGTase-I. Typically, 0.05 % NP-40 was utilized for cell lysis. This detergent, however, appeared to inhibit prenylation of GGTase-I at the concentration used (Figure 3-22 C). Therefore, cells were lysed by mechanical disruption using a 0.55 mm syringe needle.

Investigation of peptide substrate specificity of the mutants. While the obtained prenylation patterns suggested that the FTase and GGTase-I mutants orthogonally deliver biotin-geranyl to their native protein substrates, previous studies have shown that either changes in the native isoprenoid structures or mutations in the active site of FTase and GGTase-I near the CAAX peptide binding sites may influence the substrate specificities of both enzymes[295, 325, 326].

As mentioned in section 1.2.2, Beese and co-workers mutated W102β and Y365β in the FTase active site and thereby interconverted the lipid substrate specificities of FTase and GGTase-I. Surprisingly, this retained the peptide preference for CVLS, a typical FTase CAAX motif, in comparison to CVLL, a typical GGTase-I CAAX motif.

Following this line of experiment, Dr. Yao-Wen Wu (Prof. Roger S. Goody, Department of Physical Biochemistry, Max-Planck-Institut für molekulare Physiologie, Dortmund) investigated the substrate specificity of FTase$_{W102T\_Y154T}$, FTase$_{W102T\_Y154T\_Y205T}$, GGTase-I$_{F53Y\_Y126T}$, and GGTase-I$_{F52Y\_F53Y\_Y126T}$ using the described fluorescence assay with either dansyl-labeled GCVLS or GCVLL as a peptide substrate.

Wild-type FTase was discriminatory towards the two CAAX boxes CVLS and CVLL in the farnesylation process (Figure 3-23 A). The fluorescence increase observed in the presence of the CVLL probably represents residual catalytic activity.

In spite of significant changes in the active site, the triple GGTase-I mutant retained the native preference for CVLL compared to CVLS towards biotin-geranyl transfer (Figure 3-23 E).

Unexpectedly, only a minimal fluorescence increase was observed when using all other mutants in combination with BGPP (exemplary spectra shown in Figure 3-23 B). This was most probably due to a lack of increase in hydrophobicity upon prenylation, since Western

blot analyses had confirmed that biotin-geranyl was indeed transferred onto recombinant or endogenous CAAX substrates (Figure 3-20 and 3-22). Therefore, GGPP was employed as a lipid substrate for the analysis of the other mutants.

Both FTase$_{W102T\_Y154T}$ and FTase$_{W102T\_Y154T\_Y205T}$ displayed an excellent substrate specificity toward CVLS using GGPP as a lipid donor (Figure 3-23 C, D), whereas GGTase-I$_{F53Y\_Y126T}$ and GGTase-I$_{F52Y\_F53Y\_Y126T}$ preferred the native GGTase-I CAAX box CVLL over CVLS (Figure 3-23 F, G).
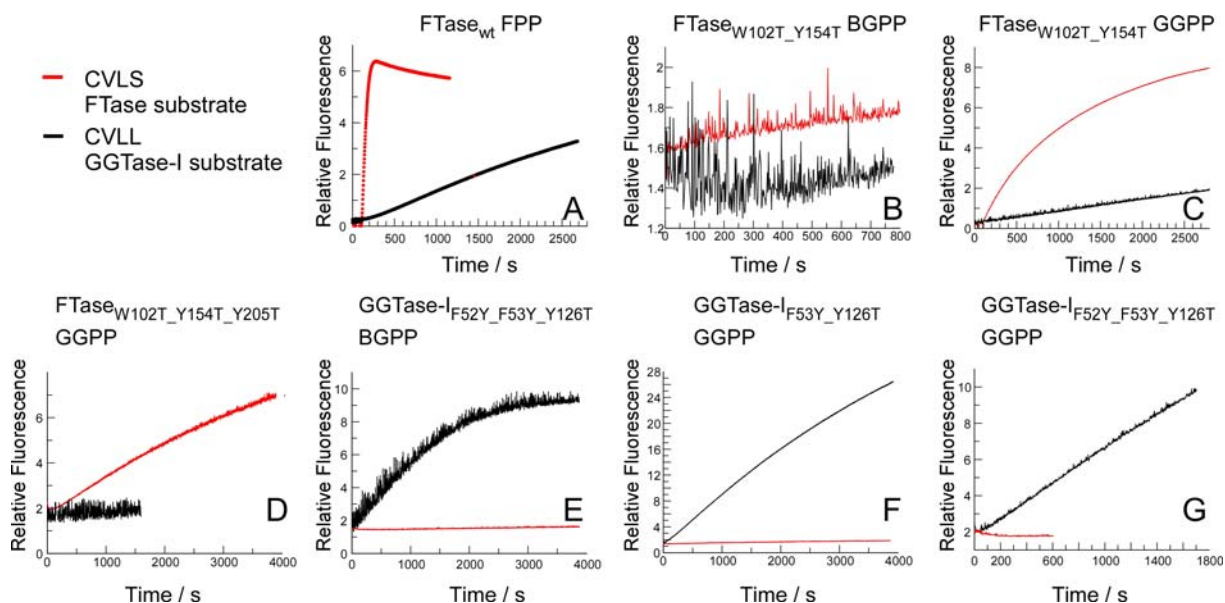
Figure 3-23 Specificity of FTase and GGTase-I mutants towards dansyl-GCVLS and dansyl-GCVLL peptide substrates. Prenylation reaction of wild-type FTase with FPP **A**, FTase$_{W102T\_Y154T}$ with BGPP **B** or GGPP **C**, FTase$_{W102T\_Y154T\_Y205T}$ with GGPP **D**, GGTase-I$_{F52Y\_F53Y\_Y126T}$ with BGPP **E** or GGPP **G**, or of GGTase-I$_{F53Y\_Y126T}$ with GGPP **F** were performed as described in Materials and Methods. Equal amounts of substrates were used for each test pair. The fluorescence increase observed in **C** where FTase$_{W102T\_Y154T}$ was incubated with GGPP and the GGTase-I substrate was also observed in case of **A** and probably represented residual catalytic activity. The experiments were performed by Dr. Yao-Wen Wu.

The analysis demonstrates that the peptide substrate specificity towards CVLL and CVLS was not significantly altered in all protein prenyltransferase mutants tested for GGPP prenylation. However, while the mutations did not eliminate the native peptide specificities of FTase and GGTase-I for CVLS and CVLL, the effects of the mutations on the overall recognition of the CAAX sequence require further investigation.

Since BGPP prenylation in most cases did not result in a fluorescence change, it cannot be excluded that BGPP changes the substrate specificity for CVLL and CVLS of those mutants tested. Many studies have reported altered peptide specificities due to modifications in the isoprenoid chains[325, 326]. It is believed, however, that changes in the first geranyl unit affect the peptide specificity of FTase, whereas modifications adjacent to the first geranyl unit do not influence the peptide preference. Therefore, it is likely that BGPP will not change the peptide

specificities of the prenyltransferase mutants. However, additional experiments are necessary to confirm this reasoning.

3.2.5 Analysis of the entire cellular prenylome

The results obtained suggest that the developed strategy enables a selective labeling of the complete set of protein prenyltransferase substrates in complex mixtures such as cellular lysates. In an attempt to tag and detect all prenylatable proteins, i.e. the prenylome, simultaneously, compactin lysate was supplemented with 2 µM RabGGTase, 2 µM REP-1, and 5 µM BGPP, and the reaction was allowed to proceed for 2 h at room temperature. Subsequently, 20 µM $ZnCl_2$ as well as 1 µM $FTase_{W102T\_Y154T}$, 1 µM $FTase_{W102T\_Y154T\_Y205T}$, 2 µM $GGTase_{F53Y\_Y126T}$, and 5 µM BGPP were added and reacted for another 4-6 h at room temperature. The prenylation mixture was subjected to SDS-PAGE and Western blot analysis. When all three enzymes acted simultaneously, a prenylation pattern was obtained that represented an overlay of those of the individual protein prenyltransferases (Figure 3-24). This further demonstrates that the mutant prenyltransferases faithfully and orthogonally deliver biotin-geranyl to their cognate substrates, resulting in the first affinity-tagging and isolation of the entire cellular mammalian prenylome reported to date.
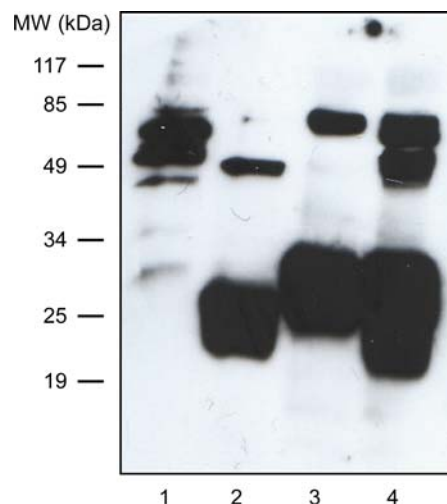
Figure 3-24 Analysis of the cellular mammalian prenylome. Cell lysates were prenylated with different engineered protein prenyltransferases. Lane 1- lysates prenylated with $FTase_{W102T\_Y154T\_Y205T}$, lane 2- with GGTase-$I_{F53Y\_Y126T}$, lane 3- with RabGGTase, lane 4- with all three protein prenyltransferases.

3.2.6 Effect of protein prenyltransferase inhibitors on the prenylome

Since the developed methodology enables the assessment of the status of all prenylatable proteins in the cell, it can be applied for monitoring the effect of prenylation-modulating drugs such as protein prenyltransferase inhibitors[327]. This is particularly important because some of the compounds that had been developed as specific inhibitors of a single protein prenyltransferase have reached clinical trials without full assessment of their cross-reactivity towards the other two enzymes, mainly owing to a lack of appropriate technologies, as described in section 1.4.
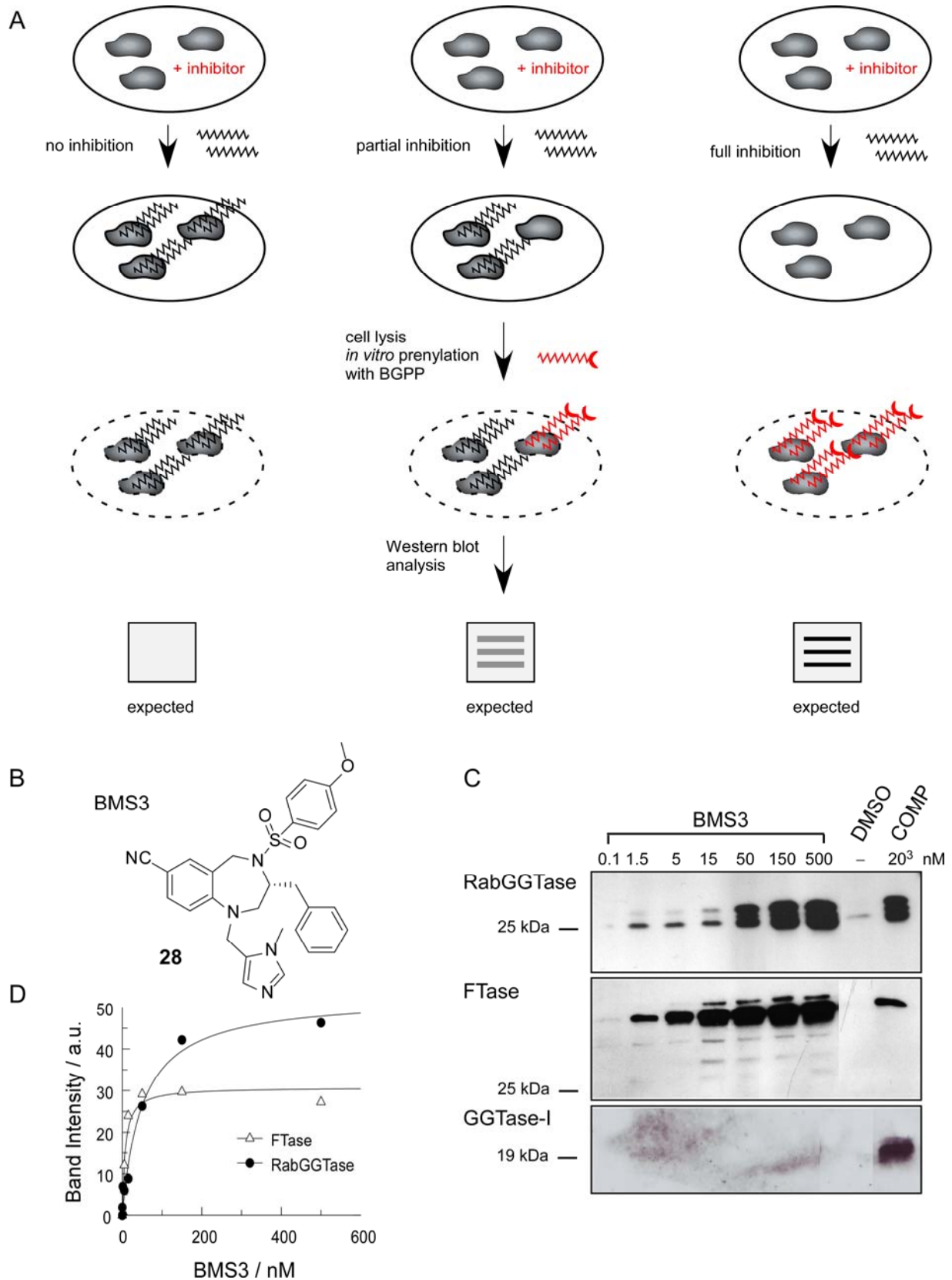
Figure 3-25 Evaluation of the *in vivo* activity of BMS3. **A** Schematic overview on inhibitor treatment of cells, lysate preparation, *in vitro* prenylation with BGPP, and Western blot analysis. **B** Chemical structure of BMS3. **C** Inhibition of protein prenylation in COS-7 cells treated with BMS3 for 18 h. The cell lysates were prenylated with the respective protein prenyltransferases (FTase$_{W102T\_Y154T}$ and FTase$_{W102T\_Y154T\_Y205T}$, GGTase-I$_{F53Y\_Y126T}$, or RabGGTase) and analyzed by Western blot. **D** Quantification of results shown in **C** and calculation of the $K_{i,app}$ values for BMS3 and the respective protein prenyltransferase.

In order to demonstrate that a prenylome-wide analysis of such off-target effects can be performed using the developed technology, the benzodiazepine compound BMS3 (Figure 3-25 B), synthesized by Dr. Robin S. Bon (Prof. Waldmann, Department of Chemical Biology, Max Planck Institute of Molecular Physiology, Dortmund), was chosen as a model inhibitor[220]. COS-7 cells were treated with increasing concentrations of BMS3 up to 500 µM for 18 h and analyzed for the presence of unprenylated proteins upon inhibition of the protein prenyltransferases by BMS3 (Figure 3-25 A). The cells were lysed, and the resulting lysate was prenylated with BGPP using either $FTase_{W102T\_Y154T}$/ $FTase_{W102T\_Y154T\_Y205T}$, GGTase-$I_{F53Y\_Y126T}$, or wild-type RabGGTase/REP-1. As references, compactin- and DMSO-treated cells were used as fully unprenylated or fully prenylated control, respectively.

Western blot analysis of the prenylation mixtures revealed that BMS3 fully inhibited RabGGTase and FTase at the highest concentrations used, while prenylation of the GGTase-I substrates remained unaffected (Figure 3-25 C), in accordance with the *in vitro* data reported by Ross-MacDonald and co-workers[220]. Evaluation of the Western blot signal intensities using the AIDA software revealed K_i values of 50 and 7 nM for FTase and RabGGTase, respectively (Figure 3-25 D). These values cannot be regarded as IC_{50} values, since the reference representing the supposedly fully inhibited situation, the compactin-treated COS-7 cells, showed less intense bands than the BMS3-treated cells. This hints at a salvage pathway for FPP synthesis other than that derived from mevalonate.

These results provide the first quantitative *in vivo* protein prenyltransferase inhibition data, demonstrating that BMS3 is a potent dual specificity inhibitor of FTase and RabGGTase *in vivo*. Compared to the IC_{50}s *in vitro*, the values are higher, most probably due to inefficient uptake inside the cell, chemical instability of the compound, and/or its metabolic degradation.

To further corroborate the utility of the developed approach as a novel and powerful method for monitoring changes in protein prenylation in eukaryotic cells in response to therapeutic compounds, the *in vivo* effects of two established commercially available protein prenyltransferase inhibitors, FTase inhibitor B581 and GGTI-298, were investigated.

COS-7 cells were treated with B581 at concentrations ranging from 2 to 100 µM[328]. In accordance with earlier studies, B581 is a selective peptomimic inhibitor of FTase[329, 330]. Surprisingly, however, it did not show complete inhibition of FTase even at a concentration of 100 µM (Figure 3-26 A-C). The discrepancy to the literature reports may be explained that the inhibitory effect of B581 was investigated on Ras and lamin A prenylation, on its reverse transforming properties in Ras-transformed cells, and on the MAPK pathway controlled by Ras, wheras the overall FTase inhibition on all its substrates as well as the extent of the overall inhibition remained unclear. The failure of complete inhibition of FTase by B581 may result from a low affinity of the inhibitor for FTase, a complex inhibition mechanism, or cross-prenylation of FTase substrates in the FTI-treated cells by GGTase-I.

In addition, the developed technology experimentally confirmed the lack of inhibitory activity of B581 towards RabGGTase (Figure 3-26 C), which had been unclear before.
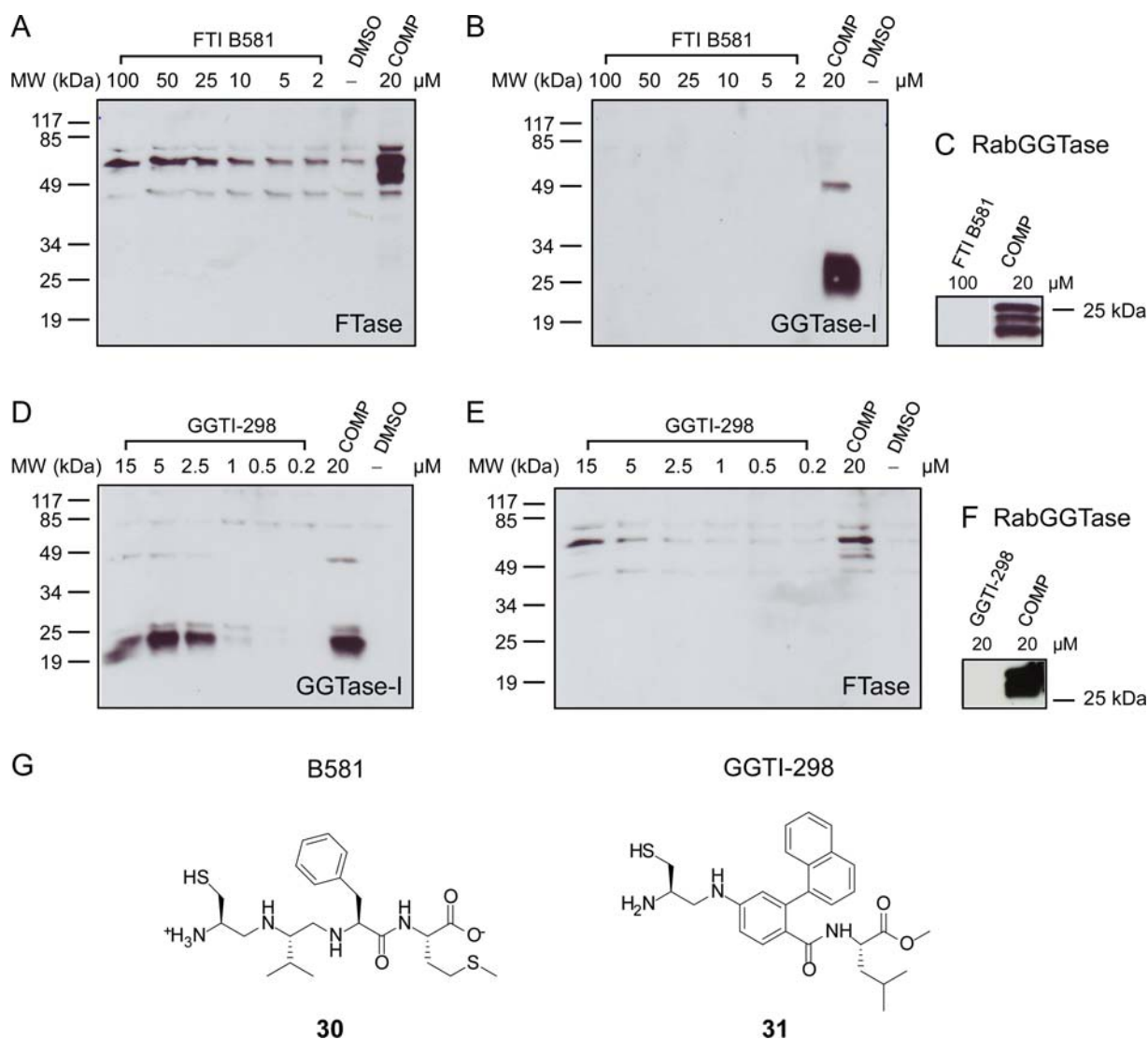
Figure 3-26 Inhibition of protein prenylation in COS-7 cells by FTI B581 and GGTI-298. The lysates of COS-7 cells were analyzed for the presence of unprenylated substrates upon inhibition of FTase **A**, **E**, GGTase-I **B**, **D**, and RabGGTase **C**, **F**. Cells were treated with the indicated concentrations of FTase inhibitor B581 **A-C** or GGTI-298 **D-F**. Lysates were collected, *in vitro* prenylated with the respective wild-type or mutant protein prenyltransferase as in Figure 3-25, and processed for Western blot with STR-HRP. **G** Chemical structure of B581 (left) and GGTI-298 (right). Cell treatment and lysate preparation were performed by Dr. Christine Delon.

GGTI-298 is regarded as a specific inhibitor of GGTase-I without affecting the processing of H-Ras *in vivo* even at concentrations of up to 15 µM. While the outcome of its influence on important signal transduction pathways has been thoroughly studied[331-335], its *in vivo* specificity towards the other two protein prenyltransferases is not established since the inhibitory effect of GGTI-298 has mainly been tested on H-Ras and lamin B prenylation only.
COS-7 cells were treated with varying concentrations of GGTI-298 up to 15 µM. The resulting lysates were prenylated with BGPP using either FTase mutants, GGTase-I mutant, or wild-type RabGGTase/REP-1. In accordance with the described studies, there was full *in vivo*

inhibition of GGTase-I at concentrations above 5 µM and no activity towards RabGGTase (Figure 3-26 D and F, respectively). Surprisingly, the compound also inhibited FTase at a concentration of 15 µM, since high molecular weight bands could be observed (Figure 3-26 E). This experiment strongly suggests that GGTI-298 is less specific *in vivo* than previously believed.
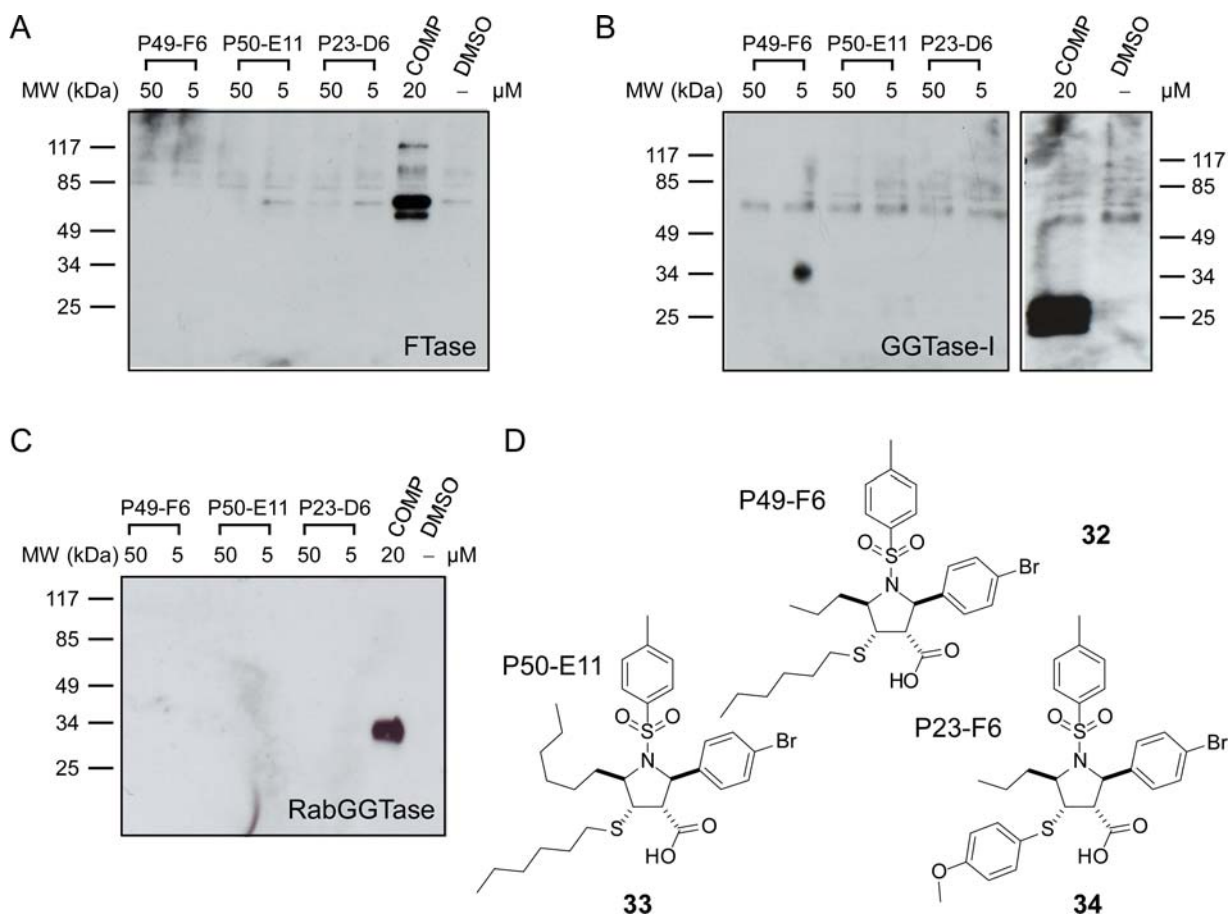
Figure 3-27 *In vivo* evaluation of pyrrolidine-derived protein prenyltransferase inhibitors. Cells were treated with 5-50 µM P49-F6, P50-E11, and P23-D6 or 20 µM compactin or DMSO as positive or negative control, respectively. The resulting lysates were biotin-geranylated using FTase mutants **A**, GGTase-I mutant **B**, or wild-type RabGGTase **C**. **D** Chemical structures of P49-F6, P50-E11, and P23-D6, which were synthesized by Dr. Céline Deraeve. Inhibitor treatment and lysate preparation was performed by Dr. Christine Delon.

Further, the *in vivo* effect of three recently described pyrrolidine-based inhibitors of RabGGTase, P49-F6, P50-E11, and P23-D6, were analyzed (Figure 3-27 D)[336]. All three compounds were demonstrated to be specific micromolar RabGGTase inhibitors *in vitro*, and the published data also suggested that P49-F6 inhibits the prenylation of Rab5B and increases its cytoplasmic localization *in vivo*.

COS-7 cells were treated with increasing amounts of P49-F6, P50-E11, and P23-D6, which were synthesized by Dr. Céline Deraeve (Prof. Waldmann, Department of Chemical Biology, Max-Planck-Institut für molekulare Physiologie, Dortmund). Subsequent biotin-geranylation of the resulting lysates demonstrated that none of the compounds showed *in vivo* inhibition of

protein prenylation at concentrations up to 50 µM and for up to 48 h (Figure 3-27 A-C). It therefore appears that the redistribution of endogenous Rab5B from the membrane to the cytosol in response to P49-F6 treatment, as described in the publication, was not a result of RabGGTase inhibition[336].

3.2.7 Quantitative analysis of the mammalian prenylome

A potential biomedical application of the developed technology is the proteome-wide analysis of protein prenyltransferase action and their protein substrates. Thus, a direct tissue- and organ-specific profiling of protein prenyltransferase substrate expression and the effect of prenylation-affecting drugs on the status of the prenylome should be achievable. A premise for such an approach is the ability to separate the protein prenyltransferase substrates into single proteins. Similar molecular weights of many prenylation substrates, in particular those of GGTase-I and RabGGTase, complicate their analysis by 1D SDS-PAGE.
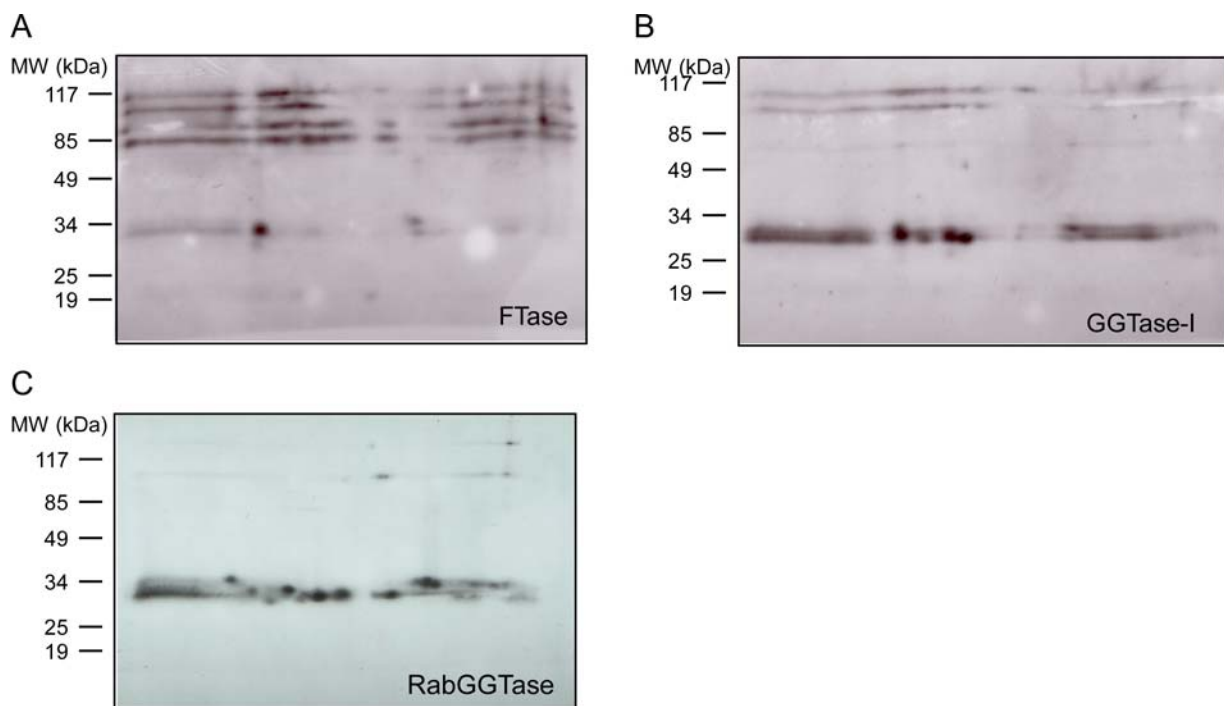
Figure 3-28 2D SDS PAGE analysis and Western blot analysis of compactin-treated COS-7 cell lysate prenylated with BGPP using engineered protein prenyltransferases **A-C**. The prenylation was carried out using FTase$_{W102T\_Y154T}$ **A**, GGTase-I$_{Y126T}$ **B**, or RabGGTase **C** and visualized by Western blotting with STR-HRP.

In an attempt to improve the separation of the products, lysates derived from compactin-treated COS-7 cells were biotin-geranylated with FTase$_{W102T\_Y154T}$, GGTase-I$_{Y126T}$, and wild-type RabGGTase and analyzed on 2D SDS-PAGE with Western blotting. Thereby, the signals were separated into a pattern of dozens of single spots or groups of spots, which showed an enzyme-specific distribution (Figure 3-28 A-C).

However, even in 2D configuration, a reliable separation of single protein prenyltransferase substrates could not be accomplished. Coupling the quantitative isolation of biotin-labeled proteins from complex lysate samples to mass spectrometry may provide a potential route for their identification and quantification. Multidimensional Protein Identification Technology (MudPIT) has proven to be suitable for such purposes. It is based on the proteolytic digestion of complex protein mixtures and multi-dimensional chromatography, followed by their separation by tandem mass spectrometry and matching of the spectra with sequence databases[337].

Lysate derived from either compactin- or DMSO-treated treated COS-7 cells were biotin-geranylated with 1 µM RabGGTase/REP-1/BGPP for 4-6 h at room temperature, enriched on magnetic streptavidin beads, and washed with 4M GdmHCl/PBS, 4 M urea/PBS, and 50 mM NH_4HCO_3, pH 8.0, three times each. To digest all associated proteins, the beads were treated with trypsin and chymotrypsin. The resulting peptides were analyzed by MudPIT, which was performed by Benjamin Fränzel and Dr. Dirk Wolters (Proteincenter, Ruhr-Universität Bochum). 42 RabGTPases were found by database search of the obtained peptide sequences; these proteins were absent in the DMSO-treated negative control (Figure 3-29 A). The lack of some known RabGTPases, such as Rab17, could be explained by their cell-type specific expression[338].

In addition to providing information about the identity of proteins in lysate mixtures, MudPIT analysis also gives a measure of protein abundance based on sequence coverage[339, 340]; this is the percentage of a protein´s amino acid sequence covered by the identified peptides. A comparison among different Rabs is feasible since RabGTPases have similar molecular weights and are expected to show a similar behavior in the mass-spectrometric experiments.

In order to obtain an absolute quantification of the data, a known amount of recombinant [^{15}N]-labeled Rab22A was spiked into the samples prior to tryptic digestion. The experiment revealed that protein abundances were substantially different among the Rab proteins, with Rab1A/B, Rab5C, Rab14, and Rab11B being the most dominant proteins, with an abundance of more than 1.5 pmol per mL lysate. Since 3 mL lysate corresponded to approximately 10 million cells, 1.5 pmol per mL lysate is equal to roughly 270,000 molecules per cell.

In contrast, Rab4A/B, Rab6C, Rab15, Rab27A/B, Rab30, Rab33B, Rab34, Rab37, Rab 39A/B, Rab41 and Rab43 were found at an abundance of less than 0.3 pmol per mL lysate each (Figure 3-29 A).

To confirm that the abundance data obtained using mass-spectrometry was reliable, we performed quantitative Western blotting of the COS-7 lysates using specific antibodies for Rab1A, Rab6A, and Rab7. Compactin-treated lysate was prenylated with RabGGTase/REP-1/BGPP, and the prenylation mixtures along with known amounts of recombinant GST-Rab1, Rab6A, or Rab7 were subjected to 1D SDS-PAGE. After transfer onto a nitrocellulose

membrane, the membrane was incubated with either anti-Rab1A, anti-Rab6A, or anti-Rab7 antibodies followed by anti-mouse or anti-rabbit antibody, depending on the source of the polyclonal antibodies.
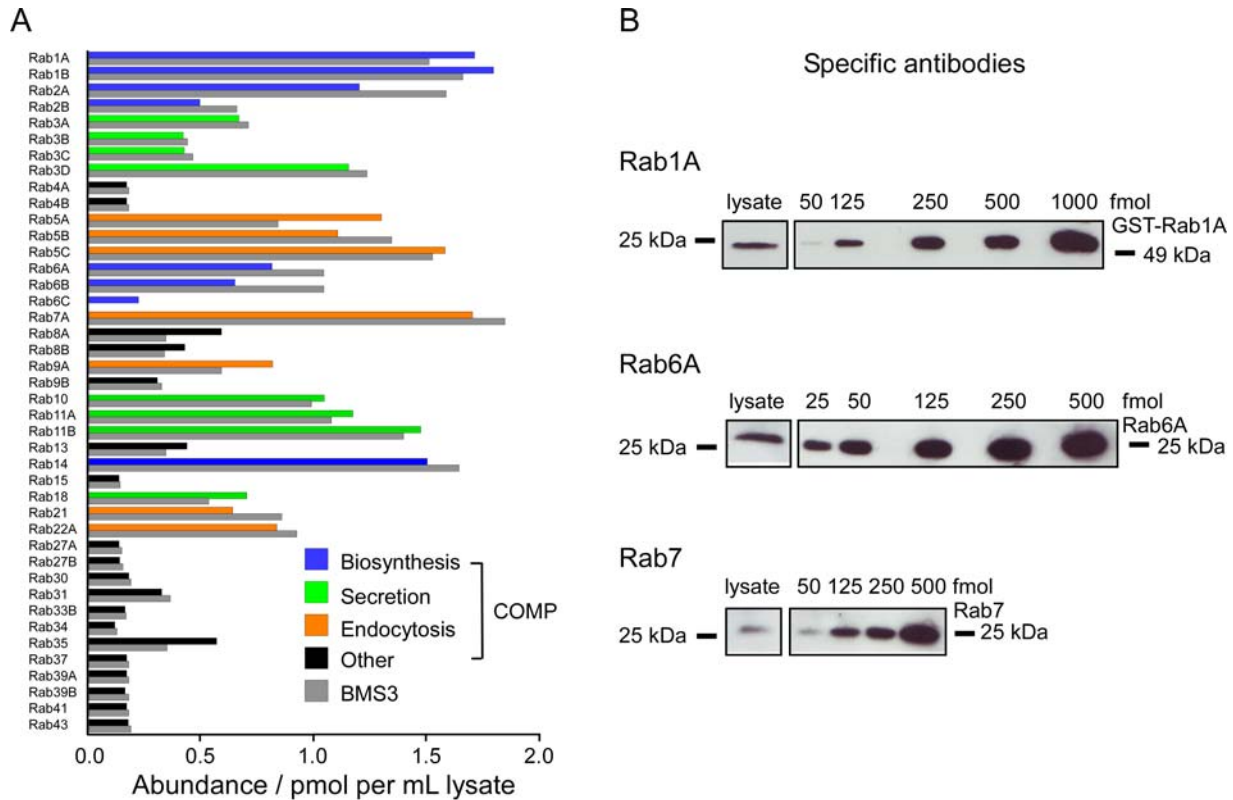
Figure 3-29 Identification and quantification of RabGTPases from compactin- and BMS3- treated COS-7 lysates. **A** Abundance of RabGTPases from compactin-treated (blue, green, red, and black bars) and BMS3-treated (gray bars) COS-7 cells using the MudPIT technology. The protein abundance is given in pmol per mL COS-7 lysate, and individual Rab proteins are colored according to their function: blue- Rabs controlling the biosynthetic pathways; green- Rabs controlling secretion; orange- Rabs controlling endocytosis; black – all other RabGTPases. **B** Lysate of COS-7 cells was resolved on SDS-PAGE gel together with the indicated amounts of recombinant GST-Rab1A (top), Rab6A (middle), or Rab7 (bottom). The gels were subjected to Western blotting with specific anti-Rab1A, anti-Rab7, or anti-Rab6A antibodies, and the antibody binding was detected using the chemiluminescent method.

The band intensities on the Western blot were judged by visual inspection, which revealed ca. 125 fmol of Rab1A (2.1 pmol per mL lysate or ~ 380,000 Rab1A molecules per cell), 25-50 fmol of Rab6A (~ 75,000-150,000 molecules per cell), and 50-125 fmol of Rab7 (~150,000-375,000 molecules per cell, Table 3-4). In good agreement with the MudPIT data, Rab1A was significantly more abundant in COS-7 cells than Rab7 and Rab6A (Figure 3-29 B). The observed abundance differences among the Rabs were larger than observed using the mass spectrometric approach. This is likely to be a result of a non-linear relationship between amounts of the proteins on the blot and the chemiluminescence capture by the photo-film.

Having confirmed that the quantitative information on the Rab abundances obtained by MudPIT was reliable, we considered the abundance of unprenylated RabGTPases found by MudPIT in the compactin-treated cells as the total abundance of expressed RabGTPases in

COS-7 cells. Analysis of this data shows that the expression of the most abundant RabGTPases found forms three clusters. The first group is formed by GTPases that control the early steps of endocytosis (Rab5A,B,C, Rab7, Rab9, Rab21 and Rab22, Figure 3-29 A in orange), the second by GTPases that control secretion (Rab3A,B,C,D, Rab10, Rab11A,B, and Rab18, Figure 3-29 A in green), and the third by RabGTPases that control the traffic in and to the Golgi apparatus (Rab1A,B, Rab2A,B, Rab6A,B,C, and Rab14, Figure 3-29 A in blue).

The obtained results suggest that the more highly abundant RabGTPases are associated with the main hubs of endocytic and biosynthetic routes, which probably reflects the number of individual fusion events in these compartments. In contrast, the less abundant proteins can be attributed to GTPases that regulate specialized trafficking processes.

Table 3-4 RabGTPase abundances in COS-7 lysate obtained by MudPIT and specific antibodies.			
MudPIT		**Specific antibodies**	
pmol per mL lysate	molecules per cell	pmol per mL lysate	molecules per cell
Rab1A 1.7	310,000	2.1	380,000
Rab6A 0.8	140,000	0.4-0.8	75,000-150,000
Rab7 1.7	310,000	0.8-2	150,000-375,000

By coupling enrichment of biotin-geranylated RabGTPases to their specific mass spectrometric identification and quantification, the BMS3-treated COS-7 lysates were reanalyzed. The aim was to determine whether BMS3-mediated inhibition of RabGGTase affected all RabGTPases to a similar extent or whether the prenylation of some proteins were inhibited more strongly than others. The latter is theoretically possible owing to (i) the very diverse structures of Rab C-terminal prenylation motifs and (ii) the lack of information on the mode of BMS3-mediated inhibition, which may result in different inhibition patterns of the single Rabs.

MudPIT analysis of the samples revealed no significant changes in the relative abundance of unprenylated Rab proteins in BMS3-treated cell lysates compared with cells that were treated with compactin (which can be regarded as the total abundance of expressed RabGTPases). The data suggests that BMS3-mediated inhibition is non-discriminatory with respect to the RabGTPases (Figure 3-29 in gray).

The results obtained demonstrate that coupling the enrichment of biotin-geranylated protein prenyltransferase substrates with the mass-spectrometric MudPIT technology provides a useful tool to identify and quantify unprenylated proteins *in vivo*.

4 SUMMARY AND OUTLOOK

Protein prenylation is one of the most extensively studied posttranslational modifications; it plays a central part in the regulation of diverse cellular processes and also underlies various pathologies, particularly cancer.

The present study was aimed at the investigation of the enzymatic protein prenylation reactions as potential tools for generic protein derivatization and for selective labeling of all protein prenyltransferase substrates in mammalian cells.

The first part of this work examined whether the PTM reaction catalyzed by FTase can serve as a universal protein labeling strategy. Three azide- and diene-functionalized isoprenoid analogs were designed, all of which were transferred by FTase to peptides and proteins equipped with the C-terminal CAAX sequence derived from mammalian K-Ras4B, albeit with different kinetics.

APO-GPP displayed a catalytic efficiency that was 3.5-fold enhanced compared to the native substrate FPP, whereas the k_{cat}/K_M values for HOM-GPP and AAA-GPP were 2- and 36-fold lower, respectively. Nevertheless, catalytic amounts of FTase and a small excess of either isoprenoid analog were sufficient to quantitatively convert the protein into the prenylated species following incubation for 12 h at room temperature.

The established reaction conditions were mild enough to preserve the native structure of the protein substrates. With regard to the biochemical properties of the prenylated proteins, APO-GPP and particularly AAA-GPP appear to represent the least invasive analogs, since the apparent hydrophobicity and the oligomerization state of the target proteins did not change upon prenylation.

We showed that the azide functionalities in APO-GPP and AAA-GPP were suitable for subsequent Staudinger ligation with a triaryl phosphine. In contrast to Diels-Alder cycloaddition, the Staudinger ligation was fully chemoselective and proceeded with rapid reaction kinetics. In particular, the azide in AAA-G was most suitable for the Staudinger ligation, since its reaction required only 1.5 h and exclusively yielded the desired product. In contrast, the azide in APO-G displayed a 3-fold decrease in reaction kinetics and also left 20 % of the target protein unligated.

In summary, AAA-GPP is the analog of choice for a two-step labeling strategy based on FTase-catalyzed prenylation of CAAX-tagged proteins and subsequent Staudinger ligation.

Compared to other labeling strategies, the FTase-mediated prenylation reaction displays the shortest peptide recognition sequence reported to date without suffering from a loss in efficiency. To compete with other technologies, especially those that can be applied *in vivo*,

several improvements have to be implemented＊. For instance, the CAAX sequence CVIM fused to the C-terminus of the target protein is only one of many protein substrates that will be recognized as a substrate *in vivo*. Engineering FTase mutants that specifically recognize a non-native CAAX sequence would therefore be an invaluable tool to broaden the applicability of the approach.

One of the methods suitable for targeted protein engineering is directed evolution. By creating a randomized library of FTase mutants with altered active sites one could identify an FTase enzyme that specifically recognizes non-native CAAX motifs. In addition, it may also be possible to move the recognition sequence from the C- to the N-terminus. This would allow for more flexibility with regard to the location of the CAAX sequence within the target protein. Furthermore, the substrate promiscuity of wild-type FTase towards the lipid donor is limited. As a result, the incorporation of substantial modifications into the lipid chain is restricted. It may be possible to replace the lipid moiety by fully non-isoprene moieties, which could help to increase the solubility of the prenylated target protein. Ongoing work in our group suggests that the β-subunit of FTase on its own may be sufficient for catalysis (Alexandrov et al., unpublished). This is an important finding with regard to the implementation of screening and selection systems to evolve FTase since the evolution of the more complex dimeric enzyme would require a co-expression of both subunits.

The second part of this work describes the development of a generic strategy to selectively label the prenylome of mammalian cells. The investigation was triggered by the observation that the biotin-functionalized isoprenoid analog BGPP functions as an efficient lipid donor for RabGGTase. This probe was used for the affinity-labeling of RabGTPases *in vitro* and in cellular lysates. Due to the extraordinarily high sensitivity of the assay, a stable pool of non-prenylated RabGTPases could be detected in untreated COS-7 lysate and mouse tissue. Based on the crystal structure of BGPP in complex with wild-type FTase, FTase and GGTase-I mutants capable of selectively labeling their cognate protein substrates were generated by site-directed mutagenesis. These mutants displayed no change in their native CAAX peptide specificity. Together with wild-type RabGGTase, the set of engineered protein prenyltransferases enabled the isolation and analysis of the entire cellular prenylome. Separation into single RabGTPases was achieved by coupling an enrichment of the biotin-geranylated proteins by means of streptavidin pulldown to mass spectrometry, which provided

---

＊ During the course of the PhD thesis, several strategies for the enzymatic incorporation of functional groups into proteins equipped with peptide tags of different sizes have been reported. In these studies, existing enzymes were re-engineered to decrease the size of the peptide label including biotin ligase (15 AA)[341] and phosphopantetheinyl transferase (8-12 AA)[342, 343]. Alternatively, the suitability of new enzymes were explored such as transglutaminase (7 AA)[344], sortase (~ 20 AA)[345], formylglycine generating enzyme (6-13 AA)[346, 347], *N*-Myristoyl transferase (15 AA)[348, 349], and lipoic acid ligase (22 AA)[350].

information on the abundances of the individual RabGTPases in the cell. The data suggests that the main hubs of vesicular transport feature more RabGTPases than specialized intracellular trafficking routes. The applicability of the methodology was demonstrated by the analysis of the *in vivo* effects of several protein prenyltransferase inhibitors including BMS3- a candidate anti-cancer therapeutic. These inhibitor studies revealed that BMS3 is a dual specificity inhibitor of RabGGTase and FTase *in vivo*. The investigation of several other commercially available inhibitors indicated that some of the inhibitors displayed the expected activities *in vivo*, whereas others either did not or targeted a broader spectrum of protein prenyltransferases than previously believed.

There are a few unique features of the described technology that set it apart from existing methodologies. The procedure (i) is simple compared to other techniques such as metabolic labeling; (ii) displays the best detection sensitivity reported to date; and (iii) allows for the isolation and analysis of the entire cellular prenylome. In combination, this enables an unbiased, proteome-wide detection of protein prenyltransferase substrates. This particularly applies to RabGTPases which cannot be predicted on the basis of a short peptide recognition sequence. We conclude that the strength of this method is its ability to detect femtomolar quantities of unprenylated proteins in cell culture, specific organs, and in whole organisms. Detection of unprenylated proteins in specific organs should be possible since we could detect a minor pool of unprenylated RabGTPases in mouse liver and brain. This is particularly important with regard to the drug distribution and efficacy of prenylation-modulating drugs such as protein prenyltransferase inhibitors or statins.

In future applications, the strategy developed for selective labeling and analysis of the mammalian prenylome is likely to serve as an important tool for providing insights into the coordination of GTPase expression and prenylation and their function in the regulation of intracellular signaling pathways as well as for elucidating their role in degenerative and infectious diseases.

SUMMARY AND OUTLOOK (german)

Die Prenylierung von Proteinen ist eine der meist untersuchtesten posttranslationalen Modifikationen. Sie nimmt in der Regulierung unterschiedlicher zellulärer Prozesse eine zentrale Rolle ein.

Ziel der vorliegenden Arbeit war die Untersuchung der enzymatischen Protein-Prenylierungsreaktionen, die potentiell für eine allgemein anwendbare Proteinderivatisierung sowie für die selektive Markierung von den gesamten Proteinprenyltransferase-Substraten in eukaryotischen Zellen ausgenutzt werden können.

Der erste Teil der vorliegenden Arbeit befasst sich mit der Fragestellung, ob die von FTase katalysierte posttranslationale Modifikationsreaktion für eine allgemein anwendbare Proteinlabeling-Strategie geeignet ist. Drei Azid- und Dien-funktionalisierte Isoprenoid-Analoga wurden entwickelt, die mit Hilfe von FTase mit unterschiedlicher Reaktionskinetik auf Peptide und Proteine, welche mit der C-terminalen CAAX-Sequenz von K-Ras4B ausgestattet wurden, übertragen werden konnten. Verglichen mit dem nativen Substrat FPP war die katalytische Effizienz von APO-GPP um 3.5-fach erhöht, die von HOM-GPP und AAA-GPP hingegen um 2- bzw. 36-fach erniedrigt. Dennoch war eine katalytische Menge an FTase und ein leichter Überschuss des jeweiligen Isoprenoid-Analogs bei einer Inkubation von 12 h bei Raumtemperatur ausreichend, um die Proteine quantitativ mit den Isoprenoid-Analogen zu prenylieren. Unter den etablierten milden Reaktionsbedingungen konnte die native Struktur des Proteinsubstrates bewahrt werden. Die Verwendung von APO-GPP und insbesondere AAA-GPP beeinflusste die biochemischen Eigenschaften der prenylierten Proteine nur gering: Sowohl die apparente Hydrophobizität als auch der Oligomerisationszustand der Proteine wurde durch die Prenylierung nicht nachteilig verändert.

Es konnte gezeigt werden, dass die Azidfunktionalitäten von AAA-GPP und APO-GPP durch die Staudinger-Ligationsreaktion mit einem Triarylphosphin modifiziert wurden. Im Gegensatz zu der Diels-Alder-Zykloaddition verlief die Staudinger-Ligation vollständig chemoselektiv und mit hoher Reaktionskinetik. Die Azidgruppe von AAA-G war insbesondere geeignet für die Staudinger-Ligation, da die Reaktion nur 1.5 h benötigte und ausschließlich das gewünschte Produkt erzielte. Die Azidgruppe in APO-G dagegen zeigte eine 3-fach langsamere Reaktionskinetik mit lediglich 80%-igem Umsatz.

Diese Ergebnisse empfehlen AAA-GPP im Vergleich zu APO-GPP für eine 2-stufige Labeling-Strategie von CAAX-modifizierten Proteinen mittels der FTase-katalysierten Prenylierung und anschließender Staudinger-Ligation.

Verglichen mit anderen Labeling-Strategien zeigt die FTase-vermittelte Prenylierungsreaktion die bisher kürzeste bekannte Peptid-Erkennungssequenz. Um sich gegen andere

Technologien behaupten zu können, insbesondere denjenigen, die *in vivo* anwendbar sind, müssen zur generellen Anwendbarkeit einige Verbesserungen implementiert werden*. Die genetisch kodierte CAAX-Sequenz CVIM am C-Terminus des Zielproteins wäre nur eine von vielen Proteinsubstraten, die als Substrat *in vivo* erkannt werden würden. Aus diesem Grunde würde das Engineering von FTase-Mutanten, die spezifisch nicht-native CAAX-Sequenzen erkennen würden, ein wertvolles Werkzeug darstellen, um die Anwendbarkeit der Methode für *in vivo*-Zwecke zu erweitern.

Ein geeigneter Ansatz für ein gezieltes Protein-Engineering ist die gerichtete Evolution. Durch die Erstellung einer randomisierten Bibliothek an FTase-Mutanten mit veränderten aktiven Zentren könnte ein Enzym identifiziert werden, das spezifisch nicht-native CAAX-Motive erkennt. Eine solche Strategie könnte auch die Verschiebung der Erkennungssequenz vom C- zum N-Terminus ermöglichen, um eine größere Flexibilität bei der Positionierung der CAAX-Sequenz zu gewährleisten. Desweiteren ist die wünschenswerte Substratpromiskuität von Wildtyp-FTase gegenüber des Lipiddonors beschränkt, so dass die Inkorporation von beträchtlichen Modifikationen innerhalb der Lipidkette limitiert ist. Es bietet sich auch die Möglichkeit, die Lipidgruppen durch nicht-Isopren-Funktionalitäten zu ersetzen. Dieses hätte den zusätzlichen Vorteil, die Löslichkeit des prenylierten Zielproteins zu erhöhen. Die Beobachtung, dass die β-Untereinheit der FTase ausreichend katalytisch kompetent ist (Alexandrov et al., unveröffentlicht), stellt eine erhebliche Vereinfachung für eine zukünftige Etablierung von Screening- und Selektionssystemen zur FTase-Evolution dar, da die Evolution des komplexeren Dimers eine Ko-Expression beider Untereinheiten erfordern würde.

Der zweite Teil dieser Arbeit befasst sich mit der Entwicklung einer allgemein anwendbaren Strategie zur selektiven und vollständigen Markierung des Prenyloms eukaryotischer Zellen. Ausgangspunkt der Untersuchung war die Beobachtung, dass die RabGGTase das Biotin-funktionalisierte Isoprenoidanalog BGPP als Lipiddonor akzeptiert. BGPP konnte dadurch zur gezielten Markierung von Rab-Proteinen *in vitro* und in Zelllysaten ausgenutzt werden. Aufgrund der außerordentlich hohen Sensitivität des Assays konnte ein Pool an nicht-prenylierten Rab-Proteinen in COS-7-Zelllysaten und in Geweben von Mäusen detektiert werden.

---

* Im Laufe der Doktorarbeit wurde über einige Strategien zur enzymatischen Inkorporation von funktionellen Gruppen in Proteine, die mit Peptid-Tags verschiedener Größe ausgestattet wurden, berichtet. In diesen Studien wurden existierende Enzyme weiterentwickelt, um die Größe des Peptidlabels zu verringern; darunter waren Biotin-Ligase (15 AA)[341] und Phosphopantetheinyl-transferase (8-12 AA)[342, 343]. Alternativ wurde die Anwendbarkeit neuer Enzyme getestet wie z. B. Transglutaminase (7 AA)[344], Sortase (~ 20 AA)[345], Formylglycine-generierende Enzyme (6-13 AA)[346, 347], *N*-Myristoyl-transferase (15 AA)[348, 349], sowie *lipoic acid ligase* (22 AA)[350].

Basierend auf der Kristallstruktur von BGPP im Komplex mit Wildtyp-FTase wurden durch zielgerichtete Mutagenese FTase- und GGTase-I-Varianten generiert, in denen die Spezifität für das CAAX-Peptidsubstrat unverändert blieb und die ihre Proteinsubstrate selektiv mit Biotin-geranyl modifizierten. Durch diese Mutanten konnte zusammen mit Wildtyp-RabGGTase die Isolierung und Analyse des gesamten zellulären Prenyloms erreicht werden. Die Auftrennung in einzelne Rab-Proteine gelang durch die Kopplung eines Streptavidin-Pulldowns der Biotin-geranylierten Proteine mit der massenspektrometrischen MudPIT-Methodik. Durch die zelluläre Quantifizierung spezifischer Rab-Proteine konnte die Vermutung bestätigt werden, dass die zentralen Prozesse des vesikulären Transports mehr Rab-Proteine aufweisen als die spezialisierten intrazellulären Transportwege.

Die Anwendung der Methode konnte anhand der Analyse von den *in vivo*-Effekten einiger Proteinprenyltransferase-Inhibitoren wie z. B. BMS3, einem potentiellen Wirkstoff in der Anti-Krebstherapie, veranschaulicht werden. Die Inhibitorstudien deuten darauf hin, dass BMS3 ein dual-spezifischer Inhibitor von RabGGTase und FTase *in vivo* ist. Weitere Untersuchungen anderer kommerziell erhältlicher Inhibitoren zeigten, dass einige davon die erwarteten Aktivitäten *in vivo* aufwiesen, andere dagegen entweder eine breiteres Spektrum an Proteinprenyltransferasen beeinflussten oder gar keine Aktivität zeigten.

Die Methode der Proteinderivatisierung mittels BGPP zeichnet sich durch zahlreiche Vorzüge gegenüber anderen existierenden Technologien aus: Die Strategie (i) ist im Vergleich zu anderen Techniken wie z. B. der metabolischen Markierung leicht durchführbar, (ii) zeigt die empfindlichste bisher bekannte Detektionssensitivität und (iii) ermöglicht die Isolierung und die Analyse des gesamten zellulären Prenyloms. Dadurch kann eine unverfälschte, Proteom-weite Detektion von Proteinprenyltransferasesubstraten erzielt werden, vor allem von Rab-Proteinen, die nicht direkt aufgrund einer kurzen Peptid-Erkennungssequenz vorausgesagt werden können. Die Stärke der hier etablierten Methode liegt in der Fähigkeit, femtomolare Mengen an unprenylierten Proteinen in der Zellkultur, spezifischen Organen und in ganzen Organismen zu bestimmen. Die Detektion von unprenylierten Proteinen in spezifischen Organen kann erwartet werden, da in dieser Arbeit ein kleiner Pool an unprenylierten Rab-Proteinen in Mäuseleber und -gehirn nachgewiesen werden konnte. Dies ist eine wichtige Erkenntnis im Hinblick auf die Verteilung und Wirksamkeit von Verbindungen, die die Prenylierung modulieren, wie z. B. Proteinprenyltransferase-Inhibitoren oder Statine.

Die etablierte Methodik zur selektiven Markierung und Analyse des eukaryotischen Prenyloms kann in Zukunft als wertvolles Werkzeug in der Analyse der Koordination von Expression und Prenylierung kleiner GTPasen sowie ihrer Rolle in der Regulation von intrazellulären Signalwegen und in den ensprechenden degenerativen und infektiösen Krankheiten dienen.

5 MATERIALS AND METHODS

5.1 Materials

5.1.1 General Materials

Table 5-1 Chemical compounds used in this study.

Supplier	Material
Applichem (Darmstadt, DE)	Acrylamide/Bisacrylamide (37.5:1, 30% w/v), Ammonium sulfate, Guadinium hydrochloride (GdmHCl), Methanol
Gerbu (Gaiberg, DE)	Dithioerythritol (DTE), Dithiothreitol (DTT), Ethylenediamine-tetraacetic acid (EDTA), Glycerol, Imidazol, 4-(2-Hydroxyethyl)-piperazine-1-ethanesulfonic acid (HEPES), Isopropyl-β-D-thiogalac-topyroanoside (IPTG), Sodium dodecylsulfate (SDS)
JT Baker (Deventer, NL)	Acetonitrile, Acetone, Dichloromethane, Disodium hydrogen-phosphate, Ethanol, Hydrochloric acid, Isopropanol, Magnesium chloride, Potassium dihydrogenphosphate, Potassium hydroxide, Sodium dihydrogenphosphate, Urea
Merck (Darmstadt, DE)	Acetic acid, Ammonium persulfate (APS), Chloramphenicol (Cam), Imidazol
Riedel-de-Haën (Seelze, DE)	Ammonium carbonate, Nickel chloride
Serva (Heidelberg, DE)	Ampicillin (Amp), Bromphenol blue, Coomassie Brilliant Blue G250+R250, β-Mercaptoethanol, Triton X-100, Zinc chloride
Sigma (Taufkirchen, DE)	Agerose, Bovine serum albumine (BSA), Ethidium bromide, Farnesyl pyrophosphate (FPP), Geranylgeranyl pyrophosphate (GGPP), Phenylmethylsulfonylfluoride (PMSF), Sinapinic acid, Sodium 2-mer-captoethanesulfonate (MESNA)
Bio-Rad (München, DE)	Bradford reagent, Electroporation cuvettes
EMD Biosciences (San Diego, USA)	Dansyl-GCVLL, Dansyl-GCVLS, FTI B581, GGTI-298
Fluka (Steinheim, DE)	Dimethylsulfoxide (DMSO), Ethanthiol, Sodium chloride, Trichloro-acetic acid (TCA), Trifluoroacetic acid (TFA)
Roth (Karlsruhe, DE)	Glycine, N,N,N´,N´-tetramethylethylendiamine (TEMED), Trihydroxy-methylaminomethane (TRIS)
GE Healthcare (Uppsala, SE)	Glutathione Sepharose, Hyperfilm ECL, ECL solution
Invitrogen (Carlsbad, USA)	IPG gel redrydration buffer, carrier ampholytes, IPG strips, NuPage LDS sample buffer, NuPage Novex Bis-Tris gels, NuPage running buffer, Dubecco´s modified Eagle´s medium, Fetal bovine serum, streptomycin
Amersham Biosciences (Uppsala, SE)	Low molecular weight marker, NAP-5 desalting column, PD-10 desal-ting column
New England Biolabs (Ipswich, USA)	Magnetic Streptavidin Beads, 6-Tube Magnetic Separation Rack, anti-Rab7 antibody
Schleicher&Schuell (Dassel, DE)	Nitrocellulose paper, Whatman FP 30/0.2, 0.4 µM cellulose filter
Qiagen GmbH (Hilden, DE)	DyeEx 2.0 Spin Kit
Biotrend (Köln, DE).	Streptavidin-horseradish peroxidase conjugate
Eppendorf (Hamburg, DE)	Eppendorf tube (0.5, 1.5, and 2.0 mL),
Falcon GmbH (Gräfeling-Locham, DE)	Falcon Tube (15 and 50 mL)
Pharmacia Biotech (Uppsala, SE)	Superdex 75/200 Gel Filtration
ILMVAC GmbH (Ilmenau, DE)	Vacuum-membrane pump
Nalgene (Rochester, USA)	ZapCap filter
Millipore (Billerica, USA)	Amicon Ultra-4, 15 (10K, 30K) Concentrator
Phenomenex (Aschaffenburg, DE)	BioSep-SEC-2000 gel filtration, Jupiter 5 µM C4 300A reverse phase column
Spectrum Lab Inc. (Racho Dominguez, USA)	Dialysis membrane tubing (MWCO: 12-14 kDa, 5-8 kDa)
Hellma Optik GmbH (Jena, DE)	Quartz cuvette (1cm)
Pharma Waldhof (Düsseldorf, DE)	Guanosine diphosphate (GDP)
Abcam (Cambridge, UK)	anti-Rab1A antibody

5.1.2 Other chemicals from contributing people

The isoprenoid analogs AAA-GPP, APO-GPP, HOM-GPP, and BGPP were synthesized by Dr. Joaquín Gomis (Prof. Waldmann, Department of Chemical Biology, Max-Planck-Institut für molekulare Physiologie, Dortmund). NBD-FPP and NBD-GPP were synthesized by Dr. Reinhard Reents and Dr. Kui-Thong Tan (Prof. Waldmann, Department of Chemical Biology, Max-Planck-Institut für molekulare Physiologie, Dortmund). The small molecules for the inhibitor studies were synthesized by Dr. Céline Deraeve and Dr. Robin S. Bon (Prof. Waldmann, Department of Chemical Biology, Max-Planck-Institut für molekulare Physiologie, Dortmund) according to literature procedures. Table 5-2 summarizes a selection of isoprenoid analogs that were coupled to C-terminal cysteines of protein prenyltransferase substrates, and protein prenyltransferase inhibitors. Synthetic procedures and analytical data can be found in the indicated references. The isoprenoids were stored at -20 °C under an atmosphere of argon or dissolved as 5.5-23.8 mM solutions in 25 mM $(NH_4)_2CO_3$. The Rab6A-specific antibody was kindly provided by Prof. A. Barnekow, Universität zu Münster. Mouse brains and livers were kindly provided by Oliver Leske (Prof. R. Heumann, Ruhr-Universität Bochum).

Table 5-2 Chemical compounds from collaborators.	
Compound	**Collaborator**
AAA-GPP[290]	
APO-GPP[290]	
HOM-GPP[290]	Dr. Joaquín Gomis
BGPP[290]	
NBD-GPP[227]	Dr. Reinhard Reents
NBD-FPP[227]	Dr. Kui-Thong Tan
BMS3[351]	Dr. Robin S. Bon
P49-F6[336]	
P50-E11[336]	Dr. Celine Deraeve
P23-D6[336]	

5.1.3 Plasmids

All molecular clonings were kindly performed and provided by Melina Terbeck, Tina Rogowsky, and Sandra Thuns.

5.1.4 General instrumentation

Table 5-3 General instrumentation.	
Supplier	**Instrument**
Pharmacia Biotech (Uppsala, SE)	Äkta prime system with REC112 recorder
Applied Biosystems (Weiterstadt, DE)	Biorad PE 9700 thermocycler
Beckman Coulter (Palo Alto, USA)	Centrifuge Allegra X-22R, Centrifuge Avanti J20-XP, Centrifuge Optima L-70K Ultracentrifuge, UV-visible Spectrometer DU 640
Eppendorf (Hamburg, DE)	Centrifuge Eppendorf 5415C/D benchtop, Thermomixer 5436 (1.5 mL)
Bio-Rad (München, DE)	Electroporation device *E.coli* pulser, Gel electrophoresis system
Millipore (Eschborn, DE)	Deionized water apparatus
Fujifilm (JP)	FLA-5000 (Fluorescence Image Reader)
Thermo BioAnalysis (Santa Fe, USA)	Fluoroskan Ascent FI type 374
Waters (Eschborn, DE)	High pressure liquid chromatography (HPLC)
Agilent Technologies (Böblingen, DE)	HPLC-ESI-MS, MALDI-TOF-MS
Microfluidics (Newton, USA)	Microfluidizer
Calimatic Knick (Berlin, DE)	pH-Meter 761
Hoefer Scientific Instruments (Hollisten, USA)	Semi-Phor semi-dry blot apparatus
Jobin Yvon Horiba Group (Edison, USA)	Spex Fluoromax-3 Specrofluorometer
Infors (Bottmingen, CH)	Shaker
Branson (Danbury, USA)	Ultrasonic cell disrupter
Fermentas (St. Leon-Rot, DE)	Prestained molecular weight marker
Invitrogen (Carlsbad, USA)	ZOOM IPG-Runner System
Falcon GmbH (Gräfeling-Locham, DE)	Falcon Tube (15 and 50 mL)
Pharmacia Biotech (Uppsala, SE)	Superdex 75/200 Gel Filtration
ILMVAC GmbH (Ilmenau, DE)	Vacuum-membrane pump
Nalgene (Rochester, USA)	ZapCap filter
Millipore (Billerica, USA)	Amicon Ultra-4, 15 (10K, 30K) Concentrator
Phenomenex (Aschaffenburg, DE)	BioSep-SEC-2000 gel filtration, Jupiter 5 µM C4 300A reverse phase column
Spectrum Lab Inc. (Racho Dominguez, USA)	Dialysis membrane tubing (MWCO: 12-14 kDa, 5-8 kDa)
Hellma Optik GmbH (Jena, DE)	Quartz cuvette (1cm)
Pharma Waldhof (Düsseldorf, DE)	Guanosine diphosphate (GDP)

Representations of crystal structures were created with the program Molsoft-ICM (Molsoft LLC, La Jolla, USA). Band intensities on SDS gels and Western blot were quantified using the software AIDA.

5.1.5 Frequently used buffers and growth media

Table 5-4 Frequently used buffers and growth media.		
Antibiotics		**Buffer A**
125 mg/L Ampicillin		50 mM NaH_2PO_4, pH 8.0
34 mg/mL Chloramphenicol		0.3 M NaCl
59 mg/mL Kanamycin		2 mM β-mercaptoethanol
Buffer B		**Breaking Buffer**
50 mM NaH_2PO_4, pH 8.0		50 mM NaH_2PO_4, pH 7.5
0.3 M NaCl		0.3 M NaCl
2 mM β-mercaptoethanol		2 mM $MgCl_2$
0.5 M Imidazole		10 µM GDP
Bug Buffer		**Coomassie staining solution**
50 mM NaH_2PO_4, pH 8.0		10 % (v/v) acetic acid
0.3 M NaCl		40 % (v/v) ethanol
		0.1 % (w/v) Coomassie Brilliant Blue R250
Destaining solution		**DNA loading buffer (5x)**
10 % (v/v) acetic acid		30 % (w/v) sucrose
		20 % (v/v) glycerol
		0.2 % (w/v) orange G
LB agar plates		**LB medium**
15 g/L Bacto agar		5 g/L yeast extract
50 mg/L Ampicillin		19 g/L tryptone
		10 g/L NaCl
PBS (20x)		**PBST (20x)**
160 g/L NaCl		160 g/L NaCl
4 g/L KCl		4 g/L KCl
28.8 g/L $Na_2HPO_4 \cdot 2H_2O$		28.8 g/L $Na_2HPO_4 \cdot 2H_2O$
4.8 g/L KH_2PO_4		4.8 g/L KH_2PO_4
		1 % Tween-20
Prenylation buffer		**Lysate prenylation buffer**
25 mM HEPES, pH 7.2		25 mM HEPES, pH 7.2
40 mM NaCl		40 mM NaCl
2 mM $MgCl_2$		2 mM $MgCl_2$
20 µM GDP (omitted for CAAX-tagged proteins other than GTPases)		20 µM GDP
2 mM DTE		2 mM DTE
20 µM $ZnCl_2$ (omitted for RabGGTase prenylation)		20 µM $ZnCl_2$ (omitted for RabGGTase prenylation)
		0.5 mM PMSF
		1/100 CLAP
SDS-PAGE loading buffer (2x)		**SDS-PAGE resolving buffer**
62.3 mM Tris-HCl, pH 6.8		1.5 M Tris-HCl, pH 8.8
2 % /w/v) SDS		0.4 % (w/v) SDS
10 % (v/v) glycerol		
5 % (v/v) β-mercaptoethanol		
0.001 % (w/v) bromphenol blue		
SDS-PAGE running buffer (10x)		**SDS-PAGE stacking gel buffer (4x)**
0.25 M Tris-HCl		0.5 M Tris-HCl, pH 6.8
2 M glycine		0.4 (w/v) SDS
1 % (w/v) SDS		

5.2 Protein expression and purification methods

5.2.1 Expression and purification of CFP-CAAX

The construct CFP-CAAX (CFP-TKCVIM) was purified from *E.coli* BL21 (DE3) Codon Plus RIL cells expressing the hexahistidine-tagged fluorescent protein bearing the 6AA K_i-Ras C-terminal peptide. In brief, after cell growth, induction, and lysis of the cells, CFP-CAAX was purified from crude homogenate using Ni-NTA Sepharose columns (Pharmacia). The fractions containing the desired protein were identified using SDS-PAGE, concentrated to ~10 mg/mL, aliquotted, shock-frozen in liquid nitrogen, and stored at -80 °C.

5.2.2 Expression and purification of FTase$_{wt}$, GGTase-I$_{wt}$ and their respective mutants, RabGGTase$_{wt}$, REP-1, MRS6p, and the small GTPases

All proteins were kindly prepared and provided by Nataliya Lupilova, Melina Terbeck, and Astrid Sander. The expression and purification was reported earlier. Mutations of the β-subunits of FTase and GGTase-I were generated using the Quikchange mutagenesis kit (Strategene) according to the manufacturer´s instructions[352].

5.2.3 Expression and purification of [^{15}N]-labelled Rab22A

[^{15}N]-labeled human hexahistidine-tagged Rab22A protein was recombinantly expressed using a pOPINE-Rab22A vector in 1 L culture using M9 minimal medium with added glucose (10 mg/mL), [^{15}N]H$_4$Cl (1 mg/mL) as the isotope source, 100 μg/mL ampicillin, and trace elements. The culture was inoculated with an aliquot of an overnight culture to an OD$_{600}$ of ~0.1 and grown at 37°C on a shaker at 100 rpm to an OD$_{600}$ of ~0.8. Recombinant expression was induced by the addition of 0.6 mM IPTG, and the culture was further grown overnight (12-15 h) at 21°C and 130 rpm. The protein was purified by a combination of affinity chromatography on a 5 mL Ni-NTA column (GE Healtcare) and gel filtration on a Superdex 75 16/60 (GE Healtcare).

5.3 Analytical methods

5.3.1 LC-ESI-MS

Liquid-**C**hromatography-**E**lectrospray-**I**onization-**M**ass-**S**pectrometry (LC-ESI-MS) analysis was performed on an Agilent 1100 series chromatography system (Hewlett Packard) equipped with an LCQ-ESI mass spectrometer (Finnigan, San José, USA) with Jupiter C4 columns (5 µm, 15 x 0.46 cm, 400 Å pore size, Phenomenex, Aschaffenburg, DE). For separation by liquid chromatography, a gradient of buffer B (0.1 % formic acid in ACN) in

buffer A (0.1 % formic acid in water) was employed with a constant flow-rate of 1mL/min. Upon sample injection, a ratio of 20 % buffer B was kept constant for 5 min. Elution was achieved with a linear gradient of 20-70 % over 10 min followed by a steep gradient with 70-90 % buffer B for 2 min. The column was extensively flushed for at least 10 min with 95 % buffer B. Under these conditions, the small GTPases as well as the fluorescent proteins typically eluted at a retention time of 12-13 min. Mass spectra data evaluation and deconvolution was carried out using the Xcalibur software package. The accuracy of the method for proteins within the molecular range of 20 kDa is about 1-2 Da.

5.3.2 MALDI-TOF mass spectrometry

Matrix-**A**ssisted-**L**aser-**D**esorbtion-**I**onization-Time-Of-Flight (MALDI-TOF) spectra were recorded on a Voyager-DE Pro Biospectrometry work station from Applied Biosystems (Weiterstadt, DE). Desalting of protein samples was achieved using small GF spin columns (DyeEx 2.0 Spin Kit, Qiagen, Hilden, DE) and mixed with an equal volum of matrix (saturated sinapinic acid solution in 0.3 % TFA/ACN 2:1

Table 5-5 Instrument settings.	
acceleration voltage	25 kV
grid voltage	93 %
extraction delay time	750 nm
guide wire	0.3 %

(v/v)). The mixture was quickly spotted onto a MALDI sample plate, and subsequently air- or fan-dried. The spectra were measured as shown in Table 5-5. In order to obtain optimal signal-to-noise ratios, the laser intensity was manually adjusted during the measurements. Spectra recording and data evaluation was performed using the supplied Voyager software package. The accuracy of the method for proteins within the molecular weight range of 20-30 kDa is about 20 Da.

5.3.3 Gel filtration chromatography (GF)

Gel **F**iltration chromatography was performed on a Waters 600 chromatography instrument equipped with a Waters 2487 absorbance detector and a Waters 2475 fluorescence detector (Waters, Milford, USA). Using a Superdex 75 HR 10/30 column (separation range: 3-70 kDa) or a Superdex 200 HR 10/30 column (separation range: 10-600 kDa, Pharmacia, Uppsala, SE), GF chromatography was carried out in running buffer (25 mM HEPES, pH 7.2, 40 mM NaCl, 2 mM MgCl$_2$, 2 mM DTE, and optionally 20 µM GDP) at a flow rate of 0.5 mL/min. For analytical gel filtration of the prenylation reactions, the crude prenylation mixtures were loaded onto a Superdex 200 10/30 gel filtration column (GE Healthcare) driven by an FPLC system. The column was pre-equilibrated with 25 mM Hepes, pH 7.2, 40 mM NaCl, 2 mM MgCl$_2$ and, in the case of Ypt7-CAAX, 10 µM GDP. The flow rate was 1 mL/min, and the absorbance of the eluent was monitored at 280 nm. Fractions of 1 mL were collected and

analyzed by SDS-PAGE (see section 5.3.4). Selected fractions were subjected to ESI-MS and/or MALDI-MS.

5.3.4 Denaturing SDS-PAGE (1D and 2D)

1-dimensional SDS-PAGE. 15 % SDS-PAGE gels were used for the analysis of small GTPases or fluorescent proteins (molecular weight range from 20-30 kDa). The corresponding volumes of the individual components were mixed as indicated in Table 5-6. The mixed solution was poured into a Biorad

Table 5-6 SDS-PAGE gel components.		
	Lower buffer	Upper buffer
Acrylamide	25 mL	5 mL
4 x buffer	12.5 mL	7.5 mL
H_2O	12.5 mL	17.5 mL
APS	250 µL	240 µL
TEMED	25 µL	30 µL

Multi-casting apparatus for 9 gels. After polymerization of the resolving gel, a stacking gel mixture was cast on top of the resolving gel. The protein samples were prepared by adding an equal volume of SDS-PAGE sample buffer (2x) and heated for 5-10 min at 95 °C. Gels were run at 50 mA per gel until the bromphenol blue front entered the buffer solution. Fluorescently labeled proteins were visualized by exposing the unstained gel to UV light or the FLA-5000 Fluorescence Image Reader (Fujifilm, JP). The proteins were subsequently stained in a solution of Coomassie brilliant blue or further processed for Western blot analysis.

2-dimensional SDS-PAGE. 2D gel electrophoresis was carried out using the ZOOM IPG-Runner System (Invitrogen) according to the manufacturer´s instructions. Briefly, 5-10 µL of samples was dissolved in IPG gel rehydration buffer containing 8 M urea, 2 % w/v 3-[(3-cholamidopropyl)-dimethylammonio]-1-propanesulfonate (CHAPS), 0.5 % v/v carrier ampholytes, pH range 3-10, and 0.002 % bromphenol blue. The IPG strips (pH 3-10) were incubated in this solution overnight at room temperature. Separation of the proteins in the first dimension was achieved through isoelectric focusing, followed by incubating the IPG strip in NuPage LDS sample buffer (Invitrogen) containing reducing agent or iodoacetamide for alkylation for 15 min each. The proteins were separated by SDS-PAGE using NuPAGE Novex Bis-Tris gels (4-12% acrylamide gradient, Invitrogen). Bio-Rad standards were used as molecular weight markers. Western blot analysis was carried out as described in the following chapter.

5.3.5 Western blot analysis

The unstained SDS-PAGE gel was sandwiched between a nitrocellulose membrane and two gel-blotting Whatman filter papers each (Schleicher&Schuell, Dassel, DE) of the same size.

The order of the sandwich was as follows: cathode - 2 sheets of cathode buffer-wetted sheets - gel - anode buffer-wetted nitrocellulose membrane - 2 sheets of anode buffer-wetted sheets - anode. The transfer was carried out for 1 h at a current of 80 mA per gel in a Semi-Phor semi-dry blot apparatus (Hoefer Scientific Instruments, San Francisco, USA). The efficiency of transfer was judged by the transfer of the prestained molecular weight marker. The membrane was cut out and blocked with 20 mL of blocking solution (5 % non-fat dry milk in 0.05 % PBST) for at least 30 min. Subsequently, the streptavidin-horseradish peroxidase conjugate (Biotrend, Köln, DE) at a concentration of 1 µg/mL in PBS containing 0.05 % Tween-20 (PBST) was added. The membrane was allowed to incubate for 2 h at room temperature. The membrane was washed three times with PBST. The horseradish peroxidase conjugates were detected using the ECL kit (Amersham, UK) and a Hyperfilm ECL (GE Healthcare).

Alternatively, the blots were incubated with specific RabGTPase antibodies (see section 5.4.5). Band intensities were judged either by visual inspection or quantified using the AIDA software.

5.4 Biochemical methods

5.4.1 *In vitro* protein prenylation

Prenylation with AAA-GPP, APO-GPP, and HOM-GPP. All protein prenylation reactions were performed in prenylation buffer (25 mM Hepes, pH 7.2, 40 mM NaCl, 2 mM $MgCl_2$), and in the case of Ypt7-CAAX 10 µM GDP. In a volume of 10 µL, 60 µM protein and 120 µM isoprenoid were preincubated for 5 min at room temperature. The prenylation reaction was initiated by the addition of 4.6 µM FTase and reacted for up to 12 h at room temperature to reach completion. Identification of the prenylated sample was performed by LC-ESI mass spectrometry. To remove excess isoprenoid, the samples were rebuffered on a NAP5 column (GE Healthcare), concentrated in a Vivaspin 500 (Vivascience) to a total protein concentration of ~ 5 mg/mL, shock-frozen and stored at -80 °C.

Prenylation with BGPP, NBD-GPP, and NBD-FPP. 2 µM protein substrate (Rab7, RhoA or GST-RhoA, K_i-Ras or CFP-CAAX) was incubated with 2 µM of the appropriate protein prenyltransferase (RabGGTase, GGTase-I, or FTase, respectively) and 10 µM BGPP or NBD-GPP (FTase) or NBD-FPP (GGTase-I and RabGGTase) in prenylation buffer (25 mM Hepes pH 7.2, 40 mM NaCl, 2 mM DTE, 2 mM $MgCl_2$, 20 μM GDP) in a final volume of 10 μL. When Rab proteins were used as protein substrate, REP-1 was also added to the mixture to a final concentration of 2 μM. For CAAX prenyltransferases, 20 µM $ZnCl_2$ was included in the reaction mixture. The mixtures were incubated for > 2 h at room temperature and then

quenched by addition of 10 μL of 2x SDS-PAGE sample buffer. The samples were heated at 95°C for 5 min, and 0.5 pmol (for subsequent Western blot of the biotin-conjugated proteins) or 20 pmol (for subsequent fluorescence scanning of the NBD-conjugated proteins) was loaded onto a 15 % SDS polyacrylamide gel. The biotin-labeled samples were transferred onto a nitrocellulose membrane and blotted with the STR-conjugate. Alternatively, NBD fluorescence was recorded using a fluorescence scanner with an excitation filter of 473 nm and an emission filter of 510 nm. LC-ESI mass analysis of prenylated samples was performed as described.

5.4.2 Streptavidin pulldown

Streptavidin pulldown and subsequent elution was successfully performed with magnetic streptavidin purchased from New England Biolabs. The amount of beads was used according to the manufacturer´s indicated binding capacity of 1.25 nmol per mL bead suspension. The prenylation mixture was incubated with the beads for 1 h on an end-to-end rotor at room temperature. In the case of *in vitro* prenylation, the beads were thoroughly washed with PBS using a magnetic separator rack (New England Biolabs), and the biotinylated proteins were eluted by boiling the beads with 50 µl 2x SDS PAGE sample buffer at 90 °C for 10 min followed by sample concentration. For subsequent MudPIT analysis, harsher washing conditions with three washes each with PBS/4 M GdmHCl, PBS/4 M urea, and with 50 mM NH_4HCO_3, pH 8, were used.

5.4.3 In lysate protein prenylation

Prenylation reactions of compactin-, DMSO, or inhibitor-treated COS-7 lysates was performed essentially as for *in vitro* prenylation in 10-30 µL of the respective lysate using a mixture of 1 µM of both $FTase_{W102T\_Y154T\_Y205T}$ and $FTase_{W102T\_Y154T}$, 2 µM $GGTase_{F53Y\_Y126T}$, or 2 µM wild-type RabGGTase/REP-1 for typically 4-6 h at room temperature. When using frozen lysate stock, 20 µM GDP and 2 mM DTE, and in the case of CAAX prenyltransferases 20 µM $ZnCl_2$, were added freshly prior to the reaction. If necessary, the samples were concentrated before loading onto the gel. For the reaction of all three protein prenyltransferases in one sample, 25 µL of compactin-treated lysate was supplemented with 2 µM RabGGTase and REP-1 as well as 5 µM BGPP. After reaction for 2 h at room temperature, 1 µM of each FTase mutant and 2 µM GGTase-I_{F53Y_Y126T} mutant along with 5 µM BGPP and 20 µM $ZnCl_2$ was added. The reaction was allowed to proceed for another 4-6 h. The reaction was stopped by SDS sample buffer. For the detection of the pool of unprenylated Rab proteins in DMSO- or cycloheximide-treated lysate, 450 µL lysate was supplemented with 1 µM of RabGGTase, REP-1, and BGPP for 6 h at room temperature. The reaction was then subjected to magnetic streptavidin-

agarose beads (New England Biolabs) and incubated for 1h on an end-to-end rocker at room temperature. After thorough washing with PBS, the biotinylated proteins were eluted by boiling the beads with 60 µl 1x SDS PAGE sample buffer at 90 °C for 10 min followed by sample concentration. For large-scale prenylation of RabGGTase, FTase, and GGTase-I mutants in compactin-treated cells for 2D SDS-PAGE, 2 µM of the respective enzyme (and REP-1) as well as 1 µM BGPP were added to 500, 2000, or 1000 µL of lysate, respectively, for 6 h at room temperature, and the samples were processed as described for the detection of the pool of unprenylated Rabs. For subsequent mass spectrometric analysis, 1 mL of compactin-, DMSO-, or BMS3-treated lysate was prenylated with 2 µM RabGGTase, REP-1, and 1 µM BGPP for 6 h at room temperature. After thorough washing (see section 5.4.2), on bead digestion and MudPIT analysis was performed by Benjamin Fränzel and Dr. Dirk Wolters[352].

5.4.4 Quantification of RabGTPase abundance in COS-7 lysate

A volume of 60 µL of lysate derived from compactin-treated COS-7 cells was supplemented with 2 µM RabGGTase, REP-1, and excess BGPP and reacted for 4 h at room temperature. The reaction was stopped by the addition of 60 µL 1 x SDS sample buffer. After concentration, the samples along with varying amounts of recombinant GST-Rab1A, Rab6A, or Rab7 were loaded on a SDS-PAGE gel. After separation, the proteins were transferred onto a nitrocellulose membrane, which was subsequently incubated with 2 µg/mL anti-Rab1A, 1:1000 dilution of anti-Rab6A provided by our collaborator, or 1:1000 dilution of anti-Rab7 in 3 % milk/PBST for 2 h at room temperature followed by incubation with either anti-goat-HRP or anti-rabbit-HRP conjugates. Further processing was performed essentially as described in section 5.3.5. The abundance of the individual RabGTPases in the lysate was judged by visual inspection of the Western blots by comparing the band intensities with the recombinant proteins of known amount.

5.4.5 Chemoselective modification of the prenylated proteins

Staudinger ligation. 50 µM CFP-CAAX prenylated with either AAA-GPP or APO-GPP was incubated with 5 eq phosphine **27** (stock solution: 5 mM in DMSO) in 25 mM Hepes, pH 7.2, 40 mM NaCl and 2 mM $MgCl_2$ for 2 h at 25 °C. As controls, 50 µM CFP-CAAX-F and 50 µM CFP-CAAX-AAA/APO-G were supplemented with 5 eq phosphine **27** and 5 (v/v) % DMSO alone, respectively. In a screen for reaction conditions, samples were incubated with or without 0.05 (v/v) % Tween-20 and/or 2 mM DTE. To investigate the time course of the reaction, CFP-CAAX-AAA/APO-G were subjected to the Staudinger ligation under the described conditions with 2 mM DTE and 0.05 (v/v) % Tween-20. At the indicated time points,

the samples were quenched by passing the reaction mixtures through a spin gel filtration column (Qiagen), and the progression of the reaction was estimated by the intensity of the mass peaks by ESI-MS.

Diels-Alder cycloaddition. The accessible cysteines in the CFP-CAAX-HOM-G-FTase mixture were blocked using Ellmann´s reagent (5,5´-dithiobis(2-nitrobenzoic acid), DTNB) as described earlier[266, 299]. The proteins were then rebuffered against either 25 mM Hepes, pH 7.2, 40 mM NaCl, 2 mM $MgCl_2$ or 50 mM Na_2HPO_4, pH 6.0, 40 mM NaCl, 2 mM $MgCl_2$. 50 µM CFP-CAAX-HOM-G at pH 7.2 or 6.0 was incubated with 40 eq 6-maleimidohexanoic acid **28** (stock: 20 mM in DMSO) 25 °C for up to 15 h. As controls, 50 µM CFP-CAAX-F and 50 µM CFP-CAAX-HOM-G were incubated with 40 eq maleimide **28** and 5 vol.-% DMSO alone, respectively. Excess dienophile **28** was removed by passing the reaction mixture through a DyeEx spin gel filtration column (Qiagen). The reaction yields were estimated by the intensity of the mass peaks by ESI-MS.

5.5 Biophysical methods

5.5.1 Fluorescence titrations- determination of K_D

Fluorescence measurements were performed on a Spex Fluoromax-3 spectrofluoro-meter (Jobin Yvon, Edison, USA). Measurements were carried out in 1 mL Quartz cuvettes (Hellma) with continuous stirring and thermostated at 25 °C unless otherwise indicated. All buffers used in these experiments were filtered through a 0.2 µm membrane filter (Whatman) and degassed on a vacuum-membrane pump (ILMVAC GmbH, Ilmenau, DE) by stirring for 1 h at room temperature. Fluorescence titrations were performed in titration buffer (50 mM HEPES, pH 7.2, 50 mM NaCl, and 5 mM DTE). The NBD fluorescence was excited at 487 nm, and data were collected at 530 nm for the interaction with FTase/GGTase-I or at 550 nm for the interaction with RabGGTase. NBD-GPP or NBD-FPP (A) was added to 1 mL buffer in a quartz cuvette and stirred until the fluorescence signal was stable. Small aliquots of the respective protein prenyltransferase (B) were added stepwise to the cuvette until the signal change reached saturation. The fluorescence signals were corrected for light scattering as well as dilution and plotted as a function of the reactant concentration. The data was fitted to the following equation using GraFit 5.0 (Erithacus Software, Surrey, UK):

$$F = F_{min} + \frac{(F_{max} - F_{min}) \cdot \left[(B + A + K) - \sqrt{(B + A + K_d)^2 - 4BA} \right]}{2B}$$

where F is the fluorescence intensity (in arbitrary units), F_{min} is the fluorescence intensity at the beginning of the titration, F_{max} is the intensity of the complex, B is the total titrant concentration, A is the concentration of the fluorescent reactant, and K_d is the dissociation

constant to be determined for the interaction. In the fit to this equation, F_{min}, F_{min}, B, and K_d were allowed to vary in the program Grafit (Erithacus Software).

For the competitive titration of FTase with AAA-GPP, APO-GPP, HOM-GPP, and BGPP, a pre-formed complex of 160 nM NBD-FPP and 210 nM FTase was titrated with the isoprenoid derivatives. The experimental data were fitted with the program Scientist (Micromath) using a model file which allows simulation and fitting to a set of three equations describing the two equilibria and the generation of the fluorescence signal. The K_d for the FTase:NBD-FPP interaction was held constant at the value determined from the direct titration.

For the competitive titration of GGTase-I and RabGGTase, a pre-formed complex of 50 or 200 nM NBD-FPP and 50 or 200 nM FPP or GGPP was titrated with the respective enzyme. In the case of BGPP, a higher concentration was used. The experimental data were fitted with the program Scientist as described above.

5.5.2 Continuous fluorometric assay for FTase and GGTase-I prenylation

To compare the enzymatic incorporation of the analogs by fluorescence spectroscopy, an established fluorescence-based assay was employed[225]. First, 2.2 µM *N*-dansyl-GCVLS (EMB Bioscience) and a saturating concentration of 20 µM of the respective isoprenoid were preincubated using the buffer reported by Poulter and colleagues, and the reaction was initiated by the addition of 50 nM FTase. Changes of dansyl fluorescence ($\lambda_{ex}/\lambda_{em}$ = 340 nm /505 nm) were monitored for 8000 s. At the saturation point, addition of excess FTase did not result in further increase in fluorescence, indicating that the peptide was completely prenylated. The total increase in fluorescence was linearly correlated to the initial peptide substrate concentration. In order to determine the kinetic parameters the initial rates of the prenylation reaction were measured from the linear region at different isoprenoid concentrations using 1-20 nM FTase. Conversion of v_i and k_{cat} into units of µM/s and 1/s, respectively, were performed as described above. The data were fitted using the Michaelis-Menten model:

$$(2) \quad v = \frac{V_{max} \cdot [S]}{K_M + [S]},$$

where V_{max} is the maximal velocity, [S] the concentration of the isoprenoid substrate and K_M the Michaelis-Menten constant.

Examination of the specificity of the enzymatic incorporation of isoprenoids for dansyl-GCVLS and dansyl-GCVLL was performed in essentially the same manner[352]. First, *N*-dansyl-GCVLS/L (6 µM, EMD Bioscience) and 107-140 nM of enzyme were preincubated in a buffer containing 50 mM Hepes, pH 7.8, 5 mM MgCl$_2$, and 2 mM DTT, and the reaction was initiated

by the addition of a saturating concentration (6-11.5 μM) of the appropriate isoprenoid. Changes in dansyl fluorescence ($\lambda_{ex}/\lambda_{em}$=340 nm/505 nm) were monitored for up to 4000 s.

5.6 COS-7 cells general maintenance and lysate preparation

COS-7 cells were grown in Dulbecco's Modified Eagle's medium (DMEM, Invitrogen), supplemented with 10% fetal bovine serum (Invitrogen) as well as 1 % penicillin and streptomycin (Invitrogen). Cells were incubated in a humidified atmosphere at 37°C in 5 % CO_2 and passaged every 2–3 days. COS-7 cells were grown to 70 % confluence in either 6 well or 15 cm dishes and fed with 0.5 % DMSO, 20 μg/mL cycloheximide, 20 μM compactin, 0.5 μM BMS3, or the indicated concentration of inhibitor. Cells were incubated for a further 12-18 h and then harvested to produce cell lysate. Cells were washed in phosphate buffered saline (137 mM NaCl, 2.7 mM KCl, 4.3 mM Na_2HPO_4, and 1.4 mM KH_2PO4) and incubated at 4°C for 15 min in prenylation buffer (50 mM Hepes pH 7.2, 50 mM NaCl, 2 mM $MgCl_2$, 2 mM DTT, 100 μM GDP, 10 μg/ml CLAP, 0.6 mM PMSF), either with or without 0.5 (v/v) % NP-40. Cells were then scraped and transferred to a reaction tube for centrifugation at 16,100 × g at 4°C for 10 min. If detergent was omitted, the cells were disrupted by pushing them 5 times through a 0.55 mm syringe needle prior to centrifugation.

Mouse brain or liver was homogenized using a Dounce homogenizer in prenylation buffer and further processed as described for COS-7 lysate preparation.

5.7 Crystallization and structure solution of the BGPP:FTase and the BGPP: FTase$_{W102T\_Y154T}$ complexes

These procedures are described in[352].

6   REFERENCES

1.   Lander, E. S., et al., Initial sequencing and analysis of the human genome. *Nature* **2001,** *409* (6822), 860-921.

2.   Venter, J. C., et al., The sequence of the human genome. *Science* **2001,** *291* (5507), 1304-51.

3.   Walsh, C. T.; Garneau-Tsodikova, S.; Gatto, G. J., Jr., Protein posttranslational modifications: the chemistry of proteome diversifications. *Angew Chem Int Ed Engl* **2005,** *44* (45), 7342-72.

4.   Meri, S.; Baumann, M., Proteomics: posttranslational modifications, immune responses and current analytical tools. *Biomol Eng* **2001,** *18* (5), 213-20.

5.   Black, D. L., Mechanisms of alternative pre-messenger RNA splicing. *Annu Rev Biochem* **2003,** *72*, 291-336.

6.   Maniatis, T.; Tasic, B., Alternative pre-mRNA splicing and proteome expansion in metazoans. *Nature* **2002,** *418* (6894), 236-43.

7.   Davis, B. G., Biochemistry. Mimicking posttranslational modifications of proteins. *Science* **2004,** *303* (5657), 480-2.

8.   Latham, J. A.; Dent, S. Y., Cross-regulation of histone modifications. *Nat Struct Mol Biol* **2007,** *14* (11), 1017-1024.

9.   Kouzarides, T., Chromatin modifications and their function. *Cell* **2007,** *128* (4), 693-705.

10.   Gelb, M. H., Protein prenylation, et cetera: signal transduction in two dimensions. *Science* **1997,** *275* (5307), 1750-1.

11.   Sakagami, Y.; Isogai, A.; Suzuki, A.; Tamura, S.; Tsuchiya, E.; Fukui, S., Isolation of a Novel Sex-Hormone, Tremerogen a-10, Controlling Conjugation Tube Formation in Tremella-Mesenterica Fries. *Agricultural and Biological Chemistry* **1978,** *42* (5), 1093-1094.

12.   Tsuchiya, E.; Fukui, S.; Kamiya, Y.; Sakagami, Y.; Fujino, M., Requirements of chemical structure of hormonal activity of lipopeptidyl factors inducing sexual differentiation in vegetative cells of heterobasidiomycetous yeasts. *Biochem Biophys Res Commun* **1978,** *85* (1), 459-63.

13.   Anderegg, R. J.; Betz, R.; Carr, S. A.; Crabb, J. W.; Duntze, W., Structure of Saccharomyces cerevisiae mating hormone a-factor. Identification of S-farnesyl cysteine as a structural component. *J Biol Chem* **1988,** *263* (34), 18236-40.

14.   Goldstein, J. L.; Brown, M. S., Regulation of the mevalonate pathway. *Nature* **1990,** *343* (6257), 425-30.

15.   Maltese, W. A.; Sheridan, K. M., Isoprenylated proteins in cultured cells: subcellular distribution and changes related to altered morphology and growth arrest induced by mevalonate deprivation. *J Cell Physiol* **1987,** *133* (3), 471-81.

16.   Schmidt, R. A.; Schneider, C. J.; Glomset, J. A., Evidence for post-translational incorporation of a product of mevalonic acid into Swiss 3T3 cell proteins. *J Biol Chem* **1984,** *259* (16), 10175-80.

17.   Maurer-Stroh, S.; Washietl, S.; Eisenhaber, F., Protein prenyltransferases. *Genome Biol* **2003,** *4* (4), 212.

18.   Casey, P. J.; Seabra, M. C., Protein prenyltransferases. *J Biol Chem* **1996,** *271* (10), 5289-92.

19.   Seabra, M. C.; Reiss, Y.; Casey, P. J.; Brown, M. S.; Goldstein, J. L., Protein farnesyltransferase and geranylgeranyltransferase share a common alpha subunit. *Cell* **1991,** *65* (3), 429-34.

20.   Taylor, J. S.; Reid, T. S.; Terry, K. L.; Casey, P. J.; Beese, L. S., Structure of mammalian protein geranylgeranyltransferase type-I. *EMBO J* **2003,** *22* (22), 5963-74.

21.   Park, H. W.; Boduluri, S. R.; Moomaw, J. F.; Casey, P. J.; Beese, L. S., Crystal structure of protein farnesyltransferase at 2.25 angstrom resolution. *Science* **1997,** *275* (5307), 1800-4.

22.   Lane, K. T.; Beese, L. S., Thematic review series: lipid posttranslational modifications. Structural biology of protein farnesyltransferase and geranylgeranyltransferase type I. *J Lipid Res* **2006,** *47* (4), 681-99.

23.   Andres, D. A.; Goldstein, J. L.; Ho, Y. K.; Brown, M. S., Mutational analysis of alpha-subunit of protein farnesyltransferase. Evidence for a catalytic role. *J Biol Chem* **1993,** *268* (2), 1383-90.

24.   Dunten, P.; Kammlott, U.; Crowther, R.; Weber, D.; Palermo, R.; Birktoft, J., Protein farnesyltransferase: structure and implications for substrate binding. *Biochemistry* **1998,** *37* (37), 13042.

25.   Zhang, H.; Seabra, M. C.; Deisenhofer, J., Crystal structure of Rab geranylgeranyltransferase at 2.0 A resolution. *Structure* **2000,** *8* (3), 241-51.

26.   Dursina, B.; Thoma, N. H.; Sidorovitch, V.; Niculae, A.; Iakovenko, A.; Rak, A.; Albert, S.; Ceacareanu, A. C.; Kolling, R.; Herrmann, C.; Goody, R. S.; Alexandrov, K., Interaction of yeast Rab geranylgeranyl transferase with its protein and lipid substrates. *Biochemistry* **2002,** *41* (21), 6805-16.

27.   Pylypenko, O.; Rak, A.; Reents, R.; Niculae, A.; Sidorovitch, V.; Cioaca, M. D.; Bessolitsyna, E.; Thoma, N. H.; Waldmann, H.; Schlichting, I.; Goody, R. S.; Alexandrov, K., Structure of Rab escort protein-1 in complex with Rab geranylgeranyltransferase. *Mol Cell* **2003,** *11* (2), 483-94.

28.   Hightower, K. E.; Huang, C. C.; Casey, P. J.; Fierke, C. A., H-Ras peptide and protein substrates bind protein farnesyltransferase as an ionized thiolate. *Biochemistry* **1998,** *37* (44), 15555-62.

29.   Huang, C. C.; Casey, P. J.; Fierke, C. A., Evidence for a catalytic role of zinc in protein farnesyltransferase. Spectroscopy of Co2+-farnesyltransferase indicates metal coordination of the substrate thiolate. *J Biol Chem* **1997,** *272* (1), 20-3.

30.   Saderholm, M. J.; Hightower, K. E.; Fierke, C. A., Role of metals in the reaction catalyzed by protein farnesyltransferase. *Biochemistry* **2000,** *39* (40), 12398-405.

31.   Reiss, Y.; Brown, M. S.; Goldstein, J. L., Divalent-Cation and Prenyl Pyrophosphate Specificities of the Protein Farnesyltransferase from Rat-Brain, a Zinc Metalloenzyme. *Journal of Biological Chemistry* **1992,** *267* (9), 6403-6408.

32.   Chen, W. J.; Moomaw, J. F.; Overton, L.; Kost, T. A.; Casey, P. J., High-Level Expression of Mammalian Protein Farnesyltransferase in a Baculovirus System - the Purified Protein Contains Zinc. *Journal of Biological Chemistry* **1993,** *268* (13), 9675-9680.

33.   Hightower, K. E.; Fierke, C. A., Zinc-catalyzed sulfur alkyation:insights from protein farnesyltransferase. *Curr Opin Chem Biol* **1999,** *3* (2), 176-81.

34.   Long, S. B.; Casey, P. J.; Beese, L. S., Cocrystal structure of protein farnesyltransferase complexed with a farnesyl diphosphate substrate. *Biochemistry* **1998,** *37* (27), 9612-8.

35. Pickett, J. S.; Bowers, K. E.; Hartman, H. L.; Fu, H. W.; Embry, A. C.; Casey, P. J.; Fierke, C. A., Kinetic studies of protein farnesyltransferase mutants establish active substrate conformation. *Biochemistry* **2003,** *42* (32), 9741-8.

36. Guo, Z.; Wu, Y. W.; Das, D.; Delon, C.; Cramer, J.; Yu, S.; Thuns, S.; Lupilova, N.; Waldmann, H.; Brunsveld, L.; Goody, R. S.; Alexandrov, K.; Blankenfeldt, W., Structures of RabGGTase-substrate/product complexes provide insights into the evolution of protein prenylation. *EMBO J* **2008,** *27* (18), 2444-56.

37. Leung, K. F.; Baron, R.; Seabra, M. C., Thematic review series: lipid posttranslational modifications. geranylgeranylation of Rab GTPases. *J Lipid Res* **2006,** *47* (3), 467-75.

38. Turek-Etienne, T. C.; Strickland, C. L.; Distefano, M. D., Biochemical and structural studies with prenyl diphosphate analogues provide insights into isoprenoid recognition by protein farnesyl transferase. *Biochemistry* **2003,** *42* (13), 3716-24.

39. Furfine, E. S.; Leban, J. J.; Landavazo, A.; Moomaw, J. F.; Casey, P. J., Protein Farnesyltransferase - Kinetics of Farnesyl Pyrophosphate Binding and Product Release. *Biochemistry* **1995,** *34* (20), 6857-6862.

40. Pompliano, D. L.; Schaber, M. D.; Mosser, S. D.; Omer, C. A.; Shafer, J. A.; Gibbs, J. B., Isoprenoid Diphosphate Utilization by Recombinant Human Farnesyl-Protein Transferase - Interactive Binding between Substrates and a Preferred Kinetic Pathway. *Biochemistry* **1993,** *32* (32), 8341-8347.

41. Strickland, C. L.; Windsor, W. T.; Syto, R.; Wang, L.; Bond, R.; Wu, Z.; Schwartz, J.; Le, H. V.; Beese, L. S.; Weber, P. C., Crystal structure of farnesyl protein transferase complexed with a CaaX peptide and farnesyl diphosphate analogue. *Biochemistry* **1998,** *37* (47), 16601-11.

42. Reid, T. S.; Terry, K. L.; Casey, P. J.; Beese, L. S., Crystallographic analysis of CaaX prenyltransferases complexed with substrates defines rules of protein substrate selectivity. *J Mol Biol* **2004,** *343* (2), 417-33.

43. Alexandrov, K.; Simon, I.; Yurchenko, V.; Iakovenko, A.; Rostkova, E.; Scheidig, A. J.; Goody, R. S., Characterization of the ternary complex between Rab7, REP-1 and Rab geranylgeranyl transferase. *Eur J Biochem* **1999,** *265* (1), 160-70.

44. Seabra, M. C.; Mules, E. H.; Hume, A. N., Rab GTPases, intracellular traffic and disease. *Trends Mol Med* **2002,** *8* (1), 23-30.

45. Wilson, A. L.; Erdman, R. A.; Castellano, F.; Maltese, W. A., Prenylation of Rab8 GTPase by type I and type II geranylgeranyl transferases. *Biochem J* **1998,** *333 (Pt 3)*, 497-504.

46. Huang, C.; Hightower, K. E.; Fierke, C. A., Mechanistic studies of rat protein farnesyltransferase indicate an associative transition state. *Biochemistry* **2000,** *39* (10), 2593-602.

47. Pickett, J. S.; Bowers, K. E.; Fierke, C. A., Mutagenesis studies of protein farnesyltransferase implicate aspartate beta 352 as a magnesium ligand. *J Biol Chem* **2003,** *278* (51), 51243-50.

48. Clausen, V. A.; Edelstein, R. L.; Distefano, M. D., Stereochemical analysis of the reaction catalyzed by human protein geranylgeranyl transferase. *Biochemistry* **2001,** *40* (13), 3920-30.

49. Edelstein, R. L.; Weller, V. A.; Distefano, M. D.; Tung, J. S., Stereochemical analysis of the reaction catalyzed by yeast protein farnesyltransferase. *Journal of Organic Chemistry* **1998,** *63* (16), 5298-5299.

50. Pais, J. E.; Fierke, C. A., Measurement of kinetic isotope effects to probe the reaction mechanism catalyzed by mammalian protein farnesyltransferase. *Faseb Journal* **2007,** *21* (5), A275-A275.

51.   Pais, J. E.; Bowers, K. E.; Fierke, C. A., Measurement of the alpha-secondary kinetic isotope effect for the reaction catalyzed by mammalian protein farnesyltransferase. *Journal of the American Chemical Society* **2006,** *128* (47), 15086-15087.

52.   Tschantz, W. R.; Furfine, E. S.; Casey, P. J., Substrate binding is required for release of product from mammalian protein farnesyltransferase. *J Biol Chem* **1997,** *272* (15), 9989-93.

53.   Dolence, J. M.; Poulter, C. D., A mechanism for posttranslational modifications of proteins by yeast protein farnesyltransferase. *Proc Natl Acad Sci U S A* **1995,** *92* (11), 5008-11.

54.   Zhang, F. L.; Moomaw, J. F.; Casey, P. J., Properties and kinetic mechanism of recombinant mammalian protein geranylgeranyltransferase type I. *J Biol Chem* **1994,** *269* (38), 23465-70.

55.   Yokoyama, K.; McGeady, P.; Gelb, M. H., Mammalian protein geranylgeranyltransferase-I: substrate specificity, kinetic mechanism, metal requirements, and affinity labeling. *Biochemistry* **1995,** *34* (4), 1344-54.

56.   Stirtan, W. G.; Poulter, C. D., Yeast protein geranylgeranyltransferase type-I: steady-state kinetics and substrate binding. *Biochemistry* **1997,** *36* (15), 4552-7.

57.   Long, S. B.; Casey, P. J.; Beese, L. S., The basis for K-Ras4B binding specificity to protein farnesyltransferase revealed by 2 A resolution ternary complex structures. *Structure* **2000,** *8* (2), 209-22.

58.   Tobin, D. A.; Pickett, J. S.; Hartman, H. L.; Fierke, C. A.; Penner-Hahn, J. E., Structural characterization of the zinc site in protein farnesyltransferase. *J Am Chem Soc* **2003,** *125* (33), 9962-9.

59.   Long, S. B.; Casey, P. J.; Beese, L. S., Reaction path of protein farnesyltransferase at atomic resolution. *Nature* **2002,** *419* (6907), 645-50.

60.   Moomaw, J. F.; Casey, P. J., Mammalian protein geranylgeranyltransferase. Subunit composition and metal requirements. *J Biol Chem* **1992,** *267* (24), 17438-43.

61.   Hartman, H. L.; Bowers, K. E.; Fierke, C. A., Lysine beta311 of protein geranylgeranyltransferase type I partially replaces magnesium. *J Biol Chem* **2004,** *279* (29), 30546-53.

62.   Troutman, J. M.; Andres, D. A.; Spielmann, H. P., Protein farnesyl transferase target selectivity is dependent upon peptide stimulated product release. *Biochemistry* **2007,** *46* (40), 11299-309.

63.   Shen, F.; Seabra, M. C., Mechanism of digeranylgeranylation of Rab proteins. Formation of a complex between monogeranylgeranyl-Rab and Rab escort protein. *J Biol Chem* **1996,** *271* (7), 3692-8.

64.   Alory, C.; Balch, W. E., Molecular basis for Rab prenylation. *J Cell Biol* **2000,** *150* (1), 89-103.

65.   Thoma, N. H.; Niculae, A.; Goody, R. S.; Alexandrov, K., Double prenylation by RabGGTase can proceed without dissociation of the mono-prenylated intermediate. *J Biol Chem* **2001,** *276* (52), 48631-6.

66.   Thoma, N. H.; Iakovenko, A.; Kalinin, A.; Waldmann, H.; Goody, R. S.; Alexandrov, K., Allosteric regulation of substrate binding and product release in geranylgeranyltransferase type II. *Biochemistry* **2001,** *40* (1), 268-74.

67.   Thoma, N. H.; Iakovenko, A.; Owen, D.; Scheidig, A. S.; Waldmann, H.; Goody, R. S.; Alexandrov, K., Phosphoisoprenoid binding specificity of geranylgeranyltransferase type II. *Biochemistry* **2000,** *39* (39), 12043-52.

112

68.   Baron, R. A.; Seabra, M. C., Rab geranylgeranylation occurs preferentially via the pre-formed REP-RGGT complex and is regulated by geranylgeranyl pyrophosphate. *Biochem J* **2008**, *415* (1), 67-75.

69.   Rak, A.; Pylypenko, O.; Niculae, A.; Pyatkov, K.; Goody, R. S.; Alexandrov, K., Structure of the Rab7:REP-1 complex: insights into the mechanism of Rab prenylation and choroideremia disease. *Cell* **2004**, *117* (6), 749-60.

70.   Alory, C.; Balch, W. E., Molecular evolution of the Rab-escort-protein/guanine-nucleotide-dissociation-inhibitor superfamily. *Mol Biol Cell* **2003**, *14* (9), 3857-67.

71.   Shilo, B. Z.; Weinberg, R. A., Unique transforming gene in carcinogen-transformed mouse cells. *Nature* **1981**, *289* (5798), 607-9.

72.   Der, C. J.; Cox, A. D., Isoprenoid modification and plasma membrane association: critical factors for ras oncogenicity. *Cancer Cells* **1991**, *3* (9), 331-40.

73.   Kontani, K.; Tada, M.; Ogawa, T.; Okai, T.; Saito, K.; Araki, Y.; Katada, T., Di-Ras, a distinct subgroup of ras family GTPases with unique biochemical properties. *J Biol Chem* **2002**, *277* (43), 41070-8.

74.   Yamane, H. K.; Farnsworth, C. C.; Xie, H. Y.; Evans, T.; Howald, W. N.; Gelb, M. H.; Glomset, J. A.; Clarke, S.; Fung, B. K., Membrane-binding domain of the small G protein G25K contains an S-(all-trans-geranylgeranyl)cysteine methyl ester at its carboxyl terminus. *Proc Natl Acad Sci U S A* **1991**, *88* (1), 286-90.

75.   Adamson, P.; Marshall, C. J.; Hall, A.; Tilbrook, P. A., Post-translational modifications of p21rho proteins. *J Biol Chem* **1992**, *267* (28), 20033-8.

76.   Nobes, C. D.; Lauritzen, I.; Mattei, M. G.; Paris, S.; Hall, A.; Chardin, P., A new member of the Rho family, Rnd1, promotes disassembly of actin filament structures and loss of cell adhesion. *J Cell Biol* **1998**, *141* (1), 187-97.

77.   Roberts, P. J.; Mitin, N.; Keller, P. J.; Chenette, E. J.; Madigan, J. P.; Currin, R. O.; Cox, A. D.; Wilson, O.; Kirschmeier, P.; Der, C. J., Rho Family GTPase modification and dependence on CAAX motif-signaled posttranslational modification. *J Biol Chem* **2008**, *283* (37), 25150-63.

78.   Nassar, N.; Hoffman, G. R.; Manor, D.; Clardy, J. C.; Cerione, R. A., Structures of Cdc42 bound to the active and catalytically compromised forms of Cdc42GAP. *Nat Struct Biol* **1998**, *5* (12), 1047-52.

79.   Hoffman, G. R.; Nassar, N.; Cerione, R. A., Structure of the Rho family GTP-binding protein Cdc42 in complex with the multifunctional regulator RhoGDI. *Cell* **2000**, *100* (3), 345-56.

80.   Kinsella, B. T.; Erdman, R. A.; Maltese, W. A., Carboxyl-terminal isoprenylation of ras-related GTP-binding proteins encoded by rac1, rac2, and ralA. *J Biol Chem* **1991**, *266* (15), 9786-94.

81.   Buss, J. E.; Quilliam, L. A.; Kato, K.; Casey, P. J.; Solski, P. A.; Wong, G.; Clark, R.; McCormick, F.; Bokoch, G. M.; Der, C. J., The COOH-terminal domain of the Rap1A (Krev-1) protein is isoprenylated and supports transformation by an H-Ras:Rap1A chimeric protein. *Mol Cell Biol* **1991**, *11* (3), 1523-30.

82.   Farrell, F. X.; Yamamoto, K.; Lapetina, E. G., Prenyl group identification of rap2 proteins: a ras superfamily member other than ras that is farnesylated. *Biochem J* **1993**, *289 (Pt 2)*, 349-55.

83.   Kinsella, B. T.; Maltese, W. A., rab GTP-binding proteins implicated in vesicular transport are isoprenylated in vitro at cysteines within a novel carboxyl-terminal motif. *J Biol Chem* **1991**, *266* (13), 8540-4.

84.   Farnsworth, C. C.; Seabra, M. C.; Ericsson, L. H.; Gelb, M. H.; Glomset, J. A., Rab geranylgeranyl transferase catalyzes the geranylgeranylation of adjacent cysteines in the small GTPases Rab1A, Rab3A, and Rab5A. *Proc Natl Acad Sci U S A* **1994,** *91* (25), 11963-7.

85.   Lai, R. K.; Perez-Sala, D.; Canada, F. J.; Rando, R. R., The gamma subunit of transducin is farnesylated. *Proc Natl Acad Sci U S A* **1990,** *87* (19), 7673-7.

86.   Yamane, H. K.; Farnsworth, C. C.; Xie, H. Y.; Howald, W.; Fung, B. K.; Clarke, S.; Gelb, M. H.; Glomset, J. A., Brain G protein gamma subunits contain an all-trans-geranylgeranylcysteine methyl ester at their carboxyl termini. *Proc Natl Acad Sci U S A* **1990,** *87* (15), 5868-72.

87.   Marrari, Y.; Crouthamel, M.; Irannejad, R.; Wedegaertner, P. B., Assembly and trafficking of heterotrimeric G proteins. *Biochemistry* **2007,** *46* (26), 7665-77.

88.   Ray, K.; Kunsch, C.; Bonner, L. M.; Robishaw, J. D., Isolation of cDNA clones encoding eight different human G protein gamma subunits, including three novel forms designated the gamma 4, gamma 10, and gamma 11 subunits. *J Biol Chem* **1995,** *270* (37), 21765-71.

89.   Ashar, H. R.; James, L.; Gray, K.; Carr, D.; Black, S.; Armstrong, L.; Bishop, W. R.; Kirschmeier, P., Farnesyl transferase inhibitors block the farnesylation of CENP-E and CENP-F and alter the association of CENP-E with the microtubules. *J Biol Chem* **2000,** *275* (39), 30451-7.

90.   Jefferson, A. B.; Majerus, P. W., Properties of type II inositol polyphosphate 5-phosphatase. *J Biol Chem* **1995,** *270* (16), 9370-7.

91.   De Smedt, F.; Boom, A.; Pesesse, X.; Schiffmann, S. N.; Erneux, C., Post-translational modification of human brain type I inositol-1,4,5-trisphosphate 5-phosphatase by farnesylation. *J Biol Chem* **1996,** *271* (17), 10419-24.

92.   Farnsworth, C. C.; Wolda, S. L.; Gelb, M. H.; Glomset, J. A., Human lamin B contains a farnesylated cysteine residue. *J Biol Chem* **1989,** *264* (34), 20422-9.

93.   Lutz, R. J.; Trujillo, M. A.; Denham, K. S.; Wenger, L.; Sinensky, M., Nucleoplasmic localization of prelamin A: implications for prenylation-dependent lamin A assembly into the nuclear lamina. *Proc Natl Acad Sci U S A* **1992,** *89* (7), 3000-4.

94.   Kutzleb, C.; Sanders, G.; Yamamoto, R.; Wang, X.; Lichte, B.; Petrasch-Parwez, E.; Kilimann, M. W., Paralemmin, a prenyl-palmitoyl-anchored phosphoprotein abundant in neurons and implicated in plasma membrane dynamics and cell process formation. *J Cell Biol* **1998,** *143* (3), 795-813.

95.   Heilmeyer, L. M., Jr.; Serwe, M.; Weber, C.; Metzger, J.; Hoffmann-Posorske, E.; Meyer, H. E., Farnesylcysteine, a constituent of the alpha and beta subunits of rabbit skeletal muscle phosphorylase kinase: localization by conversion to S-ethylcysteine and by tandem mass spectrometry. *Proc Natl Acad Sci U S A* **1992,** *89* (20), 9554-8.

96.   Anant, J. S.; Fung, B. K., In vivo farnesylation of rat rhodopsin kinase. *Biochem Biophys Res Commun* **1992,** *183* (2), 468-73.

97.   Anant, J. S.; Ong, O. C.; Xie, H. Y.; Clarke, S.; O'Brien, P. J.; Fung, B. K., In vivo differential prenylation of retinal cyclic GMP phosphodiesterase catalytic subunits. *J Biol Chem* **1992,** *267* (2), 687-90.

98.   Inglese, J.; Koch, W. J.; Caron, M. G.; Lefkowitz, R. J., Isoprenylation in regulation of signal transduction by G-protein-coupled receptor kinases. *Nature* **1992,** *359* (6391), 147-50.

99.   Wennerberg, K.; Rossman, K. L.; Der, C. J., The Ras superfamily at a glance. *Journal of Cell Science* **2005,** *118* (5), 843-846.

REFERENCES

100. Takai, Y.; Sasaki, T.; Matozaki, T., Small GTP-binding proteins. *Physiol Rev* **2001,** *81* (1), 153-208.

101. Sprang, S. R., G protein mechanisms: insights from structural analysis. *Annu Rev Biochem* **1997,** *66*, 639-78.

102. Cherfils, J.; Chardin, P., GEFs: structural basis for their activation of small GTP-binding proteins. *Trends Biochem Sci* **1999,** *24* (8), 306-11.

103. Vetter, I. R.; Wittinghofer, A., The guanine nucleotide-binding switch in three dimensions. *Science* **2001,** *294* (5545), 1299-304.

104. John, J.; Rensland, H.; Schlichting, I.; Vetter, I.; Borasio, G. D.; Goody, R. S.; Wittinghofer, A., Kinetic and structural analysis of the Mg(2+)-binding site of the guanine nucleotide-binding protein p21H-ras. *J Biol Chem* **1993,** *268* (2), 923-9.

105. Bos, J. L.; Rehmann, H.; Wittinghofer, A., GEFs and GAPs: critical elements in the control of small G proteins. *Cell* **2007,** *129* (5), 865-77.

106. Scheffzek, K.; Ahmadian, M. R.; Wittinghofer, A., GTPase-activating proteins: helping hands to complement an active site. *Trends Biochem Sci* **1998,** *23* (7), 257-62.

107. Wu, S. K.; Zeng, K.; Wilson, I. A.; Balch, W. E., Structural insights into the function of the Rab GDI superfamily. *Trends Biochem Sci* **1996,** *21* (12), 472-6.

108. Harvey, J. J., An Unidentified Virus Which Causes the Rapid Production of Tumours in Mice. *Nature* **1964,** *204*, 1104-5.

109. Barbacid, M., ras genes. *Annu Rev Biochem* **1987,** *56*, 779-827.

110. Ruta, M.; Wolford, R.; Dhar, R.; Defeo-Jones, D.; Ellis, R. W.; Scolnick, E. M., Nucleotide sequence of the two rat cellular rasH genes. *Mol Cell Biol* **1986,** *6* (5), 1706-10.

111. DeFeo, D.; Gonda, M. A.; Young, H. A.; Chang, E. H.; Lowy, D. R.; Scolnick, E. M.; Ellis, R. W., Analysis of two divergent rat genomic clones homologous to the transforming gene of Harvey murine sarcoma virus. *Proc Natl Acad Sci U S A* **1981,** *78* (6), 3328-32.

112. Ellis, R. W.; Defeo, D.; Shih, T. Y.; Gonda, M. A.; Young, H. A.; Tsuchida, N.; Lowy, D. R.; Scolnick, E. M., The p21 src genes of Harvey and Kirsten sarcoma viruses originate from divergent members of a family of normal vertebrate genes. *Nature* **1981,** *292* (5823), 506-11.

113. Hancock, J. F.; Paterson, H.; Marshall, C. J., A polybasic domain or palmitoylation is required in addition to the CAAX motif to localize p21ras to the plasma membrane. *Cell* **1990,** *63* (1), 133-9.

114. Leventis, R.; Silvius, J. R., Lipid-binding characteristics of the polybasic carboxy-terminal sequence of K-ras4B. *Biochemistry* **1998,** *37* (20), 7640-8.

115. Clarke, S., Protein isoprenylation and methylation at carboxyl-terminal cysteine residues. *Annu Rev Biochem* **1992,** *61*, 355-86.

116. Kim, E.; Ambroziak, P.; Otto, J. C.; Taylor, B.; Ashby, M.; Shannon, K.; Casey, P. J.; Young, S. G., Disruption of the mouse Rce1 gene results in defective Ras processing and mislocalization of Ras within cells. *J Biol Chem* **1999,** *274* (13), 8383-90.

117. Wright, L. P.; Philips, M. R., Thematic review series: lipid posttranslational modifications. CAAX modification and membrane targeting of Ras. *J Lipid Res* **2006,** *47* (5), 883-91.

118. Clarke, S.; Vogel, J. P.; Deschenes, R. J.; Stock, J., Posttranslational modification of the Ha-ras oncogene protein: evidence for a third class of protein carboxyl methyltransferases. *Proc Natl Acad Sci U S A* **1988,** *85* (13), 4643-7.

119. Hancock, J. F.; Magee, A. I.; Childs, J. E.; Marshall, C. J., All ras proteins are polyisoprenylated but only some are palmitoylated. *Cell* **1989,** *57* (7), 1167-77.

120. Swarthout, J. T.; Lobo, S.; Farh, L.; Croke, M. R.; Greentree, W. K.; Deschenes, R. J.; Linder, M. E., DHHC9 and GCP16 constitute a human protein fatty acyltransferase with specificity for H- and N-Ras. *J Biol Chem* **2005,** *280* (35), 31141-8.

121. Schlessinger, J., Cell signaling by receptor tyrosine kinases. *Cell* **2000,** *103* (2), 211-25.

122. Matozaki, T.; Nakanishi, H.; Takai, Y., Small G-protein networks: their crosstalk and signal cascades. *Cell Signal* **2000,** *12* (8), 515-24.

123. Bar-Sagi, D.; Hall, A., Ras and Rho GTPases: a family reunion. *Cell* **2000,** *103* (2), 227-38.

124. Mor, A.; Philips, M. R., Compartmentalized Ras/MAPK signaling. *Annu Rev Immunol* **2006,** *24*, 771-800.

125. Omerovic, J.; Laude, A. J.; Prior, I. A., Ras proteins: paradigms for compartmentalised and isoform-specific signalling. *Cell Mol Life Sci* **2007,** *64* (19-20), 2575-89.

126. Rocks, O.; Peyker, A.; Kahms, M.; Verveer, P. J.; Koerner, C.; Lumbierres, M.; Kuhlmann, J.; Waldmann, H.; Wittinghofer, A.; Bastiaens, P. I., An acylation cycle regulates localization and activity of palmitoylated Ras isoforms. *Science* **2005,** *307* (5716), 1746-52.

127. Goodwin, J. S.; Drake, K. R.; Rogers, C.; Wright, L.; Lippincott-Schwartz, J.; Philips, M. R.; Kenworthy, A. K., Depalmitoylated Ras traffics to and from the Golgi complex via a nonvesicular pathway. *J Cell Biol* **2005,** *170* (2), 261-72.

128. Sidhu, R. S.; Clough, R. R.; Bhullar, R. P., Ca2+/calmodulin binds and dissociates K-RasB from membrane. *Biochem Biophys Res Commun* **2003,** *304* (4), 655-60.

129. Fivaz, M.; Meyer, T., Reversible intracellular translocation of KRas but not HRas in hippocampal neurons regulated by Ca2+/calmodulin. *J Cell Biol* **2005,** *170* (3), 429-41.

130. Villalonga, P.; Lopez-Alcala, C.; Bosch, M.; Chiloeches, A.; Rocamora, N.; Gil, J.; Marais, R.; Marshall, C. J.; Bachs, O.; Agell, N., Calmodulin binds to K-Ras, but not to H- or N-Ras, and modulates its downstream signaling. *Mol Cell Biol* **2001,** *21* (21), 7345-54.

131. Bivona, T. G., et al., PKC regulates a farnesyl-electrostatic switch on K-Ras that promotes its association with Bcl-XL on mitochondria and induces apoptosis. *Mol Cell* **2006,** *21* (4), 481-93.

132. Simons, K.; Ikonen, E., Functional rafts in cell membranes. *Nature* **1997,** *387* (6633), 569-72.

133. Etienne-Manneville, S.; Hall, A., Rho GTPases in cell biology. *Nature* **2002,** *420* (6916), 629-35.

134. Jaffe, A. B.; Hall, A., Rho GTPases: biochemistry and biology. *Annu Rev Cell Dev Biol* **2005,** *21*, 247-69.

135. Small, J. V., Lamellipodia architecture: actin filament turnover and the lateral flow of actin filaments during motility. *Semin Cell Biol* **1994,** *5* (3), 157-63.

136. Stossel, T. P., On the crawling of animal cells. *Science* **1993,** *260* (5111), 1086-94.

137. Olofsson, B., Rho guanine dissociation inhibitors: pivotal molecules in cellular signalling. *Cell Signal* **1999,** *11* (8), 545-54.

138.   Zerial, M.; McBride, H., Rab proteins as membrane organizers. *Nat Rev Mol Cell Biol* **2001,** *2* (2), 107-17.

139.   Palade, G., Intracellular Aspects of the Process of Protein Synthesis. *Science* **1975,** *189* (4206), 867.

140.   Novick, P.; Field, C.; Schekman, R., Identification of 23 complementation groups required for post-translational events in the yeast secretory pathway. *Cell* **1980,** *21* (1), 205-15.

141.   Balch, W. E.; Dunphy, W. G.; Braell, W. A.; Rothman, J. E., Reconstitution of the transport of protein between successive compartments of the Golgi measured by the coupled incorporation of N-acetylglucosamine. *Cell* **1984,** *39* (2 Pt 1), 405-16.

142.   Mellman, I.; Warren, G., The road taken: past and future foundations of membrane traffic. *Cell* **2000,** *100* (1), 99-112.

143.   Bonifacino, J. S.; Glick, B. S., The mechanisms of vesicle budding and fusion. *Cell* **2004,** *116* (2), 153-66.

144.   Cai, H.; Reinisch, K.; Ferro-Novick, S., Coats, tethers, Rabs, and SNAREs work together to mediate the intracellular destination of a transport vesicle. *Dev Cell* **2007,** *12* (5), 671-82.

145.   Novick, P.; Zerial, M., The diversity of Rab proteins in vesicle transport. *Curr Opin Cell Biol* **1997,** *9* (4), 496-504.

146.   Grosshans, B. L.; Ortiz, D.; Novick, P., Rabs and their effectors: achieving specificity in membrane traffic. *Proc Natl Acad Sci U S A* **2006,** *103* (32), 11821-7.

147.   Bonifacino, J. S.; Lippincott-Schwartz, J., Coat proteins: shaping membrane transport. *Nat Rev Mol Cell Biol* **2003,** *4* (5), 409-14.

148.   Kirchhausen, T., Three ways to make a vesicle. *Nat Rev Mol Cell Biol* **2000,** *1* (3), 187-98.

149.   McMahon, H. T.; Mills, I. G., COP and clathrin-coated vesicle budding: different pathways, common approaches. *Curr Opin Cell Biol* **2004,** *16* (4), 379-91.

150.   Owen, D. J.; Collins, B. M.; Evans, P. R., Adaptors for clathrin coats: structure and function. *Annu Rev Cell Dev Biol* **2004,** *20*, 153-91.

151.   Barlowe, C.; Orci, L.; Yeung, T.; Hosobuchi, M.; Hamamoto, S.; Salama, N.; Rexach, M. F.; Ravazzola, M.; Amherdt, M.; Schekman, R., COPII: a membrane coat formed by Sec proteins that drive vesicle budding from the endoplasmic reticulum. *Cell* **1994,** *77* (6), 895-907.

152.   Letourneur, F.; Gaynor, E. C.; Hennecke, S.; Demolliere, C.; Duden, R.; Emr, S. D.; Riezman, H.; Cosson, P., Coatomer is essential for retrieval of dilysine-tagged proteins to the endoplasmic reticulum. *Cell* **1994,** *79* (7), 1199-207.

153.   Memon, A. R., The role of ADP-ribosylation factor and SAR1 in vesicular trafficking in plants. *Biochim Biophys Acta* **2004,** *1664* (1), 9-30.

154.   Hanna, J.; Carroll, K.; Pfeffer, S. R., Identification of residues in TIP47 essential for Rab9 binding. *Proc Natl Acad Sci U S A* **2002,** *99* (11), 7450-4.

155.   Carroll, K. S.; Hanna, J.; Simon, I.; Krise, J.; Barbero, P.; Pfeffer, S. R., Role of Rab9 GTPase in facilitating receptor recruitment by TIP47. *Science* **2001,** *292* (5520), 1373-6.

156.   McLauchlan, H.; Newell, J.; Morrice, N.; Osborne, A.; West, M.; Smythe, E., A novel role for Rab5-GDI in ligand sequestration into clathrin-coated pits. *Curr Biol* **1998,** *8* (1), 34-45.

157.   Pagano, A.; Crottet, P.; Prescianotto-Baschong, C.; Spiess, M., In vitro formation of recycling vesicles from endosomes requires adaptor protein-1/clathrin and is regulated by rab4 and the connector rabaptin-5. *Mol Biol Cell* **2004,** *15* (11), 4990-5000.

158.   Echard, A.; Jollivet, F.; Martinez, O.; Lacapere, J. J.; Rousselet, A.; Janoueix-Lerosey, I.; Goud, B., Interaction of a Golgi-associated kinesin-like protein with Rab6. *Science* **1998,** *279* (5350), 580-5.

159.   Hill, E.; Clarke, M.; Barr, F. A., The Rab6-binding kinesin, Rab6-KIFL, is required for cytokinesis. *EMBO J* **2000,** *19* (21), 5711-9.

160.   Matanis, T.; Akhmanova, A.; Wulf, P.; Del Nery, E.; Weide, T.; Stepanova, T.; Galjart, N.; Grosveld, F.; Goud, B.; De Zeeuw, C. I.; Barnekow, A.; Hoogenraad, C. C., Bicaudal-D regulates COPI-independent Golgi-ER transport by recruiting the dynein-dynactin motor complex. *Nat Cell Biol* **2002,** *4* (12), 986-92.

161.   Imamura, T.; Huang, J.; Usui, I.; Satoh, H.; Bever, J.; Olefsky, J. M., Insulin-induced GLUT4 translocation involves protein kinase C-lambda-mediated functional coupling between Rab4 and the motor protein kinesin. *Mol Cell Biol* **2003,** *23* (14), 4892-900.

162.   Huang, J.; Imamura, T.; Olefsky, J. M., Insulin can regulate GLUT4 internalization by signaling to Rab5 and the motor protein dynein. *Proc Natl Acad Sci U S A* **2001,** *98* (23), 13084-9.

163.   Hoepfner, S.; Severin, F.; Cabezas, A.; Habermann, B.; Runge, A.; Gillooly, D.; Stenmark, H.; Zerial, M., Modulation of receptor recycling and degradation by the endosomal kinesin KIF16B. *Cell* **2005,** *121* (3), 437-50.

164.   Bloom, G. S.; Goldstein, L. S., Cruising along microtubule highways: how membranes move through the secretory pathway. *J Cell Biol* **1998,** *140* (6), 1277-80.

165.   Seabra, M. C.; Coudrier, E., Rab GTPases and myosin motors in organelle motility. *Traffic* **2004,** *5* (6), 393-9.

166.   Desnos, C.; Huet, S.; Darchen, F., 'Should I stay or should I go?': myosin V function in organelle trafficking. *Biol Cell* **2007,** *99* (8), 411-23.

167.   Jordens, I.; Marsman, M.; Kuijl, C.; Neefjes, J., Rab proteins, connecting transport and vesicle fusion. *Traffic* **2005,** *6* (12), 1070-7.

168.   Marks, M. S.; Seabra, M. C., The melanosome: membrane dynamics in black and white. *Nat Rev Mol Cell Biol* **2001,** *2* (10), 738-48.

169.   Jordens, I.; Fernandez-Borja, M.; Marsman, M.; Dusseljee, S.; Janssen, L.; Calafat, J.; Janssen, H.; Wubbolts, R.; Neefjes, J., The Rab7 effector protein RILP controls lysosomal transport by inducing the recruitment of dynein-dynactin motors. *Curr Biol* **2001,** *11* (21), 1680-5.

170.   Johansson, M.; Rocha, N.; Zwart, W.; Jordens, I.; Janssen, L.; Kuijl, C.; Olkkonen, V. M.; Neefjes, J., Activation of endosomal dynein motors by stepwise assembly of Rab7-RILP-p150Glued, ORP1L, and the receptor betaIII spectrin. *J Cell Biol* **2007,** *176* (4), 459-71.

171.   Raposo, G.; Marks, M. S., The dark side of lysosome-related organelles: specialization of the endocytic pathway for melanosome biogenesis. *Traffic* **2002,** *3* (4), 237-48.

172.   Strom, M.; Hume, A. N.; Tarafder, A. K.; Barkagianni, E.; Seabra, M. C., A family of Rab27-binding proteins. Melanophilin links Rab27a and myosin Va function in melanosome transport. *J Biol Chem* **2002,** *277* (28), 25423-30.

173.   Whyte, J. R.; Munro, S., Vesicle tethering complexes in membrane traffic. *J Cell Sci* **2002,** *115* (Pt 13), 2627-37.

174. Sztul, E.; Lupashin, V., Role of tethering factors in secretory membrane traffic. *Am J Physiol Cell Physiol* **2006,** *290* (1), C11-26.

175. Orci, L.; Perrelet, A.; Rothman, J. E., Vesicles on strings: morphological evidence for processive transport within the Golgi stack. *Proc Natl Acad Sci U S A* **1998,** *95* (5), 2279-83.

176. Allan, B. B.; Moyer, B. D.; Balch, W. E., Rab1 recruitment of p115 into a cis-SNARE complex: programming budding COPII vesicles for fusion. *Science* **2000,** *289* (5478), 444-8.

177. Cao, X.; Ballew, N.; Barlowe, C., Initial docking of ER-derived vesicles requires Uso1p and Ypt1p but is independent of SNARE proteins. *EMBO J* **1998,** *17* (8), 2156-65.

178. Seals, D. F.; Eitzen, G.; Margolis, N.; Wickner, W. T.; Price, A., A Ypt/Rab effector complex containing the Sec1 homolog Vps33p is required for homotypic vacuole fusion. *Proc Natl Acad Sci U S A* **2000,** *97* (17), 9402-7.

179. Wurmser, A. E.; Sato, T. K.; Emr, S. D., New component of the vacuolar class C-Vps complex couples nucleotide exchange on the Ypt7 GTPase to SNARE-dependent docking and fusion. *J Cell Biol* **2000,** *151* (3), 551-62.

180. Chen, Y. A.; Scheller, R. H., SNARE-mediated membrane fusion. *Nat Rev Mol Cell Biol* **2001,** *2* (2), 98-106.

181. Jahn, R.; Scheller, R. H., SNAREs--engines for membrane fusion. *Nat Rev Mol Cell Biol* **2006,** *7* (9), 631-43.

182. Sutton, R. B.; Fasshauer, D.; Jahn, R.; Brunger, A. T., Crystal structure of a SNARE complex involved in synaptic exocytosis at 2.4 A resolution. *Nature* **1998,** *395* (6700), 347-53.

183. Rothman, J. E., Mechanisms of intracellular protein transport. *Nature* **1994,** *372* (6501), 55-63.

184. Fasshauer, D.; Sutton, R. B.; Brunger, A. T.; Jahn, R., Conserved structural features of the synaptic fusion complex: SNARE proteins reclassified as Q- and R-SNAREs. *Proc Natl Acad Sci U S A* **1998,** *95* (26), 15781-6.

185. Ossig, R.; Schmitt, H. D.; de Groot, B.; Riedel, D.; Keranen, S.; Ronne, H.; Grubmuller, H.; Jahn, R., Exocytosis requires asymmetry in the central layer of the SNARE complex. *EMBO J* **2000,** *19* (22), 6000-10.

186. McNew, J. A.; Weber, T.; Parlati, F.; Johnston, R. J.; Melia, T. J.; Sollner, T. H.; Rothman, J. E., Close is not enough: SNARE-dependent membrane fusion requires an active mechanism that transduces force to membrane anchors. *J Cell Biol* **2000,** *150* (1), 105-17.

187. Mayer, A.; Wickner, W.; Haas, A., Sec18p (NSF)-driven release of Sec17p (alpha-SNAP) can precede docking and fusion of yeast vacuoles. *Cell* **1996,** *85* (1), 83-94.

188. Hanson, P. I.; Roth, R.; Morisaki, H.; Jahn, R.; Heuser, J. E., Structure and conformational changes in NSF and its membrane receptor complexes visualized by quick-freeze/deep-etch electron microscopy. *Cell* **1997,** *90* (3), 523-35.

189. McBride, H. M.; Rybin, V.; Murphy, C.; Giner, A.; Teasdale, R.; Zerial, M., Oligomeric complexes link Rab5 effectors with NSF and drive membrane fusion via interactions between EEA1 and syntaxin 13. *Cell* **1999,** *98* (3), 377-86.

190. Starai, V. J.; Jun, Y.; Wickner, W., Excess vacuolar SNAREs drive lysis and Rab bypass fusion. *Proc Natl Acad Sci U S A* **2007,** *104* (34), 13551-8.

191. Goody, R. S.; Rak, A.; Alexandrov, K., The structural and mechanistic basis for recycling of Rab proteins between membrane compartments. *Cell Mol Life Sci* **2005,** *62* (15), 1657-70.

192.   Ullrich, O.; Stenmark, H.; Alexandrov, K.; Huber, L. A.; Kaibuchi, K.; Sasaki, T.; Takai, Y.; Zerial, M., Rab GDP dissociation inhibitor as a general regulator for the membrane association of rab proteins. *J Biol Chem* **1993,** *268* (24), 18143-50.

193.   Luan, P.; Balch, W. E.; Emr, S. D.; Burd, C. G., Molecular dissection of guanine nucleotide dissociation inhibitor function in vivo. Rab-independent binding to membranes and role of Rab recycling factors. *J Biol Chem* **1999,** *274* (21), 14806-17.

194.   Dirac-Svejstrup, A. B.; Sumizawa, T.; Pfeffer, S. R., Identification of a GDI displacement factor that releases endosomal Rab GTPases from Rab-GDI. *EMBO J* **1997,** *16* (3), 465-72.

195.   Gelb, M. H.; Brunsveld, L.; Hrycyna, C. A.; Michaelis, S.; Tamanoi, F.; Van Voorhis, W. C.; Waldmann, H., Therapeutic intervention based on protein prenylation and associated modifications. *Nat Chem Biol* **2006,** *2* (10), 518-28.

196.   Lowy, D. R.; Willumsen, B. M., Function and regulation of ras. *Annu Rev Biochem* **1993,** *62*, 851-91.

197.   Rolfe, B. E.; Worth, N. F.; World, C. J.; Campbell, J. H.; Campbell, G. R., Rho and vascular disease. *Atherosclerosis* **2005,** *183* (1), 1-16.

198.   Stein, M. P.; Dong, J.; Wandinger-Ness, A., Rab proteins and endocytic trafficking: potential targets for therapeutic intervention. *Adv Drug Deliv Rev* **2003,** *55* (11), 1421-37.

199.   Griscelli, C.; Durandy, A.; Guy-Grand, D.; Daguillard, F.; Herzog, C.; Prunieras, M., A syndrome associating partial albinism and immunodeficiency. *Am J Med* **1978,** *65* (4), 691-702.

200.   van den Hurk, J. A.; Schwartz, M.; van Bokhoven, H.; van de Pol, T. J.; Bogerd, L.; Pinckers, A. J.; Bleeker-Wagemakers, E. M.; Pawlowitzki, I. H.; Ruther, K.; Ropers, H. H.; Cremers, F. P., Molecular basis of choroideremia (CHM): mutations involving the Rab escort protein-1 (REP-1) gene. *Hum Mutat* **1997,** *9* (2), 110-7.

201.   D'Adamo, P., et al., Mutations in GDI1 are responsible for X-linked non-specific mental retardation. *Nat Genet* **1998,** *19* (2), 134-9.

202.   van Slegtenhorst, M., et al., Identification of the tuberous sclerosis gene TSC1 on chromosome 9q34. *Science* **1997,** *277* (5327), 805-8.

203.   Tamanoi, F.; Gau, C. L.; Jiang, C.; Edamatsu, H.; Kato-Stankiewicz, J., Protein farnesylation in mammalian cells: effects of farnesyltransferase inhibitors on cancer cells. *Cell Mol Life Sci* **2001,** *58* (11), 1636-49.

204.   Basso, A. D.; Kirschmeier, P.; Bishop, W. R., Lipid posttranslational modifications. Farnesyl transferase inhibitors. *J Lipid Res* **2006,** *47* (1), 15-31.

205.   Karp, J. E., et al., Clinical and biologic activity of the farnesyltransferase inhibitor R115777 in adults with refractory and relapsed acute leukemias: a phase 1 clinical-laboratory correlative trial. *Blood* **2001,** *97* (11), 3361-9.

206.   Alsina, M., et al., Farnesyltransferase inhibitor tipifarnib is well tolerated, induces stabilization of disease, and inhibits farnesylation and oncogenic/tumor survival pathways in patients with advanced multiple myeloma. *Blood* **2004,** *103* (9), 3271-7.

207.   Rao, S., et al., Phase III double-blind placebo-controlled study of farnesyl transferase inhibitor R115777 in patients with refractory advanced colorectal cancer. *J Clin Oncol* **2004,** *22* (19), 3950-7.

208.   Macdonald, J. S.; McCoy, S.; Whitehead, R. P.; Iqbal, S.; Wade, J. L., 3rd; Giguere, J. K.; Abbruzzese, J. L., A phase II study of farnesyl transferase inhibitor R115777 in pancreatic

cancer: a Southwest oncology group (SWOG 9924) study. *Invest New Drugs* **2005,** *23* (5), 485-7.

209. Greenwood, J.; Steinman, L.; Zamvil, S. S., Statin therapy and autoimmune disease: from protein prenylation to immunomodulation. *Nat Rev Immunol* **2006,** *6* (5), 358-70.

210. Sepp-Lorenzino, L.; Ma, Z.; Rands, E.; Kohl, N. E.; Gibbs, J. B.; Oliff, A.; Rosen, N., A peptidomimetic inhibitor of farnesyl:protein transferase blocks the anchorage-dependent and -independent growth of human tumor cell lines. *Cancer Res* **1995,** *55* (22), 5302-9.

211. Chien, Y.; White, M. A., RAL GTPases are linchpin modulators of human tumour-cell proliferation and survival. *EMBO Rep* **2003,** *4* (8), 800-6.

212. Khosravi-Far, R.; Solski, P. A.; Clark, G. J.; Kinch, M. S.; Der, C. J., Activation of Rac1, RhoA, and mitogen-activated protein kinases is required for Ras transformation. *Mol Cell Biol* **1995,** *15* (11), 6443-53.

213. Clark, E. A.; Golub, T. R.; Lander, E. S.; Hynes, R. O., Genomic analysis of metastasis reveals an essential role for RhoC. *Nature* **2000,** *406* (6795), 532-5.

214. Feig, L. A., Ral-GTPases: approaching their 15 minutes of fame. *Trends Cell Biol* **2003,** *13* (8), 419-25.

215. Gildea, J. J.; Harding, M. A.; Seraj, M. J.; Gulding, K. M.; Theodorescu, D., The role of Ral A in epidermal growth factor receptor-regulated cell motility. *Cancer Res* **2002,** *62* (4), 982-5.

216. Lim, K. H.; Baines, A. T.; Fiordalisi, J. J.; Shipitsin, M.; Feig, L. A.; Cox, A. D.; Der, C. J.; Counter, C. M., Activation of RalA is critical for Ras-induced tumorigenesis of human cells. *Cancer Cell* **2005,** *7* (6), 533-45.

217. Philips, M. R.; Cox, A. D., Geranylgeranyltransferase I as a target for anti-cancer drugs. *J Clin Invest* **2007,** *117* (5), 1223-5.

218. Cheng, K. W.; Lahad, J. P.; Kuo, W. L.; Lapuk, A.; Yamada, K.; Auersperg, N.; Liu, J.; Smith-McCune, K.; Lu, K. H.; Fishman, D.; Gray, J. W.; Mills, G. B., The RAB25 small GTPase determines aggressiveness of ovarian and breast cancers. *Nat Med* **2004,** *10* (11), 1251-6.

219. He, H.; Dai, F.; Yu, L.; She, X.; Zhao, Y.; Jiang, J.; Chen, X.; Zhao, S., Identification and characterization of nine novel human small GTPases showing variable expressions in liver cancer tissues. *Gene Expr* **2002,** *10* (5-6), 231-42.

220. Lackner, M. R., et al., Chemical genetics identifies Rab geranylgeranyl transferase as an apoptotic target of farnesyl transferase inhibitors. *Cancer Cell* **2005,** *7* (4), 325-36.

221. Puccetti, L.; Acampa, M.; Auteri, A., Pharmacogenetics of statins therapy. *Recent Patents Cardiovasc Drug Discov* **2007,** *2* (3), 228-36.

222. Konstantinopoulos, P. A.; Karamouzis, M. V.; Papavassiliou, A. G., Post-translational modifications and regulation of the RAS superfamily of GTPases as anticancer targets. *Nat Rev Drug Discov* **2007,** *6* (7), 541-55.

223. Denoyelle, C.; Albanese, P.; Uzan, G.; Hong, L.; Vannier, J. P.; Soria, J.; Soria, C., Molecular mechanism of the anti-cancer activity of cerivastatin, an inhibitor of HMG-CoA reductase, on aggressive human breast cancer cells. *Cell Signal* **2003,** *15* (3), 327-38.

224. Pais, J. E.; Bowers, K. E.; Stoddard, A. K.; Fierke, C. A., A continuous fluorescent assay for protein prenyltransferases measuring diphosphate release. *Anal Biochem* **2005,** *345* (2), 302-11.

225.   Cassidy, P. B.; Dolence, J. M.; Poulter, C. D., Continuous fluorescence assay for protein prenyltransferases. *Methods Enzymol* **1995,** *250*, 30-43.

226.   Owen, D. J.; Alexandrov, K.; Rostkova, E.; Scheidig, A. J.; Goody, R. S.; Waldmann, H., Chemo-enzymatic synthesis of fluorescent Rab 7 proteins: Tools to study vesicular trafficking in cells. *Angewandte Chemie-International Edition* **1999,** *38* (4), 509-512.

227.   Dursina, B.; Reents, R.; Delon, C.; Wu, Y.; Kulharia, M.; Thutewohl, M.; Veligodsky, A.; Kalinin, A.; Evstifeev, V.; Ciobanu, D.; Szedlacsek, S. E.; Waldmann, H.; Goody, R. S.; Alexandrov, K., Identification and specificity profiling of protein prenyltransferase inhibitors using new fluorescent phosphoisoprenoids. *J Am Chem Soc* **2006,** *128* (9), 2822-35.

228.   Pompliano, D. L.; Gomez, R. P.; Anthony, N. J., Intramolecular Fluorescence Enhancement - a Continuous Assay of Ras Farnesyl - Protein Transferase. *Journal of the American Chemical Society* **1992,** *114* (20), 7945-7946.

229.   Kale, T. A.; Hsieh, S. A.; Rose, M. W.; Distefano, M. D., Use of synthetic isoprenoid analogues for understanding protein prenyltransferase mechanism and structure. *Curr Top Med Chem* **2003,** *3* (10), 1043-74.

230.   Peter, M.; Chavrier, P.; Nigg, E. A.; Zerial, M., Isoprenylation of rab proteins on structurally distinct cysteine motifs. *J Cell Sci* **1992,** *102 (Pt 4)*, 857-65.

231.   Hancock, J. F., Reticulocyte lysate assay for in vitro translation and posttranslational modification of Ras proteins. *Methods Enzymol* **1995,** *255*, 60-5.

232.   Benetka, W.; Koranda, M.; Maurer-Stroh, S.; Pittner, F.; Eisenhaber, F., Farnesylation or geranylgeranylation? Efficient assays for testing protein prenylation in vitro and in vivo. *BMC Biochem* **2006,** *7*, 6.

233.   Mendola, C. E.; Backer, J. M., Lovastatin blocks N-ras oncogene-induced neuronal differentiation. *Cell Growth Differ* **1990,** *1* (10), 499-502.

234.   Das, N. P.; Allen, C. M., Inhibition of farnesyl transferases from malignant and non-malignant cultured human lymphocytes by prenyl substrate analogues. *Biochem Biophys Res Commun* **1991,** *181* (2), 729-35.

235.   Gaon, I.; Turek, T. C.; Weller, V. A.; Edelstein, R. L.; Singh, S. K.; Distefano, M. D., Photoactive Analogs of Farnesyl Pyrophosphate Containing Benzoylbenzoate Esters: Synthesis and Application to Photoaffinity Labeling of Yeast Protein Farnesyltransferase. *J Org Chem* **1996,** *61* (22), 7738-7745.

236.   Gibbs, R. A.; Krishnan, U.; Dolence, J. M.; Poulter, C. D., A Stereoselective Palladium Copper-Catalyzed Route to Isoprenoids - Synthesis and Biological Evaluation of 13-Methylidenefarnesyl Diphosphate. *Journal of Organic Chemistry* **1995,** *60* (24), 7821-7829.

237.   Gaon, I.; Turek, T. C.; Distefano, M. D., Farnesyl and geranylgeranyl pyrophosphate analogs incorporating benzoylbenzyl ethers: Synthesis and inhibition of yeast protein farnesyltransferase. *Tetrahedron Letters* **1996,** *37* (49), 8833-8836.

238.   Turek, T. C.; Gaon, I.; Distefano, M. D., Analogs of farnesyl pyrophosphate containing benzophenones: Synthesis and photoaffinity labeling of yeast protein farnesyltransferase. *Abstracts of Papers of the American Chemical Society* **1996,** *212*, 166-ORGN.

239.   Turek, T. C.; Gaon, I.; Gamache, D.; Distefano, M. D., Synthesis and evaluation of benzophenone-based photoaffinity labeling analogs of prenyl pyrophosphates containing stable amide linkages. *Bioorganic & Medicinal Chemistry Letters* **1997,** *7* (16), 2125-2130.

122

240. Turek, T. C.; Gaon, I.; Distefano, M. D.; Strickland, C. L., Synthesis of farnesyl diphosphate analogues containing ether-linked photoactive benzophenones and their application in studies of protein prenyltransferases. *J Org Chem* **2001,** *66* (10), 3253-64.

241. Chehade, K. A.; Andres, D. A.; Morimoto, H.; Spielmann, H. P., Design and synthesis of a transferable farnesyl pyrophosphate analogue to Ras by protein farnesyltransferase. *J Org Chem* **2000,** *65* (10), 3027-33.

242. Dursina, B. E.; Reents, R.; Niculae, A.; Veligodsky, A.; Breitling, R.; Pyatkov, K.; Waldmann, H.; Goody, R. S.; Alexandrov, K., A genetically encodable microtag for chemo-enzymatic derivatization and purification of recombinant proteins. *Protein Expr Purif* **2005,** *39* (1), 71-81.

243. Prescher, J. A.; Bertozzi, C. R., Chemistry in living systems. *Nat Chem Biol* **2005,** *1* (1), 13-21.

244. Miller, L. W.; Cornish, V. W., Selective chemical labeling of proteins in living cells. *Curr Opin Chem Biol* **2005,** *9* (1), 56-61.

245. Chen, I.; Ting, A. Y., Site-specific labeling of proteins with small molecules in live cells. *Curr Opin Biotechnol* **2005,** *16* (1), 35-40.

246. Farinas, J.; Verkman, A. S., Receptor-mediated targeting of fluorescent probes in living cells. *Journal of Biological Chemistry* **1999,** *274* (12), 7603-7606.

247. Marks, K. M.; Braun, P. D.; Nolan, G. P., A general approach for chemical labeling and rapid, spatially controlled protein inactivation. *Proc Natl Acad Sci U S A* **2004,** *101* (27), 9982-7.

248. Marks, K. M.; Rosinov, M.; Nolan, G. P., In vivo targeting of organic calcium sensors via genetically selected peptides. *Chem Biol* **2004,** *11* (3), 347-56.

249. Guignet, E. G.; Hovius, R.; Vogel, H., Reversible site-selective labeling of membrane proteins in live cells. *Nat Biotechnol* **2004,** *22* (4), 440-4.

250. Griffin, B. A.; Adams, S. R.; Tsien, R. Y., Specific covalent labeling of recombinant protein molecules inside live cells. *Science* **1998,** *281* (5374), 269-72.

251. Griffin, B. A.; Adams, S. R.; Jones, J.; Tsien, R. Y., Fluorescent labeling of recombinant proteins in living cells with FlAsH. *Methods Enzymol* **2000,** *327*, 565-78.

252. Adams, S. R.; Campbell, R. E.; Gross, L. A.; Martin, B. R.; Walkup, G. K.; Yao, Y.; Llopis, J.; Tsien, R. Y., New biarsenical ligands and tetracysteine motifs for protein labeling in vitro and in vivo: synthesis and biological applications. *J Am Chem Soc* **2002,** *124* (21), 6063-76.

253. Tsien, R. Y., The green fluorescent protein. *Annu Rev Biochem* **1998,** *67*, 509-44.

254. Zhang, J.; Campbell, R. E.; Ting, A. Y.; Tsien, R. Y., Creating new fluorescent probes for cell biology. *Nat Rev Mol Cell Biol* **2002,** *3* (12), 906-18.

255. Keppler, A.; Gendreizig, S.; Gronemeyer, T.; Pick, H.; Vogel, H.; Johnsson, K., A general method for the covalent labeling of fusion proteins with small molecules in vivo. *Nat Biotechnol* **2003,** *21* (1), 86-9.

256. Keppler, A.; Kindermann, M.; Gendreizig, S.; Pick, H.; Vogel, H.; Johnsson, K., Labeling of fusion proteins of O6-alkylguanine-DNA alkyltransferase with small molecules in vivo and in vitro. *Methods* **2004,** *32* (4), 437-44.

257. Keppler, A.; Pick, H.; Arrivoli, C.; Vogel, H.; Johnsson, K., Labeling of fusion proteins with synthetic fluorophores in live cells. *Proc Natl Acad Sci U S A* **2004,** *101* (27), 9955-9.

258. Giriat, I.; Muir, T. W., Protein semi-synthesis in living cells. *J Am Chem Soc* **2003,** *125* (24), 7180-1.

REFERENCES

259.   Buskirk, A. R.; Ong, Y. C.; Gartner, Z. J.; Liu, D. R., Directed evolution of ligand dependence: small-molecule-activated protein splicing. *Proc Natl Acad Sci U S A* **2004,** *101* (29), 10505-10.

260.   Yeo, D. S.; Srinivasan, R.; Uttamchandani, M.; Chen, G. Y.; Zhu, Q.; Yao, S. Q., Cell-permeable small molecule probes for site-specific labeling of proteins. *Chem Commun (Camb)* **2003,** (23), 2870-1.

261.   Yin, J.; Liu, F.; Li, X.; Walsh, C. T., Labeling proteins with small molecules by site-specific posttranslational modification. *J Am Chem Soc* **2004,** *126* (25), 7754-5.

262.   George, N.; Pick, H.; Vogel, H.; Johnsson, N.; Johnsson, K., Specific labeling of cell surface proteins with chemically diverse compounds. *J Am Chem Soc* **2004,** *126* (29), 8896-7.

263.   Chen, I.; Howarth, M.; Lin, W.; Ting, A. Y., Site-specific labeling of cell surface proteins with biophysical probes using biotin ligase. *Nat Methods* **2005,** *2* (2), 99-104.

264.   Howarth, M.; Takao, K.; Hayashi, Y.; Ting, A. Y., Targeting quantum dots to surface proteins in living cells with biotin ligase. *Proc Natl Acad Sci U S A* **2005,** *102* (21), 7583-8.

265.   Mahal, L. K.; Yarema, K. J.; Bertozzi, C. R., Engineering chemical reactivity on cell surfaces through oligosaccharide biosynthesis. *Science* **1997,** *276* (5315), 1125-8.

266.   de Araujo, A. D.; Palomo, J. M.; Cramer, J.; Kohn, M.; Schroder, H.; Wacker, R.; Niemeyer, C.; Alexandrov, K.; Waldmann, H., Diels-Alder ligation and surface immobilization of proteins. *Angew Chem Int Ed Engl* **2005,** *45* (2), 296-301.

267.   Rostovtsev, V. V.; Green, L. G.; Fokin, V. V.; Sharpless, K. B., A stepwise huisgen cycloaddition process: copper(I)-catalyzed regioselective "ligation" of azides and terminal alkynes. *Angew Chem Int Ed Engl* **2002,** *41* (14), 2596-9.

268.   Tornoe, C. W.; Christensen, C.; Meldal, M., Peptidotriazoles on solid phase: [1,2,3]-triazoles by regiospecific copper(i)-catalyzed 1,3-dipolar cycloadditions of terminal alkynes to azides. *J Org Chem* **2002,** *67* (9), 3057-64.

269.   Saxon, E.; Armstrong, J. I.; Bertozzi, C. R., A "traceless" Staudinger ligation for the chemoselective synthesis of amide bonds. *Org Lett* **2000,** *2* (14), 2141-3.

270.   Kohn, M.; Breinbauer, R., The Staudinger ligation-a gift to chemical biology. *Angew Chem Int Ed Engl* **2004,** *43* (24), 3106-16.

271.   Agard, N. J.; Prescher, J. A.; Bertozzi, C. R., A strain-promoted [3 + 2] azide-alkyne cycloaddition for covalent modification of biomolecules in living systems. *J Am Chem Soc* **2004,** *126* (46), 15046-7.

272.   Agard, N. J.; Baskin, J. M.; Prescher, J. A.; Lo, A.; Bertozzi, C. R., A comparative study of bioorthogonal reactions with azides. *ACS Chem Biol* **2006,** *1* (10), 644-8.

273.   Luchansky, S. J.; Argade, S.; Hayes, B. K.; Bertozzi, C. R., Metabolic functionalization of recombinant glycoproteins. *Biochemistry* **2004,** *43* (38), 12358-66.

274.   Saxon, E.; Bertozzi, C. R., Cell surface engineering by a modified Staudinger reaction. *Science* **2000,** *287* (5460), 2007-10.

275.   Kohn, M.; Wacker, R.; Peters, C.; Schroder, H.; Soulere, L.; Breinbauer, R.; Niemeyer, C. M.; Waldmann, H., Staudinger ligation: a new immobilization strategy for the preparation of small-molecule arrays. *Angew Chem Int Ed Engl* **2003,** *42* (47), 5830-4.

276.   Soellner, M. B.; Dickson, K. A.; Nilsson, B. L.; Raines, R. T., Site-specific protein immobilization by Staudinger ligation. *J Am Chem Soc* **2003,** *125* (39), 11790-1.

277. Speers, A. E.; Cravatt, B. F., Chemical strategies for activity-based proteomics. *Chembiochem* **2004,** *5* (1), 41-7.

278. Link, A. J.; Tirrell, D. A., Cell surface labeling of Escherichia coli via copper(I)-catalyzed [3+2] cycloaddition. *J Am Chem Soc* **2003,** *125* (37), 11164-5.

279. Baskin, J. M.; Prescher, J. A.; Laughlin, S. T.; Agard, N. J.; Chang, P. V.; Miller, I. A.; Lo, A.; Codelli, J. A.; Bertozzi, C. R., Copper-free click chemistry for dynamic in vivo imaging. *Proc Natl Acad Sci U S A* **2007,** *104* (43), 16793-7.

280. Chaiet, L.; Wolf, F. J., The Properties of Streptavidin, a Biotin-Binding Protein Produced by Streptomycetes. *Arch Biochem Biophys* **1964,** *106*, 1-5.

281. Duckworth, B. P.; Zhang, Z.; Hosokawa, A.; Distefano, M. D., Selective labeling of proteins by using protein farnesyltransferase. *Chembiochem* **2007,** *8* (1), 98-105.

282. Xu, J.; Degraw, A. J.; Duckworth, B. P.; Lenevich, S.; Tann, C. M.; Jenson, E. C.; Gruber, S. J.; Barany, G.; Distefano, M. D., Synthesis and reactivity of 6,7-dihydrogeranylazides: reagents for primary azide incorporation into peptides and subsequent staudinger ligation. *Chem Biol Drug Des* **2006,** *68* (2), 85-96.

283. Rose, M. W.; Rose, N. D.; Boggs, J.; Lenevich, S.; Xu, J.; Barany, G.; Distefano, M. D., Evaluation of geranylazide and farnesylazide diphosphate for incorporation of prenylazides into a CAAX box-containing peptide using protein farnesyltransferase. *J Pept Res* **2005,** *65* (6), 529-37.

284. Rose, M. W.; Xu, J.; Kale, T. A.; O'Doherty, G.; Barany, G.; Distefano, M. D., Enzymatic incorporation of orthogonally reactive prenylazide groups into peptides using geranylazide diphosphate via protein farnesyltransferase: implications for selective protein labeling. *Biopolymers* **2005,** *80* (2-3), 164-71.

285. Labadie, G. R.; Viswanathan, R.; Poulter, C. D., Farnesyl diphosphate analogues with omega-bioorthogonal azide and alkyne functional groups for protein farnesyl transferase-catalyzed ligation reactions. *J Org Chem* **2007,** *72* (24), 9291-7.

286. Duckworth, B. P.; Xu, J.; Taton, T. A.; Guo, A.; Distefano, M. D., Site-specific, covalent attachment of proteins to a solid surface. *Bioconjug Chem* **2006,** *17* (4), 967-74.

287. Gauchet, C.; Labadie, G. R.; Poulter, C. D., Regio- and chemoselective covalent immobilization of proteins through unnatural amino acids. *J Am Chem Soc* **2006,** *128* (29), 9274-5.

288. Kho, Y.; Kim, S. C.; Jiang, C.; Barma, D.; Kwon, S. W.; Cheng, J.; Jaunbergs, J.; Weinbaum, C.; Tamanoi, F.; Falck, J.; Zhao, Y., A tagging-via-substrate technology for detection and proteomics of farnesylated proteins. *Proc Natl Acad Sci U S A* **2004,** *101* (34), 12479-84.

289. Duckworth, B. P.; Chen, Y.; Wollack, J. W.; Sham, Y.; Mueller, J. D.; Taton, T. A.; Distefano, M. D., A universal method for the preparation of covalent protein-DNA conjugates for use in creating protein nanostructures. *Angew Chem Int Ed Engl* **2007,** *46* (46), 8819-22.

290. Nguyen, U. T.; Cramer, J.; Gomis, J.; Reents, R.; Gutierrez-Rodriguez, M.; Goody, R. S.; Alexandrov, K.; Waldmann, H., Exploiting the substrate tolerance of farnesyltransferase for site-selective protein derivatization. *Chembiochem* **2007,** *8* (4), 408-23.

291. Micali, E.; Chehade, K. A.; Isaacs, R. J.; Andres, D. A.; Spielmann, H. P., Protein farnesyltransferase isoprenoid substrate discrimination is dependent on isoprene double bonds and branched methyl groups. *Biochemistry* **2001,** *40* (41), 12254-65.

292. Yokoyama, K.; Zimmerman, K.; Scholten, J.; Gelb, M. H., Differential prenyl pyrophosphate binding to mammalian protein geranylgeranyltransferase-I and protein farnesyltransferase and its consequence on the specificity of protein prenylation. *J Biol Chem* **1997,** *272* (7), 3944-52.

293. Dudler, T.; Gelb, M. H., Replacement of the H-Ras farnesyl group by lipid analogues: implications for downstream processing and effector activation in Xenopus oocytes. *Biochemistry* **1997,** *36* (41), 12434-41.

294. Roberts, M. J.; Troutman, J. M.; Chehade, K. A.; Cha, H. C.; Kao, J. P.; Huang, X.; Zhan, C. G.; Peterson, Y. K.; Subramanian, T.; Kamalakkannan, S.; Andres, D. A.; Spielmann, H. P., Hydrophilic anilinogeranyl diphosphate prenyl analogues are Ras function inhibitors. *Biochemistry* **2006,** *45* (51), 15862-72.

295. Troutman, J. M.; Subramanian, T.; Andres, D. A.; Spielmann, H. P., Selective modification of CaaX peptides with ortho-substituted anilinogeranyl lipids by protein farnesyl transferase: competitive substrates and potent inhibitors from a library of farnesyl diphosphate analogues. *Biochemistry* **2007,** *46* (40), 11310-21.

296. Subramanian, T.; Liu, S.; Troutman, J. M.; Andres, D. A.; Spielmann, H. P., Protein farnesyltransferase-catalyzed isoprenoid transfer to peptide depends on lipid size and shape, not hydrophobicity. *Chembiochem* **2008,** *9* (17), 2872-82.

297. Chehade, K. A.; Kiegiel, K.; Isaacs, R. J.; Pickett, J. S.; Bowers, K. E.; Fierke, C. A.; Andres, D. A.; Spielmann, H. P., Photoaffinity analogues of farnesyl pyrophosphate transferable by protein farnesyl transferase. *J Am Chem Soc* **2002,** *124* (28), 8206-19.

298. Cui, G.; Wang, B.; Merz, K. M., Jr., Computational studies of the farnesyltransferase ternary complex part I: substrate binding. *Biochemistry* **2005,** *44* (50), 16513-23.

299. de Araujo, A. D.; Palomo, J. M.; Cramer, J.; Seitz, O.; Alexandrov, K.; Waldmann, H., Diels-Alder ligation of peptides and proteins. *Chemistry* **2006,** *12* (23), 6095-109.

300. Speers, A. E.; Adam, G. C.; Cravatt, B. F., Activity-based protein profiling in vivo using a copper(i)-catalyzed azide-alkyne [3 + 2] cycloaddition. *J Am Chem Soc* **2003,** *125* (16), 4686-7.

301. Watzke, A.; Gutierrez-Rodriguez, M.; Kohn, M.; Wacker, R.; Schroeder, H.; Breinbauer, R.; Kuhlmann, J.; Alexandrov, K.; Niemeyer, C. M.; Goody, R. S.; Waldmann, H., A generic building block for C- and N-terminal protein-labeling and protein-immobilization. *Bioorg Med Chem* **2006,** *14* (18), 6288-306.

302. Watzke, A.; Kohn, M.; Gutierrez-Rodriguez, M.; Wacker, R.; Schroder, H.; Breinbauer, R.; Kuhlmann, J.; Alexandrov, K.; Niemeyer, C. M.; Goody, R. S.; Waldmann, H., Site-selective protein immobilization by Staudinger ligation. *Angew Chem Int Ed Engl* **2006,** *45* (9), 1408-12.

303. Kiick, K. L.; Saxon, E.; Tirrell, D. A.; Bertozzi, C. R., Incorporation of azides into recombinant proteins for chemoselective modification by the Staudinger ligation. *Proc Natl Acad Sci U S A* **2002,** *99* (1), 19-24.

304. Lin, F. L.; Hoyt, H. M.; van Halbeek, H.; Bergman, R. G.; Bertozzi, C. R., Mechanistic investigation of the staudinger ligation. *J Am Chem Soc* **2005,** *127* (8), 2686-95.

305. Handlon, A. L.; Oppenheimer, N. J., Thiol reduction of 3'-azidothymidine to 3'-aminothymidine: kinetics and biomedical implications. *Pharm Res* **1988,** *5* (5), 297-9.

306. Soellner, M. B.; Tam, A.; Raines, R. T., Staudinger ligation of peptides at non-glycyl residues. *J Org Chem* **2006,** *71* (26), 9824-30.

307. Lindstrom, U. M., Stereoselective organic reactions in water. *Chem Rev* **2002,** *102* (8), 2751-72.

126

308.   Otto, S.; Engberts, J. B., Hydrophobic interactions and chemical reactivity. *Org Biomol Chem* **2003,** *1* (16), 2809-20.

309.   Grieco, P. A.; Walker, J. K., Intramolecular cationic [5+2] cycloaddition reactions promoted by trimethylsilyl triflate in 3.0 M lithium perchlorate-ethyl acetate: Application to a formal total synthesis of (+/-)-isocomene. *Tetrahedron* **1997,** *53* (26), 8975-8996.

310.   Hill, K. W.; Taunton-Rigby, J.; Carter, J. D.; Kropp, E.; Vagle, K.; Pieken, W.; McGee, D. P.; Husar, G. M.; Leuck, M.; Anziano, D. J.; Sebesta, D. P., Diels--Alder bioconjugation of diene-modified oligonucleotides. *J Org Chem* **2001,** *66* (16), 5352-8.

311.   Husar, G. M.; Anziano, D. J.; Leuck, M.; Sebesta, D. P., Covalent modification and surface immobilization of nucleic acids via the Diels-Alder bioconjugation method. *Nucleosides Nucleotides Nucleic Acids* **2001,** *20* (4-7), 559-66.

312.   Pozsgay, V.; Vieira, N. E.; Yergey, A., A method for bioconjugation of carbohydrates using Diels-Alder cycloaddition. *Org Lett* **2002,** *4* (19), 3191-4.

313.   Houseman, B. T.; Mrksich, M., Carbohydrate arrays for the evaluation of protein binding and enzymatic modification. *Chem Biol* **2002,** *9* (4), 443-54.

314.   Houseman, B. T.; Huh, J. H.; Kron, S. J.; Mrksich, M., Peptide chips for the quantitative evaluation of protein kinase activity. *Nat Biotechnol* **2002,** *20* (3), 270-4.

315.   Dillmore, W. S.; Yousaf, M. N.; Mrksich, M., A photochemical method for patterning the immobilization of ligands and cells to self-assembled monolayers. *Langmuir* **2004,** *20* (17), 7223-31.

316.   Touchot, N.; Chardin, P.; Tavitian, A., Four additional members of the ras gene superfamily isolated by an oligonucleotide strategy: molecular cloning of YPT-related cDNAs from a rat brain library. *Proc Natl Acad Sci U S A* **1987,** *84* (23), 8210-4.

317.   Troutman, J. M.; Roberts, M. J.; Andres, D. A.; Spielmann, H. P., Tools to analyze protein farnesylation in cells. *Bioconjug Chem* **2005,** *16* (5), 1209-17.

318.   Lin, H. P.; Hsu, S. C.; Wu, J. C.; Sheen, I. J.; Yan, B. S.; Syu, W. J., Localization of isoprenylated antigen of hepatitis delta virus by anti-farnesyl antibodies. *J Gen Virol* **1999,** *80 (Pt 1)*, 91-6.

319.   Baron, R.; Fourcade, E.; Lajoie-Mazenc, I.; Allal, C.; Couderc, B.; Barbaras, R.; Favre, G.; Faye, J. C.; Pradines, A., RhoB prenylation is driven by the three carboxyl-terminal amino acids of the protein: evidenced in vivo by an anti-farnesyl cysteine antibody. *Proc Natl Acad Sci U S A* **2000,** *97* (21), 11626-31.

320.   Terry, K. L.; Casey, P. J.; Beese, L. S., Conversion of protein farnesyltransferase to a geranylgeranyltransferase. *Biochemistry* **2006,** *45* (32), 9746-55.

321.   Ko, T. P.; Chen, Y. K.; Robinson, H.; Tsai, P. C.; Gao, Y. G.; Chen, A. P.; Wang, A. H.; Liang, P. H., Mechanism of product chain length determination and the role of a flexible loop in Escherichia coli undecaprenyl-pyrophosphate synthase catalysis. *J Biol Chem* **2001,** *276* (50), 47474-82.

322.   Ohnuma, S.; Narita, K.; Nakazawa, T.; Ishida, C.; Takeuchi, Y.; Ohto, C.; Nishino, T., A role of the amino acid residue located on the fifth position before the first aspartate-rich motif of farnesyl diphosphate synthase on determination of the final product. *J Biol Chem* **1996,** *271* (48), 30748-54.

323.   Ohnuma, S.; Hirooka, K.; Ohto, C.; Nishino, T., Conversion from archaeal geranylgeranyl diphosphate synthase to farnesyl diphosphate synthase. Two amino acids before the first

aspartate-rich motif solely determine eukaryotic farnesyl diphosphate synthase activity. *J Biol Chem* **1997,** *272* (8), 5192-8.

324. Ohnuma, S.; Hirooka, K.; Tsuruoka, N.; Yano, M.; Ohto, C.; Nakane, H.; Nishino, T., A pathway where polyprenyl diphosphate elongates in prenyltransferase. Insight into a common mechanism of chain length determination of prenyltransferases. *J Biol Chem* **1998,** *273* (41), 26705-13.

325. Reigard, S. A.; Zahn, T. J.; Haworth, K. B.; Hicks, K. A.; Fierke, C. A.; Gibbs, R. A., Interplay of isoprenoid and peptide substrate specificity in protein farnesyltransferase. *Biochemistry* **2005,** *44* (33), 11214-23.

326. Krzysiak, A. J.; Rawat, D. S.; Scott, S. A.; Pais, J. E.; Handley, M.; Harrison, M. L.; Fierke, C. A.; Gibbs, R. A., Combinatorial modulation of protein prenylation. *ACS Chem Biol* **2007,** *2* (6), 385-9.

327. Guo, Z.; Wu, Y. W.; Tan, K. T.; Bon, R. S.; Guiu-Rozas, E.; Delon, C.; Nguyen, T. U.; Wetzel, S.; Arndt, S.; Goody, R. S.; Blankenfeldt, W.; Alexandrov, K.; Waldmann, H., Development of selective RabGGTase inhibitors and crystal structure of a RabGGTase-inhibitor complex. *Angew Chem Int Ed Engl* **2008,** *47* (20), 3747-50.

328. Battaglia, A.; Pak, K.; Brors, D.; Bodmer, D.; Frangos, J. A.; Ryan, A. F., Involvement of ras activation in toxic hair cell damage of the mammalian cochlea. *Neuroscience* **2003,** *122* (4), 1025-35.

329. Cox, A. D.; Garcia, A. M.; Westwick, J. K.; Kowalczyk, J. J.; Lewis, M. D.; Brenner, D. A.; Der, C. J., The CAAX peptidomimetic compound B581 specifically blocks farnesylated, but not geranylgeranylated or myristylated, oncogenic ras signaling and transformation. *J Biol Chem* **1994,** *269* (30), 19203-6.

330. Garcia, A. M.; Rowell, C.; Ackermann, K.; Kowalczyk, J. J.; Lewis, M. D., Peptidomimetic inhibitors of Ras farnesylation and function in whole cells. *J Biol Chem* **1993,** *268* (25), 18415-8.

331. Qian, Y.; Vogt, A.; Vasudevan, A.; Sebti, S. M.; Hamilton, A. D., Selective inhibition of type-I geranylgeranyltransferase in vitro and in whole cells by CAAL peptidomimetics. *Bioorg Med Chem* **1998,** *6* (3), 293-9.

332. Finder, J. D.; Litz, J. L.; Blaskovich, M. A.; McGuire, T. F.; Qian, Y.; Hamilton, A. D.; Davies, P.; Sebti, S. M., Inhibition of protein geranylgeranylation causes a superinduction of nitric-oxide synthase-2 by interleukin-1beta in vascular smooth muscle cells. *J Biol Chem* **1997,** *272* (21), 13484-8.

333. Miquel, K.; Pradines, A.; Sun, J.; Qian, Y.; Hamilton, A. D.; Sebti, S. M.; Favre, G., GGTI-298 induces G0-G1 block and apoptosis whereas FTI-277 causes G2-M enrichment in A549 cells. *Cancer Res* **1997,** *57* (10), 1846-50.

334. Vogt, A.; Sun, J.; Qian, Y.; Hamilton, A. D.; Sebti, S. M., The geranylgeranyltransferase-I inhibitor GGTI-298 arrests human tumor cells in G0/G1 and induces p21(WAF1/CIP1/SDI1) in a p53-independent manner. *J Biol Chem* **1997,** *272* (43), 27224-9.

335. McGuire, T. F.; Qian, Y.; Vogt, A.; Hamilton, A. D.; Sebti, S. M., Platelet-derived growth factor receptor tyrosine phosphorylation requires protein geranylgeranylation but not farnesylation. *J Biol Chem* **1996,** *271* (44), 27402-7.

336. Watanabe, M.; Fiji, H. D.; Guo, L.; Chan, L.; Kinderman, S. S.; Slamon, D. J.; Kwon, O.; Tamanoi, F., Inhibitors of protein geranylgeranyltransferase I and Rab geranylgeranyltransferase identified from a library of allenoate-derived compounds. *J Biol Chem* **2008,** *283* (15), 9571-9.

337. Delahunty, C. M.; Yates, J. R., 3rd, MudPIT: multidimensional protein identification technology. *Biotechniques* **2007,** *43* (5), 563, 565, 567 passim.

338. Lutcke, A.; Jansson, S.; Parton, R. G.; Chavrier, P.; Valencia, A.; Huber, L. A.; Lehtonen, E.; Zerial, M., Rab17, a novel small GTPase, is specific for epithelial cells and is induced during cell polarization. *J Cell Biol* **1993,** *121* (3), 553-64.

339. Florens, L., et al., A proteomic view of the Plasmodium falciparum life cycle. *Nature* **2002,** *419* (6906), 520-6.

340. Zybailov, B.; Coleman, M. K.; Florens, L.; Washburn, M. P., Correlation of relative abundance ratios derived from peptide ion chromatograms and spectrum counting for quantitative proteomic analysis using stable isotope labeling. *Anal Chem* **2005,** *77* (19), 6218-24.

341. Chen, I.; Choi, Y. A.; Ting, A. Y., Phage display evolution of a peptide substrate for yeast biotin ligase and application to two-color quantum dot labeling of cell surface proteins. *J Am Chem Soc* **2007,** *129* (20), 6619-25.

342. Zhou, Z.; Cironi, P.; Lin, A. J.; Xu, Y.; Hrvatin, S.; Golan, D. E.; Silver, P. A.; Walsh, C. T.; Yin, J., Genetically encoded short peptide tags for orthogonal protein labeling by Sfp and AcpS phosphopantetheinyl transferases. *ACS Chem Biol* **2007,** *2* (5), 337-46.

343. Zhou, Z.; Koglin, A.; Wang, Y.; McMahon, A. P.; Walsh, C. T., An eight residue fragment of an acyl carrier protein suffices for post-translational introduction of fluorescent pantetheinyl arms in protein modification in vitro and in vivo. *J Am Chem Soc* **2008,** *130* (30), 9925-30.

344. Lin, C. W.; Ting, A. Y., Transglutaminase-catalyzed site-specific conjugation of small-molecule probes to proteins in vitro and on the surface of living cells. *J Am Chem Soc* **2006,** *128* (14), 4542-3.

345. Popp, M. W.; Antos, J. M.; Grotenbreg, G. M.; Spooner, E.; Ploegh, H. L., Sortagging: a versatile method for protein labeling. *Nat Chem Biol* **2007,** *3* (11), 707-8.

346. Rush, J. S.; Bertozzi, C. R., New aldehyde tag sequences identified by screening formylglycine generating enzymes in vitro and in vivo. *J Am Chem Soc* **2008,** *130* (37), 12240-1.

347. Wu, P.; Shui, W.; Carlson, B. L.; Hu, N.; Rabuka, D.; Lee, J.; Bertozzi, C. R., Site-specific chemical modification of recombinant proteins produced in mammalian cells by using the genetically encoded aldehyde tag. *Proc Natl Acad Sci U S A* **2009**.

348. Heal, W. P.; Wickramasinghe, S. R.; Bowyer, P. W.; Holder, A. A.; Smith, D. F.; Leatherbarrow, R. J.; Tate, E. W., Site-specific N-terminal labelling of proteins in vitro and in vivo using N-myristoyl transferase and bioorthogonal ligation chemistry. *Chem Commun (Camb)* **2008,** (4), 480-2.

349. Heal, W. P.; Wickramasinghe, S. R.; Leatherbarrow, R. J.; Tate, E. W., N-Myristoyl transferase-mediated protein labelling in vivo. *Org Biomol Chem* **2008,** *6* (13), 2308-15.

350. Fernandez-Suarez, M.; Baruah, H.; Martinez-Hernandez, L.; Xie, K. T.; Baskin, J. M.; Bertozzi, C. R.; Ting, A. Y., Redirecting lipoic acid ligase for cell surface protein labeling with small-molecule probes. *Nat Biotechnol* **2007,** *25* (12), 1483-7.

351. Chen, B. C.; Sundeen, J. E.; Guo, P.; Bednarz, M. S.; Zhao, R., Novel triethylsilane mediated reductive N-alkylation of amines: improved synthesis of 1-(4-imidazolyl)methyl-4-sulfonylbenzodiazepines new farnesyltransferase inhibitors. *Tetrahedron Letters* **2001,** *42* (7), 1245-1246.

352. Nguyen, U. T.; Guo, Z.; Delon, C.; Wu, Y.; Deraeve, C.; Franzel, B.; Bon, R. S.; Blankenfeldt, W.; Goody, R. S.; Waldmann, H.; Wolters, D.; Alexandrov, K., Analysis of the eukaryotic prenylome by isoprenoid affinity tagging. *Nat Chem Biol* **2009**.

7 ACKNOWLEDGEMENTS

ACKNOWLEDGEMENTS

8 DECLARATION/EIDESSTATTLICHE ERKLÄRUNG

Hiermit versichere ich an Eides statt, dass ich die vorliegende Arbeit selbständig und nur mit den angegebenen Hilfsmitteln angefertigt habe.

Dortmund, April 2009

Thi Thanh Uyen Nguyen